NOVA IMS Information Management School

DOCTORAL PROGRAMME

Information Management

The Role of Synthetic Data in Improving Supervised Learning Methods

The Case of Land Use/Land Cover Classification

João Pedro Martins Ribeiro da Fonseca

A thesis submitted in partial fulfillment of the requirements for the degree of Doctor in Information Management

NOVA Information Management School
Instituto Superior de Estatística e Gestão de Informação

Universidade Nova de Lisboa

[this page should not be included in the digital version. Its purpose is only for the printed version]

NOVA Information Management School
Instituto Superior de Estatística e Gestão de Informação
Universidade Nova de Lisboa

The Role of Synthetic Data in Improving Supervised Learning Methods: The Case of Land Use/Land Cover Classification

by

João Pedro Martins Ribeiro da Fonseca

Doctoral Thesis presented as partial requirement for obtaining the PhD in Information Management

Supervisor: Professor Fernando Bação, PhD

February 2023

Statement of Integrity

I hereby declare having conducted this academic work with integrity. I confirm that I have not usedplagiarism or any form of undue use of information or falsification of results along the process leadingto its elaboration. I further declare that I have fully acknowledge the Rules of Conduct and Code of Honor from the NOVA Information Management School.

Lisbon, February 1, 2023

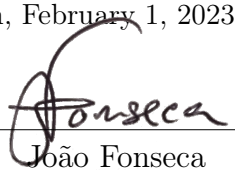

João Fonseca

Dedication

To my parents, José Manuel and Maria de Lurdes Fonseca.

Acknowledgements

MIT Portugal - funding

Fernando Bacao - advisor

Georgios Douzas - discussions, tips and help on technical implementations throughout the research work

English professor from NOVA IMS - proofreading multiple chapters of this dissertation

My parents, José Manuel and Maria de Lurdes, my siblings, Hugo and Inês, my grandmother, Teresa, my girlfriend, Yasmina El Fassi and my brother-in-law, Hugo Nunes.

My friends, Pedro Rodrigues, Francisco Martins, Miguel Meco, Andrew Bell, Rafaela Henriques, Margarida Saragoça, Manvel Khudinyan, Francisco Braga, Miguel Portas, Mari Reyes, Ana Vieira, Ana Correia, Oumaima Derfoufi

My secondary school's biology teacher, Regina Lucena, who taught us life skills well beyond the courses' syllabi, and tremendously inspired me towards a research-oriented path (without me realising it).

Professor Marco Painho and my friends from the doctoral program, Vicente Tang, Maria Anastasiadou and Darina Vorobeva

Abstract

In remote sensing, Land Use/Land Cover (LULC) maps constitute important assets for various applications, promoting environmental sustainability and good resource management. Although, their production continues to be a challenging task. There are various factors that contribute towards the difficulty of generating accurate, timely updated LULC maps, both via automatic or photo-interpreted LULC mapping. Data preprocessing, being a crucial step for any Machine Learning task, is particularly important in the remote sensing domain due to the overwhelming amount of raw, unlabeled data continuously gathered from multiple remote sensing missions. However a significant part of the state-of-the-art focuses on scenarios with full access to labeled training data with relatively balanced class distributions. This thesis focuses on the challenges found in automatic LULC classification tasks, specifically in data preprocessing tasks. We focus on the development of novel Active Learning (AL) and imbalanced learning techniques, to improve ML performance in situations with limited training data and/or the existence of rare classes. We also show that much of the contributions presented are not only successful in remote sensing problems, but also in various other multidisciplinary classification problems. The work presented in this thesis used open access datasets to test the contributions made in imbalanced learning and AL. All the data pulling, preprocessing and experiments are made available at https://github.com/joaopfonseca/publications. The algorithmic implementations are made available in the Python package *ml-research* at https://github.com/joaopfonseca/ml-research.

Keywords: LULC classification; Active Learning; Imbalanced Learning; Synthetic Data; Oversampling;

Sustainable Development Goals (SDG):

Contents

List of Figures

List of Tables

1. Introduction

Accurate LULC maps constitute a unique resource for a variety of applications. Its applications range from environmental monitoring, land change detection, and natural hazard assessment to agriculture and water/wetland monitoring [1]. However, the production of LULC maps often require the involvement of multiple photo-interpreters with specialized skills, making the process expensive and time-consuming and unsuitable for operational LULC mapping over large areas [2]. Therefore, the manual production of LULC maps are often outdated by the time they are completed, limiting its value to the analysis past conditions in the area of interest.

An alternative method to address the limitations found in the photo-interpreted approach to produce LULC maps is automated mapping. This method uses remotely sensed data, especially multi and hyper-spectral images, to train ML algorithms to automatically detect the different LULC classes. To do this, the usage of recent supervised learning techniques seems to be a promising path to achieve reliable and updated maps [3]. However, the practical application of this approach is hampered by various limitations:

1. Human error. The quality of the classifiers produced is heavily dependent on the quality of its training data. In this case, the training dataset is extracted from manually labeled land cover patches using typically satellite imagery. The target LULC map's minimum mapping unit, as well as the quality of orthophotos and satellite images being used are some of the factors that may lead to label noise in the training data [4].

2. High dimensionality. The high dimensionality of multi and hyper-spectral images contain useful information to improve ML classification tasks. However, it also introduces an additional layer of complexity and redundancy in classification [5]. If the training data is not large enough, it may cause the classification task to be affected by the curse of dimensionality.

3. Class separability. Some LULC classes sometimes contain overlapping spectral signatures which makes the separation of the two classes particularly challenging in some cases [6].

4. Infrequent LULC classes. Depending on the region of study, some land cover classes may be more or less frequent when compared to other regions [7]. However, the accurate identification of rare classes is often equally or more important than the identification of the remaining classes. This problem is known, in ML community, as imbalanced learning. As an example, the classification of a desert region with 3 classes of interest, bare soil, urban and water, would be an imbalanced learning problem. In this case, a classifier that would predict bare soil for the entire area of study would have very high overall accuracy scores but would not be useful.

5. Scarcity of labeled data. The increasing number of remote sensing missions in the past decades are generating large amounts of high quality data. However, only a small portion of this data has some sort of LULC ground truth and can be used for supervised learning. In these scenarios the production of automated LULC maps is particularly challenging and involves the usage of techniques that are able to leverage information from both labeled and unlabeled data and simultaneously maximize the value of the data annotation process [8].

The latter two challenges, imbalanced learning (*i.e.*, infrequent LULC classes) and scarcity of labeled data, are the focus of this thesis. However, these two challenges may be addressed in various different ways.

The asymmetry frequently found on LULC class distributions affects the performance of ML classifiers. In this scenario, during the ML classifier's learning phase, the minority classes contribute less to the minimization of accuracy, the typical objective function, biasing the classifier towards the most frequent classes. The possible approaches to deal with imbalanced learning can be divided into three main groups [9]:

1. Cost-sensitive solutions. These methods use a cost matrix to adjust the misclassification cost to benefit the minority classes.
2. Algorithmic-level solutions. These methods introduce algorithmic solutions to improve the learning process on the minority classes.
3. Resampling solutions. They modify the training data to balance the class distribution by removing observations from the majority class(es) or adding observations belonging to the minority class(es).

The latter set of methods, resampling solutions, benefit from their simplicity. This type of approaches do not require domain knowledge to define a cost matrix and dispense the usage of specialized classifiers. These methods can be further divided into (1) Oversampling, where an algorithm generates artificial observations belonging to the minority class, (2) Undersampling, where an algorithm removes observations belonging to the majority class or (3) Hybrid approaches, which combine oversampling and undersampling together. In this thesis, we will focus on oversampling methods and generalize these as a corner case of augmentation methods for tabular data in later chapters. In Section 1.1 this topic is discussed to a greater extent.

The second challenge this thesis focuses on is the implementation of useful ML algorithms in environments with scarce availability of labeled data. There are three different types of techniques to address this problem, which fall in between supervised and unsupervised learning:

1. Semi-supervised Learning. Uses both labeled and unlabeled data in the training phase to improve the classifier's performance [10]. It pushes the decision boundaries of classifiers to regions with lower density of observations while maximizing the performance over the labeled training dataset [11].
2. Self-supervised Learning. Uses unlabeled data to perform secondary/pretext tasks to learn representations of the input space [12]. These methods typically use neural network architectures [13].
3. Active Learning. Iteratively samples the most informative/representative observation out of a pool of unlabeled data in order to be labeled and included into the training dataset [14]. This approach attempts to optimize the classifier's performance with as least data as possible.

The latter method, Active Learning, benefits from the possibility of including different techniques into its pipeline, including the former two. It is therefore one of the main focus of this thesis. In Section 1.2 this topic is discussed to a greater extent.

1.1. Data Augmentation

Data Augmentation methods expand the training dataset by introducing new and informative observations [15]. The production of artificial data may be done via the introduction of perturbations on the input [16], feature [17] or output space [15]. Data Augmentation methods may be divided into Heuristic and Neural Network-based approaches [18]. In addition, they may also be distinguished based on its data generation policy, whether local (considers a local/specific subset of the dataset) or global (considers the overall distribution of the training dataset). Figure 1.1 shows the general taxonomy of Heuristic Data Augmentation methods. Finding the appropriate Data Augmentation method generally depends on

the domain [17], although some studies discuss which methods are more appropriate according to the domain [18, 19, 20].

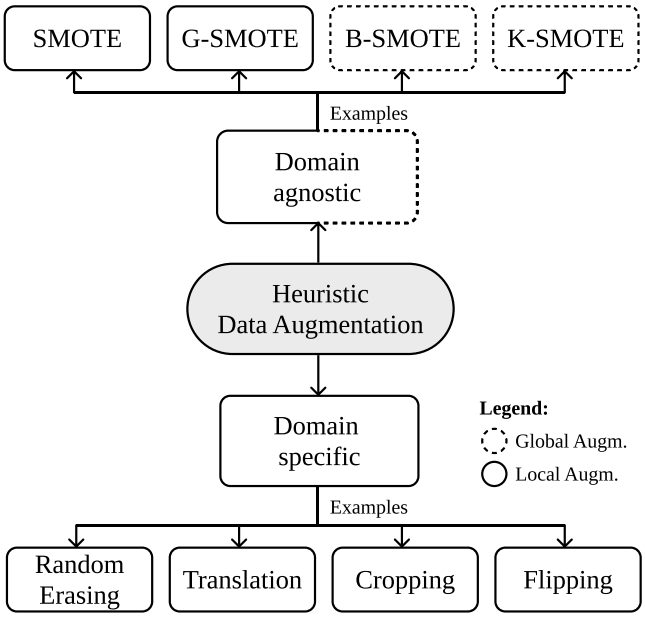

Figure 1.1.: Schema containing a general Heuristic Data Augmentation taxonomy.

Heuristic approaches attempt to generate new and relevant observations through the application a predefined procedure, usually incorporating some degree of randomness [21]. Since these methods typically occur in the input space, they require less data and computational power when compared to Neural Network methods. Neural Network approaches, on the other hand, map the original input space into a lower-dimensional representation, known as the feature space [17]. The generation of artificial data occurs in the feature space and is reconstructed into the input space. Although these methods allow the generation of less noisy data in high-dimensional contexts and more plausible artificial data, they are significantly more computationally intensive. Considering the scope of this thesis, the computational power available for this experiment and the breadth of datasets used in the different experimental procedures, we will focus on domain-agnostic heuristic data augmentation methods.

While some techniques may depend on the domain, others are domain-agnostic. For example, Random Erasing [16], Translation, Cropping and Flipping are image data-specific augmentation methods. Other methods, such as most of the variants of the Synthetic Minority Oversampling TEchnique (SMOTE) [22], may be considered domain agnostic. However, SMOTE methods were originally developed as oversamplers, whose goal is to balance the class frequencies of the target variable in the training dataset and address the class imbalance bias. Therefore, oversampling methods may be considered a subset of Data Augmentation. Data Augmentation strategies may follow varying augmentation strategies, which does not necessarily depend on the target class distribution. An example of the differences among general data augmentation and oversampling generation strategies is shown in Figure 1.2.

The simplest approach found in the literature is randomly duplicating existing training observations. As a non-informed data generation method, although simple to implement, it increases the risk of overfitting and generally performs worse than other informed heuristic methods [2].

The SMOTE method generates artificial data via the linear interpolation between a random observation and one of its k-nearest neighbors (also randomly selected) [22]. Although simple and effective, it also contains several limitations which motivated the development other variants, discussed below. Specifically, its selection mechanism does not consider the global structure of the dataset while its generation mechanism

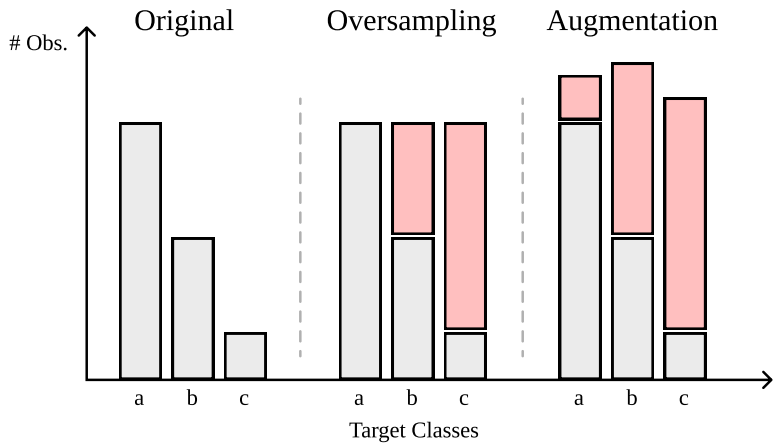

Figure 1.2.: Examples of data augmentation Strategies. The salmon-colored bars represent artificial data using the normal oversampling (center group) and an example of augmentation (right group) strategies.

introduces little variability into the training dataset [23]. Borderline-SMOTE (B-SMOTE) [24] improves the selection mechanism by attributing a larger importance to the observations closer to the decision boundaries. The selected observations are used to run the SMOTE method in order to produce better defined decision boundaries. A more recent improvement of the selection mechanism is K-means SMOTE (K-SMOTE) [25]. This method uses a clustering-based approach to overcome imbalances between and within classes, while considering the densities of each region of the input space.

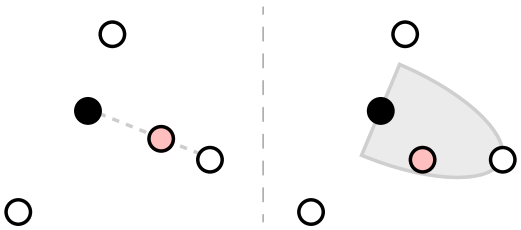

Figure 1.3.: Examples of data generation using SMOTE and G-SMOTE. In this example, both G-SMOTE's deformation and truncation parameters assume values around 0.5.

G-SMOTE [23] modifies SMOTE's generation mechanism. Instead of generating an observation as a linear combination between 2 others, it generates observations within an hypersphere defined using the selected observation as its center and one of its nearest neighbors as its boundary. The hypersphere contains two hyperparameters, the truncation and deformation factors, which limit the area of the hypersphere. The difference between SMOTE and G-SMOTE is shown in Figure 1.3.

1.2. Active Learning

Supervised ML algorithms typically perform well in contexts where labeled data is abundant and accessible. However, in a practical setting, finding this data is frequently a challenging task. Depending on the domain, collecting large volumes of data may not be feasible since the labeling of such data becomes labor and time intensive and may involve domain experts throughout the process [26]. AL maximizes a

classifier's performance while annotating as least observations as possible. It assumes that observations within the same dataset have a different contribution to the training of ML classifiers [27]. Consequently, the data annotation cost can be minimized via the annotation of the most valuable observations within an unlabeled input space. The goal is to iteratively maximize the classification performance of ML algorithms while minimizing the required amount of training data to reach a certain performance threshold [28]. It allows the implementation of ML classifiers with a good performance and minimal effort when compared to randomly selecting data or labeling the entire unlabeled dataset [29]. Therefore, it addresses the labeling problem in scenarios with a limited budget, time, or availability of labeled data.

AL methods may be divided into 2 different stages, initialization and iteration. Figure 1.4 shows a diagram that represents the typical AL initialization. Assuming the AL task is initialized without any previously labeled data, it is typically composed of 3 steps [30]:

1. Collection of an unlabeled dataset, where the procedure depends on the domain of application.
2. Selection of an initial data subset. Typically, when there is no a priori labeled dataset, the initial data subset is randomly picked from the unlabeled dataset.
3. Data labeling. The supervisor is presented with the data subset, where its goal is to label each observation. Some of the research refers to the supervisor as the oracle [31, 32].

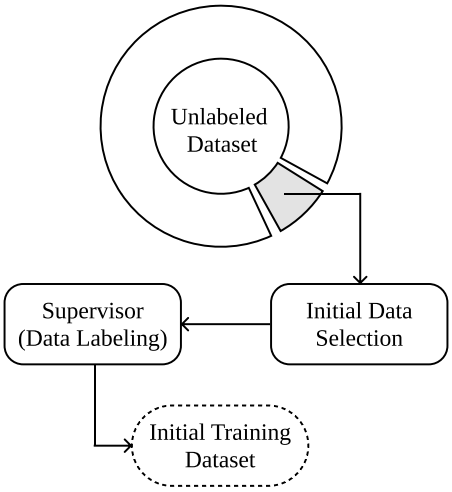

Figure 1.4.: Diagram depicting an AL initialization.

Once an initial training dataset is set up, the iterative process of AL takes place. An AL iteration is completed once a new batch of labeled data is added to the training dataset. A standard AL process is shown in Figure 1.5 and is composed of the following steps [33, 34]:

1. Setting up a classification algorithm and uncertainty criterion. The classifier is trained using the labeled dataset (*i.e.,* the Current Training Dataset), and is used to predict the class membership probabilities of the observations found in the unlabeled dataset. The class probabilities are passed into an Uncertainty Criterion, which will return the classification uncertainty of the classification algorithm for each unlabeled observation. The combination of the classifier, along with the uncertainty criterion is sometimes referred to as the Query/Acquisition function [35].
2. Selecting the top N observations. Since it is not possible to determine a priori whether the classifier's prediction is correct or not, the N observations with highest uncertainty may have been unknowingly correctly classified. However, regardless of the classification quality, these observations are expected to provide the most meaningful information to train the classifier in the next iteration.

3. Labeling the selected N observations and updating the current training dataset with the new training observations. The selected observations from the unlabeled dataset are presented to the supervisor, which is responsible for manually labeling the observations. The new (labeled) training observations are added to the training dataset and the iteration is completed.

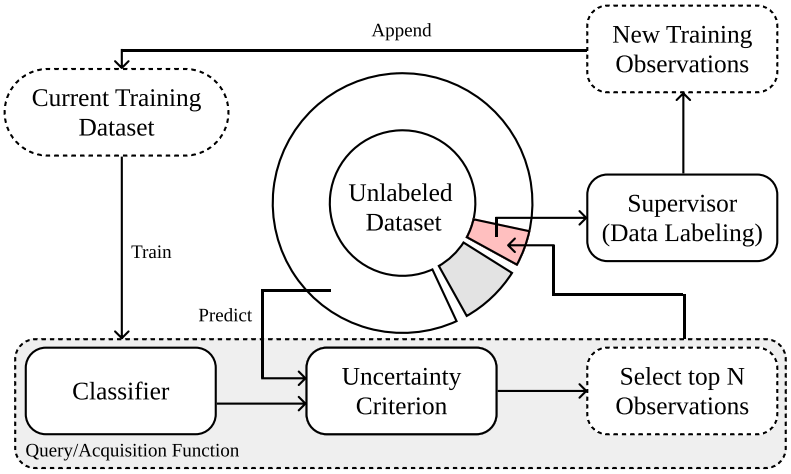

Figure 1.5.: Diagram depicting an AL iteration. In the first iteration, the training set collected during the initialization process becomes the "Current Training Dataset".

Two common challenges found in AL implementations is the consistency and efficiency of AL in practical scenarios [36]. On the one hand, the consistency problem refers to the high variance in performance (regarding classification and data selection) over different initializations (*i.e.,* different initial training datasets) of active learners. On the other hand, the efficiency problem refers to the maximization of the quality of the collected data over a run. Therefore, a good active learner is capable of having a consistent performance over different initializations while ensuring the production of high-performing classifiers with the least possible amount of data. There are various factors that may affect the consistency and efficiency of the AL framework: (1) Human error during data labeling [37], (2) Non-informative initial training dataset [38] and (3) Lack of an appropriate uncertainty criterion [35]. AL research has typically been focused on the specification of uncertainty criteria, as well as domain-specific applications. Query functions can be divided into two different categories [39, 40]:

1. Informative-based query strategies. These strategies use the classifier's output to assess the importance of each observation towards the performance of the classifier. These strategies focus on quantifying the class uncertainty of the unlabeled observations. Since these techniques do not account for the relationships between the unlabeled observations and treats each observation independently [41].

2. Representative-based query strategies. These strategies estimate the optimal set of observations that will optimize the classifier's performance. This strategy contains 3 main approaches: Density-based, Diversity-based and Exploration of graph structures. Although this method addresses the problem of sampling bias and redundant instance selection, these strategies typically require more observations in order to reach the desired classification performance [40].

Although there are significant contributions towards the development of more robust query functions and classifiers in AL, modifications to AL's basic structure is rarely explored. In [31] the authors introduce a loss prediction module in the AL framework to replace the uncertainty criterion. This model implements a second classifier to predict the expected loss of the unlabeled observations (using the actual losses collected during the training of the original classifier) and return the unlabeled observations with the highest expected loss. Although this contribution is specific to neural networks (and more specifically, to

deep neural networks), they were able to significantly improve the efficiency of data selection in AL. In [8] the authors propose the usage of semi-supervised learning during both the initialization of the AL and the iterative process as well. However, this method was proposed specifically for deep learning applications.

A query strategy/function encompasses all the steps prior to the data labeling within an AL iteration. They focus on finding the observations' informativeness, representativeness or both [39, 40]. Representative query strategies are generally less efficient in data selection than Informative query strategies [40]. However, recent research often use representative approaches alongside informative approaches [39, 42]. Representative query strategies are explored via 3 main approaches [40]:

1. Density-based, which select representative observations from high density regions. [43, 44, 45] used a density-based approach using clustering algorithms to select the observations closest to the centroid of each cluster.
2. Diversity-based, which select the N observations at each iteration that maximize the diversity in the training data. The diversity-based approach was developed to avoid the selection of redundant observations in batch-mode learning [46].
3. Graph-based, which find the most representative nodes and edges of a graph network [47]. Since these methods are specific to graph network data, they have a more limited applicability.

Informative query strategies, unlike representative query strategies, do not account for the structure of the unlabeled dataset. As a result, this type of strategy may lead to the inefficient selection of observations (*i.e.,* redundant observations with similar profiles) [40]. Research on more robust selection criteria attempts to address the efficiency problem. This is motivated by the importance of the selection criteria in AL's iterative process [35]. Specifically, Settles [48] observed that in some datasets informative query strategies fail to outperform the random selection of observations. Generally, the Random Selection query method is used as a baseline. This method disregards the class membership probabilities produced by the classifier and returns N random points from the dataset without following any specific criteria.

A frequently used query strategy is Uncertainty Sampling, originally proposed in [49]. Using this method, the estimation of an observation's uncertainty is based on the target class with the highest probability (p_a, according to the classifier) and the uncertainty is calculated as $1 - p_a$. However, since this method dismissed the classifier's predictions on the remaining labels, the Breaking Ties criterion was proposed to address this limitation for multiclass problems [50]. This method uses the two target classes with highest probability (p_a and p_b, according to the classifier) and the uncertainty is calculated as $p_a - p_b$ (in this case, the lower the output value, the higher the uncertainty). Recent variants of the Breaking Ties criterion, such as the Modified Breaking Ties, attempted to fix some limitations of the original method [51, 52].

Another common informative query strategy is the calculation of Shannon's Entropy. This metric measures the level of uncertainty based on the probabilities of a set of possible events. Its formula is given by $H(p) = -\sum_{i=0}^{n} p_i \log_2 p_i$, having p as the set of probabilities of all target classes. The application of the Entropy uncertainty criterion is also frequently applied in Deep Active Learning [32]. Other Entropy-based methods were also developed for more specific applications. For example, an ensemble querying approach known as Entropy Querying-by-Bagging uses the predictions of all estimators to find the maximum entropy of each observation [53].

The Query by Committee (QBC) strategy was developed to address ensemble classifiers. It is a disagreement based strategy attempts to maximize the information gain at each iteration by computing the disagreement of the predictions over the estimators that form the ensemble. The Entropy Querying-by-Bagging and Query-by-Boosting methods are also ensemble strategies. Query by boosting and bagging methods were found to achieve a good performance over various datasets [54], while the performance between the two strategies appears to differ significantly across various scenarios [55].

Other classifier-specific query strategies were also developed for different applications. However, these methods have the disadvantage of depending on the classifier being used. For example, Margin Sampling is a well studied strategy that uses a Support Vector Machine as its classifier in order to select the unlabeled observations closest to its decision boundaries [40]. Although, since this method is known to lead to the excessive selection of observations in dense regions [56], it was improved in various ways. In [56] the authors extend this strategy by applying the manifold-preserving graph reduction algorithm beyond the normal Margin Sampling method.

1.3. Research Questions

The main research questions (RQ) and goals of the work plan are the following:

1. What are the main research lines in data augmentation?
    - Development of a literature review to study existing data augmentation methods and the core fields where they are being used.
2. How can automatic LULC mapping achieve an increased and consistent quality?
    - Exploration of imbalanced learning methods in the context of LULC.
3. How to perform automated LULC mapping efficiently under limited ground-truth data availability?
    - Development of an improved active learning framework in the remote sensing domain using artificial data generation.
4. How to oversample data with both continuous and categorical features?
    - Development of an improved oversampling method to be used with mixed data types.

1.4. Main Objectives

This research aims to apply and develop new data preprocessing techniques to LULC classification, with a focus on AL and oversampling techniques. The main objective is to optimize ML classifiers' performance with minimal labeled data and/or imbalanced learning scenarios. This objective was decomposed into four research questions. We start by performing a literature review of data augmentation techniques (RQ1). Second, we apply a state-of-the-art oversampling method to understand its effect in LULC classification tasks (RQ2). Third, we modify the AL framework to include a generator and optimize its augmentation policy to further reduce the amount of required labeled data for ML classifiers to reach a satisfactory performance (RQ3). Finally, we propose a new oversampling method for datasets with both continuous and categorical features (RQ4).

Each contribution towards the different RQs is divided into different studies. All chapters refer to a different RQ with the exception Chapters 4 and 5, which refer to RQ3. The future steps necessary to complete the PhD plan are described in Chapter 7. The current structure of the thesis is shown in Table 1.1.

RQ1 aims to investigate and consolidate data augmentation methods. This was done by conducting a literature review to study the main areas of application of data augmentation methods. To do this, we created a database of research papers containing the author list, year of publication, journal/conference, keywords, title, abstract and number of citation of a large number of papers related to data augmentation. This study was done with Natural Language Processing (NLP) techniques to extract topics and knowledge

graphs based on keywords to understand the different relationships among studies. This approach resulted in a compilation of the most important and current research in the field, allowing both researchers and practitioners to use this work as a starting point for their own work. Finally, the development of this work represents a crucial step towards the identification of new opportunities within the field and consequently towards the following research question and objectives. The results of this work is available in Chapter **??**.

The most relevant methods found in Chapter **??** will be used for posterior work. Specifically, we address RQ2 using a heuristic data augmentation method, K-means SMOTE [25], as described in Chapter 3. Since datasets produced for LULC classification often contain irrelevant, redundant, noisy and/or unreliable data, knowledge discovery is hindered and ultimately leads to the poor training of predictors. Consequently, data preprocessing becomes an important contribution to the quality of the predictors developed. In this case, we used K-means SMOTE to oversample minority regions belonging to the same land cover class. This was motivated by the challenges faced in producing automated LULC maps using a training dataset with rare classes. In this scenario, the spectral signature of a given class often depends on its geographical distribution and the time of the year the image was captured. Cluster-based oversamplers, such as K-means SMOTE, allow for a more accurate generation of minority samples, since it can identify and isolate variations in spectral signatures within a land cover class.

At a later stage, in RQ3, we addressed a different instance of the problem of rare land cover classes in the training dataset. Specifically, in a context of limited sample-collection budget, the collection of the most informative samples capable of optimally increasing the classification accuracy of a LULC map is of particular interest [33]. Active learning attempts to minimize the human-computer interaction involved in photo-interpretation by selecting the data points to include into the annotation process. Although, current state-of-the-art techniques are mostly focused on the improvement of the acquisition function. We study this problem via the modification of the typical AL framework. We focus on the usage of data augmentation techniques and an augmentation policy optimizer to improve the quality of the data generated. These modifications are presented in Chapters 4 and 5:

- Chapter 4 introduces the generator component into the typical AL framework.
- Chapter 5 introduces the augmentation policy optimizer, while generalizing the generator component for augmentation policies beyond oversampling strategies.

One of the main limitations uncovered in RQ1 (see Section **??**) is the lack of oversampling methods applicable to datasets containing categorical features. In fact, only two oversamplers were found to be capable of oversampling data with categorical features, SMOTENC [22] and random oversampling. However, in a practical setting, datasets with mixed feature types are common but the methods available are outdated. RQ4 will be addressed through the modification of a State-of-the-art oversampling method by mixing its data generation mechanism with the one found in SMOTENC. However, this work is still in progress.

1.5. Methods

The methodology used for all contributions follow a similar approach, with exception to the work presented in Chapter **??**. It is composed as follows:

1. Collection of a large number of (LULC, multidisciplinary or image) classification datasets.
2. Identification of related literature and limitations to be addressed.
3. Design and implementation of contributions.
4. Definition and implementation of experimental settings.

5. Analysis of results and statistical significance testing.
6. Publish results.

The methodological approach to the proposed doctoral work is depicted in Figure 1.6. All of the work presented was developed while ensuring full reproducibility. Contributions at the algorithm-level are implemented in the Python open-source package ML-Research.

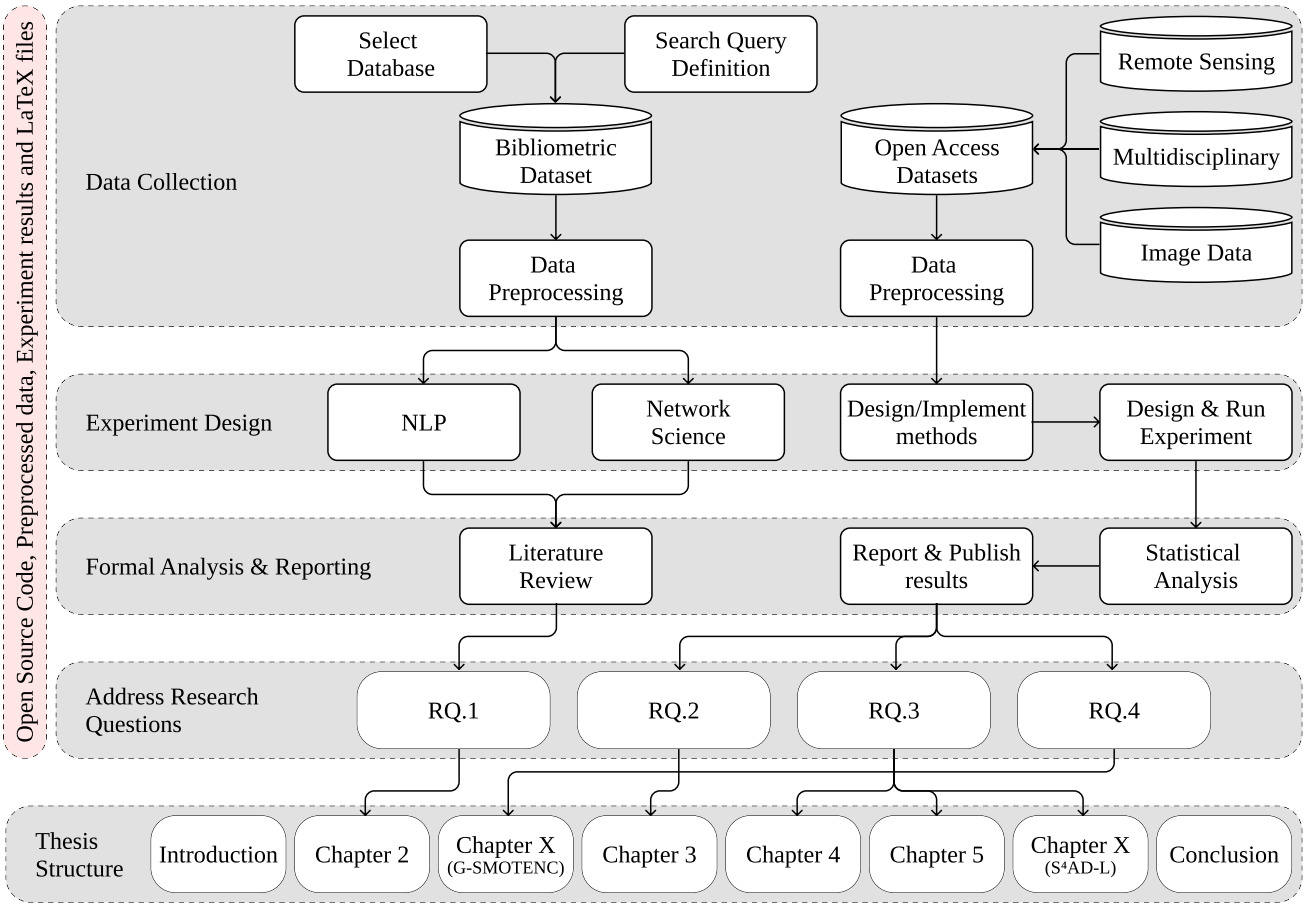

Figure 1.6.: Planned structure and methodological approach of the doctoral work.

1.6. Path of Research

The work developed is organized in different papers of related subjects, namely AL and imbalanced learning. Every submitted or published research output is available at this GitHub repository, along with the LaTeX scripts, data, source code (for data pulling, preprocessing, experiments and analysis), experiments' raw outputs and analysis outputs (figures, tables and diagrams). The current stage of each of the studies is presented in Table 1.1.

Chapter	RQ	Study Name	Current stage
??	1	Research Trends and Applications of Data Augmentation Algorithms	Under Review (Initial submission)
3	2	Improving Imbalanced Land Cover Classification with K-means SMOTE: Detecting and Oversampling Distinctive Minority Spectral Signatures	Published in the journal Information
4	3	Increasing the Effectiveness of Active Learning: Introducing Artificial Data Generation in Active Learning for Land Use/Land Cover Classification	Published in the journal Remote Sensing
5	3	Improving Active Learning Performance Through the Use of Data Augmentation	Under Review (2^{nd} round)
n/a	3	S^4AD-Learning: Self-supervised Semi-supervised Active Deep Learning	Work in Progress
n/a	4	Geometric SMOTENC: A geometrically enhanced drop-in replacement for SMOTENC	Work in Progress

Table 1.1.: Current stage of the planned studies in the scope of the doctoral program and PhD grant.

2. Tabular and Latent Space Synthetic Data Generation: A Literature Review

Submitted as Joao Fonseca, Fernando Bacao, to a Q1 Journal, 2022

The generation of synthetic data can be used for anonymization, regularization, oversampling, semi-supervised learning, self-supervised learning and various other tasks. Such broad potential motivated the development of new algorithms, specialized in data generation for specific data formats and Machine Learning (ML) tasks. However, one of the most common data formats used in industry applications, tabular data, is generally overlooked; Literature analyses are scarce, state-of-the-art methods are spread across domains and ML tasks and there is little to no distinction among the main types of mechanism underlying synthetic data generation algorithms. In this paper, we analyse tabular and latent space synthetic data generation algorithms. Specifically, we propose a unified taxonomy as an extension and generalization of previous taxonomies, review 70 generation algorithms across six ML problems, distinguish the main generation mechanisms identified into six categories, describe each type of generation mechanism, discuss metrics to evaluate the quality of synthetic data and provide recommendations for future research. We expect this study to assist researchers and practitioners identify relevant gaps in the literature and design better and more informed practices regarding synthetic data.

Keywords: Synthetic Data; Data Augmentation; Oversampling; Regularization; Privacy

2.1. Introduction

Tabular data consists of a database structured in tabular form, composed of columns (features) and rows (observations) [57]. It is one of the most commonly used data structures within a wide range of domains. However, ML techniques developed for tabular data can be applied to any type of data; input data, regardless of its original format, can be mapped into a manifold, lower-dimensional abstraction of the input data and mapped back into its original input space [58, 59]. This abstraction is often referred to as embeddings, encodings, feature space or latent space. In this paper, we will refer to this concept as latent space.

Synthetic data is obtained from a generative process based on properties of real data [60]. The generation of synthetic data is essential for several objectives. For example, it is used as a form of regularizing ML classifiers (*i.e.*, data augmentation) [61]. One form of anonymizing datasets is via the production of synthetic observations (*i.e.*, synthetic data generation) [62]. In settings where only a small portion of training data is labeled, some techniques generate artificial data using both labeled and unlabeled data with a modified loss function to train neural networks (*i.e.*, semi-supervised learning) [63]. In imbalanced learning contexts, synthetic data can be used to balance the target classes' frequencies and reinforce the learning of minority classes (*i.e.*, oversampling) [64]. Some active learning frameworks use synthetic data

to improve data selection and classifier training [65]. Other techniques employ data generation to train neural networks without labeled data (*i.e.*, self-supervised learning) [12].

The breadth of these techniques span multiple domains, such as facial recognition [66], Land Use/Land Cover mapping [67], medical image processing [68], Natural Language Processing (NLP) [69] or credit card default prediction [70]. According to the domain and data type, the data generation techniques used may vary significantly. In addition, several synthetic data generation methods are specific to the domain, data type or target ML task. Generally, these methods rely on the domain data's structure, which are not easily transferable to tabular data.

Overall, synthetic data generation techniques for tabular data are not as explored as image or text data, despite its popularity and ubiquity [71]. Furthermore, these techniques are invariant to the original data format; they can be applied to both the latent space [59] or tabular data. On one hand, data generation in the latent space uses a generative model to learn a manifold, lower-dimensional abstraction over the input space [58]. At this level, any tabular data generation mechanism can be applied and reconstructed into the input space if necessary. On the other hand, synthetic data generation on tabular data can be applied to most problems. Although, the choice of generation mechanism depends on (1) the importance of the original statistical information and the relationships among features, (2) the target ML task and (3) the role synthetic data plays in the process (*i.e.*, anonymization, regularization, class balancing, etc.). For example, when generating data to address an imbalanced learning problem (*i.e.*, oversampling), the relationships between the different features are not necessarily kept, since the goal is to reinforce the learning of the minority class by redefining an ML classifier's decision boundaries. If the goal is to anonymize a dataset, perform some type of descriptive task, or ensure consistent model interpretability, statistical information must be preserved.

Depending on the context, evaluating the quality of the generated data is a complex task. For example, for image and time series data, perceptually small changes in the original data can lead to large changes in the euclidean distance [60, 72]. The evaluation of generative models typically account primarily for the performance in a specific task, since good performance in one criterion does not imply good performance on another [72]. However, in computationally intensive tasks it is often impracticable to search for the optimal configurations of generative models. To address this limitation, other evaluation methods have been proposed to assist in this evaluation, which typically use statistical divergence metrics, averaged distance metrics, statistical similarity measurements, or precision/recall metrics [73, 74]. The relevant performance metrics found in the literature are discussed in Section 2.6.

2.1.1. Motivation, Scope and Contributions

This literature review focuses on generation mechanisms applied to tabular data across the main ML techniques where tabular synthetic data is used. We also discuss generation mechanisms used in the latent space, since the generation mechanisms in tabular data and latent space may be used interchangeably. In addition, we focus on the ML perspective of synthetic data, as opposed to the practical perspective; according to the practical perspective, synthetic data is used as a proxy of real data. It is assumed to be inaccessible, essential and a secondary asset for tasks like education, software development, or systems demonstrations [75].

We focus on data generation techniques in the tabular and latent space (*i.e.*, embedded inputs) with a focus on classification and associated ML problems. Related literature reviews are mostly focused on specific algorithmic or domain applications, with little to no emphasis on the core generative process. For this reason, these techniques often appear "sandboxed", even though there is a significant overlap between them. There are some related reviews published since 2019. Assefa et al. [60] provides a general overview of synthetic data generation for time series data anonymization in the finance sector. Hernandez et al. [76] reviews data generation techniques for tabular health records anonymization. Raghunathan [77] reviews synthetic data anonymization techniques that preserve the statistical properties of a dataset.

Table 2.1.: Related literature reviews published since 2019.

Reference	Data type	ML problem	Domain	Observations
Assefa et al. [60]	—	Data privacy	Finance	Analysis of applications, motivation and properties of synthetic data for anonymization.
Hernandez et al. [76]	Tabular	Data privacy	Healthcare	Focus on GANs.
Raghunathan [77]	Tabular	Data privacy	Statistics	Focus on general definitions such as differential privacy and statistical disclosure control.
Nalepa et al. [78]	Image	Segmentation	Medicine	Analysis of algorithmic applications on a 2018 brain-tumor segmentation challenge.
Bayer et al. [79]	Text	Classification	—	Distinguish 100 methods into 12 groups.
Shorten et al. [80]	Text	Deep Learning	—	General overview of text data augmentation.
Chen et al. [81]	Text	Few-shot Learning	—	Augmentation techniques for machine learning with limited data
Feng et al. [69]	Text	—	—	Overview of augmentation techniques and applications on NLP tasks.
Liu et al. [82]	Text	—	Various	Analysis of industry use cases of data augmentation in NLP. Emphasis on input level data augmentation.
Yi et al. [68]	Image	—	Medicine	Emphasis on GANs.
Wang et al. [83]	Image	Deep Learning	—	Regularization techniques using facial image data. Emphasis on Deep Learning generative models.
Shorten et al. [84]	Image	Deep Learning	—	Emphasis on data augmentation as a regularization technique.
Khosla et al. [85]	Image	—	—	Broad overview of image data augmentation. Emphasis on traditional approaches.
Khalifa et al. [86]	Image	—	Various	General overview of image data augmentation and relevant domains of application.
Iwana et al. [87]	Time series	Classification	—	Defined a taxonomy for time series data augmentation.
Wen et al. [88]	Time series	Various	—	Analysis of data augmentation methods for classification, anomaly detection and forecasting.
Zhao et al. [89]	Graph	Various	—	Graph data augmentation for supervised and self-supervised learning.

Nalepa et al. [78] reviews data augmentation techniques for brain-tumor segmentation. Bayer et al. [79] distinguishes augmentation techniques for text classification into latent and data space, while providing an extensive overview of augmentation methods within this domain. However, the taxonomy proposed and latent space augmentation methods are not necessarily specific to the domain. Shorten et al. [80], Chen et al. [81], Feng et al. [69] and Liu et al. [82] also review data augmentation techniques for text data. Yi et al. [68] review Generative Adversarial Network architectures for medical imaging. Wang et al. [83] reviews face data augmentation techniques. Shorten et al. [84], Khosla et al. [85] and Khalifa et al. [86] discuss techniques for image data augmentation. Iwana et al. [87] and Wen et al. [88] also review time series data augmentation techniques. Zhao et al. [89] review data augmentation techniques for graph data. The analysis of related literature reviews [1] is shown in Table 2.1.

[1] Results obtained using Google Scholar, limited to articles published since 2019, using the search query `("synthetic data generation" OR "oversampling" OR "imbalanced learning" OR "data augmentation") AND ("literature review" OR "survey")`. Retrieved on August 11^{th}, 2022. More articles were added later whenever found relevant.

The different taxonomies established in the literature follow a similar philosophy, but vary in terminology and are often specific to the technique discussed. Regardless, it is possible to establish a broader taxonomy without giving up on specificity. This study provides a joint overview of the different data generation approaches, domains and ML techniques where data generation is being used, as well as a common taxonomy across domains. It extends the analyses found in these articles and uses the compiled knowledge to identify research gaps. We compare the strengths and weaknesses of the models developed within each of these fields. Finally, we identify possible future research directions to address some of the limitations found. The contributions of this paper are summarized below:

- Bridge different ML concepts using synthetic data generation in its core;
- Propose a synthetic data generation/data augmentation taxonomy to address the ambiguity in the various taxonomies proposed in the literature;
- Characterize all the relevant data generation methods using the proposed taxonomy;
- Discuss the ML techniques in which synthetic data generation is used and consolidate the current generation mechanisms across the different techniques;
- Highlight the key challenges of synthetic data generation and discuss possible future research directions.

2.1.2. Paper Organization

The rest of this paper is organized as follows: Section 2.2 defines and formalizes the different concepts, goals, trade-offs and motivations related to synthetic data generation. Section 2.3 defines the taxonomy used to categorize all the algorithms analysed in this study. Section 2.4 analyses all the algorithms using synthetic data generation, distinguished by learning problem. Section 2.5 describes the main generation mechanisms found, distinguished by generation type. Section 2.6 reviews performance evaluation methods of synthetic data generation mechanisms. Section 2.7 summarizes the main findings and general recommendations for good practices on synthetic data usage. Section 2.8 discusses limitations, research gaps and future research directions. Section 2.9 presents the main conclusions drawn from this study.

2.2. Background

In this section we define basics concepts, common goals, trade-offs and motivations regarding the generation of synthetic data in ML. We define synthetic data generation as the production of artificial observations that resemble naturally occurring ones within a certain domain, using a generative model. It requires access to a training dataset, a generative process, or a data stream. However, the constraints imposed to this process largely depends on the target ML task. For example, to generate artificial data for regularization purposes in supervised learning (*i.e.*, data augmentation) the training dataset must be annotated. The production of anonymized datasets using synthetic data generation requires synthetic datasets to be different from the original data, while following similar statistical properties. Domain knowledge may also be necessary to encode specific relationships among features into the generative process.

2.2.1. Relevant Learning Problems

The breach of sensitive information is an important barrier to the sharing of datasets, especially when it concerns personal information [90]. One solution for this problem is the generation of synthetic data without identifiable information. Generally speaking, ML tasks that require data with sensitive information are not compromised when using synthetic data. The experiment conducted by Patki et al. [62] using relational datasets showed that in 11 out 15 comparisons ($\approx 73\%$), practitioners performing predictive modelling tasks using fully synthetic datasets performed the same or better than those using the original dataset. Optionally, anonymized synthetic data may be produced with theoretical privacy guarantees, using differential privacy techniques. This topic is discussed in Section 2.4.1.

A common problem in the training of deep neural networks are their capacity to generalize [91] (*i.e.*, reduce the difference in classification performance between known and unseen observations). Data augmentation is a common method to address this problem for any type of ML classifier. The generation of synthetic observations increases the range of the input space used in the training phase and reduces the difference in performance between known and new observations. Although other regularization methods exist, data augmentation is a useful method since it does not affect the choice in the architecture of the ML classifier and does not exclude the usage of other regularization methods. In domains such as computer vision and NLP, data augmentation is also used to improve the robustness of models against adversarial attacks [92, 93]. These topics are discussed into higher detail in Section 2.4.2.

In supervised learning, synthetic data generation is often motivated by the need to balance target class distributions (*i.e.*, oversampling). Since most ML classifiers are designed to perform best with balanced datasets, defining an appropriate decision boundary to distinguish rare classes becomes difficult [94]. Although there are other approaches to address imbalanced learning, oversampling techniques are generally easier to implement since they do not involve modifications to the classifier. This topic is discussed into higher detail in Section 2.4.3.

In supervised learning tasks where labeled data is not readily available, but can be labeled, an Active Learning (AL) method may be used to improve the efficiency of the labelling process. AL aims to reduce the cost of producing training datasets by finding the most informative observations to label and feed into the classifier [95]. In this case, the generation of synthetic data is particularly useful to reduce the amount of labelled data required for a successful ML project. This topic is discussed in Section 2.4.4.

Two other techniques reliant on synthetic data generation are Semi-supervised Learning (Semi-SL) and Self-Supervised Learning (Self-SL). The former leverages both labeled and unlabeled data in the training phase, simultaneously, while several methods apply perturbations on the training data as part of the training procedure [96]. The latter, Self-SL, is a technique used to train neural networks in the absence of labeled data. Several Semi-SL and Self-SL methods use synthetic data generation as a core element. These methods are discussed in Sections 2.4.5 and 2.4.6.

2.2.2. Problem Formulation

The original dataset, $\mathcal{D} = \mathcal{D}_L \cup \mathcal{D}_U$, is a collection of real observations and is distinguished according to whether a target feature exists, $\mathcal{D}_L = ((x_i, y_i))_{i=1}^{l}$, or not, $\mathcal{D}_U = (x_i)_{i=1}^{u}$. All three datasets, $\mathcal{D}$, $\mathcal{D}_L$ and $\mathcal{D}_U$ consist of ordered collections with lengths $l + u$, l and u, respectively. Synthetic data generation is performed using a generator, $f_{gen}(x; \tau) = x^s$, where τ defines the generation policy (*i.e.*, its hyperparameters), $x \in \mathcal{D}$ is an observation and $x^s \in \mathcal{D}^s$ is a synthetic observation. Analogous to $\mathcal{D}$, the synthetic dataset, $\mathcal{D}^s$, is also distinguished according to whether there is an assignment of a target feature, $\mathcal{D}_L^s = ((x_j^s, y_j^s))_{j=1}^{l'}$, or not, $\mathcal{D}_U^s = (x_j^s)_{j=1}^{u'}$.

Depending on the ML task, it may be relevant to establish metrics to measure the quality of $\mathcal{D}^s$. In this case, a metric $f_{qual}(\mathcal{D}^s, \mathcal{D})$ is used to determine the level of similarity/dissimilarity between $\mathcal{D}$ and $\mathcal{D}^s$. In

addition, a performance metric to estimate the performance of a model on the objective task, f_{per}, may be used to determine the appropriateness of a model with parameters θ, *i.e.*, f_θ. The generator's goal is to generate $\mathcal{D}^s$ with arbitrary length, given $\mathcal{D} \sim \mathbb{P}$ and $\mathcal{D}^s \sim \mathbb{P}^s$, such that $\mathbb{P}^s \approx \mathbb{P}$, $x_i \neq x_j \forall x_i \in \mathcal{D} \wedge x_j \in \mathcal{D}^s$. $f_{gen}(x;\tau)$ attempts to generate a $\mathcal{D}^s$ that maximizes either f_{per}, f_{qual}, or a combination of both.

2.3. Data Generation Taxonomy

The taxonomy proposed in this paper is a combination of different definitions found in the literature, extended with other traits that vary among domains and generation techniques. Within image data studies, Shorten et al. [84] and Khalifa et al. [86] divide data augmentation techniques into "basic" or "classical" approaches and deep learning approaches. In both cases, the former refers to domain-specific generation techniques, while the latter may be applied to any data structure. Iwana et al. [87] proposes a time-series data augmentation taxonomy divided in four families: (1) Random transformation, (2) Pattern mixing, (3) Generative models and (4) Decomposition. With exception to generative models, the majority of the methods presented in the remaining families are well established and domain specific. Hernandez et al. [76] defines a taxonomy for synthetic tabular data generation approaches divided in three types of approaches: (1) Classical, (2) Deep learning and (3) Others. Most taxonomies follow similar definitions, while varying in terminology or distinction criteria. In addition, all taxonomies with categories defined as "basic", "traditional" or "classical" use these to characterize domain-specific transformations.

Within the taxonomies found, none of them consider how a generation mechanism employs $\mathcal{D}$ into the generation process or, if applicable, the training phase. However, it is important to understand whether a generation mechanism randomly selects x and a set of close neighbors, thus considering local information only, or considers the overall dataset or data distribution for the selection of x and/or generation of x^s. Our proposed taxonomy is depicted in Figure 2.1. It characterizes data generation mechanisms using four properties:

1. Architecture. Defines the broader type of data augmentation. It is based on domain specificity, architecture type or data transformations using a heuristic or random perturbation process. Data generation based on data sampling from a probability function is considered probability-based. Generation techniques that apply a form of random perturbation, interpolation or geometric transformation to the data with some degree of randomness are considered randomized approaches. Typical, domain-specific data generation techniques are considered domain-specific approaches. These techniques apply transformations to a data point leveraging relationships in the structure of the data (which is known *a priori*). Generative models based on neural network architectures are defined as network-based. These architectures attempt to either generate observations in the latent space and/or by producing observations that are difficult to distinguish from the original dataset.

2. Application level. Refers to the phase of the ML pipeline where the generative process is included. Generative models are considered internal if they are used alongside the primary ML task, whereas models used prior to the development of the primary ML task are considered external.

3. Scope. Considers the usage of the original dataset's properties. Generative models that consider the density of the data space, statistical properties of $\mathcal{D}$, or attempt to replicate/manipulate specific relationships found in $\mathcal{D}$ are considered to have a global scope, whereas generative models that consider a single observation and/or a set of close neighbors are considered to have a local scope. On the one hand, generative models with a local scope do not account for $\mathbb{P}^s$ but allow for the generation of x^s within more precise regions in the latent/input space. On the other hand, generative models with a global scope have a higher capacity to model $\mathbb{P}^s$ but produce x^s with less precision within the latent/input space.

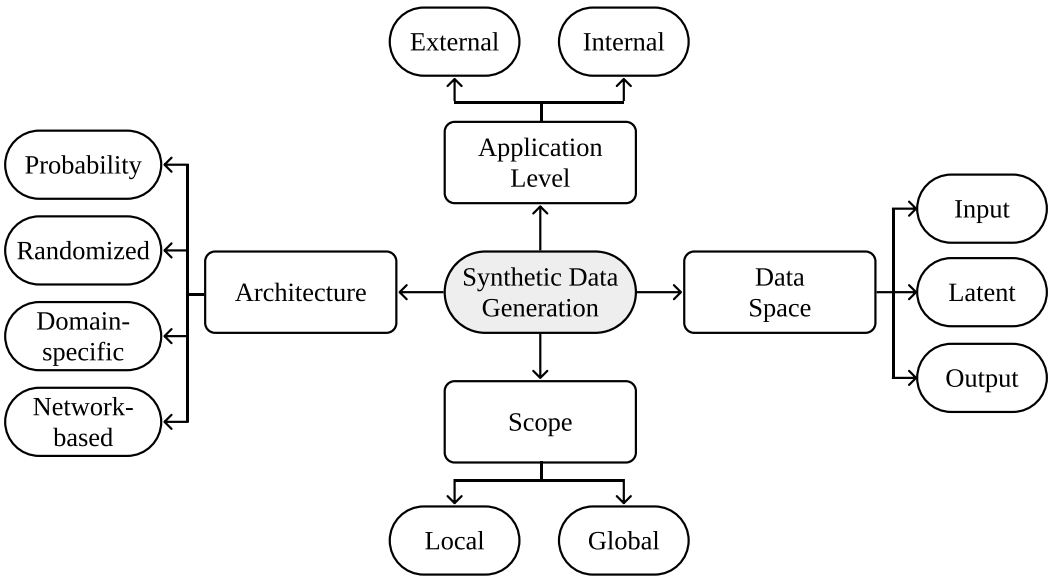

Figure 2.1.: General taxonomy of data generation mechanisms proposed in this paper.

4. Data space. Refers to the type of data representation used to apply the generative model. Generation mechanisms can be applied using the raw dataset (*i.e.*, on the input space), an embedded representation of the data (*i.e.*, on the latent space) or based on the target feature (*i.e.*, on the output space). Although some studies discuss the need to generate synthetic data on the input space [90, 62], there are various studies that successfully apply synthetic data generation techniques on a latent space.

Throughout the analysis of the different types of generation mechanisms, all relevant methods were characterized using this taxonomy and listed in Table 2.2.

Table 2.2.: Summary of the synthetic data generation methods discussed in this work.

Algorithm	ML Problem	Type	Architecture	Level	Data Space	Scope
SDV [62]	Anon.	PDF	Probabilistic	External	Input	Global
MST [97]	DP	PGM	Probabilistic	External	Input	Global
MWEM [98]	DP	Other	Probabilistic	External	Input	Global
MWEM-PGM [99]	DP	PGM	Probabilistic	External	Input	Global
PrivBayes [100]	DP	PGM	Probabilistic	External	Input	Global
DPGAN [101]	DP	GAN	Network	External	Latent	Global
DPCTGAN [102]	DP	GAN	Network	External	Latent	Global
PATE-GAN [103]	DP	GAN	Network	External	Lat. + Out.	Global
PATECTGAN [102]	DP	GAN	Network	External	Lat. + Out.	Global
FEM [104]	DP	Perturb.	Probabilistic	External	Input	Global
RAP [105]	DP	Perturb.	Probabilistic	External	Input	Global
PDF [106, 107]	—	PDF	Probabilistic	External	Input	Global
Kamino [108]	DP	PDF	Probabilistic	External	Input	Global
RON-GAUSS [109]	DP	PDF	Probabilistic	Internal	Latent	Global
HDMM [110]	DP	Perturb.	Probabilistic	External	Input	Global
DualQuery [111]	DP	Other	Probabilistic	External	Input	Global
ROS(E) [112]	Ovs	Perturb.	Randomized	External	Input	Local
SMOTE [113]	Ovs	Linear	Randomized	External	Input	Local
SMOTENC [113]	Ovs	Linear	Randomized	External	Input	Local
SMOTEN [113]	Ovs	—	—	External	Input	Local

Continued on next page

Table 2.2.: Summary of the synthetic data generation methods discussed in this work.

Algorithm	ML Problem	Type	Architecture	Level	Data Space	Scope
Borderline-SMOTE [114]	Ovs	Linear	Randomized	External	Input	Local
G-SMOTE [115]	Ovs	Geometric	Randomized	External	Input	Local
ADASYN [116]	Ovs	Linear	Randomized	External	Input	Local
KernelADASYN [117]	Ovs	PDF	Probabilistic	External	Input	Local
MOKAS [118]	Ovs	Other	Network	External	Latent	Global
SOMO [119]	Ovs	Linear	Net.+Rand.	External	Input	Global
G-SOMO [120]	Ovs	Geometric	Net.+Rand.	External	Input	Global
GMM-SENN [121]	Ovs	PDF	Probabilistic	External	Input	Global
GMF-SMOTE [122]	Ovs	Linear	Randomized	External	Input	Global
C-VAE [123]	Ovs	AE	Network	External	Latent	Global
Safe-level SMOTE [124]	Ovs	Linear	Randomized	External	Input	Local
LR-SMOTE [125]	Ovs	Linear	Randomized	External	Input	Global
K-means SMOTE [126]	Ovs	Linear	Randomized	External	Input	Global
DBSMOTE [127]	Ovs	Linear	Randomized	External	Input	Local
CGAN [128]	Ovs	GAN	Network	External	Latent	Global
K-means CTGAN [129]	Ovs	GAN	Network	External	Latent	Global
SMOTER [130]	Ovs + Reg	Linear	Randomized	External	Input	Local
G-SMOTER [131]	Ovs + Reg	Linear	Randomized	External	Input	Local
RACOG [132]	Ovs	PGM	Probabilistic	External	Input	Global
wRACOG [132]	Ovs	PGM	Probabilistic	External	Input	Global
RWO [133]	Ovs	PGM	Probabilistic	External	Input	Global
PDFOS [134]	Ovs	PDF	Probabilistic	External	Input	Global
Mixup [135]	DA	Linear	Randomized	External	In.+Out.	Local
M-Mixup [136]	DA	Linear	Network	Internal	Lat.+Out.	Global
NL-Mixup [137]	DA	Geometric	Randomized	External	In.+Out.	Local
AE-DA [138]	DA	AE	Network	External	In./Lat.+Out.	Local
MODALS [139]	DA	—	Network	Internal	Latent	Global
LSI [140]	DA	AE	Network	External	Lat.+Out.	Global
Gibbs [71]	DA	PGM	Probabilistic	External	Input	Global
MedGAN [141]	DA	GAN	Network	External	Latent	Global
GANBLR [142]	DA	PGM	Probabilistic	External	Input	Global
Table-GAN [143]	DA	GAN	Network	External	Latent	Global
CTGAN [144]	DA	GAN	Network	External	Latent	Global
TVAE [144]	DA	AE	Network	External	Latent	Global
AE [145]	DA	AE	Network	External	Latent	Global
InfoMixup [65]	AL	Linear	Network	Internal	Lat.+Out.	Global
VAEACGAN [146]	AL	AE	Network	Internal	Latent	Global
AL-G-SMOTE [95]	AL	Geometric	Randomized	Internal	Input	Local
DAE [147]	Semi-SL	AE	Network	Internal	Input	Global
Π-model [148]	Semi-SL	Perturb.	Randomized	Internal	In.+Lat.	Local
Mean Teacher [149]	Semi-SL	Perturb.	Randomized	Internal	In.+Lat.	Local
ICT [150]	Semi-SL	Linear	Randomized	Internal	Input	Local
Mixmatch [151]	Semi-SL	Linear	Randomized	Internal	Input	Local
SDAT [152]	Semi-SL	AE+PDF	Net.+Prob.	Internal	Latent	Global
MCoM [153]	Semi-SL	Linear	Randomized	Int.+Ext.	Inp.+Lat.	Global
C-Mixup [154]	Semi/Self-SL	AE+Lin.	Net+Rand.	Internal	Latent	Global
VIME [57]	Semi/Self-SL	Perturb.	Randomized	Internal	Input	Local
SubTab [155]	Self-SL	Perturb.	Rand.+Prob.	Internal	Input	Local
Scarf [156]	Self-SL	Perturb.	Randomized	Internal	Input	Local
A-SFS [157]	Self-SL	Perturb.	Randomized	Internal	Input	Local

2.4. Algorithmic applications

In this section we discuss the data generation mechanisms for the different contexts where they are applied. We emphasize the constraints in each problem that condition the way generation mechanisms are used. The literature search was conducted with the Google Scholar database, using multiple keywords related to each learning problem. Additional studies were collected by checking the citing and cited articles of each study found initially. The related work discussed these studies was used to check for additional missing methods. Although a larger preference was given to studies published in or after 2019, our analysis includes relevant papers from previous years, including seminal/classical publications in the field. All the steps involved in the literature collection were conducted manually and individually for each learning problem.

2.4.1. Privacy

Synthetic data generation is a technique used to produce synthetic, anonymized versions of datasets [90]. It is considered a good approach to share sensitive data without compromising significantly a given data mining task [158, 143]. Traditional data anonymization techniques, as well as federated learning are two other viable solutions for privacy-preserving data publishing tasks, but contain drawbacks [76]. On one hand, traditional data anonymization requires domain knowledge, is labor intensive and remains susceptible to disclosure [159]. On the other hand, federated learning is a technically complex task that consists on training ML classifiers on edge devices and aggregating temporarily updated parameters on a centralized server, instead of aggregating the training data [160]. Although it prevents sharing sensitive data, its applicability is dependent on the task. Dataset anonymization via synthetic data generation attempts to balance disclosure risk and data utility in the final synthetic dataset. The goal is to ensure observations are not identifiable and the relevant data mining tasks are not compromised [161, 162].

The generation of synthetic datasets allow a more flexible approach to implement ML tasks. To do this, it is important to guarantee that sensitive information in $\mathcal{D}$ is not leaked into $\mathcal{D}^s$. Differential privacy (DP), a formalization of privacy, offers strict theoretical privacy guarantees [102]. A differentially private generation mechanism produces a synthetic dataset, regulated by the privacy parameter ϵ, with statistically indistinguishable results when using either $\mathcal{D}$ or neighboring datasets $\mathcal{D}' = \mathcal{D} \backslash \{x\}$, for any $x \in \mathcal{D}$. A synthetic data generation model (f_{gen}) guarantees (ϵ, δ)-differential privacy if $\forall S \subseteq Range(f_{gen})$ all $\mathcal{D}, \mathcal{D}'$ differing on a single entry [98]:

$$Pr[f_{gen}(\mathcal{D}) \in S] \leq e^{\epsilon} \cdot Pr[f_{gen}(\mathcal{D}') \in S] + \delta \tag{2.1}$$

In this case, ϵ is a non-negative number defined as the privacy budget. A lower ϵ guarantees a higher level of privacy, but reduces the utility of the produced synthetic data. DP synthetic data is especially appealing since it is not affected by post-processing; any ML pipeline may be applied on $\mathcal{D}^s$ while maintaining (ϵ, δ)-differential privacy [163].

However, there are popular synthetic data-based anonymization approaches to perform anonymization without DP guarantees. For example, the Synthetic Data Vault (SDV) [62] anonymizes databases using Gaussian copula models to generate synthetic data. However, this method allows the usage of other generation mechanisms. A posterior extension of SDV was proposed to generate data using a CTGAN [144] and to handle sequential tabular data using a conditional probabilistic auto-regressive neural network [164].

The choice of the most appropriate DP synthetic data generation techniques depends on the task to be developed (if known) and the domain. However, marginal-based algorithms appear to perform well across various tests [165]. A well-known method for the generation of DP synthetic datasets is the combination

of the Multiplicative Weights update rule with the Exponential Mechanism (MWEM) [98]. MWEM is an active learning-style algorithm that maintains an approximation of $\mathcal{D}^s$. At each time step, MWEM selects the worst approximated query (determined by a scoring function) using the Exponential Mechanism and improves the accuracy of the approximating distribution using the Multiplicative Weights update rule. A known limitation of this method is its lack of scalability. Since this method represents the approximate data distribution in datacubes, this method becomes infeasible for high-dimensional problems [99]. This limitation was addressed with the integration of a Probabilistic Graphical Model-based (PGM) estimation into MWEM (MWEM-PGM) and a subroutine to compute and optimize the clique marginals of the PGM, along with other existing privacy mechanisms [99]. Besides MWEM, this method was used to modify and improve the quality of other DP algorithms: PrivBayes [100], HDMM [110] and DualQuery [111].

PrivBayes [100] addresses the curse of dimensionality by computing a differentially private Bayesian Network (*i.e.*, a type of PGM). Instead of injecting noise into the dataset, they inject noise into the lower-dimensional marginals. The high-dimensional matrix mechanism (HDMM) [110] mechanism is designed to efficiently answer a set of linear queries on high-dimensional data, which are answered using the Laplace mechanism. The DualQuery algorithm [111] is based on the two-player interactions in MWEM, and follows a similar synthetic data generation mechanism as the one found in MWEM.

FEM [104] follows a similar data generation approach as MWEM. It also uses the exponential mechanism and replaces the multiplicative weights update rule with the follow-the-perturbed-leader (FTPL) algorithm [166]. The Relaxed Adaptive Projection (RAP) algorithm [105] uses the projection mechanism [167] to answer queries on the private dataset using a perturbation mechanism and attempts to find the synthetic dataset that matches the noisy answers as accurately as it can.

Kamino [108] introduces denial constraints in the data synthesis process. It builds on top of the probabilistic database framework [106, 107], which models a probability distribution function (PDF) and integrates denial constraints as parametric factors, out of which the synthetic observations are sampled. RON-GAUSS [109] combines the random orthonormal (RON) dimensionality reduction technique and synthetic data sampling using either a Gaussian generative model or a Gaussian mixture model. The motivation for this model stems from the *Diaconis-Freedman-Meckes* effect [168], which states that most high-dimensional data projections follow a nearly Gaussian distribution. Since RON-GAUSS includes a feature extraction step (using RON) and the synthetic data generated is not projected back into the input space, we consider RON-GAUSS an internal approach to the ML pipeline.

The Maximim Spanning Tree (MST) algorithm [97] is a marginal estimation-based approach that produces differentially private data. It uses the Private-PGM mechanism [99] that relies on the PGM approach to generate synthetic data. PGM models are most commonly used when it is important to maintain the pre-existing statistical properties and relationships between features [169].

Another family of DP synthetic data generation techniques relies on the usage of Generative Adversarial Networks (GAN). DPGAN [101] modifies the original GAN architecture to make it differentially private by introducing noise to gradients during the learning procedure. This approach was also applied on a conditional GAN architecture directed towards tabular data (CTGAN) [144], which resulted in the DPCTGAN [102] algorithm. Another type of GAN-based DP data synthesis method is based on the combination of a GAN architecture and the Private Aggregation of Teacher Ensembles (PATE) [170] approach. Although the PATE method generates a DP classifier, it served as the basis for PATE-GAN [103], a DP synthetic data generation mechanism. PATE-GAN replaces the discriminator component of a GAN with the PATE mechanism, which guarantees DP over the generated data. The PATE mechanism is used in the learning phase to train an ensemble of classifiers to distinguish real from synthetic data. As a second step, the predicted labels are passed (with added noise) to another discriminator, which is used to train the generator network.

2.4.2. Regularization

When the training data is clean, labeled, balanced, and sampled from a fixed data source, the resulting ML classifier is expected to achieve good generalization performance [171]. However, if one or more of these assumptions do not hold, the ML model becomes prone to overfitting [172]. Regularization techniques are used to address problems like overfitting, small training dataset, high dimensionality, outliers, label noise and catastrophic forgetting [173, 174, 175, 176]. They can be divided into three groups [177]:

1. Output level modifications. Transforms the labels in the training data.
2. Algorithmic level modifications. Modifies the classifier's architecture, loss function or other components in the training procedure.
3. Input level modifications. Modifies the training dataset by expanding it with synthetic data.

The last approach, input level modifications, is known as data augmentation. It is used to increase the size and variability of a training dataset, by producing synthetic observations [178, 20]. Since it is applied at the data level, it can be used for various types of problems and classifiers [15]. Earlier definitions of data augmentation refer to methods based on iterative optimization or sampling algorithms that introduce unobserved data or latent variables [179]. In the current ML literature, data augmentation techniques mostly refer to the former, while the latter is better known as feature extraction. Although data augmentation is commonly used and extensively studied in computer vision [84] and natural language processing [69], its research on tabular data is less common.

Mixup [135] consists of a linear interpolation between two randomly selected observations and their target feature values, $(x_i, y_i), (x_j, y_j) \in \mathcal{D}_L$, such that given $\lambda \sim \text{Beta}(\alpha, \alpha)$, $x^s = \lambda x_i + (1 - \lambda)x_j$ and $y^s = \lambda y_i + (1 - \lambda)y_j$, where α is a predetermined hyperparameter. This method was the source of Manifold Mixup (M-Mixup) [136]. It generates synthetic data in the latent space of a neural network classifier's hidden layers. Another Mixup-based data augmentation approach, Nonlinear Mixup (NL-Mixup) [137], applies a nonlinear interpolation policy. In this case, Λ is a set of mixing policies sampled from a beta distribution applied to each feature. This approach modifies the original mixup approach to generate data within a hyperrectangle/orthotope: $x^s = \Lambda \odot x_i + (1 - \Lambda) \odot x_j$, where $\odot$ denotes the Hadamard product.

Feng et al. [138] proposed an autoencoder-based data augmentation (AE-DA) approach where the training of the autoencoder is done for each target class, non-iteratively, which reduces the amount of time required compared to the batch processing approach. The decoding weights of an autoencoder are scaled and linearly combined with an observation from another class using a coefficient that follows a beta distribution. The latter step varies from typical interpolation-based approaches, since this coefficient is usually drawn from a uniform distribution.

The Modality-Agnostic Automated Data Augmentation in the Latent Space model (MODALS) [139] leverages on the concept discussed by DeVries et al. [59], as well as the Latent Space Interpolation method (LSI) [140] and M-Mixup [136]. However, MODALS introduces a framework for data augmentation internally. It contains a feature extraction step, trained using a combination of adversarial loss, classification loss and triplet loss, where latent space generation mechanisms are applied. The classifier is trained using the original and the synthetic observations generated in the latent space. In this study the authors discuss difference transform augmentation method (among others already described in this study). It generates within-class synthetic data by selecting a x^c and two random observations within the same class, x_i, x_j, to compute $x^s = x^c + \lambda(x_i - x_j)$. In addition they also experiment with Gaussian noise and Hard example extrapolation, determined by $x^s = x^c + \lambda(x^c - \mu)$, where μ is the mean of the observations within a given class.

In the model distillation approach proposed in [71] the student model is trained with synthetic data generated with Gibbs sampling. Although Gibbs sampling is infrequently used in recent literature, two

oversampling methods using Gibbs sampling appear to achieve state-of-the-art performance [132]. However, probabilistic-based approaches for data augmentation are uncommon; there are some methods proposed for the more specific case of oversampling, but no more related methods for data augmentation were found.

A well-known approach to GAN-based data augmentation is Table-GAN [143]. It utilizes the vanilla GAN approach to the generation of synthetic data. However, vanilla GAN does not allow the controlled generation of synthetic data given conditional attributes such as the target feature values in supervised learning tasks and may be the cause for aggravated categorical feature imbalance. These limitations were addressed with the CTGAN [144] algorithm, which implements the conditional GAN approach to tabular data. Another GAN-based architecture, MedGAN [141], can also be adapted for tabular data and is used as a benchmark in related studies (*e.g.*, [144, 142]). When compared to the remaining GAN-based approaches, MedGAN's architecture is more complex and is generally underperforms in the experiments found in the literature. The GANBLR [142] modifies vanilla GAN architectures with a Bayesian network as both generator and discriminator to create synthetic data. This approach benefits from its interpretability and reduced complexity, while maintaining state-of-the-art performance across various evaluation criteria.

Another less popular approach for network-based synthetic data generation are autoencoder architectures. TVAE, proposed in [144] achieved state-of-the art performance. It consists of the VAE algorithm with an architecture modified for tabular data (*i.e.*, 1-dimensional). However, as discussed by the authors, this method contains limitations since it is difficult to achieve DP with AE-based models since they access the original data during the training procedure, unlike GANs. Delgado et al. [145] studies the impact of data augmentation on supervised learning with small datasets. The authors compare four different AE architectures: Undercomplete, Sparse, Deep and Variational AE. Although all of the tested AE architectures improved classification performance, the deep and variational autoencoders were the best overall performing models.

2.4.3. Oversampling

Since most supervised ML classifiers are designed to expect classes with similar frequencies, training them over imbalanced datasets can result in limited classification performance. With highly skewed distributions in $\mathcal{D}_L$, the classifier's predictions tend to be biased towards overrepresented classes [64]. For example, one can predict correctly with over 99% accuracy whether credit card accounts were defrauded using a constant classifier. This issue can be addressed in 3 different ways: resampling, algorithmic modifications and cost-sensitive solutions [67]. Resampling techniques are more general approaches when opposed to algorithmic and cost-sensitive methods. They modify $\mathcal{D}_L$ to ensure balanced class frequencies by removing majority class observations (*i.e.*, undersampling), producing synthetic minority class observations (*i.e.*, oversampling), or a combination of both. However, since undersampling removes observations from $\mathcal{D}_L$, it has the disadvantage of information loss [180] and lacks effectiveness when compared to oversampling methods [181, 182]. Oversampling can be considered a specific setting of data augmentation.

Oversampling is an appropriate technique when, given a set of n target classes, there is a collection C_{maj} containing the majority class observations and C_{min} containing the minority class observations such that $\mathcal{D}_L = \bigcup_{i=1}^{n} C_i$. The training dataset $\mathcal{D}_L$ is considered imbalanced if $|C_{maj}| > |C_{min}|$. This imbalance is quantified using the Imbalance Ratio (IR), expressed as $IR = \frac{|C_{maj}|}{|C_{min}|}$. An oversampling algorithm with a standard generation policy will generate a $\mathcal{D}_L^s = \bigcup_{i=1}^{n} C_i^s$ that guarantees $|C_i \cup C_i^s| = |C_{maj}|, \forall i \in \{1, \ldots, n\}$. The model f_θ will be trained using an artificially balanced dataset $\mathcal{D}'_L = \mathcal{D}_L \cup \mathcal{D}_L^s$.

Random Oversampling (ROS) is considered a classical approach to oversampling. It oversamples minority classes by randomly picking samples with replacement. It is a bootstrapping approach that, if generated in a smoothed manner (*i.e.*, by adding perturbations to the synthetic data), is also known as Random

Oversampling Examples (ROSE) [112]. However, the random duplication of observations often leads to overfitting [183].

The Synthetic Minority Oversampling Technique (SMOTE) [113] attempts to address the data duplication limitation in ROS with a two stage data generation mechanism:

1. Selection phase. A minority class observation, $x^c \in C_{min}$, and one of its k-nearest neighbors, $x^{nn} \in C_{min}$, are randomly selected.
2. Generation phase. A synthetic observation, x^s, is generated along a line segment between x^c and x^{nn}: $x^s = \alpha x^c + (1-\alpha)x^{nn}, \alpha \sim \mathcal{U}(0,1)$.

Although the SMOTE algorithm addresses the limitations in ROS, it brings other problems, which motivated the development of several SMOTE-based variants [115]: (1) it introduces noise when a noisy minority class observation is assigned to x^c or x^{nn}, (2) it introduces noise when x^c and x^{nn} belong to different minority-class clusters, (3) it introduces near duplicate observations when x^c and x^{nn} are too close and (4) it does not account for within-class imbalance (*i.e.*, different input space regions should assume a different importance according to the concentration of minority class observations).

Borderline-SMOTE [114] modifies SMOTE's selection mechanism. It calculates the k-nearest neighbors for all minority class observations and selects the ones that are going to be used as x^c in the generation phase. An observation is selected based on the number of neighbors belonging to a different class, where the observations with no neighbors belonging to C_{min} and insufficient number of neighbors belonging C_{maj} are not considered for the generation phase. This approximates the synthetic observations to the border of the expected decision boundaries. Various other methods were proposed since then to modify selection mechanism, such as K-means SMOTE [126]. This approach addresses within-class imbalance and the generation of noisy synthetic data by generating data within clusters. The data generation is done according to each cluster's imbalance ratio and dispersion of minority class observations. DBSMOTE [127] also modifies the selection strategy by selecting as x^c the set of core observations in a DBSCAN clustering solution.

The Adaptive Synthetic Sampling approach (ADASYN) [116] uses a comparable approach to Borderline-SMOTE. It calculates the ratio of non-minority class observations within the k-nearest neighbors of each $x \in C_{min}$. The amount of observations to be generated using each $x \in C_{min}$ as x^c is determined according to this ratio; the more non-minority class neighbors an observation contains, the more synthetic observations are generated using it as x^c. The generation phase is done using the linear mechanism in SMOTE. However, this approach tends to aggravate the limitation (1) discussed previously. A second version of this method, KernelADASYN [117], replaces the generation mechanism with a weighted kernel density estimation. The weighing is done according to ADASYN's ratio and the synthetic data is sampled using the calculated Gaussian Kernel function whose bandwidth is passed as an additional hyperparameter.

Modifications to SMOTE's generation mechanism are less common and generally attempt to address problem of noisy synthetic data generation. Safe-level SMOTE [124] truncates the line segment between x^c and x^{nn} according to a safe level ratio. Geometric-SMOTE (G-SMOTE) [115] it generates synthetic data within a deformed and truncated hypersphere to also avoid the generation of near-duplicate synthetic data. It also introduces a modification of the selection strategy to combine the selection of majority class observations as x^{nn} to avoid the introduction of noisy synthetic data.

LR-SMOTE [125] modifies both the selection and generation mechanisms. The set of observations to use as x^c contains the misclassified minority class observations using a SVM classifier, out of which the potentially noisy observations are removed. The k-means clustering method is used to find the closest observations to the cluster centroids, which are used as x^c. The observations with a higher number of majority class neighbors are more likely to be selected as x^{nn}. Although the generation mechanism synthesizes observations as a linear combination between x^c and x^{nn}, it restricts or expands this range by

setting $\alpha \sim \mathcal{U}(0, M)$, where M is a ratio between the average euclidean distance of each cluster's minority class observations to x^c and the euclidean distance between x^c and x^{nn}.

The Minority Oversampling Kernel Adaptive Subspaces algorithm (MOKAS) [118] adopts a different approach when compared to SMOTE-based mechanisms. It uses the adaptive subspace self-organizing map (ASSOM) [184] algorithm to learn sub-spaces (*i.e.*, different latent spaces for each unit in the SOM), out of which synthetic data is generated. The synthetic data is generated using a lower dimensional representation of the input data to ensure the reconstructed data is different from the original observations. Overall, the usage of SOMs for oversampling is uncommon. Another two examples of this approach, SOMO [119] and G-SOMO [120] use a similar approach as K-means SMOTE. In the case of G-SOMO, the SMOTE generation mechanism is replaced by G-SMOTE's instead.

Oversampling using GMM was found in a few recently proposed algorithms. GMM-SENN [121] fits a GMM and uses its inverse weights to sample data, followed by the application of SMOTEENN to leverage the Edited Nearest Neighbors (ENN) methods as a means to reduce the noise in the training dataset. The GMM Filtering-SMOTE (GMF-SMOTE) [122] algorithm applies a somewhat inverse approach; a GMM is used to detect and delete boundary samples the synthetic data is generated with SMOTE.

Dai et al. [123] propose a contrastive learning-based VAE approach for oversampling, adapted from the architecture proposed in [185]. They address a limitation found in most oversampling methods, where these methods focus almost exclusively on the distribution of the minority class, while largely ignoring the majority class distribution. Their VAE architecture uses two encoders trained jointly, using both a majority and a minority class observation. The synthetic observation is generated by sampling from one of the sets of latent variables (which follows a Gaussian distribution) and projecting it into the decoder.

Another set of network-based methods that fully replace SMOTE-based mechanisms are GAN-based architectures. One example of this approach is CGAN [128]. It uses an adversarial training approach to generate data that approximates the original data distribution and indistinguishable from the original dataset (according to the adversarial classifier). A more recent GAN-based oversampler, K-means CTGAN [129] uses a K-means clustering method as an additional attribute to train the CTGAN. In this case, cluster labels allow the reduction of within-class imbalance. These types of approaches benefit from learning the overall per-class distribution, instead of using local information only. However, GANs require more computational power to train, their performance is sensitive to the initialization and are prone to the "mode collapse" problem.

Statistical-based oversampling approaches are less common. Some methods, such as RACOG and wRACOG [132] are based on Gibbs sampling, PDFOS [134] is based on probability density function estimations and RWO [133] uses a random walk algorithm. Although oversampling for classification problems using continuous features appears as a relatively well explored problem, there is a general lack of research on oversampling using nominal features or mixed data types (*i.e.*, using both nominal and continuous features) and regression problems. SMOTENC [113] introduces a SMOTE adaptation for mixed data types. It calculates the nearest neighbors of x^c by including in the euclidean distance metric the median of the standard deviations of the continuous features for every nominal feature values that are different between x^c and x^{nn}. The generation is done using the normal SMOTE procedure for the continuous features and the nominal features are determined with their modes within x^c's nearest neighbors. The SMOTEN [113] is an oversampling algorithm for nominal features only. It uses the nearest neighbor approach proposed in Cost et al. [186] and generates x^s using the modes of the features in x^c's nearest neighbors. Solutions to oversampling in regression problems are generally also based on SMOTE, such as SMOTER [130] and G-SMOTER [131].

2.4.4. Active Learning

AL is an informed approach to data collection and labeling. In classification problems, when $|\mathcal{D}_U| \gg |\mathcal{D}_L|$ and it is possible to label data according to a given budget, AL methods will search for the most informative unlabeled observations. Once labeled and included into the training set, these observations are expected to improve the performance of the classifier to a greater extent when compared to randomly selecting observations. AL is an iterative process where an acquisition function $f_{acq}(x, f_\theta) : \mathcal{D}_U \rightarrow \mathbb{R}$ computes a classification uncertainty score for each unlabeled observation, at each iteration. f_{acq} provides the selection criteria based on the uncertainty scores, f_θ and the labeling budget [65].

One way to improve an AL process is via the generation of synthetic data. In this case, synthetic data is expected to improve classification with a better definition of the classifier's decision boundaries. This allows the allocation of the data collection budget over a larger area of the input space. These methods can be divided into AL with pipelined data augmentation approaches and AL with within-acquisition data augmentation [65]. Pipelined data augmentation is the more intuitive approach, where at each training phase the synthetic data is produced to improve the quality of the classifier and is independent from f_{acq}. In Fonseca et al. [95], the pipelined approach in tabular data achieves a superior performance compared to the traditional AL framework using the G-SMOTE algorithm and the oversampling generation policy. Other methods, although developed and tested on image data, could also be adapted for tabular data: in the Bayesian Generative Active Deep Learning framework [146] the authors propose VAEACGAN, which uses a VAE architecture along with an auxiliary-classifier generative adversarial network (ACGAN) [187] to generate synthetic data.

The Look-Ahead Data Acquisition via augmentation algorithm [65] proposes an acquisition function that considers the classification uncertainty of synthetic data generated using a given unlabeled observation, instead of only estimating classification uncertainty of the unlabeled observation itself. This approach considers both the utility of the augmented data and the utility of the unlabeled observation. This goal is achieved with the data augmentation method InfoMixup, which uses M-Mixup [136] along with the distillation of the generated synthetic data using f_{acq}. The authors additionally propose InfoSTN, although the original Spatial Transform Networks (STN) [188] were originally designed for image data augmentation.

2.4.5. Semi-supervised Learning

Semi-supervised learning (Semi-SL) techniques modify the learning phase of ML algorithms to leverage both labeled and unlabeled data. This approach is used when $|\mathcal{D}_U| \gg |\mathcal{D}_L|$ (similarly to AL settings), but additional labeled data is too difficult to acquire. In recent years, the research developed in this area directed much of its focus to neural network-based models and generative learning [96]. Overall, Semi-SL can be distinguished between transductive and inductive methods. In this section, we will focus on synthetic data generation mechanisms in inductive, perturbation-based Semi-SL algorithms, applicable to tabular or latent space data.

The ladder network [147] is a semi-supervised learning architecture that learns a manifold latent space using a Denoising Autoencoder (DAE). The synthetic data is generated during the learning phase; random noise is introduced into the input data and the DAE learns to predict the original observation. Although this method was tested with image data, DAE networks can be adapted for tabular data [189].

The Π-model simultaneously uses both labeled and unlabeled data in the training phase [148]. Besides minimizing cross-entropy, they add to the loss function the squared difference between two input level transformations (Gaussian noise and other image-specific methods) in the network's output layer. Mean Teacher algorithm [149] built upon the Π-model, which used the same types of augmentation. The Interpolation Consistency Training (ICT) [150] method combined the mean teacher and the Mixup approach, where synthetic observations are generated using only the unlabeled observations and their

predicted label using the teacher model. In Mixmatch [151], the Mixup method is used by randomly selecting any pair of observations and their true labels (if it's a labeled observation) or predicted label (if it's unlabeled).

The Semi-SL Data Augmentation for Tabular data (SDAT) algorithm [152] uses an autoencoder to generate synthetic data in the latent space with Gaussian perturbations. The Contrastive Mixup (C-Mixup) [154] algorithm generates synthetic data using the Mixup mechanism with observation pairs within the same target label. The Mixup Contrastive Mixup algorithm (MCoM) [153] proposes the triplet Mixup method using three observations where $x^s = \lambda_i x_i + \lambda_j x_j + (1 - \lambda_i - \lambda_j)x_k$, where $\lambda_i, \lambda_j \sim \mathcal{U}(0, \alpha)$, $\alpha \in (0, 0.5]$ and x_i, x_j and x_k belong to the same target class. The same algorithm also uses the M-Mixup method as part of the latent space learning phase.

2.4.6. Self-supervised Learning

Self-supervised learning (Self-SL), although closely related to Semi-SL, assumes $\mathcal{D}_L = \emptyset$. These models focus on representation learning using $\mathcal{D}_U$ via secondary learning tasks, which can be adapted to multiple downstream tasks [13]. This family of techniques allow the usage of raw, unlabeled data, which is generally cheaper to acquire when compared to processed, curated and labeled data. Although not all Self-SL methods rely on data augmentation (*e.g.*, STab [190]), the majority of state-of-the-art tabular Self-SL methods use data augmentation as a central concept for the training phase.

The value imputation and mask estimation method (VIME) [57] is a Semi-SL and Self-SL approach that introduces Masking, a tabular data augmentation method. It is motivated by the need to generate corrupted, difficult to distinguish synthetic data in a computationally efficient way for Self-SL training. They replace with probability p_m the feature values in x_i with another randomly selected value of each corresponding feature. To do this, the authors use a binomial mask vector $m = [m_1, \ldots, m_d]^\perp \in \{0, 1\}^d$, $m_j \sim \text{Bern}(p_m)$, observation x_i and the noise vector ϵ (*i.e.*, the vector of possible replacement values). A synthetic observation is produced as $x^s = (1 - m) \odot x_i + m \odot \epsilon$. A subsequent study proposed the SubTab [155] framework present a multi-view approach; analogous to cropping in image data or feature bagging in ensemble learning. In addition, the authors propose an extension of the masking approach proposed in VIME by introducing noise using different approaches: Gaussian noise, swap-noise (*i.e.*, the approach proposed in VIME) and zero-out noise (*i.e.*, randomly replace a feature value by zero).

The Self-supervised contrastive learning using random feature corruption method (Scarf) [156] uses a similar synthetic data generation approach as VIME. Scarf differs from VIME by using contrastive loss instead of the denoising auto-encoder loss used in VIME. A-SFS [157] is a Self-SL algorithm designed for feature extraction. It achieved higher performance compared to equivalent state-of-the-art augmentation-free approaches such as Tabnet [191] and uses the masking generation mechanism described in VIME.

2.5. Generation mechanisms

In this section we provide a general description of the synthetic data generation mechanisms found in the learning problems in Section 2.4. Table 2.3 summarizes the assumptions and usage of the generation mechanisms across the selected works and learning problems.

We focus on 2 key conditions for the data generation process, smoothness and manifold space (adapted from the background in [96]). The smoothness condition requires that if two observations x_i, x_j are close, then it's expected that y_i, y_j have the same value. The manifold condition requires synthetic data generation to occur within locally euclidean topological spaces. Therefore, a generation mechanism with the smoothness requirement also requires a manifold, while the opposite is not necessarily true.

Table 2.3.: Analysis of synthetic data generation mechanisms.

Type	Mechanism	Smoothness	Manifold	Priv.	Reg.	Ovs.	AL	Semi-SL	Self-SL
Perturbation	Random	✓	✓	×	×	✓	×	×	×
	Laplace	✓	✓	✓	×	×	×	×	×
	Gaussian	✓	✓	✓	✓	×	×	✓	✓
	Swap-noise	×	×	×	×	×	×	✓	✓
	Zero-out noise	×	×	×	×	×	×	×	✓
PDF	Gaussian Gen.	×	✓	✓	×	✓	×	×	×
	Gaussian Mix.	×	✓	✓	×	✓	×	×	×
	KDE	×	✓	×	×	✓	×	×	×
PGM	Bayesian Net.	×	×	✓	✓	×	×	×	×
	Gibbs	×	×	×	✓	✓	×	×	×
	Random Walk	×	×	×	×	✓	×	×	×
Linear	Between-class Int.	×	✓	×	✓	×	✓	✓	×
	Within-class Int.	✓	✓	×	✓	✓	✓	✓	×
	Extrapolation	✓	✓	×	✓	✓	×	×	×
	Hard Extra.	✓	✓	×	✓	✓	×	×	×
	Inter.+Extra.	✓	✓	×	×	✓	×	×	×
	Difference Transf.	✓	✓	×	✓	×	×	×	×
Geometric	Hypersphere	✓	✓	×	×	✓	✓	×	×
	Triangular	✓	✓	×	×	×	×	✓	×
	Hyperrectangle	×	✓	×	✓	×	×	×	×
Neural nets.	GAN	×	×	✓	✓	✓	✓	×	×
	AE	×	×	×	✓	✓	✓	✓	×
Others	Exponential M.	×	×	✓	×	×	×	×	×
	Reconstruction err.	×	×	×	×	✓	×	×	×

In the remaining subsections we will describe the main synthetic data generation mechanisms found in the literature, based on the studies discussed in Section 2.4.

2.5.1. Perturbation Mechanisms

The general perturbation-based synthetic data generation mechanism is defined as $x^s = x_i + \epsilon$, where ϵ is the noise vector sampled from a certain distribution. The random perturbation mechanism can be thought of as the non-informed equivalent of PGMs and PDFs. It samples $|\epsilon|$ values from a uniform distribution, *i.e.*, $e_i \sim \mathcal{U}(\cdot,\cdot), \forall e_i \in \epsilon$, while the minimum and maximum values depend on the context and level of perturbation desired, typically centered around zero.

Laplace (commonly used in DP algorithms) and Gaussian perturbations sample ϵ with $e_i \sim \text{Lap}(\cdot,\cdot)$ and $e_i \sim \mathcal{N}(\cdot,\cdot)$, respectively. Within the applications found, in the presence of categorical features, these methods tend to use n-way marginals (also known as conjunctions or contingency tables [111]) to ensure the generated data contains variability in the categorical features and the distribution of categorical feature values follows some given constraint. Although various other distributions could be used to apply perturbations, the literature found primarily focuses on introducing noise via uniform, Laplace and Gaussian distributions.

Masking modifies the original perturbation based approach by introducing a binomial mask vector, $m = [m_1, \ldots, m_d]^\perp \in \{0,1\}^d, m_i \sim \text{Bern}(p_m)$ and the generation mechanism is defined as $x^s = (1-m) \odot x_i + m \odot \epsilon$ [57]. The ϵ variable is defined according to the perturbation used. The Gaussian approach generates the noise vector as $\epsilon = x_i + \epsilon'$, where $e'_i \sim \mathcal{N}(\cdot,\cdot), \forall e'_i \in \epsilon'$. The swap-noise approach shuffles the

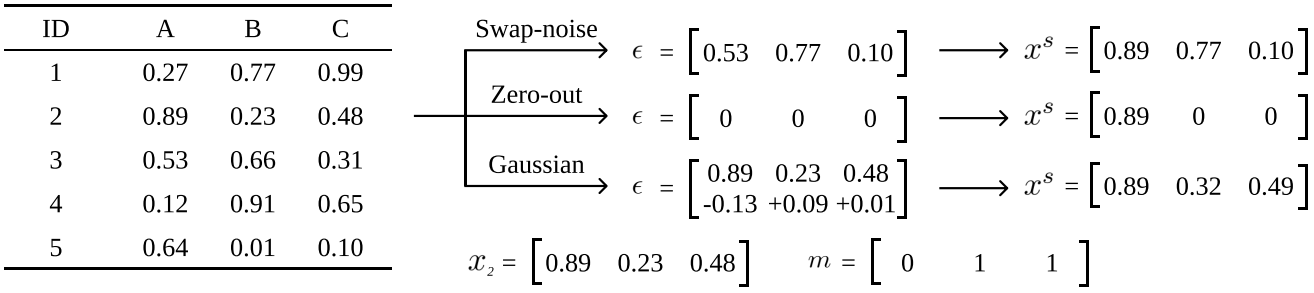

Figure 2.2.: Examples of synthetic observations generated with different masking approaches.

feature values from all observations to form ϵ, while the zero-out noise approach sets all ϵ values to zero. Intuitively, the masking technique modifies an observation's feature values with probability p_m, instead of adding perturbations over the entire observation. Figure 2.2 shows a visual depiction of the masking technique.

2.5.2. Probability Density Function Mechanisms

The Gaussian generative model, despite unfrequently used when compared to the remaining Probaility Density Function mechanisms discussed in this subsection, is an essential building block for these mechanisms. In particular, we focus on the multivariate gaussian approach, which follows near-Gaussian distribution assumptions, which is rarely reasonable on the input space. However, for high-dimensional data, it is possible to motivate this approach via the *Diaconis-Freedman-Meckes* effect [168], which states that high-dimensional data projections generally follow a nearly Gaussian distribution. The Gaussian generative model produces synthetic data from a Gaussian distribution $x^s \sim \mathcal{N}(\mu, \Sigma)$, where $\mu \in \mathbb{R}^d$ is a vector with the features' means and $\Sigma \in \mathbb{R}^{d \times d}$ is the covariance matrix. It follows the following density function [109]:

$$f(x) = \frac{1}{\sqrt{(2\pi)^d \det(\Sigma)}} \exp\left(-\frac{1}{2}(x-\mu)^T \Sigma^{-1}(x-\mu)\right) \tag{2.2}$$

Consequently, to define a Gaussian generative model it is only necessary to estimate the dataset's mean and covariance matrix.

A Gaussian mixture model (GMM) comprises several Gaussian distributions that aim to represent subpopulations within a dataset. Its training procedure allows the model to iteratively learn the subpopulations using the Expectation Maximization algorithm. A GMM becomes more appropriate than the Gaussian generative model when the data is expected to have more than one higher-density regions, leading to a poor fit of unimodal Gaussian models.

Kernel Density Estimation (KDE) methods use a kernel function to estimate the density of the dataset's distribution at each region of the input/latent space. Despite the various kernel options, the Gaussian kernel is commonly used for synthetic data generation [117]. The general kernel estimator is defined as follows:

$$\hat{p}(x) = \frac{1}{N+h} \sum_{i=1}^{N} K\left(\frac{x - x_i}{h}\right) \tag{2.3}$$

Where $N = |\mathcal{D}|$, h is a smoothing parameter known as bandwidth and K is the kernel function. The Gaussian kernel is defined as follows:

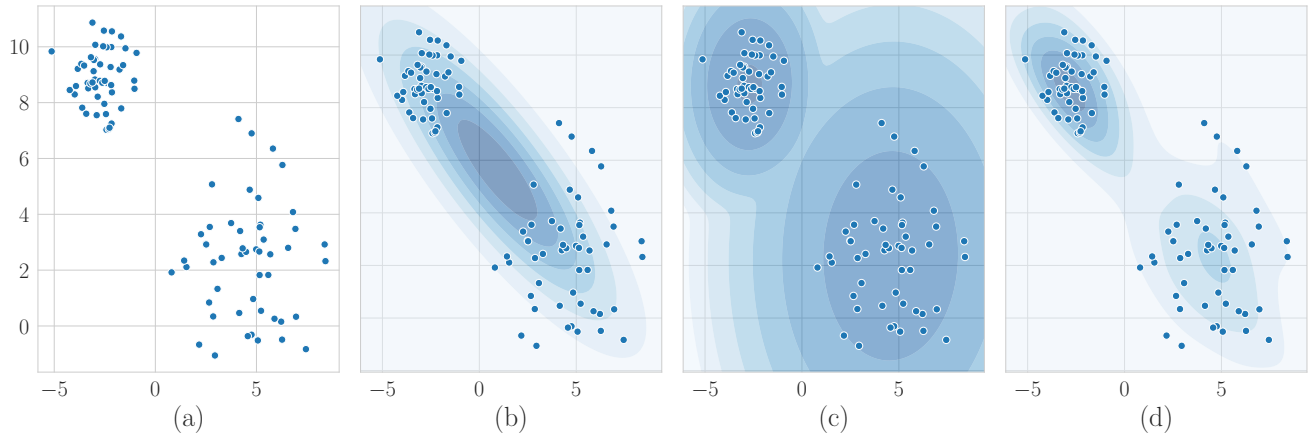

Figure 2.3.: Examples of PDF mechanisms fitted to a mock dataset. Legend: (a) Original dataset, (b) Gaussian generative model, (c) Gaussian Mixture Model and (d) Gaussian Kernel Density Estimation.

$$G_i(x) = K\left(\frac{x - x_i}{h}\right) = \frac{1}{(\sqrt{2\pi}h)^d}\exp\left(-\frac{1}{2}\frac{(x - x_i)^T(x - x_i)}{h}\right) \tag{2.4}$$

Therefore, the Gaussian KDE approach can also be expressed as $\hat{p}(x) = \frac{1}{N+h}\sum_{i=1}^{N} G_i(x)$, while the data is sampled from the estimated probability distribution. Figure 2.3 shows a visualization of the PDF mechanisms discussed, applied to a mock dataset.

2.5.3. Probabilistic Graphical Models

A Bayesian network can be thought of as a collection of as a collection of conditional distributions. It represents the joint probability distribution over the cross-product of the feature domains in $\mathcal{D}$. It is a directed acyclic graph that represents $\mathcal{D}$'s features as nodes and their conditional dependencies as directed edges. The set of features pointing directly to feature $v \in V, d = |V|$ via a single edge are known as the parent variables, $pa(v)$. A Bayesian network calculates $p(x)$ as the product of the individual density functions, based on the conditional probabilities of the parent variables:

$$p(x) = \prod_{v \in V} p(x_v | x_{pa(v)}) \tag{2.5}$$

Since the construction of a directed acyclic graph can be labor intensive, different ML approaches were developed for the learning of these structures [192]. Bayesian networks can be used for synthetic data generation when the relationship between variables is known (or can be learned) and when the data is high dimensional, making the sampling process non-trivial.

Random walk algorithms comprise the general process of iterating through a set of random steps. Although uncommon, random walk approaches may be used to sample data. The random walk approach described in Zhang et al. [133] uses the Gaussian noise mechanism over minority class observations to create synthetic observations. The Gibbs sampling mechanism also performs a random walk by iterating through sampled feature values.

Gibbs sampling is a Markov Chain Monte Carlo algorithm that iteratively samples a synthetic observation's feature values. It is a suitable method to sample synthetic data from a Bayesian network. The process

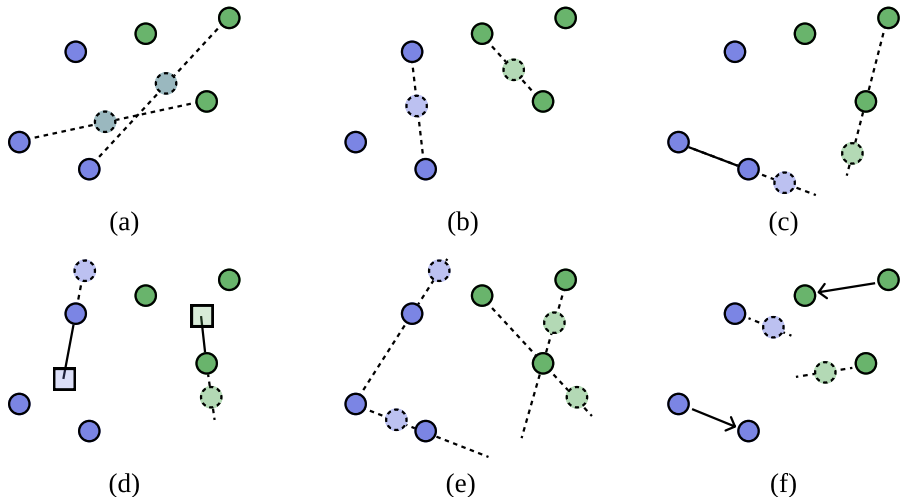

Figure 2.4.: Examples of linear transformation mechanisms. Legend: (a) Between-class interpolation, (b) Within-class interpolation, (c) Observation-based extrapolation, (d) Hard extrapolation, (e) Combination of interpolation and extrapolation and (f) Difference transform.

starts with an initial observation selected from $\mathcal{D}$, x_0 and is used to begin the sampling process. In its original format, the sampling of each feature value v in x_i^s is conditioned by x_{i-1}^s and the feature values already sampled from x_i^s, such that $x_{i,v}^s \sim p(x_{i,v}^s | x_{i,1}^s, \ldots, x_{i,v-1}^s, x_{i-1,v+1}^s, \ldots, x_{i-1,d}^s)$. Therefore, Gibbs sampling is a special case of the Metropolis-Hastings algorithm.

2.5.4. Linear Transformations

Linear interpolation mechanisms can be split into two subgroups: between and within-class interpolation. Both mechanisms follow a similar approach; they use a scaling factor λ, typically sampled from either $\mathcal{U}(0,1)$ or Beta(α,α):

$$x^s = \lambda x_i + (1-\lambda)x_j = x_j + \lambda(x_i - x_j) \tag{2.6}$$

The within-class interpolation mechanism selects two observations from the same class, while the between-class interpolation mechanism selects two observations from different classes and also interpolates the one-hot encoded target classes y_i and y_j. However, the approach to select observations might vary according to the ML task and data generation algorithm. For example, most SMOTE-based methods select a center observation and a random observation within its k-nearest neighbors belonging to the same class, while the Mixup method selects two random observations, regardless of their class membership.

The observation-based linear extrapolation mechanism modifies Equation 2.6 such that $x^s = x_i + \lambda(x_i - x_j)$, while the hard extrapolation mechanism uses the mean of a class' observations, μ^c and a randomly selected observation to generate $x^s = x_i^c + \lambda(x_i^c - \mu^c)$. Some methods also combine both interpolation and extrapolation. This can be achieved using Equation 2.6 and modifying λ's range to either decreasing its minimum value below zero or increasing its maximum value above one.

The difference transform mechanism uses two observations to compute a translation vector (multiplied by the scaling factor λ) and apply it on a third observation:

$$x^s = x_i + \lambda(x_j - x_k) \tag{2.7}$$

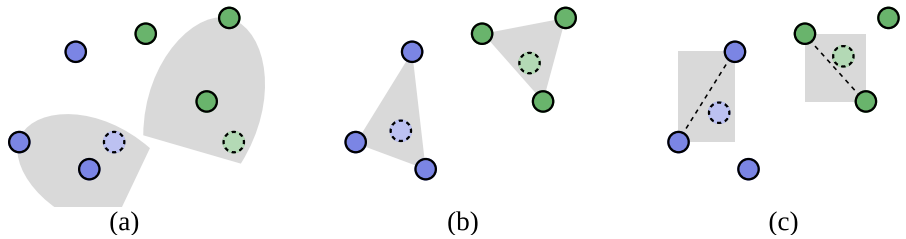

Figure 2.5.: Examples of geometric transformation mechanisms. Legend: (a) hypersphere mechanism, (b) triangular mechanism and (c) hyperrectangle mechanism.

Although there are various linear transformation mechanisms in the literature, the majority of the studies applied linear interpolation mechanisms. Within-class interpolation was frequently found in oversampling methods, while between-class interpolation was found most often in regularization methods. A depiction of the linear transformation mechanisms found in the literature are presented in Figure 2.4.

2.5.5. Geometric Transformations

Overall, geometric transformation mechanisms were not frequently found in the literature. They are primarily used to develop Mixup or SMOTE-based variants. Figure 2.5 shows a visual example of the related mechanisms.

The hypersphere mechanism generates data within a distorted, n-dimensional hyperspheroid. It is formed using an observation to define the center of the geometry and another to define its edge. It is defined with two hyperparameters, the deformation factor, $\alpha_{def} \in [0, 1]$, and the truncation factor, $\alpha_{trunc} \in [-1, 1]$. The deformation factor deforms the hypersphere into an elliptic shape, where $\alpha_{def} = 1$ applies no deformation and $\alpha_{def} = 0$ creates a line segment. The truncation factor limits the generation area of the hyperspheroid within a subset of the hypersphere, where $\alpha_{trunc} = 0$ applies no truncation, $\alpha_{trunc} = 1$ uses the half of the area between the two selected observations and $\alpha_{trunc} = -1$ uses the opposing area. In Figure 2.5a, the two generation areas were formed using approximately $\alpha_{trunc} = \alpha_{def} = 0.5$.

The triangular mechanism selects three observations to generate $x^s = \lambda_i x_i + \lambda_j x_j + (1 - \lambda_i - \lambda_j)x_k$, where $\lambda_i, \lambda_j \sim \mathcal{U}(0, \alpha)$, $\alpha \in (0, 0.5]$. The hyperrectangle mechanism uses an approach similar similar to Equation 2.6. However, the scaling factor is changed into a scaling vector, $\Lambda = [\lambda_1, \ldots, \lambda_d] \in [0, 1]^d, \lambda_i \sim$ Beta(α, α), where α is a hyperparameter used to define the Beta distribution. A synthetic observation is generated with $x^s = \Lambda \odot x_i + (1 - \Lambda) \odot x_j$, where $\odot$ denotes the Hadamard product. This operation originates a generation area like the ones presented in Figure 2.5c.

2.5.6. Neural Networks

Generative Adversarial Network (GAN) architectures are structured as a minimax two-player game composed of two models, a generator and a discriminator. Both models are trained simultaneously throughout the learning phase, to learn to generate data with similar statistical properties when compared to the original data. The generative model captures the data distribution, while the discriminator estimates the probability of an observation coming from the training data. The goal of the generator model is to produce synthetic observations that are capable of fooling the discriminator, making it difficult for the discriminator to distinguish real from synthetic observations. Although they were originally developed in an unsupervised learning setting [193], subsequent contributions proposed GANs with several different architectures, for semi-SL, supervised learning (for both regularization and oversampling) and reinforcement learning.

An autoencoder (AE) is a type of neural network architecture that learns manifold representations of an input space. These models are typically trained by regenerating the input and are designed with a bottleneck in the hidden layers that corresponds to the learned latent space. It contains two parts, an encoder and a decoder. The encoder transforms the input data into lower-dimensional representations (*i.e.*, the latent space), while the decoder projects these representations into the original input space. Since it was first proposed [194], many variants were developed for multiple applications. However, based on the literature found, the variational AE architecture appears to be the most popular approach.

2.6. Evaluating the Quality of Synthetic Data

The vast majority of synthetic data generation models are evaluated on a ML utility basis. Compared to research on the development of actual synthetic data generation algorithms, there is a general lack of research on the development of metrics to evaluate their quality beyond performance metrics such as Overall Accuracy (OA) or F1-score. One motivation to do this is the ability to anticipate the quality of the data for the target task before training a ML classifier, which may be expensive and time-consuming. This is a challenging problem, since the usefulness of synthetic data generators depend on the assumptions imposed according to the dataset, domain and ML problem [73]. This section focuses on the main evaluation approaches found in the literature beyond classification performance, as well as recently proposed methods. For a more comprehensive analysis of performance metrics for synthetic data evaluation, the reader is referred to [195] and [72].

The GANBLR model [142] was evaluated on three aspects: (1) ML utility, (2) Statistical similarity, and (3) Interpretability. In Xu et al. [144], the authors evaluate the CTGAN and TVAE models using a likelihood fitness metric (to measure statistical similarity) and ML efficacy (*i.e.*, utility). Hittmeir et al. [196] evaluate synthetic data generators using a 2-step approach: Similarity comparison and data utility. According to Alaa et al. [74], the evaluation of generative models should quantify three key aspects of synthetic data:

1. Fidelity. The synthetic observations must resemble real observations;
2. Diversity. The synthetic observations should cover $\mathcal{D}$'s variability;
3. Generalization. The synthetic observations should not be copies of real observations;

Ensuring these properties are met will secure the objectives defined in Section 2.2.2: $\mathbb{P}^s \approx \mathbb{P}$ and $x_i \neq x_j \forall x_i \in \mathcal{D} \wedge x_j \in \mathcal{D}^s$.

The effective evaluation of synthetic data generation methods is a complex task. A good performance with respect to one evaluation method does not necessarily imply a good performance on the primary ML task, results from different evaluation methods seem to be independent, and evaluating the models directly onto the target application is generally recommended [72]. Therefore, each evaluation procedure must be carefully implemented and adapted according to the use case.

2.6.1. Quantitative approaches

The Kullback-Leibler (KL) divergence (and equivalently the log-likelihood) is a common approach to evaluate generative models [72]. Other commonly used metrics, like Parzen window estimates, appear to be a generally poor quality estimation method and are not recommended for most applications [72]. KL divergence is defined as follows:

$$D_{KL}(P||Q) = \sum_{x \in \mathcal{X}} P(x) \log \frac{P(x)}{Q(x)} \tag{2.8}$$

Where $\mathcal{X}$ is a probability space, P and Q are estimated probability distributions based on $\mathbb{P}$ and $\mathbb{P}^s$, respectively. The KL divergence is a non symmetric measurement that represents how a reference probability distribution (P) differs from another (Q). A D_{KL} close to zero means Q is similar to P. However, metrics like the KL divergence or the log-likelihood are generally difficult to interpret, do not scale well for high dimensional data and fail to highlight model failures [74]. Another related metric, used in [197], is the Jensen-Shannon (JS) divergence. It consists of a symmetrized and smoothed variation of the KL divergence. Having $M = \frac{P+Q}{2}$, it is calculated as:

$$D_{JS}(P||Q) = \frac{D_{KL}(P||M) + D_{KL}(Q||M)}{2} \tag{2.9}$$

The Wasserstein Distance is another relevant metric to estimate the distance between two distribution functions. It was also used to develop GAN variants since it improves the stability in the training of GANs [198, 199].

In past literature, the propensity score was considered an appropriate performance metric to measure the utility of masked data [200]. This metric is estimated using a classifier (typically a logistic regression) trained on a dataset with both the original and synthetic data, using as target the source of each observation (synthetic or original). The goal of this classifier is to predict the likelihood of an observation to be synthetic. Therefore, this approach guarantees observation-level insights regarding the faithfulness of each observation. Woo et al. [200] suggest a summarization of this metric, also defined as the propensity Mean Squared Error (pMSE) [73]:

$$U_p = pMSE = \frac{1}{N} \sum_{i=1}^{N} (\hat{p}_i - c)^2 \tag{2.10}$$

Where $N = |\mathcal{D} \cup \mathcal{D}^s|$, $c = \frac{|\mathcal{D}^s|}{N}$ and $\hat{p}_i$ is the estimated propensity score for observation i. When a synthetic dataset is indistinguishable from real data, $pMSE$ will be close to zero. Specifically, when the data source is indistinguishable, the expected pMSE is given by [201]:

$$E(pMSE) = \frac{(k-1)(1-c)^2 c}{N} \tag{2.11}$$

Where k is the number of parameters in the logistic regression model (including bias). When the synthetic dataset is easily distinguishable from the original dataset, U_p will be close to $(1-c)^2$. Dankar et al. [90], established a generally consistent, weak negative correlation between U_p and OA.

Chundawat et al. [73] proposed TabSynDex to address the lack of uniformity of synthetic data evaluation, which can also be used as a loss function to train network-based models. It is a single metric evaluation approach bounded within $[0, 1]$ that consists of a combination between (1) the relative errors of basic statistics (mean, median and standard deviation), (2) the relative errors of correlation matrices, (3) a pMSE-based index, (4) a support coverage-based metric for histogram comparison and (5) the performance difference in a ML efficacy-based metric between models trained on real and synthetic data.

The three-dimensional metric proposed by Alaa et al. [74] presents an alternative evaluation approach. It combines three metrics (α-Precision, β-Recall and Authenticity) for various application domains. It extends the Precision and Recall metrics defined in [202] into α-Precision and β-Recall, which are used to quantify fidelity and diversity. Finally, the authenticity metric is estimated using a classifier that is trained

based on the distance (denoted as d) between x^s and its nearest neighbor in $\mathcal{D}$, x_{i^*}; if $d(x^s, x_{i^*})$ is smaller than the distance between x_{i^*} and its nearest neighbor in $\mathcal{D}\backslash\{x_{i^*}\}$, x^s will likely be considered unauthentic. This approach provides a three fold perspective over the quality of $\mathcal{D}^s$ and allows a sample-level analysis of the generator's performance. Furthermore, there is a relative trade-off between the two metrics used to audit the generator and the synthetic data; a higher α-Precision score will generally correspond to a lower Authenticity score and vice versa.

A less common evaluation approach is to attempt to replicate the results of studies using synthetic data [203, 204, 205]. Another method is the computation of the average distance among synthetic observations and their nearest neighbors within the original dataset [196]. The Confidence Interval Overlap and Average Percentage Overlap metrics may be used to evaluate synthetic data specifically for regression problems [206, 207].

2.6.2. Qualitative approaches

One of the qualitative approaches found in the literature is the comparison of the features' distributions with synthetic data and the original data using histogram plots [196]. This comparison can be complemented with the quantification of these distribution differences [203]. A complementary approach is the comparison of correlation matrices via heat map plots [196].

Another way to assess the quality of synthetic data is the subjective assessment by domain experts [203]. The goal of such test is to understand whether domain experts are able to distinguish synthetic from real data, which could be quantified with classification performance metrics. A low classification performance implies synthetic data that is difficult to distinguish from real data.

2.7. Discussion

The generation of tabular and latent space synthetic data has applications in multiple ML tasks and domains. Specifically, we found six areas that were shown to benefit from synthetic data: data privacy, regularization, oversampling, active learning, semi-supervised learning and self-supervised learning. Synthetic data may be used either as an accessory task to improve a ML model's performance over a primary task (*e.g.*, regularization and oversampling), an intermediate task (*e.g.*, feature extraction), or as a final product itself (*e.g.*, data anonymization). The analysis of data generation algorithms for each relevant learning problem led to the proposal of a general purpose taxonomy primarily focused on the underlying mechanisms used for data generation. We characterized every algorithm discussed in this work into four categories: (1) architecture, (2) application level, (3) data space and (4) scope. The successful implementation of synthetic data generation generally requires a few considerations:

1. Ensuring the dataset's features are comprised within similar, fixed boundaries. For example, any method using a neighbors-based approach will rely on distance measurements (typically the euclidean distance), which is sensitive to the scale of the data and a nearest-neighbors estimation may vary depending on whether the data was scaled *a priori*. This can be achieved with data scaling.

2. Various generation mechanisms require a manifold. There are two approaches to address non-manifold input data: (1) Adopt methods sensitive to the presence of non-metric features, or (2) project the input data into a manifold (*i.e.*, a latent space).

3. The smoothness assumption is prevalent in linear and perturbation-based data generation mechanisms. If a classification problem has low class separation and difficult to solve, the choice in the design of the generator algorithm is also difficult. Generally, generation algorithm with a global scope might adapt better to classification problems with low separability. On the other hand, problems

with higher separability might require a definition of more uniform decision boundaries to prevent overfitting, which can be achieved with generation algorithms with a local scope.

4. Considering the trade-off between performance and computational power. It is generally understood that computationally-intensive approaches tend to produce synthetic data with higher quality. When trained properly, neural network mechanisms typically lead to synthetic data that is more difficult to distinguish compared to the remaining approaches. Geometric mechanisms have also achieved good results but often require a careful tuning of their hyperparameters. Linear and perturbation mechanisms do not require much training and use less hyperparameters, but have been know for often producing low diversity synthetic data (*vis a vis* the original dataset).

This work focused primarily on the mechanisms used to generate synthetic observations; preprocessing, learning phase design, latent space learning and ML task-specific contributions were secondary objectives for analysis. Consequently, understanding of how the constraints within each task condition the choice and design of the synthetic data generator is a subject of future work.

Throughout the analysis of the literature, we identified six types of generation mechanisms and discuss more specific methods used in classical and state-of-the-art techniques. Techniques for data privacy via synthetic data rely primarily on perturbation mechanisms, PDFs, PGMs and Neural networks. Regularization approaches frequently employ Linear mechanisms. Other less commonly used mechanisms are PGMs, Neural network approaches, geometric and perturbation mechanisms. Various Oversampling algorithms have been proposed using each of the mechanisms found. However, the most prevalent mechanisms used were linear-based. AL methods rarely employ synthetic data. The few studies found employ primarily linear and geometric mechanisms, and a minority used AE models for latent space augmentation. Most Semi-SL methods used perturbation and linear mechanisms, while geometric mechanisms are rarely used. All tabular Self-SL methods used perturbation mechanisms.

Designing an approach to measure the quality of synthetic data depends on the target ML problem. A wholistic evaluation approach for synthetic data should consider the analysis of (1) ML utility, (2) Statistical similarity, (3) interpretability. The analysis of statistical similarity can be further divided into (1) fidelity, (2) diversity and (3) generalization. However, balancing the analysis between these three perspectives is not a straightforward task. For example, duplicating a dataset to form a synthetic dataset will result into the best possible fidelity and diversity, but bad generalization. Overall, there is a paucity of research into the development of comprehensive analyses of synthetic data, as well as understanding the balance between the different types of analyses.

2.8. Future Work

As discussed throughout our analysis, it appears the synthetic data generation research is generally isolated within ML problems and/or domains, even though all of these areas integrate synthetic data in its core. Given the breadth and complexity of input-level and latent-level data generation mechanisms, it is increasingly important to find an *a priori* approach to efficiently determine appropriate data generation policies and techniques. However, the complexity of this task is determined by various factors: different data types, ML problems, model architectures, computational resources, performance metrics and contextual constraints. Auto-augmentation and meta learning aim to address this challenge and are still subject to active research.

It is understood that, if learned properly, the latent space is expected to be convex and isotropic. In that case, using linear generation techniques in the latent space would produce synthetic data without introducing noise [139]. However, it is unclear which types of model/architectures and training procedures contribute to the learning of a good latent space according to the context. Furthermore, we found a limited amount of research on tabular data augmentation using auto-encoder architectures. Although

there are studies performing data augmentation on tabular data in various domains [145], defining the architecture and learning phase of an AE is not an intuitive task. Generally, autoencoders are used to learn a manifold for more complex data types. As long as the method used to generate the latent space is appropriate, the methods discussed in this study could be used in the latent space regardless of the type of data.

The quality of synthetic data generation in high-dimensional scenarios appears as a prevailing limitation in various applications, especially within linear and geometric mechanisms. This limitation can be addressed with dimensionality reduction techniques, as well as latent space learning. However, research on data generation in the latent space is mostly focused on GAN architectures, which require significant computational power. Other methods to learn manifold latent spaces could be explored to address this limitation.

It remains an open question which generation mechanisms, or types of mechanisms, create better synthetic data [139]. Although there is not necessarily a one-size-fits-all solution, a general set of rules of thumb could be explored, such as understanding how certain characteristics of a problem will affect the choice of the generation policy, which types of mechanisms are more appropriate for different types of dataset, ML model architecture, domains and target ML problem, or the trade-offs between the different types of generation mechanism. A better understanding of the relationship between recently proposed methods for evaluating synthetic data (as discussed in Section 2.6) and the performance on the target ML problem might contribute to answer this question. Furthermore, determining the use cases, quality and general performance of data generation on the input, latent and output space should be further developed. Finally, it still unclear why synthetic data generation works for each of the ML tasks discussed. Research on this topic lacks depth and fails to address the theoretical underpinnings [69, 208].

The evaluation of anonymization techniques lack standardized, objective and reliable performance metrics and benchmark datasets to allow an easier comparison across classifiers to evaluate key aspects of data anonymization (resemblance, utility, privacy and performance). These datasets should contain mixed data types (*i.e.*, a combination of categorical, ordinal, continuous and discrete features) and the metrics should evaluate the performance of different data mining tasks along with the anonymization reliability. This problem appears to be universal across domains. For example, Hernandez et al. [76] observed the lack of a universal method or metric to report the performance synthetic data generation algorithms for tabular health records. Therefore, in order to facilitate the usage of these techniques in industry domains, these benchmarks must also be realistic. Rosenblatt et al. [102] attempts to address this problem by proposing a standardized evaluation methodology using standard datasets and real-world industry applications.

Unlike data privacy solutions, studies on data augmentation techniques generally do not consider the similarity/dissimilarity of synthetic data. The study of quality metrics for supervised learning may reduce computational overhead and experimentation time. Only one study related to the relationship of quality metrics and performance in the primary ML task was found in [90], which was done only for the pMSE metric.

Neural network mechanisms typically involve a higher computational cost compared to the remaining types of mechanisms. This problem is further aggravated with their inconsistent performance, since different initializations may result in very different performances. This problem may be observed in [128]. More generally, latent space representations of training data raises the challenge of interpretability; the ability to interpret latent space representations could guide the design of data generation techniques.

In non-tabular data domains, a common approach for data augmentation is the combination of several data augmentation methods to increase the diversification of synthetic data. This is true for both text classification [79] and image classification [12]. However, for tabular data, no studies were found that discuss the potential of ensembles of generation mechanisms on tabular data, *i.e.*, understanding how selecting with different probabilities different generation mechanisms to generate synthetic data would affect the performance of the primary ML task. The formalization and analysis carried out in this work,

regarding the different types of synthetic data generation mechanisms and quality metrics for latent and tabular synthetic data at an observation level, may facilitate this work.

Various oversampling methods have been proposed to address imbalanced learning limitations. However, there is still a major limitation in the literature regarding the oversampling of datasets with mixed data types or with exclusively non metric features at the input space. In addition, the research on oversampling using PDFs or PGMs is scarce.

To the best of our knowledge, research on few-shot learning for tabular data is scarce. Few-shot learning research using synthetic data generation techniques has been extensively developed using image [209, 210] and text data [211], but they are rarely adapted or tested for tabular data. One of the few studies found achieved a good performance in both few-shot and zero-shot learning through the adaptation of a Large Language model for tabular data [212].

Oversampling does not seem to be a relevant source of bias in behavioral research and does not appear to have an appreciably different effect on results for directly versus indirectly oversampled variables [213]. However, most oversampling methods do not account for the training dataset's distribution, which is especially important for features with sensitive information (*e.g.*, gender or ethnicity). Therefore, the application of oversampling methods on user data may further increase the bias in classification between gender or ethnicity groups.

Finally, various synthetic data generation algorithms are research-based, and might not be usable or feasible to be implemented by practitioners [79]. One way to address this problem is to publish the code developed, and ideally make them available as open source libraries for out-of-the-box usage.

2.9. Conclusions

This literature review analyses various synthetic data generation-based algorithms for tabular data, with a focus on external level applications. Since synthetic data generation is a crucial step for various ML applications and domains, it is essential to understand and compare which techniques and types of algorithms are used for each of these problems. The usage of synthetic data is an effective approach to better prepare datasets and ML pipelines for a wide range of applications and/or address privacy concerns. Our work proposed a taxonomy based on four key characteristics of generation algorithms, which was used to characterize 70 data generation algorithms across six ML problems. This analysis resulted in the categorization and description of the generation mechanisms underlying each of the selected algorithms into six main categories. Finally, we discussed several techniques to evaluate synthetic data, as well as general recommendations and research gaps based on the insights collected throughout the analysis of the literature.

Despite the extensive research developed on various different methods for synthetic data generation, there are still open questions regarding the theoretical underpinnings of synthetic data adoption for each of the techniques, as well as limitations in the different types of generation mechanisms and evaluation procedures. However, the empirical work presented in the literature show significant performance improvements and promising research directions for future work.

3. Improving Imbalanced Land Cover Classification with K-means SMOTE: Detecting and Oversampling Distinctive Minority Spectral Signatures

Published as Joao Fonseca, Georgios Douzas, Fernando Bacao, in Information Journal, 2021

Land cover maps are a critical tool to support informed policy development, planning, and resource management decisions. With significant upsides, the automatic production of Land Use/Land Cover maps has been a topic of interest for the remote sensing community for several years, but it is still fraught with technical challenges. One such challenge is the imbalanced nature of most remotely sensed data. The asymmetric class distribution impacts negatively the performance of classifiers and adds a new source of error to the production of these maps. In this paper, we address the imbalanced learning problem, by using K-means and the Synthetic Minority Oversampling TEchnique (SMOTE) as an improved oversampling algorithm. K-Means SMOTE improves the quality of newly created artificial data by addressing both the between-class imbalance, as traditional oversamplers do, but also the within-class imbalance, avoiding the generation of noisy data while effectively overcoming data imbalance. The performance of K-means SMOTE is compared to three popular oversampling methods (Random Oversampling, SMOTE and Borderline-SMOTE) using seven remote sensing benchmark datasets, three classifiers (Logistic Regression, K-Nearest Neighbors and Random Forest Classifier) and three evaluation metrics using a 5-fold cross-validation approach with 3 different initialization seeds. The statistical analysis of the results show that the proposed method consistently outperforms the remaining oversamplers producing higher quality land cover classifications. These results suggest that LULC data can benefit significantly from the use of more sophisticated oversamplers as spectral signatures for the same class can vary according to geographical distribution.

Keywords: LULC Classification; Imbalanced Learning; Oversampling; Data Augmentation; Clustering

3.1. Introduction

The increasing amount of remote sensing missions granted the access to dense time series (TS) data at a global level and provides up-to-date, accurate land cover information [214]. This information is often materialized through Land Use and Land Cover (LULC) maps. While Land Cover maps define the biophysical cover found on the surface of the earth, Land Use maps define how it is used by humans [215]. Both Land Use and Land Cover maps constitute an essential asset for various purposes, such as land cover change detection, urban planning, environmental monitoring and natural hazard assessment [1]. However, the timely production of accurate and updated LULC maps is still a challenge within the remote sensing

community [216]. LULC maps are produced based on two main approaches: photo-interpreted by the human eye, or automatic mapping using remotely sensed data and classification algorithms.

While photo-interpreted LULC maps rely on human operators and can be more reliable, they also present some significant disadvantages. The most important disadvantage is the cost of production, in fact photo-interpretation consumes significant resources, both in terms of money and time. Because of that, they are not frequently updated and not suitable for operational mapping over large areas. Finally, there is also the issue of overlooking rare or small-area classes, due to factors such as the minimum mapping unit being used.

Automatic mapping with classification algorithms based on machine-learning (ML) have been extensively researched and used to speed up and reduce the costs of the production process [1, 217, 218]. Improvements in classification algorithms are sure to have significant impact in the efficiency with which remote sensing imagery is used. Several challenges have been identified in order to improve automatic classification:

1. Improve the ability to handle high-dimensional datasets, in cases such as Multi-spectral TS composites high-dimensionality increases the complexity of the problem and creates a strain on computational power [5].
2. Improve class separability, as the production of an accurate LULC map can be hindered by the existence of classes with similar spectral signatures, making these classes difficult to distinguish [6].
3. Resilience to mislabelled LULC patches, as the use of photo-interpreted training data poses a threat to the quality of any LULC map produced with this strategy, since factors such as the minimum mapping unit tend to cause the overlooking of small-area LULC patches and generates noisy training data that may reduce the prediction accuracy of a classifier [4].
4. Dealing with rare land cover classes, due to the varying levels of area coverage for each class. In this case using a purely random sampling strategy will amount to a dataset with a roughly proportional class distribution as the one on the multi/hyperspectral image. On the other hand, the acquisition of training datasets containing balanced class frequencies is often unfeasible. This causes an asymmetry in class distribution, where some classes are frequent in the training dataset, while others have little expression [219, 220].

The latter challenge is known, in machine learning, as the imbalanced learning problem [221]. It is defined as a skewed distribution of instances found in a dataset among classes in both binary and multi-class problems [222]. This asymmetry in class distribution negatively impacts the performance of classifiers, especially in multi-class problems. The problem comes from the fact that during the learning phase, classifiers are optimized to maximize an objective function, with overall accuracy being the most common one [223]. This means that instances belonging to minority classes contribute less to the optimization process, translating into a bias towards majority classes. As an example, a trivial classifier can achieve 99% overall accuracy on a binary dataset where 1% of the instances belong to the minority class if it classifies all instances as belonging to the majority class. This is an especially significant issue in the automatic classification of LULC maps, as the distribution of the different land-use classes tends to be highly imbalanced. Therefore, improvements in the ability to deal with imbalanced datasets will translate into important progress in the automatic classification of LULC maps.

There are three different types of approaches to deal with the class imbalance problem [9, 218]:

1. Cost-sensitive solutions. Introduces a cost matrix to the learning phase with misclassification costs attributed to each class. Minority classes will have a higher cost than majority classes, forcing the algorithm to be more flexible and adapt better to predict minority classes.
2. Algorithmic level solutions. Specific classifiers are modified to reinforce the learning on minority classes. Consists on the creation or adaptation of classifiers.

3. Resampling solutions. Rebalances the dataset's class distribution by removing majority class instances and/or generating artificial minority instances. This can be seen as an external approach, where the intervention occurs before the learning phase, benefitting from versatility and independency from the classifier used.

Since resampling strategies represent a set of methods that are detached from classifiers by operating at the data level, they allow the use of any off the shelf algorithm, without the need for any type of changes or adaptions to the algorithm. Specifically, in the case of oversampling (defined below), the user is able to balance the dataset's class distribution by without the loss of information, which is not the case with undersampling techniques. This is a significant advantage especially considering that most users in remote sensing are not expert machine learning engineers.

Within resampling approaches there are three subgroups of approaches [9, 218, 224]:

1. Undersampling methods, which rebalance class distribution by removing instances from the majority classes.
2. Oversampling methods, which rebalance datasets by generating new artificial instances belonging to the minority classes.
3. Hybrid methods, which are a combination of both oversampling and undersampling, resulting in the removal of instances in the majority classes and the generation of artificial instances in the minority classes.

Resampling methods can be further distinguished between non-informed and heuristic (i.e., informed) resampling techniques [9, 224, 225]. The former consist of methods that duplicate/remove a random selection of data points to set class distributions to user-specified levels, and are therefore a simpler approach to the problem. The latter consists of more sophisticated approaches that aim to perform over/undersampling based on the points' contextual information within their data space.

The imbalanced learning problem is not new in machine learning but its relevancy has been growing, as attested by [226]. The problem has also been addressed in the context of remote sensing [2]. In this paper, we propose the application of a recent oversampler based on SMOTE [22], the K-means SMOTE [25] oversampler, to address the imbalanced learning problem in a multiclass context for LULC classification using various remote sensing datasets. Specifically, we use seven land use datasets commonly used in research literature, that vary among agricultural and urban land use. The K-means SMOTE algorithm couples two different procedures in the generation of artificial data. The algorithm starts by grouping the instances into clusters by using the K-means algorithm; next, the generation of the artificial data is done using the smote algorithm, taking into consideration the distribution of majority/minority cases in each individual cluster. The idea of starting with a clustering procedure before the data generation phase is important in remote sensing because the spectral signature of the different classes can change significantly based on the geographical area in which it is represented. In other words, the spectral signature of a specific class can vary greatly depending on the geography, meaning that often we will be facing within-class imbalance [227].

In fact, we can decompose class imbalance into two different types: between-class imbalance and within-class imbalance [25, 228]. While the first refers to the overall asymmetry between majority and minority classes, the second results from the fact that in different areas of the input space there might be different levels of imbalance. Depending on the complexity of the input space, different subclusters of minority and majority instances may be present. In order to achieve a balance between minority and majority instances, these subclusters should be treated separately. Assuming that the role of a classifier is to create rules in such a way that it is able to isolate the different relevant sub-concepts that represent both the majority and minority classes, the classifier will create multiple disjunct rules that describe these concepts. If the input space is simple and the classes' instances are grouped together in a unique cluster, the classifier will only need to create (general) rules that comprise large portions of instances belonging to the same class.

To the contrary, if the input space is complex and scatters through multiple small clusters, the classifier will need to learn a more complex set of (specific) rules, which can be seen in Figure 3.1. It is important to note that small clusters can happen both in the minority and majority class, although they will tend to be more frequent in the minority class due to its underrepresentation.

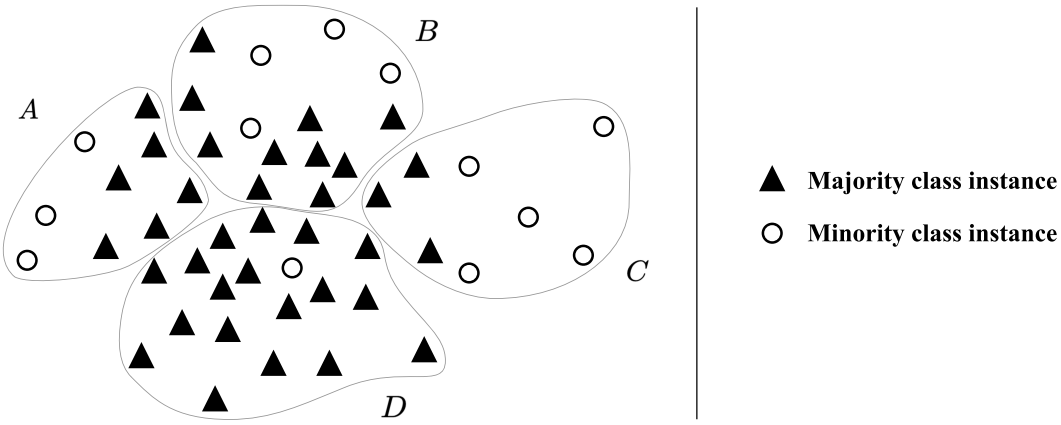

Figure 3.1.: Example of a complex input space. In this example, a classifier would need to separate the minority class' samples across 4 distinguishable clusters (A, B, C and D).

The efficacy of K-means SMOTE is tested using different types of classifiers. To do so, we employ both commonly used and/or state-of-the-art oversamplers as benchmarking methods: Random oversampling (ROS), SMOTE and Borderline-SMOTE (B-SMOTE) [24]. Also as a baseline score we include classification results without the use of any resampling method.

This paper is organized in 5 sections: section 3.2 provides an overview of the state-of-art, section 3.3 describes the proposed methodology, section 3.4 covers the results and discussion and section 3.5 presents the conclusions taken from this study.

This paper's main contributions are:

- Propose a cluster-based multiclass oversampling method appropriate for LULC classification and compare its performance with the remaining oversamplers in a multiclass context with seven benchmark LULC classification datasets. Allows us to check the oversamplers' performance across benchmark LULC datasets.
- Introducing a cluster-based oversampling algorithm within the remote sensing domain, as well as comparing its performance with the remaining oversamplers in a multiclass context.
- Make available to the remote sensing community the implementation of the algorithm in a Python library and the experiment's source code.

3.2. Imbalanced Learning Approaches

Imbalanced learning has been addressed in three different ways: over/undersampling, cost-sensitive training and changes/adaptations in the learning algorithms [218]. These approaches impact different phases of the learning process, while over/undersampling can be seen as a pre-processing step, cost-sensitive and changes in the algorithm imply a more customized and complex intervention in the algorithms. In this

section, we focus on previous work related with resampling methods, while providing a brief explanation of cost-sensitive and algorithmic level solutions.

All of the most common classifiers used for LULC classification tasks [1, 217] are sensitive to class imbalance [229]. Algorithm-based approaches typically focus on adaptations based on ensemble classification methods [230] or common non-ensemble based classifiers such as Support Vector Machines [231]. In [232], the reported results show that algorithm-based methods have comparable performance to resampling methods.

Cost-sensitive solutions refer to changes in the importance attributed to each instance through a cost matrix [233, 234, 235]. A relevant cost sensitive solution [233] uses the inverse class frequency (i.e., $1/|C_i|$, where C_i refers to the frequency of class i) to give higher weight to minority classes. Cui et al. [234] extended this method by adding a hyperparameter β to class weights as $(1-\beta)/(1-\beta^{|C_i|})$. When $\beta = 0$, no re-weighting is done. When $\beta \to 1$, weights are the inverse of the frequency class matrix. Another method [235] explores adaptations of Cross-entropy classification loss by adding different formulations of class rectification loss.

Resampling (over/undersampling) is the most common approach to imbalanced learning in machine learning in general and remote sensing in particular [220]. The generation of artificial instances (i.e., augmenting the dataset), based on rare instances, is done independently of any other step in the learning process. Once the procedure is applied, any standard machine learning algorithm can be used. Its simplicity makes resampling strategies particularly appealing for any user (especially the non-sophisticated user) interested in applying several classifiers, while maintaining a simple approach. It is also important to notice that over/undersampling methods can also be easily applied to multiclass problems, common in LULC classification tasks.

3.2.1. Non-informed resampling methods

There are two main non-informed resampling methods. Random Oversampling (ROS) generates artificial instances through random duplication of minority class instances. This method is used in remote sensing for its simplicity [236, 237], even though its mechanism makes the classifier prone to overfitting [238]. [237] found that using ROS returned worse results than keeping the original imbalance in their dataset.

A few of the recent remote sensing studies employed Random Undersampling (RUS) [239], which randomly removes instances belonging to majority classes. Although it's not as prone to overfitting as ROS, it incurs into information loss by eliminating instances from the majority class [220], which can be detrimental to the quality of the results.

Another disadvantage of non-informed resampling methods is their performance-wise inconsistency across classifiers. ROS' impact on the Indian Pines dataset was found inconsistent between Random Forest Classifiers (RFC) and Support Vector Machines (SVM) and lowered the predictive power of an artificial neural network (ANN) [223]. Similarly, RUS is found to generally lead to a lower overall accuracy due to the associated information loss [223].

3.2.2. Heuristic methods

The methods presented in this section appear as a means to overcome the insufficiencies found in non-informed resampling. They use either local or global information to generate new, relevant, non-duplicated instances to populate the minority classes and/or remove irrelevant instances from majority classes. In a comparative analysis between over- and undersamplers' performance for LULC classification [7] using the rotation forest ensemble classifier, authors found that oversampling methods consistently outperform undersampling methods. This result led us to exclude undersampling from our study.

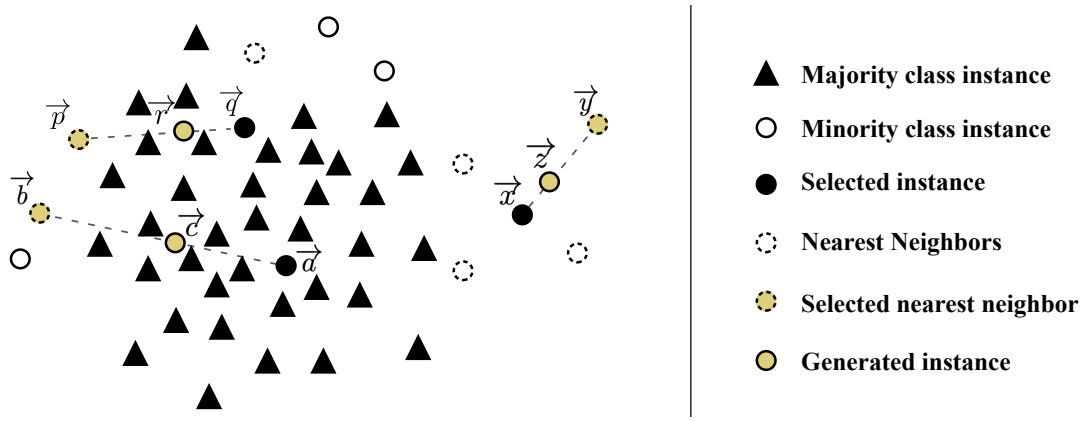

Figure 3.2.: Example of SMOTE's data generation process. SMOTE randomly selects instance $\vec{x}$ and randomly selects one of its k-nearest neighbors $\vec{y}$ to produce $\vec{z}$. Noisy instance $\vec{r}$ was generated by randomly selecting $\vec{q}$ and randomly selecting its nearest neighbor $\vec{p}$ from a different minority class cluster. Noisy instance $\vec{c}$ was generated by randomly selecting the noisy minority class instance $\vec{a}$ and one of its nearest neighbors $\vec{b}$.

SMOTE [22] was the first heuristic oversampling algorithm to be proposed and has been the most popular one since then, likely due to its fair degree of simplicity and quality of generated data. It takes a random minority class sample and introduces synthetic instances along the line segment that join a random k minority class nearest neighbor to the selected sample. Specifically, a single synthetic sample $\vec{z}$ is generated within the line segment of a randomly selected minority class instance $\vec{x}$ and one of its k nearest neighbors $\vec{y}$ such that $\vec{z} = \alpha\vec{x} + (1-\alpha)\vec{y}$, where α is a random real number between 0 and 1, as shown in Figure 3.2.

A number of studies implement SMOTE within the LULC classification context and reported improvements on the quality of the trained predictors [240, 241]. Another study proposes an adaptation of SMOTE on an algorithmic level for deep learning applications [242]. This method combines both typical computer vision data augmentation techniques, such as image rotation, scaling and flipping on the generated instances to populate minority classes. Another algorithmic implementation is the variational semi-supervised learning model [243]. It consists of a generative model that allows learning from both labeled and unlabeled instances while using SMOTE to balance the data.

Despite SMOTE's popularity, its limitations have motivated the development of more sophisticated oversampling algorithms [23, 24, 244, 245, 25, 246]. [23] identify four major weaknesses of the SMOTE algorithm, which can be summarized as:

1. Generation of noisy instances due to random selection of a minority instance to oversample. The random selection of a minority instance makes SMOTE oversampling prone to the amplification of existing noisy data. This has been addressed by variants such as B-SMOTE [24] and ADASYN [246].
2. Generation of noisy instances due to the selection of the k nearest neighbors. In the event an instance (or a small number thereof) is not noisy but is isolated from the remaining clusters, known as the "small disjuncts problem" [247], much like sample $\vec{b}$ from Figure 3.2, the selection of any nearest neighbor of the same class will have a high likelihood of producing a noisy sample.
3. Generation of nearly duplicated instances. Whenever the linear interpolation is done between two instances that are close to each other, the generated instance becomes very similar to its parents and

increases the risk of overfitting. G-SMOTE [23] attempts to address both the k nearest neighbor selection mechanism problem as well as the generation of nearly duplicated instances problem.

4. Generation of noisy instances due to the use of instances from two different minority class clusters. Although an increased k could potentially avoid the previous problem, it can also lead to the generation of artificial data between different minority clusters, as depicted Figure 3.2 with the generation of point $\overrightarrow{r}$ using minority class instances $\overrightarrow{p}$ and $\overrightarrow{q}$. Cluster-based oversampling methods attempt to address this problem.

This last issue, the generation of noisy instances due to the existence of several minority class clusters, is particularly relevant in remote sensing. It is frequent that instances belonging to the same minority class can have different spectral signatures, meaning that they will be clustered in different parts of the input space. For example, in the classification of a hyperspectral scene dominated by agricultural activities, patches relating to urban areas may constitute a minority class. These patches frequently refer to different types of land use, such as housing regions, small gardens, asphalt roads, etc., all these containing different spectral signatures. In this context, the use of SMOTE will lead to the generation of noisy instances of the minority class. This problem can be efficiently mitigated through the use of a cluster-based oversampling method. According to our literature review cluster-based oversampling approaches have never been applied in the context of remote sensing. On the other hand, while there are references of the application of cluster-based oversampling in the context of machine learning [248, 245, 244, 25], the multiclass case is rarely addressed, which is a fundamental requirement for the application of oversampling in the context of LULC.

Cluster-based oversampling approaches introduce an additional layer to SMOTE's selection mechanism, which is done through the inclusion of a clustering process. This ensures that both between-class data balance and within-class balance is preserved. The self-organizing map oversampling (SOMO) [245] algorithm transforms the dataset into a 2-dimensional input, where the areas with the highest density of minority samples are identified. SMOTE is then used to oversample each of the identified areas separately. ClUstered REsampling SMOTE (CURE-SMOTE) [244] applies a hierarchical clustering algorithm to discard isolated minority instances before applying SMOTE. Although it avoids noise generation problems, it ignores within-class data distribution. Another method [248] uses K-means to cluster the entire input space and applies SMOTE to clusters with the fewest instances, regardless of their class label. The label of the generated instance is copied from one of its parents. This method cannot ensure a balanced dataset since class imbalance is not specifically addressed, but rather dataset imbalance.

K-means SMOTE [25] avoids noisy data generation by modifying the data selection mechanism. It employs k-means clustering to identify safe areas using cluster-specific Imbalance Ratio (IR, defined by $\frac{count(C_{majority})}{count(C_{minority})}$) and determine the quantity of generated samples per cluster based on a density measure. These samples are finally generated using the SMOTE algorithm. The K-means SMOTE's data generation process is depicted in Figure 3.3. Note that the number of samples generated for each cluster varies according to the sparsity of each cluster (the sparser the cluster is, the more samples will be generated) and a cluster is rejected if the cluster's IR surpasses the threshold. Therefore, this method can be combined with any data generation mechanism, such as G-SMOTE. Also K-means SMOTE includes the SMOTE algorithm as a special case when the number of clusters is set to one. Consequently, K-means SMOTE returns results as good as or better than SMOTE.

Although no other study was found to implement cluster-based oversampling, another study [2] compared the performance of SMOTE, ROS, ADASYN, B-SMOTE and G-SMOTE in a highly imbalanced LULC classification dataset. The authors found that G-SMOTE consistently outperformed the remaining oversampling algorithms regardless of the classifier used.

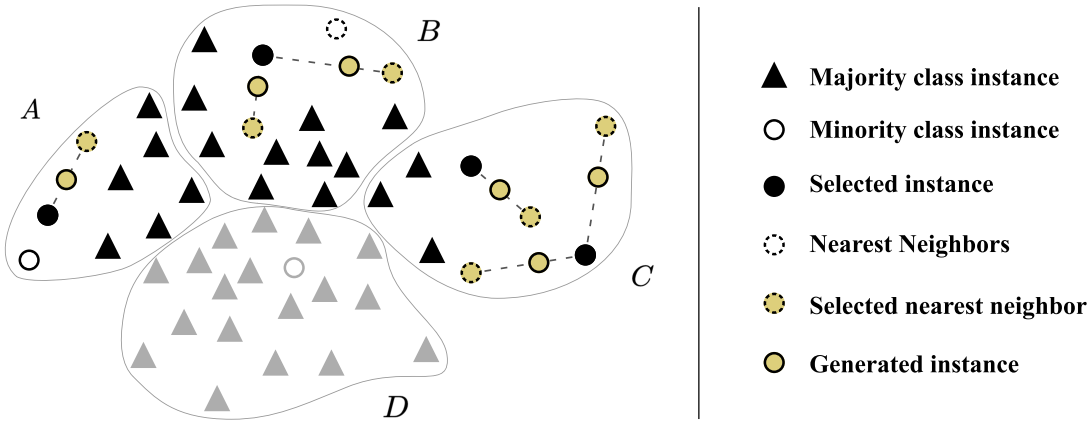

Figure 3.3.: Example of K-means SMOTE's data generation process. Clusters A, B and C are selected for oversampling, whereas cluster D was rejected due to its high imbalance ratio. The oversampling is done using the SMOTE algorithm and the k nearest neighbors selection only considers instances within the same cluster.

3.3. Methodology

The purpose of this work is to understand the performance of K-means SMOTE as opposed to other popular and/or state-of-the-art oversamplers for LULC classification. This is done using 7 datasets with predominantly land use information, along with 3 evaluation metrics and 3 classifiers to evaluate the performance of oversamplers. In this section we describe the datasets, evaluation metrics, oversamplers, classifiers and software used as well as the procedure developed.

3.3.1. Datasets

The datasets used were extracted from publicly available hyperspectral scenes. Information regarding each of these scenes is provided in this subsection. The data collection and preprocessing pipeline is shown in Figure 3.4 and is common to all hyperspectral scenes:

1. Data collection of publicly available hyperspectral scenes. The original hyperspectral scenes and ground truth data were collected from a single publicly available data repository available here.
2. Conversion of each hyperspectral scene to a structured dataset and removal of instances with no associated LULC class. This done to reshape the dataset from $(h, w, b + gt)$ into a conventional dataframe of shape $(h * w, b + gt)$, where gt, h, w and b represents the ground truth, height, width and number of bands in the scene, respectively. The pixels without ground truth information are discarded from further analysis.
3. Stratified random sampling to maintain similar class proportions on a sample of 10% of each dataset. This is done by computing the relative class frequencies in the original hyperspectral scene (minus the class representing no ground truth availability) and retrieving a sample that ensures the original relative class frequencies remain unchanged.
4. Removal of instances belonging to a class with frequency lower than 20 or higher than 1000. This is done to maintain the datasets to a practicable size due to computational constraints, while conserving the relative LULC class frequencies and data distribution.

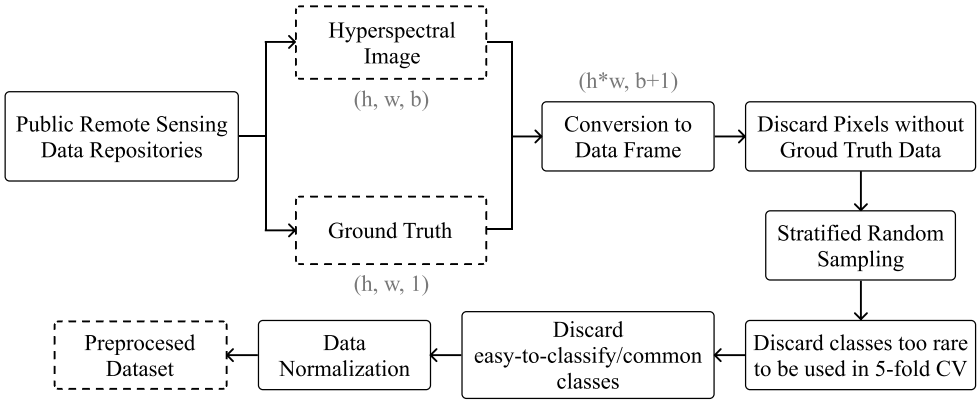

Figure 3.4.: Data collection and preprocessing pipeline.

Dataset	Features	Instances	Min. Instances	Maj. Instances	IR	Classes
Botswana	145	288	20	41	2.05	11
Pavia Centre	102	3898	278	879	3.16	7
Kennedy Space Center	176	497	23	80	3.48	11
Salinas A	224	535	37	166	4.49	6
Pavia University	103	2392	89	679	7.63	8
Salinas	224	4236	91	719	7.9	15
Indian Pines	220	984	21	236	11.24	11

Table 3.1.: Description of the datasets used for this experiment.

5. Data normalization using the MinMax scaler. This ensures all features (i.e., bands) are in the same scale. In this case, the data was rescaled between 0 and 1.

Table 3.1 provides a description of the final datasets used for this work, sorted according to its IR. Figure 3.5 shows the original hyperspectral scene out of which the dataset used in this experiment were extracted. In the representation of the ground truth of these scenes, the blue regions in the ground truth of each hyperspectral scene represent unlabeled regions (i.e., no ground truth is available). Particularly, in the Botswana and Kennedy Space Center scenes the truth was photointerpreted in more limited regions of the scene. However, the scenes are still represented as they are in order to maintain a standardized analysis over all datasets extracted for the experiment.

Botswana

The Botswana scene was acquired by the Hyperion sensor on the NASA EO-1 satellite over the Okavango Delta, Botswana in 2001-2004 at a 30m spatial resolution. Data preprocessing was performed by the UT Center for Space Research. The scene comprises a 1476×256 pixels with 145 bands and 14 classes regarding land cover types in seasonal and occasional swamps, as well as drier woodlands (see Figure 3.5a). The classes with rare instances are Short mopane and Hippo grass.

Pavia Center and University

Both Pavia Center and University scenes were acquired by the ROSIS sensor. These scenes are located in Pavia, northern Italy. Pavia Center is a 1096×1096 pixels image with 102 spectral bands, whereas Pavia

University is a 610×610 pixels image with 103 spectral bands. Both images have a geometrical resolution of 1.3m and their ground truths are composed of 9 classes each (see Figures 3.5b and 3.5c). After data preprocessing, the classes with rare instances are Asphalt and Bitumen (the class Shadows was removed for being too rare for cross validation after random sampling).

Kennedy Space Center

The Kennedy Space Center scene was acquired by the AVIRIS sensor over the Kennedy Space Center, Florida, on March 23, 1996. Out of the original 224 bands, water absorption and low SNR bands were removed and a total of 176 bands at a spatial resolution of 18m are used. The scene is a 512×614 pixel image and contains a total of 16 classes (see figure 3.5d). The classes with rare instances are hardwood swamp, slash pine and willow swamp (both hardwood swamp and slash pine were removed for being too rare for cross validation after random sampling).

Salinas and Salinas-A

These scenes were collected by the AVIRIS sensor over Salinas Valley, California and contain at-sensor radiance data. Salinas is a 512×217 pixels image with 224 bands and 16 classes regarding vegetables, bare soil and vineyard fields (see Figure 3.5e). Salinas-A, a subscene of Salinas, comprises 86×83 pixels and contains 6 classes regarding vegetables (see Figure 3.5f). These scenes have a geometrical resolution of 3.7m. Salinas-A's minority class has the label "Brocoli_green_weeds_1" and Salina's minority class has the label "Lettuce_romaine_6wk"

Indian Pines

The Indian Pines scene [249] was collected on June 12, 1992 and consists of AVIRIS hyperspectral image data covering the Indian Pine Test Site 3, located in North-western Indiana, USA. As a subset of a larger scene, it is composed of 145×145 pixels (see Figure 3.5g) and 220 spectral reflectance bands in the wavelength range 400 to 2500 nanometers at a spatial resolution of 20m. Approximately two thirds of this scene is composed by agriculture and the other third is composed of forest and other natural perennial vegetation. Additionally, the scene also contains low density buildup areas. The classes with rare instances are Alfalfa, Oats, Grass-pasture-mowed, Wheat and Stone-Steel-Towers (which removed for being too rare for cross validation after random sampling). After data preprocessing, the classes with rare instances are Corn, Buildings-Grass-Trees-Drives and Grass-Pasture.

3.3.2. Machine Learning Algorithms

To assess the quality of the K-means SMOTE algorithm, three other oversampling algorithms were used for benchmarking. ROS and SMOTE were chosen for their simplicity and popularity. B-SMOTE chosen as a popular variation of the SMOTE algorithm. We also include the classification results of no oversampling (NONE) as a baseline.

To assess the performance of each oversampler, we use the classifiers Logistic Regression (LR) [250], K-Nearest Neighbors (KNN) [251] and Random Forest (RF) [252]. This choice was based on the classifiers' popularity for LULC classification, learning type and training time [223, 217]. Since this is a multinomial classification task, for the LR classification we adopted a one-versus-all approach for each label. The predicted label is assigned according to the class predicted with highest probability.

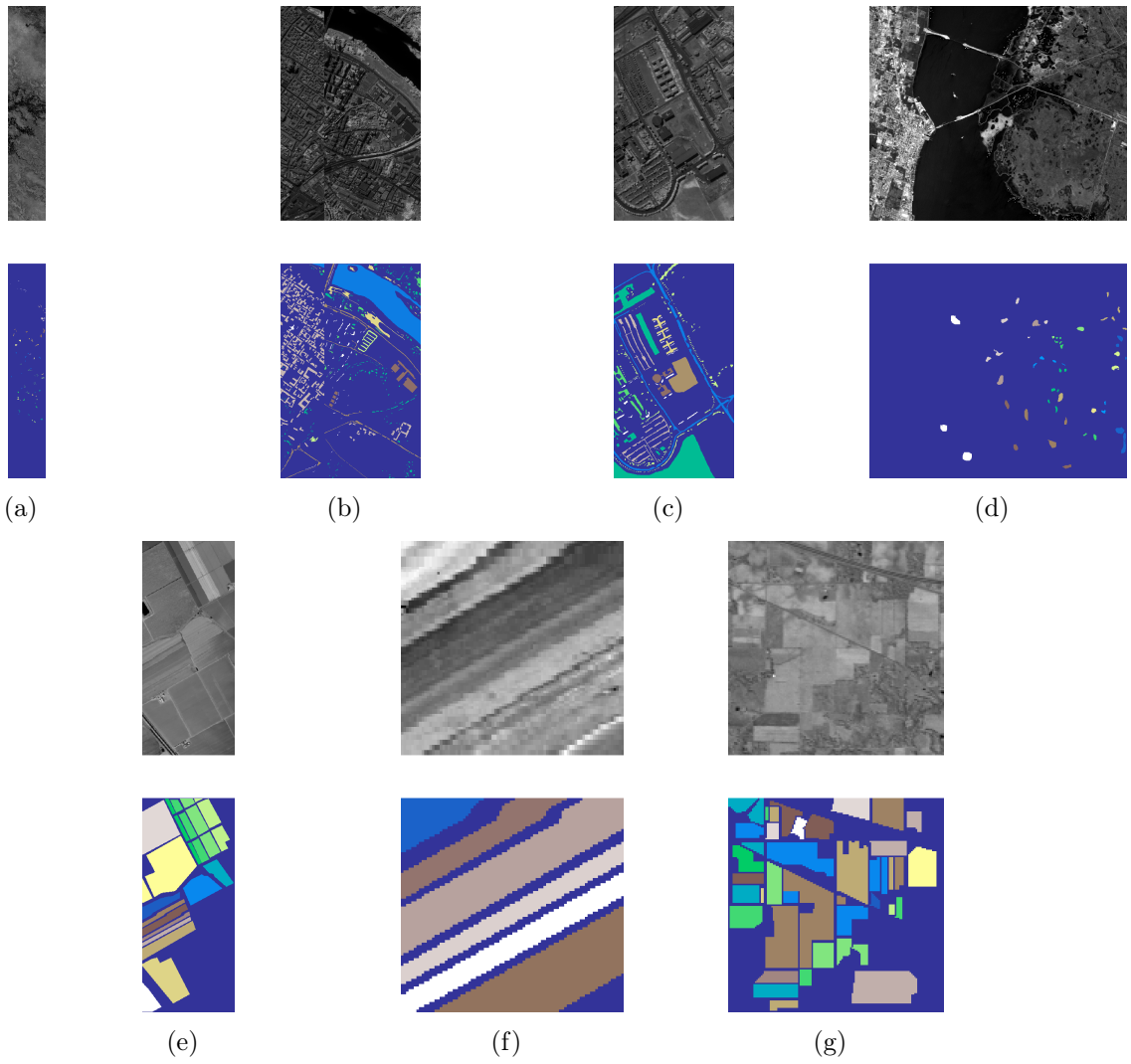

Figure 3.5.: Gray scale visualization of a band (top row) and ground truth (bottom row) of each scene used in this study. (a) Botswana, (b) Pavia Center, (c) Pavia University, (d) Kennedy Space Center, (e) Salinas, (f) Salinas A, (g) Indian Pines.

3.3.3. Evaluation Metrics

Most of the satellite-based LULC classification studies (nearly 80%) employ *Overall Accuracy* (OA) and the *Kappa Coefficient* [217]. Although, some authors argue that both evaluation metrics, even when used simultaneously, are insufficient to fully address the area estimation and uncertainty information needs [253, 254]. Other metrics like User's Accuracy (or *Precision*) and Producer's Accuracy (or *Recall*) are also common metrics to evaluate per-class prediction power. These metrics consist of ratios employing the True and False Positives (*TP* and *FP*, number of correctly/incorrectly classified instances of a given class) and True and False Negatives (*TN* and *FN*, number of correctly/incorrectly classified instances as not belonging to a given class). These metrics are formulated as $Precision = \frac{TP}{TP+FP}$ and $Recall = \frac{TP}{TP+FN}$. While metrics like OA and *Kappa Coefficient* are significantly affected by imbalanced class distributions, *F-Score* is less sensitive to data imbalance and a more appropriate choice for performance evaluation [255].

The datasets used present significantly high IRs (see Table 3.1). Therefore, it is especially important to attribute equal importance to the predictive power of all classes, which does not happen with OA and *Kappa Coefficient*. In this study, we employ 3 evaluation metrics: 1) *G-mean*, since it is not affected by skewed class distributions, 2) *F-Score*, as it proved to be a more appropriate metric for this problem when compared to other commonly used metrics [255], and 3) *Overall Accuracy*, for discussion purposes.

- The *G-mean* consists of the geometric mean of $Specificity = \frac{TN}{TN+FP}$ and *Sensitivity* (also known as *Recall*). For multiclass problems, The *G-mean* is expressed as:

$$G\text{-}mean = \sqrt{\overline{Sensitivity} \times \overline{Specificity}}$$

- *F-score* is the harmonic mean of *Precision* and *Recall*. The *F-score* for the multi-class case can be calculated using their average per class values [256]:

$$F\text{-}score = 2\frac{\overline{Precision} \times \overline{Recall}}{\overline{Precision} + \overline{Recall}}$$

- *Overall Accuracy* is the number of correctly classified instances divided by the total amount of instances. Having c as the label of the various classes, *Accuracy* is given by the following formula:

$$Accuracy = \frac{\sum_c \mathrm{TP}_c}{\sum_c (\mathrm{TP}_c + \mathrm{FP}_c)}$$

In the case of *G-mean* and *F-score*, both metrics are computed for each label and their unweighted mean is calculated (*i.e.*, following a "macro" approach). In this study we assume that all labels have an equivalent importance for the classification task.

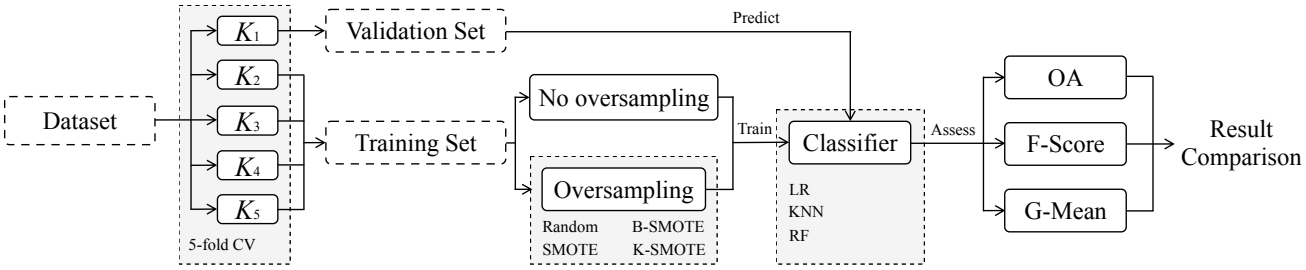

Figure 3.6.: Experimental procedure. The performance metrics are averaged over the 5 folds across each of the 3 different initializations of this procedure for a given combination of oversampler, classifier and hyperparameter definition.

Classifier	Hyperparameters	Values
LR	maximum iterations	10000
KNN	# neighbors	3, 5, 8
RF	maximum depth	None, 3, 6
	# estimators	50, 100, 200
Oversampler		
K-means SMOTE	# neighbors	3, 5
	# clusters (as % of number of instances)	1*, 0.1, 0.3, 0.5, 0.7, 0.9
	Exponent of mean distance	auto, 2, 5, 7
	IR threshold	auto, 0.5, 0.75, 1.0
SMOTE	# neighbors	3, 5
BORDERLINE SMOTE	# neighbors	3, 5

Table 3.2.: Hyper-parameters grid. * One cluster is generated in total, a corner case that mimics the behavior of SMOTE

3.3.4. Experimental Procedure

The procedure for the experiment started with the definition of a hyperparameter search grid, where a list of possible values for each relevant hyperparameter in both classifiers and oversamplers is stored. Based on this search grid, all possible combinations of oversamplers, classifiers and hyperparameters are formed. Finally, for each dataset, hyperparameter combination and initialization we use the evaluation strategy shown in Figure 3.6: k-fold cross-validation strategy where $k = 5$ to train each model defined and save the averaged scores of each split.

In the 5-fold cross validation strategy, a combination of oversampler, classifier and hyperparameters vector is fit 5 times per dataset. Before the training phase, the training set (containing $\frac{4}{5}$ of the dataset) is oversampled using one of the methods described (except for the baseline method NONE), creating an augmented dataset with the exact same number of instances for each class. The newly formed training dataset is used to train the classifier and the test set ($\frac{1}{5}$ of the dataset) is used to evaluate the performance of the classifier. The evaluation scores are then averaged over the 5 times the process is repeated. The range of hyperparameters used are shown in table 3.2. The definition of hyperparameters for the K-means SMOTE oversampler is defined according to the recommendations discussed in the original K-means SMOTE paper [25].

Classifier	Metric	NONE	ROS	SMOTE	B-SMOTE	K-SMOTE
LR	Accuracy	0.906 ± 0.039	0.904 ± 0.04	0.904 ± 0.04	0.901 ± 0.04	**0.909 ± 0.038**
LR	F-score	0.891 ± 0.041	0.893 ± 0.042	0.893 ± 0.042	0.890 ± 0.042	**0.898 ± 0.04**
LR	G-mean	0.936 ± 0.025	0.940 ± 0.025	0.940 ± 0.025	0.937 ± 0.025	**0.943 ± 0.024**
KNN	Accuracy	0.879 ± 0.043	0.865 ± 0.048	0.867 ± 0.05	0.862 ± 0.054	**0.881 ± 0.045**
KNN	F-score	0.859 ± 0.05	0.853 ± 0.049	0.861 ± 0.047	0.851 ± 0.053	**0.866 ± 0.048**
KNN	G-mean	0.919 ± 0.03	0.920 ± 0.029	0.926 ± 0.027	0.918 ± 0.03	**0.927 ± 0.027**
RF	Accuracy	0.898 ± 0.032	0.901 ± 0.031	0.900 ± 0.031	0.898 ± 0.032	**0.905 ± 0.031**
RF	F-score	0.879 ± 0.041	0.885 ± 0.037	0.887 ± 0.036	0.883 ± 0.037	**0.891 ± 0.036**
RF	G-mean	0.930 ± 0.024	0.935 ± 0.022	0.937 ± 0.021	0.935 ± 0.021	**0.939 ± 0.02**

Table 3.3.: Mean cross-validation scores of oversamplers.

3.3.5. Software Implementation

The experiment was implemented using the Python programming language, using the Scikit-Learn [257], Imbalanced-Learn [258], Geometric-SMOTE, Cluster-Over-Sampling and Research-Learn libraries. All functions, algorithms, experiments and results are provided at the GitHub repository of the project.

3.4. Results & Discussion

When evaluating the performance of an algorithm across multiple datasets, it is generally recommended to avoid direct score comparisons and use classification rankings instead [259]. This is done by assigning a ranking to oversamplers based on the different combinations of classifier, metric and dataset used. These rankings are also used for the statistical analyses presented in Section 3.4.2.

The rank values are assigned based on the mean validation scores resulting from the experiment described in Section 3.3. The averaged ranking results are computed over 3 different initialization seeds and a 5 fold cross validation scheme, returning a real number within the interval $[1, 5]$.

The hyperparameter optimization ensures that both oversamplers and classifiers are well adapted to each of the datasets used in the experiment. Specifically, the optimization of classifiers' hyperparameters is not particularly relevant since our focus is to study the relative performance scores across oversamplers. This will provide insights on the quality of the artificial data generated by each oversampler. The classifiers' hyperparameter tuning was done to avoid the over/underfitting of classifiers, since they are trained on the same data subsets along with artificial data generated with different methods.

3.4.1. Results

The mean ranking of oversamplers is presented in Figure 3.7. This ranking was computed by averaging the ranks of the mean cross-validation scores per dataset, oversampler and classifier. K-means SMOTE achieves the best mean ranking across datasets with low standard deviation.

The mean cross-validation scores are shown in Table 3.3. As discussed previously in this section, the disparity of performance levels across datasets makes the analysis of these scores less informative.

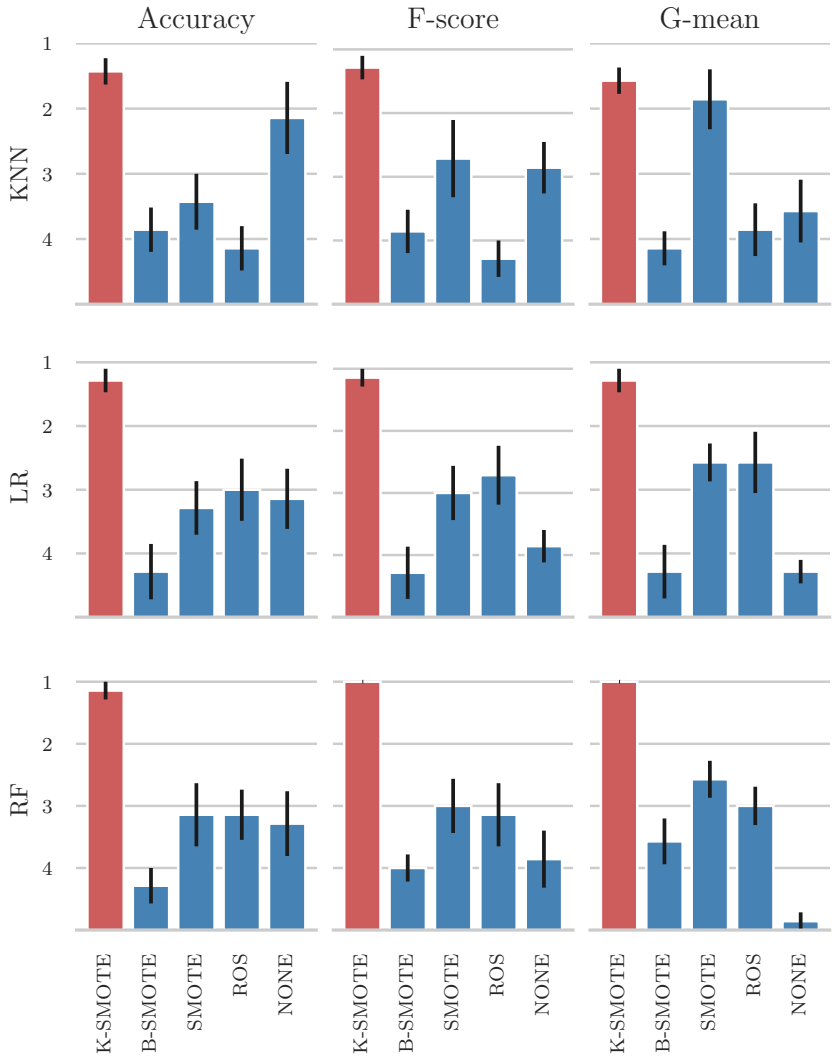

Figure 3.7.: Results for mean ranking of oversamplers across datasets.

The mean cross-validation scores for each dataset are presented in Table A.1 (see appendix). This table allows the direct comparison of the performance metrics being analysed.

3.4.2. Statistical Analysis

The experiment's multi-dataset context was used to perform a Friedman test [260]. Table 3.4 shows the results obtained in the Friedman test performed, where the null hypothesis is rejected in all cases. The rejection of the null hypothesis implies that the differences between the differences among the different oversamplers are not random, in other words, these differences are statistically significant.

Classifier	Metric	p-value	Significance
LR	Accuracy	9.8e-03	True
LR	F-score	2.3e-03	True
LR	G-mean	9.8e-04	True
KNN	Accuracy	4.3e-03	True
KNN	F-score	4.3e-03	True
KNN	G-mean	3.0e-03	True
RF	Accuracy	5.5e-03	True
RF	F-score	2.9e-03	True
RF	G-mean	1.8e-04	True

Table 3.4.: Results for Friedman test. Statistical significance is tested at a level of $\alpha = 0.05$. The null hypothesis is that there is no difference in the classification outcome across oversamplers.

A Wilcoxon signed-rank test [261] was also performed to understand whether K-means SMOTE's superiority was statistically significant across datasets and oversamplers, as suggested in [259]. This method is used as an alternative to the paired Student's t-test, since the distribution of the differences between the two samples cannot be assumed as normally distributed. The null hypothesis of the test is that K-means SMOTE's performance is similar to the compared oversampler (i.e., the oversamplers used follow a symmetric distribution around zero).

Dataset	NONE	ROS	SMOTE	B-SMOTE
Botswana	**3.1e-02**	**3.9e-03**	**3.9e-03**	**3.9e-03**
Pavia Centre	**3.1e-02**	**3.9e-03**	**1.2e-02**	**3.9e-03**
Kennedy Space Center	**3.1e-02**	**3.9e-03**	**2.7e-02**	**3.9e-03**
Salinas A	**3.1e-02**	**3.9e-03**	**1.2e-02**	**3.9e-03**
Pavia University	**3.1e-02**	**3.9e-03**	**3.9e-03**	**3.9e-03**
Salinas	**3.1e-02**	5.5e-02	**2.7e-02**	**3.9e-03**
Indian Pines	**3.1e-02**	**3.9e-03**	**7.8e-03**	**3.9e-03**

Table 3.5.: *p-values* of the Wilcoxon signed-rank test. Boldface values are statistically significant at a significance level of $\alpha = 0.05$.

3.4.3. Discussion

The mean rankings presented in Figure 3.7 show that on average, K-means SMOTE produced the best results for every classifier and performance metric used. This is due to the clustering phase and subsequent selection of data to be considered for oversampling. By successfully clustering and selecting the relevant areas in the data space to oversample, the generation of artificial instances is done only in the context of minority regions that represent well their spectral signature.

As previously discussed, the direct comparison of performance metrics averaged over various datasets is not recommended due to the varying levels of performance of classifiers across datasets [259]. Nonetheless, these results are shown in Table 3.3 to provide a fuller picture of the results obtained in the experiment. We found that on average K-means SMOTE provides increased performance, regardless of the classifier and performance metric used. More importantly, K-means SMOTE guaranteed a more consistent performance across datasets and with less variability, which can be attested in Figure 3.7 and Tables 3.3 and A.1.

As discussed in Subsection 3.3.3, Evaluation Metrics, our results are consistent with the findings in [253, 254]. Particularly, we consider the results obtained in our experiment using Overall Accuracy to be less informative than the results obtained with the remaining performance metrics, since this metric is affected by imbalanced class distributions. The majority class bias in this metric can be observed in our experiment in Figure 3.7 with the classifiers LR and KNN, where the control method (NONE) is only outperformed by K-means SMOTE. This effect is observed with more detail in Table 3.3, where the benchmark oversamplers are outperformed by the control method in 16 out of 63 tests (approximately 25%). Out of these, most refer to tests using overall accuracy among the four datasets with highest IR, showing the overall accuracy's class imbalance bias discussed in [253, 254]. The K-means SMOTE oversampler is only outperformed by the control method in 3 of tests (all of them using overall accuracy). This is an improvement over the benchmark oversamplers, showing that generally K-means SMOTE is the best choice even when overall accuracy is used as the main performance metric.

In the majority of the cases, K-means SMOTE was able to generate higher quality data due to the non-random selection of data spaces to oversample. This can be seen in the performance of the classifiers trained on top of this data generation step, making it a more informed data generation method in the context of LULC.

The performance of both oversamplers and classifiers is generally dependent on the dataset being used. Although both absolute and relative scores between the different oversamplers are dependent on the choice of metric and classifier, K-means SMOTE's relative performance is consistent across datasets and generally outperforms the remaining oversampling methods in 56 of the 63 tests (approximately 89%). The mean cross-validation results found in Table A.1 show that performance-wise, K-means SMOTE is always better than or as good as SMOTE, with the exception of 4 situations (representing 6% of the tests done), in which cases the percentage point difference is neglectable (≤ 0.1 percentage points).

The statistical tests showed that not only there is a statistically significant difference across the oversamplers used in this problem (found in the Friedman test presented in Table 3.4), but also that K-means SMOTE's superior performance is statistically significant at a level of 0.05 in 27 out of 28 tests in the Wilcoxon signed-rank test shown in Table 3.5 (approximately 96% of the tests performed). This shows that, in most cases, the usage of k-Means SMOTE improves the quality of LULC classification when compared to using SMOTE in its original format, which remains the most popular oversampler among the remote sensing community.

Although the usage of K-means SMOTE successfully captured the spectral signatures of the minority classes, it was done using K-means, a problem-agnostic clusterer. Consequently, the implementation of this method using a GIS-specific clusterer that considers the geographical traits of different regions (e.g., using the sampled pixels' geographical coordinates), may be a promising direction towards the development of more appropriate oversampling techniques in the remote sensing domain.

3.5. Conclusion

This research paper was motivated by the challenges faced when classifying rare classes for LULC mapping. Cluster-based oversampling is especially useful in this context because the spectral signature of a given class often varies, depending on its geographical distribution and the time period within which the image was acquired. This induces the representation of minority classes as small clusters in the input space. As a result, training a classifier capable of identifying LULC minority classes in the hyper/multi-spectral scene over different areas or periods becomes particularly challenging. The clustering procedure, performed before the data generation phase, allows for a more accurate generation of minority samples, as it identifies these minority clusters.

A number of existing methods to address the imbalanced learning problem were identified and their limitations discussed. Typically, algorithm-based approaches and cost-sensitive solutions are not only difficult to implement, but they are also context dependent. In this paper we focused on oversampling methods due to their widespread usage, easy implementation and flexibility. Specifically, this paper demonstrated the efficacy of a recent oversampler, K-Means SMOTE, applied in a multi-class context for Land Cover Classification tasks. This was done with sampled data from seven well known and naturally imbalanced benchmark datasets: Indian Pines, Pavia Center, Pavia University, Salinas, Salinas A, Botswana and Kennedy Space Center. For each combination of dataset, oversampler and classifier, the results of every classification task was averaged across a 5 fold stratification strategy with 3 different initialization seeds, resulting in a mean validation score of 15 classification tasks. The mean validation score of each combination was then used to perform the analyses presented in this report.

In 56 out of 63 classification tasks (approximately 89%), K-means SMOTE led to better results than ROS, SMOTE, B-SMOTE and no oversampling. More importantly, we found that K-Means SMOTE is always better or equal than the second best oversampling method. K-means SMOTE's performance was independent from both the classifier and performance metric under analysis. In general, K-means SMOTE shows a higher performance among the non tree-based classifiers employed (LR and KNN) when compared with the remaining oversamplers, where these oversamplers generally failed to improve the quality of classification. Although these findings are case dependent, they are consistent with the results presented in [25]. The proposed method also had the most consistent results across datasets, since it produced the lowest standard deviations across datasets in 7 out of 9 cases for both analyses, either based on ranking or mean cross-validation scores.

The proposed algorithm is a generalization of the original SMOTE algorithm. In fact, the SMOTE algorithm represents a corner case of K-means SMOTE i.e., when the number of clusters equals to 1. Its data selection phase differs from the one used in SMOTE and Borderline SMOTE, providing artificially augmented datasets with less noisy data than the commonly used methods. This allows the training of classifiers with better defined decision boundaries, especially in the most important regions of the data space (the ones populated by a higher percentage of minority class instances).

As stated previously, the usage of this oversampler is technically simple. It can be applied to any classification problem relying on an imbalanced dataset, alongside any classifier. K-means SMOTE is available as an open source implementation for the Python programming language (see Subsection 3.3.5). Consequently, it can be a useful tool for both remote sensing researchers and practitioners.

4. Increasing the Effectiveness of Active Learning: Introducing Artificial Data Generation in Active Learning for Land Use/Land Cover Classification

Published as Joao Fonseca, Georgios Douzas, Fernando Bacao, in Remote Sensing, 2021

In remote sensing, Active Learning (AL) has become an important technique to collect informative ground truth data "on-demand" for supervised classification tasks. In spite of its effectiveness, it is still significantly reliant on user interaction, which makes it both expensive and time consuming to implement. Most of the current literature focuses on the optimization of AL by modifying the selection criteria and the classifiers used. Although improvements in these areas will result in more effective data collection, the use of artificial data sources to reduce human-computer interaction remains unexplored. In this paper, we introduce a new component to the typical AL framework, the data generator, a source of artificial data to reduce the amount of user-labeled data required in AL. The implementation of the proposed AL framework is done using Geometric SMOTE as data generator. We compare the new AL framework to the original one using similar acquisition functions and classifiers over three AL-specific performance metrics in seven benchmark datasets. We show that this modification of the AL framework significantly reduces cost and time requirements for a successful AL implementation in all of the datasets used in the experiment.

Keywords: Active Learning; Artificial Data Generation; Land Use/Land Cover Classification; Oversampling; SMOTE

4.1. Introduction

The technological development of air and spaceborne sensors, as well as the increasing number of remote sensing missions have allowed the continuous collection of large amounts of high quality remotely sensed data. This data is often composed of multi and hyper spectral satellite imagery, essential for numerous applications, such as Land Use/Land Cover (LULC) change detection, ecosystem management [262], agricultural management [263], water resource management [264], forest management, and urban monitoring [1]. Despite LULC maps being essential for most of these applications, their production is still a challenging task [217, 216]. They can be updated using one of the following strategies:

1. Photo-interpretation. This approach consists of evaluating a patch's LULC class by a human operator based on orthophoto and satellite image interpretation [265]. This method guarantees a decent level of accuracy, as it is dependent on the interpreter's expertise and human error. Typically,

it is an expensive, time-consuming task that requires the expertise of a photo-interpreter. This task is also frequently applied to obtain ground-truth labels for training and/or validating Machine Learning (ML) algorithms for related tasks [266, 267].

2. Automated mapping. This approach is based on the usage of a ML method or a combination of methods in order to obtain an updated LULC map. The development of a reliable automated method is still a challenge among the ML and remote sensing community, since the effectiveness of existing methods varies across applications and geographical areas [217]. Typically, this method requires the existence of ground-truth data, which is frequently outdated or nonexistent for the required time frame [262]. On the other hand, employing a ML method provides readily available and relatively inexpensive LULC maps. The increasing quality of state-of-the-art classification methods have motivated the application and adaptation of these methods in this domain [223].

3. Hybrid approaches. These approaches employ photo-interpreted data to augment the training dataset and improve the quality of automated mapping [268]. It attempts to accelerate the photo-interpretation process by selecting a smaller sample of the study area to be interpreted. The goal is to minimize the inaccuracies found in the LULC map by supplying high-quality ground-truth data to the automated method. The final (photo-interpreted) dataset consists of only the most informative samples, *i.e.*, patches that are typically difficult to classify for a traditional automated mapping method [269].

The latter method is best know as AL. It is especially useful whenever there is a shortage or even absence of ground-truth data and/or the mapping region does not contain updated LULC maps [33]. In a context of limited sample-collection budget, the collection of the most informative samples capable of optimally increasing the classification accuracy of a LULC map is of particular interest [33]. AL attempts to minimize the human-computer interaction involved in photo-interpretation by selecting the data points to include in the annotation process. These data points are selected based on an uncertainty measure and represent the points close to the decision borders. Afterwards, they are passed on for photo-interpretation and added to the training dataset, while the points with the lowest uncertainty values are ignored for photo-interpretation and classification. This process is repeated until a convergence criterion is reached [270].

The relevant work developed within AL is described in detail in Section 4.2. This paper attempts to address some of the challenges found in AL, mainly inherited from automated and photo-interpreted mapping: mapping inaccuracies and time consuming human-computer interactions. These challenges have different sources:

1. Human error. The involvement of photo-interpreters in the data labeling step carries an additional risk to the creation of LULC patches. The minimum mapping unit being considered, as well as the quality of the orthophotos and satellite images being used, are some of the factors that may lead to the overlooking of small-area LULC patches and label-noisy training data [4].

2. High-dimensional datasets. Although the amount of bands (*i.e.*, features) present in multi and hyper spectral images contain useful information for automated classification, they also introduce an increased level of complexity and redundancy in the classification step [5]. These datasets are often prone to the Hughes phenomenon, also known as the curse of dimensionality.

3. Class separability. Producing an LULC map considering classes with similar spectral signatures makes them difficult to separate [6]. A lower pixel resolution of the satellite images may also imply mixed-class pixels, which may lead to both lower class separability as well as higher risk of human error.

4. Existence of rare land cover classes. The varying morphologies of different geographical regions naturally implies an uneven distribution of land cover classes [7]. This is particularly relevant in the context of AL since the data selection method is based on a given uncertainty measure over data

points whose class label is unknown. Consequently, AL's iterative process of data selection may disregard wrongly classified land cover areas belonging to a minority class.

Research developed in the field of AL typically focus on the reduction of human error by minimizing the human interaction with the process through the development of more efficient classifiers and selection criteria within the generally accepted AL framework. Concurrently, the problem of rare land cover classes is rarely addressed. This is a frequent problem in the ML community, known as the Imbalanced Learning problem. This problem exists whenever there is an uneven between-class distribution in the dataset [221]. Specifically, most classifiers are optimized and evaluted using accuracy-like metrics, which are designed to work primarily with balanced datasets. Consequently, these metrics tend to introduce a bias towards the majority class by attributing an importance to each class proportional to its relative frequency [223]. As an example, such a classifier could achieve an overall accuracy of 99% on a binary dataset where the minority class represents 1% of the overall dataset and still be useless. A number of methods have been developed to deal with this problem. They can be categorized into three different types of approaches [9, 218]. Cost-sensitive solutions perform changes to the cost matrix in the learning phase. Algorithmic level solutions modify specific classifiers to reinforce learning on minority classes. Resampling solutions modify the training data by removing majority samples and/or generating artificial minority samples. The latter is independent from the context and can be used alongside any classifier. Since we are interested in the introduction of artificial data generation in AL, we will analyze the state-of-the-art on resampling techniques (specifically oversampling) in Section 4.3.

In this paper, we propose a novel AL framework to address two limitations commonly found in the literature: minimize human-computer interaction and reduce the class imbalance bias. This is done with the introduction of an additional component in the iterative AL procedure (the generator) that is used to generate artificial data to both balance and augment the training dataset. The introduction of this component is expected to reduce the number of iterations required until the classifier reaches a satisfactory performance.

This paper is organized as follows: Section 4.1 explains the problem and its context, Sections 4.2 and 4.3 describe the state of the art in AL and Oversampling techniques, Section 4.4 explains the proposed method, Section 4.5 covers the datasets, evaluation metrics, ML classifiers and experimental procedure, Section 4.6 presents the experiment's results and discussion and Section 4.7 presents the conclusions drawn from our findings.

4.2. Active Learning Approaches

As the amount of unlabeled data increases, the interest and practical usefulness of AL follows that trend [36]. AL is used as the general definition of frameworks aiming to train a learning system in multiple steps, where a set of new data points are chosen and added to the training dataset each time [268]. Typically, an AL framework is composed of the following elements [34, 33, 268]:

1. Unlabeled dataset. Consists of the original data source (or a sample thereof). It is used in combination with the chooser and the selection criterion to expand the training dataset in regions where the classification uncertainty is higher. Therefore, the unlabeled dataset is used for both producing the initial training dataset by selecting a set of instances for the supervisor to annotate (discussed in point 3) and calculating the uncertainty map to augment the training dataset.
2. Supervisor. A human annotator (or team of human annotators) to which the uncertainty map is presented to. The supervisor is responsible for annotating unlabeled instances to be added to the augmented dataset. In remote sensing, the supervisor is typically a photo-interpreter, as is the case in [37]. Some of the research also refers to the supervisor as the *oracle* [268, 31, 32, 271].

3. Initial training dataset. It is a small, labeled sample of the original data source used to initiate the first AL iteration. The size of the initial training sample normally varies between no instances at all and 10% of the unlabeled dataset [272].
4. Current and expanded training dataset. It is the concatenation of the initial training dataset and the datasets labeled by the supervisor in past iterations (discussed in point 2).
5. Chooser (classifier). Produces the class probabilities for each unlabeled instance.
6. Selection criterion. It quantifies the chooser's uncertainty level for each instance belonging to the unlabeled dataset. It is typically based on the class probabilities assigned by the chooser. In some situations, the chooser and the selection criterion are grouped together under the concept *acquisition function* [268] or *query function* [33]. Some of the literature refers to the selection criterion by using the concept *sampling scheme* [269].

Figure 4.1 schematizes the steps involved in a complete AL iteration. For a better context within the remote sensing domain, the prediction output can be identified as the LULC map. This framework starts by collecting unlabeled data from the original data source. It is used to generate a random initial training sample and is labeled by the supervisor. In practical applications, the supervisor is frequently a group of photo-interpreters [36]. The chooser is trained on the resulting dataset and is used to predict the class probabilities on the unlabeled dataset. The class probabilities are fed into a selection criterion to estimate the prediction's uncertainty, out of which the instances with the highest uncertainty will be selected. This calculation is motivated by the absence of labels in the uncertainty dataset. Therefore, it is impossible to estimate the prediction's accuracy in the unlabeled dataset in a real case scenario. The iteration is completed when the selected points are tagged by the supervisor and added to the training dataset (*i.e.*, the augmented dataset).

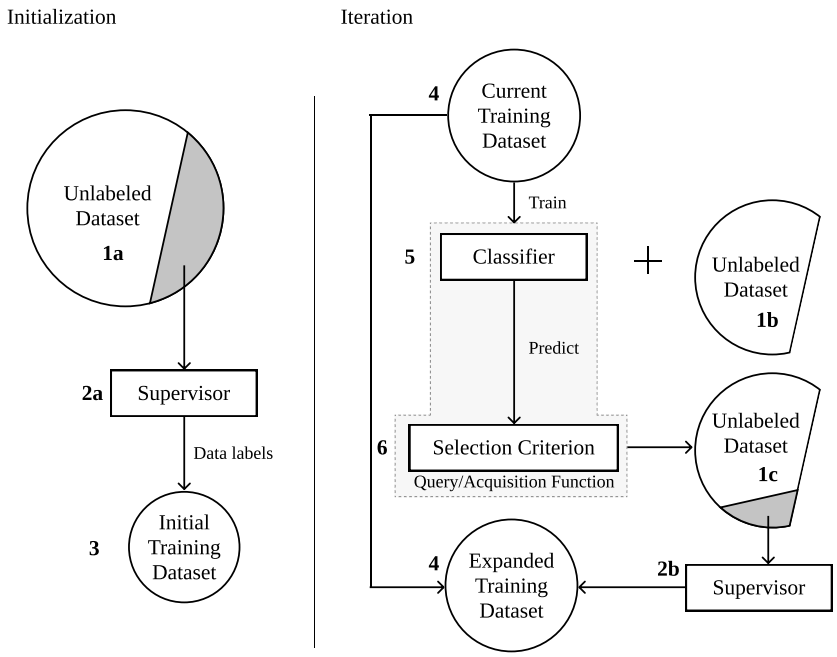

Figure 4.1.: Diagram depicting the typical AL framework.

A common challenge found in AL tasks is ensuring the consistency of AL over different initializations [36]. There are two factors involved in this phenomenon. On one hand, the implementation of the same method over different initializations may result in significantly different initial training samples, amounts to varying accuracy curves. On the other hand, the lack of a robust selection criterion and/or classifier may

also result in inconsistencies across AL experiments with different initializations. This phenomenon was observed and documented in a LULC classification context in [273].

The classification method plays a central role in the efficacy of AL. The classifier used should be able to generalise with a relatively small training dataset. Specifically, deep learning models are used in image classification due to its capability of producing high quality predictions. Although, to make such models generalizable the training set must be large enough, making its suitability for AL applications an open challenge [26, 274, 275]. Some studies in the Remote Sensing domain were developed to address this gap. In [26, 275], the authors propose a deep learning-based AL approach by training the same Convolutional Neural Network incrementally across iterations and smoothen the decision boundaries of the model using the Markov Random Field model and a Best-versus-Second Best labelling approach. This allows the introduction of additional data variability in the final training dataset. Another study [274] combined transfer learning, active classification and segmentation techniques for vehicle detection. By combining different techniques, they were able to produce a classification mechanism that performed well when the amount of training data is limited. However, the exploration of advanced deep learning classifiers in AL is still limited. In [276], the authors show that deep learning classifiers performs well on LULC classification, but are still not generalizable for different geographical regions or periods. Specifically, AL methods are still incapable of providing generalizable deep learning classifiers, which benefit from multiple advantages. The development of Convolutional Neural Networks with both 2 and 3-dimensional convolutions was explored in [277] and reported superior classification performance on benchmark datasets. However, a large amount of training data was used to produce the final classification map.

Selecting an efficient selection criterion is particularly important to find the instances closest to the decision border (*i.e.*, instances difficult to classify) [28]. Therefore, many AL related studies focus on the design of the query/acquisition function [33].

4.2.1. Non-informed selection criteria

Only one non-informed (*i.e.*, random) selection criterion was found in the literature. Random sampling selects unlabeled instances without considering any external information produced by the chooser. Since the method for selecting the unlabeled instances is random, this method disregards the usage of a chooser and is comparatively worse than any other selection criterion. However, random sampling is still a powerful baseline method [271].

4.2.2. Ensemble-based selection criteria

Ensemble disagreement is based on the class predictions of a set of classifiers. The disagreement between all the predictions for a given instance is a common measure for uncertainty, although computationally inefficient [268, 270]. It is calculated using the set of classifications over a single instance, given by the number of votes assigned to the most frequent class [28]. This method was implemented successfully for complex applications such as deep active learning [268].

Multiview [278] consists on the training of multiple independent classifiers using different views, which correspond to the selection of subsets of features or instances in the dataset. Therefore, it can be seen as a bootstrap aggregation (bagging) ensemble disagreement method. It is represented by the maximum disagreement score out of set of disagreements calculated for each view [28]. A lower value for this metric means a higher classification uncertainty. Multiview-based maximum disagreement has been successfully applied to hyper-spectral image classification in [279] and [56].

An adapted disagreement criterion for an ensemble of k-nearest neighbors has been proposed in [270]. This method employs a k-nearest neighbors classifier and computes an instance's classification uncertainty based on the neighbors' class frequency using the maximum disagreement metric over varying values for k.

As a result, this method is comparable to computing the dominant class' score over a weighted k-nearest neighbors classifier. This method was also used on a multimetric active learning framework [280].

Another relevant ensemble-based selection criterion is the binary random forest-based query model [33]. This method employs a one-versus-one ensemble method to demonstrate an efficient data selection method using the estimated probability of each binary random forest and determining the classification uncertainty based on the probabilities closest to 0.5 (*i.e.*, the least separable pair of classes are used to determine the uncertainty value). However, this study fails to compare the proposed method with other benchmark methods, such as random sampling.

4.2.3. Entropy-based criteria

A number of contributions have focused on entropy-based querying. The application of entropy is common among active deep learning applications [32], where the training of an ensemble of classifiers is often too expensive.

Entropy query-by-bagging (EQB), also defined as maximum entropy [269], is an ensemble approach of the entropy selection criterion, originally proposed in [281]. This strategy uses the set of predictions produced by the ensemble classifier to calculate those many entropy measurements. The estimated uncertainty measure for one instance is given by the maximum entropy within that set. EQB was observed to be an efficient selection criterion. Specifically, [28] applied EQB on hyper-spectral remote sensing imagery using Support Vector Machines (SVM) and Extreme Learning Machines (ELM) as choosers, achieving optimal results when combining EQB with ELM. Another study successfully implemented this method on an active deep learning application [269]. Another study improved over this method with a normalized EQB selection criterion [282].

4.2.4. Other relevant criteria

Margin Sampling is a SVM-specific criterion, based on the distance of a given point to the SVM's decision boundary [28]. This method is less popular than the remaining methods because it is limited to one type of chooser (SVMs). One extension of this method is the multiclass level uncertainty [28], calculated by subtracting the instance's distance to the decision boundaries of the two most probable classes [283].

The Mutual Information-based (MI) criterion selects the new training instances by maximizing the mutual information between the classifier and class labels in order to select instances from regions that are difficult to classify. Although this method is commonly used, it is frequently outperformed by the breaking ties selection criterion [284, 51].

The breaking ties (BT) selection criterion was originally introduced in [285]. It consists of the subtraction between the probabilities of the two most likely classes. Another related method is Modified Breaking Ties scheme (MBT), which aims at finding the instances containing the largest probabilities for the dominant class [51, 286]

Another type of selection criteria identified is the loss prediction method [31]. This method replaces the selection criterion with a predictor whose goal is to estimate the chooser's loss for a given prediction. This allows the new classifier to estimate the prediction loss on unlabeled instances and select the ones with the highest predicted loss.

Some of the literature fails to specify the strategy employed, although inferring it is generally intuitive. For example, [287] successfully used AL to address the imbalanced learning problem. They employed an ensemble of SVMs as the chooser, as well as an ensemble-based selection criterion. All of the research found related to this topic focused on the improvement of AL through modifications on the selection

criterion and classifiers used. None of these publications proposed significant variations to the original AL framework.

4.3. Artificial Data Generation Approaches

The generation of artificial data is a common approach to address imbalanced learning tasks [218], as well as improving the effectiveness of supervised learning tasks [17]. In recent years some sophisticated data generation approaches were developed. However, the scope of this work is to propose the integration of a generator within the AL framework. To do this, we will focus on heuristic data generation approaches, specifically, oversamplers.

Heuristic data resampling methods employ local and/or global information to generate new, relevant, non-duplicate instances. These methods are most commonly used to populate minority classes and balance the between-class distribution of a dataset. The Synthetic Minority Oversampling Technique (SMOTE) [22] is a popular heuristic oversampling algorithm, proposed in 2002. The simplicity and effectiveness of this method contributes to its prevailing popularity. It generates a new instance through a linear interpolation of a randomly selected minority-class instance and one of its randomly selected k-nearest neighbors. The implementation of SMOTE for LULC classification tasks has been found to improve the quality of the predictors used [240, 241]. Despite its popularity, its drawbacks motivated the development of other oversampling methods [23].

Geometric SMOTE (G-SMOTE) [23] introduces a modification of the SMOTE algorithm in the data generation mechanism to produce artificial instances with higher variability. Instead of generating artificial data as a linear combination of the parent instances, it is done within a deformed, truncated hyper-spheroid. G-SMOTE generates an artificial instance $\overrightarrow{z}$ within a hyper-spheroid, formed by selecting a minority instance $\overrightarrow{x}$ and one of its nearest neighbors $\overrightarrow{y}$, as shown in Figure 4.2. The truncation and deformation parameters define the shape of the spheroid's geometry. The method also modifies the selection strategy for the k-nearest neighbors, accepting the generation of artificial instances using instances from different classes, as shown in Figure 4.2d. The modification of both selection and generation mechanisms addresses the main drawbacks found in SMOTE, the generation of both noisy data (*i.e.,* generate minority class instances within majority class regions) and near-duplicate minority class instances [23]. G-SMOTE has shown superior performance when compared with other oversampling methods for LULC classification tasks, regardless of the classifier sed [2].

4.4. Proposed method

Within the literature identified, most of the work developed in the AL domain revolved around improving the quality of classification algorithms and/or selection criteria. Although these methods allow earlier convergence of the AL iterative process, the impact of these methods are only observed between iterations. Consequently, none of these contributions focused on the definition of decision borders within iterations. The method proposed in this paper modifies the AL framework by introducing an artificial data generation step within AL's iterative process. We define this component as the generator and is intended to be integrated into the AL framework as shown in Figure 4.3.

This modification, by using a new source of data to augment the training set, leverages the data annotation work conducted by the human operator. The artificial data that is generated between iterations reduces the amount of labeled data required to reach optimal performance and lower the amount of human labor

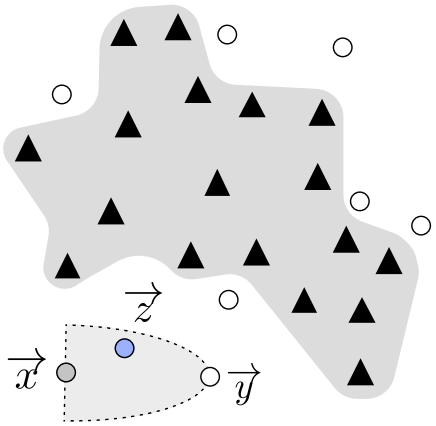

Figure 4.2.: Example of G-SMOTE's generation process. G-SMOTE randomly selects instance $\overrightarrow{x}$ and one of its nearest neighbors $\overrightarrow{y}$ to produce instance $\overrightarrow{z}$.

required to train a classifier to its optimal performance. This process lowers the annotation and overall training costs by translating some of the annotation cost into computational cost.

This method leverages the capability of artificial data to introduce more data variability into the augmented dataset and facilitate the chooser's training phase with a more consistent definition of the decision boundaries at each iteration. Therefore, any algorithm capable of producing artificial data, be it agnostic or specific to the domain, can be employed. The artificial data is only used to train the classifiers involved in the process and is discarded once the training phase is completed. The remaining steps in the AL framework remain unchanged. This method addresses the limitations found in the previous sections:

1. The convergence of classification performance should be anticipated with the clearer definition of the decision boundaries across iterations.
2. Annotation cost is expected to reduce as the need for labeled instances reduces along with the early convergence of the classification performance.
3. The class imbalance bias observed in typical classification tasks, as well as in AL is mitigated by balancing the class frequencies at each iteration.

Although the performance of this method is shown within a LULC classification context, the proposed framework is independent from the domain. The high dimensionality of remotely sensed imagery make its classification particularly challenging when the availability of labeled data is scarce and/or comes at a high cost, being subjected to the curse of dimensionality. Consequently, it is a relevant and appropriate domain to test this method.

4.5. Methodology

In this section we describe the datasets, evaluation metrics, oversampler, classifiers, software used and the procedure developed. We demonstrate the proposed method's efficiency over 7 datasets, sampled from publicly available, well-known remote sensing hyperspectral scenes frequently found in remote sensing literature. The datasets and sampling strategy are described in Subsection 4.5.1. On each of these datasets, we apply 3 different classifiers over the entire training set to estimate the optimal classification performance, the original AL framework as the baseline reference and the proposed method using G-SMOTE as a

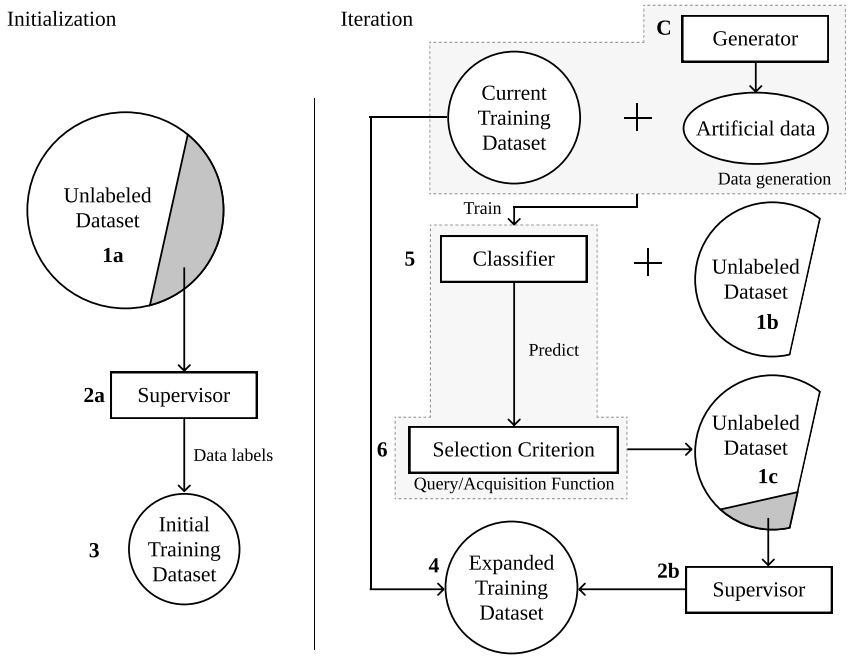

Figure 4.3.: Proposed AL framework. This paper's contribution comprises a change in the AL framework through the introduction of a data generation mechanism, represented as the generator (marked with C), which is used to add artificial instances to the training dataset.

generator, described in Subsection 4.5.2. The metrics used to estimate the performance of these algorithms are described in Subsection 4.5.3. Finally, the experimental procedure is described in Subsection 4.5.4.

Our methodology focuses on two objectives: (1) Comparison of optimal classification performance among active learners and traditional supervised learning and (2) Comparison of classification convergence efficiency among AL frameworks.

4.5.1. Datasets

The datasets used were extracted from publicly available repositories containing hyperspectral images and ground truth data. Additionally, all datasets were collected using the same sampling procedure. The description of the hyperspectral scenes used in this study is provided in Table 4.1. These scenes were chosen because of their popularity in the research community and their high baseline classification scores. Consequently, demonstrating an outperforming method in this context is particularly challenging and valuable.

The Indian Pines scene [249] is composed of agriculture fields in approximately two thirds of its coverage, low density buildup areas and natural perennial vegetation in the remainder of its area (see Figure 4.4a). The Pavia Centre and University scenes are hyperspectral, high-resolution images containing ground truth data composed of urban-related coverage (see Figures 4.4b and 4.4c). The Salinas and Salinas A scenes contain at-sensor radiance data. As subset of Salinas, the Salinas A scene contains contains the vegetables fields present in Salinas and the latter is also composed of bare soils and vineyard fields (see Figures 4.4d and 4.4e). The Botswana scene contains ground truth data composed of seasonal swamps, occasional swamps, and drier woodlands located in the distal portion of the Delta (see Figure 4.4f). The Kennedy

Dataset	Sensor	Location	Dimension	Bands	Res. (m)	Classes
Botswana	Hyperion	Okavango Delta	1476 x 256	145	30	14
Salinas A	AVIRIS	California, USA	86 x 83	224	3.7	6
Kennedy Space Center	AVIRIS	Florida, USA	512 x 614	176	18	16
Indian Pines	AVIRIS	NW Indiana, USA	145 x 145	220	20	16
Salinas	AVIRIS	California, USA	512 x 217	224	3.7	16
Pavia University	ROSIS	Pavia, Italy	610 x 610	103	1.3	9
Pavia Centre	ROSIS	Pavia, Italy	1096 x 1096	102	1.3	9

Table 4.1.: Description of the hyperspectral scenes used in this experiment. The column "Res. (m)" refers to the resolution of the sensors (in meters) that captured each of the scenes.

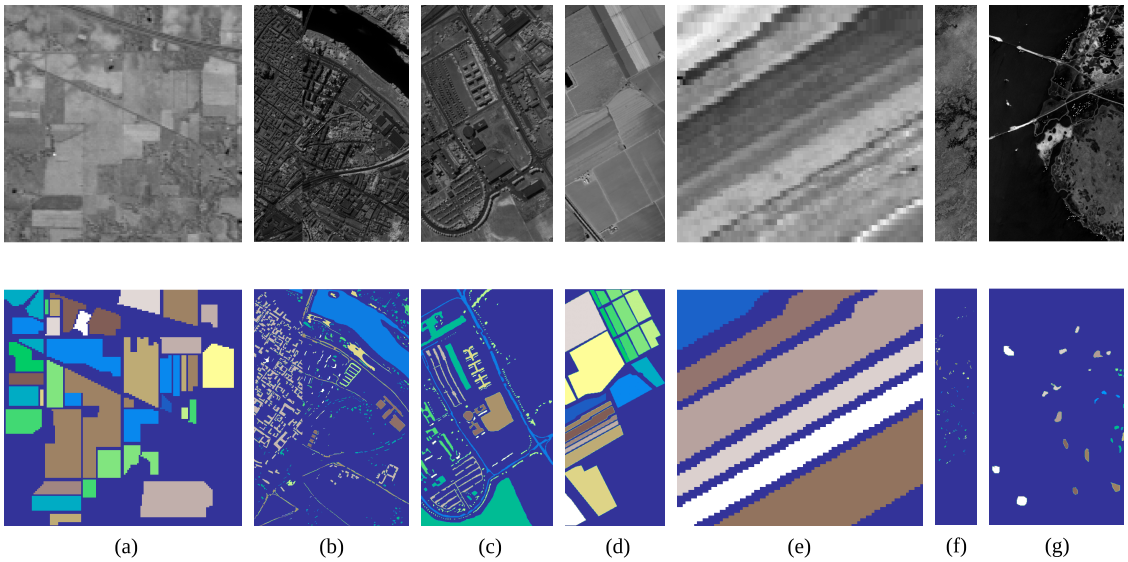

Figure 4.4.: Gray scale visualization of a band (top row) and ground truth (bottom row) of each scene used in this study. (a) Indian Pines, (b) Pavia Centre, (c) Pavia University, (d) Salinas, (e) Salinas A, (f) Botswana, (g) Kennedy Space Center

Space Center scene contains a ground truth composed of both vegetation and urban-related coverage (see Figure 4.4g).

The sampling strategy is similar to all datasets. The pixels without a ground truth label are first discarded. All the classes with cardinality lower than 150 are also discarded. This is done to maintain feasible Imbalance Ratios (IR) across datasets (where $IR = \frac{count(C_{maj})}{count(C_{min})}$). Finally, a stratified sample of 1500 instances are selected for the experiment. The resulting datasets are described in Table 4.2. The motivation for this strategy is three fold: (1) reduce the datasets to a manageable size and allow the experimental procedure to be completed within a feasible time frame, (2) ensure the relative class frequencies in the scenes are preserved and (3) ensure equivalent analyses across datasets and AL frameworks. In this context, a fixed number of instances per dataset is especially important to standardize the AL-related performance metrics.

4.5.2. Machine Learning Algorithms

Dataset	Features	Instances	Min. Instances	Maj. Instances	IR	Classes
Botswana	145	1500	89	154	1.73	12
Salinas A	224	1500	109	428	3.93	6
Kennedy Space Center	176	1500	47	272	5.79	12
Indian Pines	220	1500	31	366	11.81	12
Salinas	224	1500	25	312	12.48	16
Pavia University	103	1500	33	654	19.82	9
Pavia Centre	102	1500	27	668	24.74	9

Table 4.2.: Description of the datasets collected from each corresponding scene. The sampling strategy is similar to all scenes.

We use two different types of ML algorithms. A data generation algorithm, used to form the generator, and classification algorithms, used to calculate the classification uncertainties in the unlabeled dataset and predict the class labels in the validation and test sets.

Although any method capable of generating artificial data can be used as a generator, the one used in this experiment is an oversampler, originally developed to deal with imbalanced learning problems. Specifically, we chose G-SMOTE, a state-of-the-art oversampler.

Three classification algorithms are used. We use different types of classifiers to test the framework's performance under varying situations: neighbors-based, linear and ensemble models. The neighbors-based classifier chosen was K-nearest neighbors (KNN) [251], a logistic regression (LR) [250] is used as the linear model and a random forest classifier (RFC) [288] was used as the ensemble model.

The acquisition function is completed by testing three different selection criteria. Random selection is used as a baseline selection criterion, whereas entropy and breaking ties are used due to their popularity and independence of the classifier used.

4.5.3. Evaluation Metrics

Since the datasets used in this experiment have an imbalanced distribution of class frequencies, metrics such as the *Overall Accuracy* (OA) and *Kappa coefficient* are insufficient to accurately depict classification performance [253, 254]. Instead, metrics such as Producer's Accuracy (or *Recall*) and User's Accuracy (or *Precision*) can be used. Since they consist of ratios based on True/False Positives (TP and FP) and Negatives (TN and FN), they provide per class information regarding the classifier's classification performance. However, in this experiment, the meaning and number of classes available in each dataset varies, making these metrics difficult to synthesize.

The performance metric *Geometric mean* (G-mean) and *F-score* are less sensitive to the data imbalance bias [255, 289]. Therefore, we employ both of these scorers. G-mean consists of the geometric mean of $Specificity = \frac{TN}{TN+FP}$ and $Sensitivity = \frac{TP}{TP+FN}$ (also known as *Recall*) [289]. Both metrics are calculated in a multiclass context considering a one-versus-all approach. For multiclass problems, the *G-mean* scorer is calculated as its average per class values:

$$G\text{-}mean = \sqrt{\overline{Sensitivity}_i \times \overline{Specificity}_i}$$

The F-score performance metric is the harmonic mean of *Precision* and *Recall*. The two metrics are also calculated considering a one-versus-all approach. The *F-score* for the multi-class case can be calculated using its average per class values [256]:

$$F\text{-}score = 2\frac{\overline{Precision} \times \overline{Recall}}{\overline{Precision} + \overline{Recall}}$$

The comparison of classification convergence across AL frameworks and selection criteria is done using 2 AL-specific performance metrics. Particularly, we follow the recommendations found in [36]. Each AL configuration is evaluated using the *Area Under the Learning Curve* (AULC) performance metric. It is the sum of the classification performance values of all iterations. To facilitate the analysis of the results, we fix the range of this metric between $[0, 1]$ by dividing it with the total amount of iterations (*i.e.*, the maximum performance area).

The *Data Utilization Rate* (DUR) [290] metric consists of the ratio between the number of instances required to reach a given G-mean score threshold by an AL strategy and an equivalent baseline strategy. For easier interpretability, we simplify this metric by using the percentage of training data used by an AL strategy to reach the performance threshold, instead of presenting these values as a ratio of the baseline strategy. The DUR metric is measured at 9 different performance levels, between 0.6 and 0.95 G-mean scores at a 0.05 step.

4.5.4. Experimental Procedure

A common practice in methodological evaluations is the implementation of an offline experiment [291]. It consists of using an existing set of labeled data as a proxy for the population of unlabeled instances. Because the dataset is already fully labeled, the supervisor's typical annotation process involved in each iteration is done at zero cost. Each AL and classifier configuration is tested using a stratified 5-fold cross validation testing scheme. For each round, the larger partition is split in a stratified fashion to form a training and validation set (containing 20% of the original partition). The validation set is used to evaluate the convergence efficiency of active learners; the chooser's classification performance metrics and amount of data points used at each iteration are used to compute the AULC and DUR. Additionally, within the AL iterative process, the classifier with optimal performance on the validation set is evaluated using the test set. In order to further reduce possible initialization biases, this procedure is repeated 3 times with different initialization seeds and the results of all runs are averaged (*i.e.*, each configuration is trained and evaluated 15 times). Finally, the maximum performance lines are calculated using the same approach. In those cases, the validation set is not used. The experimental procedure is depicted in Figure 4.5.

To make the AL-specific metrics comparable among active learners, the configurations of the different frameworks must be similar. For each dataset, the number of instances is constant to facilitate the analysis of the same metrics.

In most practical AL applications it is assumed that the number of instances in the initial training sample is too small to perform hyperparameter tuning. Consequently, in order to ensure realistic results, our experimental procedure does not include hyperparameter optimization. The predefined hyperparameters are shown in Table 4.3. They were set up based on general recommendations and default settings for the classifiers and generators used.

The AL iterative process is set up with a randomly selected initial training sample with 15 initial samples. At each iteration, 15 additional samples are added to the training set. This process is stopped after

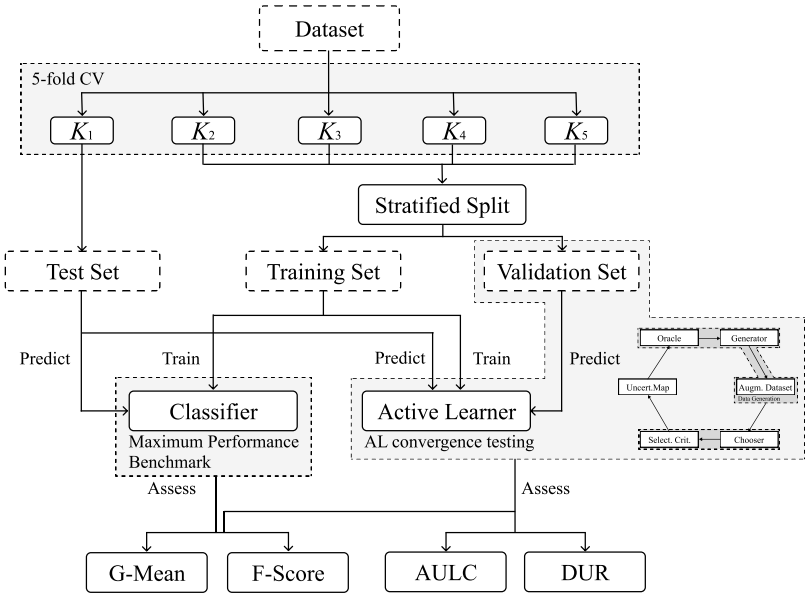

Figure 4.5.: Experimental procedure. The datasets extracted from hyperspectral scenes are split in 5 folds. 1 of those (*e.g.*, K_1) is used to test the optimal performance of AL algorithms and the classification without AL. The training set is used to iterate AL algorithms and train classifiers. The validation set is used to test the convergence of AL algorithms. The results are averaged over the 5 folds across each of the 3 different initializations of this procedure.

49 iterations, once 50% of the entire dataset (*i.e.*, 78% of the training set) is added to the augmented dataset.

4.5.5. Software Implementation

The experiment was implemented using the Python programming language, along with the Python libraries Scikit-Learn [257], Imbalanced-Learn [258], Geometric-SMOTE, Cluster-Over-Sampling and Research-Learn libraries. All functions, algorithms, experiments and results are provided in the GitHub repository of the project.

4.6. Results & Discussion

The evaluation of the different AL frameworks in a multiple dataset context should not rely uniquely on the mean of the performance metrics across datasets. [259] recommends the use of mean ranking scores, since the performance levels of the different frameworks varies according to the data it is being used on. Consequently, evaluating these performance metrics solely based on their mean values might lead to inaccurate analyses. Accordingly, the results of this experiment are analysed using both the mean ranking and absolute scores for each model. The rank values are assigned based on the mean scores resulting from three different initializations of 5-fold cross validation for each classifier and active learner. The goal of this analysis is to understand whether the proposed framework (AL with the integration of an artificial data generator) is capable of using less data from the original dataset while simultaneously achieving better classification results than the standard AL framework, *i.e.*, guarantee a faster classification convergence.

Classifier	Hyperparameters	Values
LR	maximum iterations	10000
	solver	sag
	penalty	None
KNN	# neighbors	5
	weights	uniform
	metric	euclidean
RF	maximum tree depth	None
	# estimators	100
	criterion	gini
Generator		
G-SMOTE	# neighbors	5
	deformation factor	0.5
	truncation factor	0.5

Table 4.3.: Hyper-parameter definition for the classifiers and generator used in the experiment.

Classifier	Evaluation Metric	Standard	Proposed
KNN	F-score	2.00 ± 0.0	**1.00 ± 0.0**
KNN	G-mean	2.00 ± 0.0	**1.00 ± 0.0**
LR	F-score	1.71 ± 0.45	**1.29 ± 0.45**
LR	G-mean	2.00 ± 0.0	**1.00 ± 0.0**
RF	F-score	1.86 ± 0.35	**1.14 ± 0.35**
RF	G-mean	2.00 ± 0.0	**1.00 ± 0.0**

Table 4.4.: Mean rankings of the AULC metric over the different datasets (7), folds (5) and runs (3) used in the experiment. This means that the use of G-SMOTE almost always improves the results of the original framework.

4.6.1. Results

Table 4.4 shows the average rankings and standard deviations across datasets of the AULC scores for each active learner.

The mean AULC absolute scores are provided in Table 4.5. These values are computed as the mean of the sum of the scores of a specific performance metric over all iterations (for an AL configuration). In other words, these values correspond to the average AULC over 7 $datasets \times 5$ $folds \times 3$ $initializations$.

The average DURs are shown in Table 4.6. They were calculated for various G-mean scores thresholds, varying at a step of 5% between 60% and 95%. Each row shows the percentage of training data required by the different AL configurations to reach that specific G-mean score.

G-mean Score	Classifier	Standard	Proposed
0.60	KNN	4.0%	**2.1%**
0.60	LR	2.2%	**2.1%**
0.60	RF	2.2%	**2.1%**
0.65	KNN	5.6%	**2.8%**

G-mean Score	Classifier	Standard	Proposed
0.65	LR	3.0%	**2.7%**
0.65	RF	3.1%	**2.6%**
0.70	KNN	7.9%	**4.1%**
0.70	LR	4.2%	**4.1%**
0.70	RF	4.5%	**3.6%**
0.75	KNN	13.5%	**7.1%**
0.75	LR	7.2%	**6.6%**
0.75	RF	6.6%	**5.4%**
0.80	KNN	24.4%	**16.9%**
0.80	LR	13.1%	**11.7%**
0.80	RF	11.6%	**9.2%**
0.85	KNN	29.8%	**23.6%**
0.85	LR	19.8%	**18.8%**
0.85	RF	23.1%	**17.3%**
0.90	KNN	41.0%	**36.1%**
0.90	LR	28.1%	**24.8%**
0.90	RF	37.1%	**30.3%**
0.95	KNN	71.3%	**69.1%**
0.95	LR	45.8%	**40.2%**
0.95	RF	64.6%	**62.2%**

Table 4.6.: Mean data utilization of AL algorithms, as a percentage of the training set.

The DUR of the proposed method relative to the baseline method is shown in Figure 4.6. A DUR below 1 means that the proposed framework requires less data to reach the same performance threshold (as a percentage, relative to the amount of data required by the baseline framework). For instance, in the upper left graphic we can see that the proposed framework achieves 90% classification using F-score while using 91% of the amount of data used by the traditional AL framework, in other words 9% less data.

The averaged optimal classification scores are shown in Table 4.7. The maximum performance (MP) classification scores are shown as a benchmark and represent the performance of the corresponding classifier using the entire training set.

4.6.2. Statistical Analysis

The methods used to test the experiment's results must be appropriate for a multi-dataset context. Therefore the statistical analysis is performed using the Wilcoxon signed-rank test [261] as a post-hoc analysis. The variable used for this test is the data utilization rate based on the G-mean performance metric, considering the various performance thresholds from Table 4.6.

The Wilcoxon signed-rank test results are shown in Table 4.8. We test as null hypothesis that the performance of the proposed framework is the same as the original AL framework. The null hypothesis was rejected in all datasets.

Classifier	Evaluation Metric	Standard	Proposed
KNN	F-score	0.762 ± 0.131	**0.794 ± 0.123**
KNN	G-mean	0.864 ± 0.079	**0.886 ± 0.073**
LR	F-score	0.839 ± 0.119	**0.843 ± 0.116**
LR	G-mean	0.907 ± 0.074	**0.911 ± 0.071**
RF	F-score	0.810 ± 0.109	**0.819 ± 0.1**
RF	G-mean	0.890 ± 0.068	**0.901 ± 0.059**

Table 4.5.: Average AULC of each AL configuration tested. Each AULC score is calculated using the G-mean scores of each iteration in the validation set. By the end of the iterative process, each AL configuration used a total of 750 instances of the 960 instances that compose the training set.

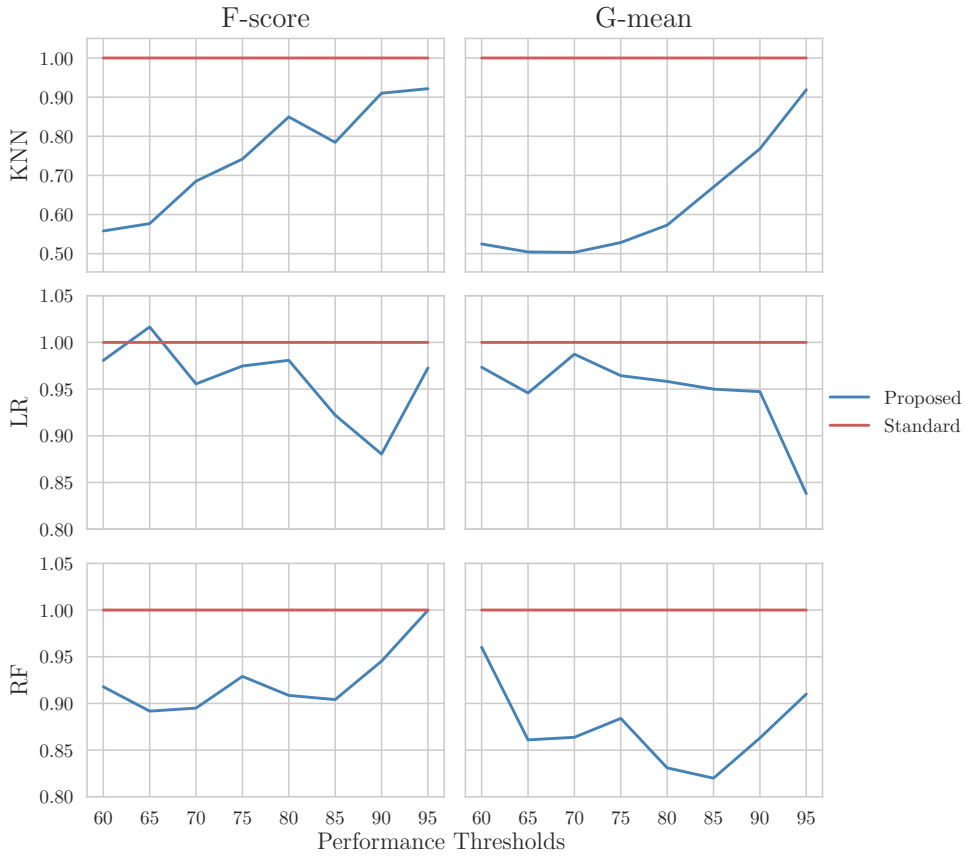

Figure 4.6.: Mean data utilization rates. The y-axis shows the percentage of data (relative to the baseline AL framework) required to reach the different performance thresholds.

Classifier	Evaluation Metric	MP	Standard	Proposed
KNN	F-score	0.838 ± 0.106	0.835 ± 0.115	**0.843 ± 0.105**
KNN	G-mean	0.907 ± 0.063	0.904 ± 0.069	**0.912 ± 0.061**
LR	F-score	**0.890 ± 0.084**	0.883 ± 0.096	0.887 ± 0.097
LR	G-mean	0.935 ± 0.052	0.931 ± 0.059	**0.938 ± 0.055**
RF	F-score	0.859 ± 0.083	0.866 ± 0.081	**0.869 ± 0.08**
RF	G-mean	0.918 ± 0.051	0.921 ± 0.051	**0.930 ± 0.043**

Table 4.7.: Optimal classification scores. The Maximum Performance (MP) classification scores are calculated using classifiers trained using the entire training set.

Dataset	p-value	Significance
Botswana	3.8e-03	True
Indian Pines	2.3e-04	True
Kennedy Space Center	1.3e-04	True
Pavia Centre	4.3e-03	True
Pavia University	4.6e-05	True
Salinas	4.6e-05	True
Salinas A	3.0e-03	True

Table 4.8.: Adjusted p-values using the Wilcoxon signed-rank method. Bold values are statistically significant at a level of $\alpha = 0.05$. The null hypothesis is that the performance of the proposed framework is similar to that of the original framework.

4.6.3. Discussion

This paper expands the AL framework by adding an artificial data generator into its iterative process. This modification is done to accelerate the classification convergence of the standard AL procedure, which is reflected in the reduction of the amount of data necessary to reach better classification results.

The convergence efficiency of the proposed method is always higher than the baseline AL framework, with the exception of one comparison, as shown in Table 4.4 and Figure 4.6. This means the proposed AL framework using data generation was able to outperform the baseline AL in nearly all scenarios.

The mean AULC scores in Table 4.5 show a significant improvement in the performance of AL when a generator is used. The mean performance of the proposed framework is always better than the baseline framework. This improvement is explained by:

1. Earlier convergence of AL, *i.e.*, requiring less data to achieve comparable performance levels. This effect is shown in Table 4.6, where we found that the proposed framework always uses less data for similar performance levels, regardless of the classifier used.
2. Higher optimal classification performance, *i.e.*, reaching higher performance levels overall. This effect is shown in Table 4.7, where we found that using a generator in AL led to a better classification performance and was capable of outperforming the MP threshold.

Our results show statistical significance in every dataset. The proposed framework had a superior performance with statistical significance on each dataset at a level of $\alpha = 0.05$. This indicates that regardless of the context under which an AL algorithm is used, the proposed framework reduces the amount of data necessary in the AL's iterative process.

This paper introduces the concept of applying data a generation algorithm in the AL framework. This was done with the implementation of a recent state of the art generalization of a popular data generation algorithm. Although, since this algorithm is based on heuristics, future work should focus on improving these results through the design of new data generation mechanisms, at the cost of additional computational power. In addition, we also noticed significant standard errors in our experimental results (see Subsection 4.6.1). This indicates that AL procedures seem to be particularly sensitive to the initialization method, which is still a limitation of AL, regardless of the framework and configurations used. This is consistent with the findings in [36], which future work should attempt to address. Although using a generator marginally reduced this standard error, it is not sufficient to address this specific limitation.

4.7. Conclusion

The aim of this experiment was to test the effectiveness of a new AL framework that introduces artificial data generation in its iterative process. The experiment was designed to test the proposed method under particularly challenging conditions, where the maximum performance line is naturally high in most datasets. The element that constitute the Generator component was set up in a plug-and-play scheme, without significant tuning of the G-SMOTE oversampler. Using a generator in AL improved the original AL framework in all scenarios. These results could be further improved through the modification and more intense tuning of the data generation strategy. In our experiment, artificial data was generated only to match each non-majority class frequency with the majority class frequency, strictly balancing the class distribution. Generating a larger amount of data for all classes can further improve these results.

The high performance scores for the baseline AL framework made the achievement of significant improvements over the traditional AL framework under these conditions particularly meaningful. The advantage of the proposed AL framework is shown in Table 4.6. In most of the presented scenarios there is a substantial reduction of data necessary to reach a given performance threshold.

The results from this experiment show that using a data generator in the AL framework will improve the convergence of the method. This framework successfully anticipate the predictor's optimal performance, as shown in Tables 4.4, 4.5 and 4.6. Therefore, in a real application, the annotation cost would have been reduced since less iterations and labeled instances are necessary to reach near optimal classification performance.

5. Improving Active Learning Performance Through the Use of Data Augmentation

Published as Joao Fonseca, Fernando Bacao, in International Journal of Intelligent Systems, 2023

Active Learning (AL) is a well-known technique to optimize data usage in training, through the interactive selection of unlabeled observations, out of a large pool of unlabeled data, to be labeled by a supervisor. Its focus is to find the unlabeled observations that, once labeled, will maximize the informativeness of the training dataset, therefore reducing data related costs. The literature describes several methods to improve the effectiveness of this process. Nonetheless, there is a paucity of research developed around the application of artificial data sources in AL, especially outside image classification or NLP. This paper proposes a new AL framework, which relies on the effective use of artificial data. It may be used with any classifier, generation mechanism and data type, and can be integrated with multiple other state-of-the-art AL contributions. This combination is expected to increase the ML classifier's performance and reduce both the supervisor's involvement and the amount of required labeled data, at the expense of a marginal increase in computational time. The proposed method introduces a hyperparameter optimization component to improve the generation of artificial instances during the AL process, as well as an uncertainty-based data generation mechanism. We compare the proposed method to the standard framework and an oversampling-based active learning method for more informed data generation in an AL context. The models' performance was tested using four different classifiers, two AL-specific performance metrics and three classification performance metrics over 15 different datasets. We demonstrate that the proposed framework, using data augmentation, significantly improves the performance of AL, both in terms of classification performance and data selection efficiency.[1]

Keywords: Active Learning; Data Augmentation; Oversampling

5.1. Introduction

The importance of training robust ML models with minimal data requirements is substantially increasing [292, 34, 44]. Although the growing amount of valuable data sources and formats being developed and explored is affecting various domains [293], this data is often unlabeled. Only a tiny amount of the data being produced and stored can be helpful in supervised learning tasks. In addition, it is often difficult and expensive to label data for specific Machine Learning (ML) projects, especially when data-intensive ML techniques are involved (*e.g.,* Deep Learning classifiers) [292]. In this scenario, labeling the full dataset becomes impractical, time-consuming and expensive. Two different ML techniques attempt to address this problem: Semi-Supervised Learning (SSL) and Active Learning (AL). Even though they address the

[1] All the code and preprocessed data developed for this study is available at https://github.com/joaopfonseca/publications/.

same problem, the two follow different approaches. SSL focuses on observations with the most certain predictions, whereas AL focuses on observations with the least certain predictions [8].

SSL attempts to use a small, predefined set of labeled and unlabeled data to produce a classifier with superior performance. This method uses the unlabeled observations to help define the classifier's decision boundaries [294]. Simultaneously, the amount of labeled data required to reach a given performance threshold is also reduced. It is a particular case of ML because it falls between the supervised and unsupervised learning perspectives. AL, instead of optimizing the informativeness of an existing training set, expands the dataset to include the most informative and/or representative observations [295]. It is an iterative process where a supervised model is trained and simultaneously identifies the most informative unlabeled observations to increase the performance of that classifier. The combination of SSL with AL has been explored in the past, achieving state-of-the-art results [296].

Several studies have pointed out the limitations of AL within an Imbalanced Learning context [297, 298]. With imbalanced data, AL approaches frequently have low performance, high computational time, or data annotation costs. Studies addressing this issue tend to adopt classifier-level modifications, such as the Weighted Extreme Learning Machine [297, 299, 300]. However, classifier or query function-level modifications (See Section 5.2.1) have limited applicability since a universally good AL strategy has not yet been found [295]. Other methods address imbalanced learning by weighing the observations as the function of the observation's class imbalance ratio [301]. Alternatively, other techniques reduce the imbalanced learning bias by combining Informative and Representative-based query approaches (see Section 5.2.1) [302]. Another approach to deal with imbalanced data and data scarcity, in general, is generating synthetic data [256]. This approach has the advantage of being classifier-agnostic, it potentially reduces the imbalanced learning bias, and also works as a regularization method in data-scarce environments, such as AL implementations [303]. However, most recent studies improve the AL performance by modifying the design/choice of the classifier and query functions used.

Recently, synthetic data generation techniques gathered attention among ML researchers for its effectiveness over a wide range of applications: regularization, oversampling, semi-supervised learning, self-supervised learning, etc. Data augmentation generates synthetic observations to complement naturally occurring observations. It aims to reinforce the definition of a ML classifier's decision boundary during the learning phase and improve the generalization of the algorithm. These techniques have the advantage of being a data level technique (despite the existence of augmentation methods applied internally in the ML classifier). Therefore, they can be implemented in a way that will not affect the choice of classifier and does not exclude the usage of other regularization approaches. In an AL context, the generation of synthetic data becomes particularly appealing, especially with randomized and statistical-based approaches; it ensures better model performance with reduced involvement of a human agent, at the expense of a marginal increase in computational power. In addition, synthetic data is expected to reduce the amount labeled data required for a good AL implementation.

Figure 5.1 illustrates the difference across AL iterations between the standard AL approach and the proposed method. Synthetic data allowed for a quicker expansion of the labeled input area at an early stage of the process, with better defined decision boundaries and near-covergence of the ML classifier's performance at the third iteration. Data augmentation influences the choice of unlabeled observations for labeling into regions where synthetic data is not being able to represent the unlabeled data pool.

5.1.1. Motivation and contributions

The usage of data augmentation in AL is not new. The literature found on the topic (see Section 5.2.3) focuses on either image classification or Natural Language Processing and uses Deep Learning-based data augmentation to improve the performance of neural network architectures in AL. These methods, although showing promising results, represent a limited perspective of the potential of data augmentation in a real-world setting:

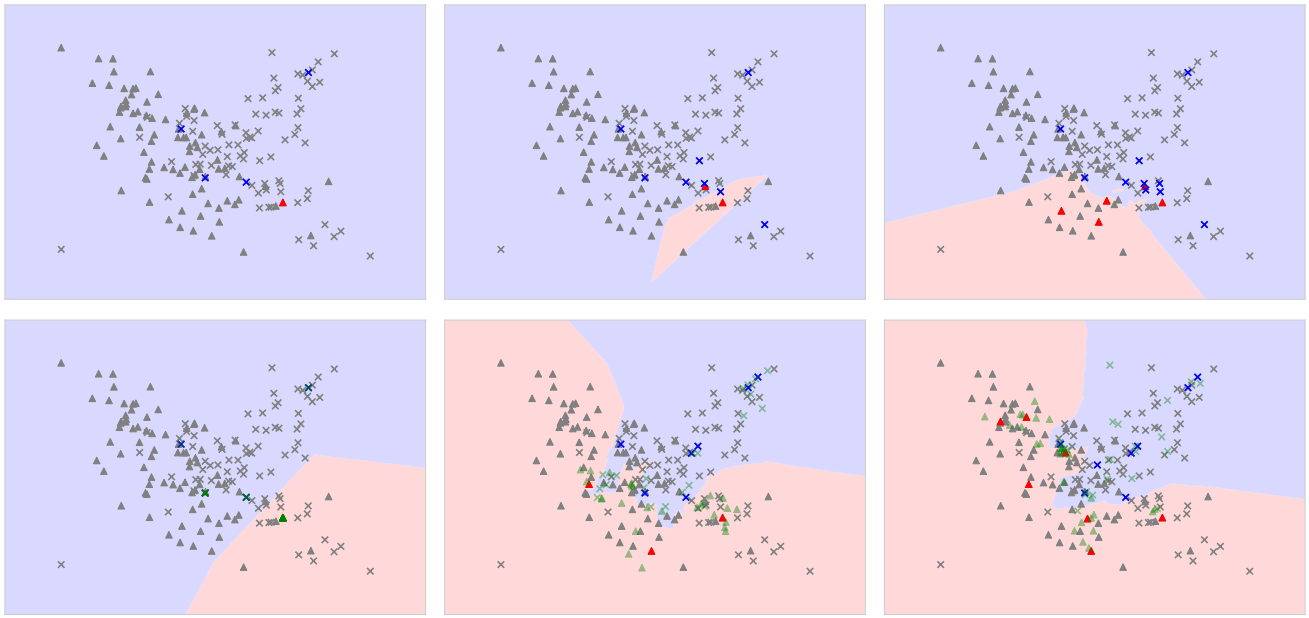

(a) (b) (c)

Figure 5.1.: Illustration of the different acquisition processes in AL using a K-Nearest Neighbors classifier and Shannon's entropy as the uncertainty estimation function, with five observations being collected and labeled per iteration. The top row shows the behavior of a standard AL implementation, while the bottom row shows the behavior of the proposed method. Column (a), (b) and (c) show the decision boundaries at iterations 1 (after the collection of five random initial training observations), 2 (with 10 labeled observations) and 3 (with 15 labeled observations), respectively. The initial labeled dataset for both approaches is the same. The two classes are distinguished with $\triangle$ and $\times$, and are colored as red and blue (respectively) if they are labeled. The transparent green observations are synthetic observations (bottow row only).

1. Using Deep Learning in an iterative setting requires access to significant computational power.
2. These models tend to use sophisticated data augmentation methods, whose implementation may not be accessible to non-sophisticated users.
3. They require a significant amount of processing time per iteration and are inappropriate for settings with limited time budgets.
4. The studies found on the topic are specific to the domain, classifier, and data augmentation method. In addition, all of the related methods found (except one) focus on either image or natural language processing classification problems.

Consequently, the direct effect of data augmentation is unclear: these studies implement different neural network-based techniques for different classification problems, whose performance may be attributed to various elements within the AL framework.

In this study, we explore the effect of data augmentation in AL in a context-agnostic setting, along with two different data augmentation policies: oversampling (where the amount of data generated for each class equals the amount of data belonging to the majority class) and non-constant data augmentation policies (where the amount of data generated exceeds the amount of data belonging to the majority class in varying quantities) between iterations. We start by conceptualizing the AL framework and each of its elements, as well as the modifications involved to implement data augmentation in the AL iterative process. We argue

that simple, non-domain specific data augmentation heuristics are sufficient to improve the performance of AL implementations, without the need to resort to deep learning-based data augmentation algorithms. These contributions can be summarized as follows:

1. We propose a flexible AL framework with pipelined data augmentation for tabular data that may be adapted for any domain or data type. This implementation is directed towards use cases with limited computational power and/or processing time.
2. We use a geometric-based data augmentation method for non-network based classifiers and adapt it to leverage information from the AL process. To the best of our knowledge, most existing methods use domain/classifier-specific augmentations or the Mixup approach, which is incompatible with most classifiers that are not neural network-based.
3. We provide empirical evidence that the integration of varying data augmentation policies between iterations in the AL framework not only further reduces the amount of labeled data required, but is also a viable training strategy for fully supervised learning settings.

When compared to the standard AL framework, the proposed framework contains two additional components: the Generator and the Hyperparameter Optimizer. We implement a modified version of the Geometric Synthetic Minority Oversampling Technique (G-SMOTE) [23] as a data augmentation method with an optimized generation policy (explained in Section 1.1). We also propose a hyperparameter optimization module, which is used to find the best data augmentation policy at each iteration. We test the effectiveness of the proposed method in 15 datasets of different domains. We implement three AL frameworks (standard, oversampling and varying data augmentation) using four different classifiers, three different performance metrics and calculate two AL-specific performance metrics.

The remainder of this manuscript is structured as follows: Section 5.2 introduces relevant topics discussed in the paper and describes the related work. Section 5.3 elucidates the proposed method. Section 5.4 details the methodology of the study's experiment. Section 5.5 presents the results obtained from the experiment, as well as a discussion of these results. Section 5.6 presents the conclusions drawn from this study.

5.2. Background

In this section we describe the AL problem, data augmentation techniques, and review the literature that combines AL with data augmentation. Table 5.1 describes the notations used throughout the rest of this study.

Table 5.1.: Description of all notations and symbols used throughout the manuscript.

Symbol	Meaning
f_c	ML classifier.
x_i	Observation at index i.
$f_{acq}(x_i; f_c)$	Acquisition function.
$f_{aug}(x_i; \tau)$	Augmentation function.
τ	Augmentation policy.
$\mathcal{D}$	Data pool. Contains both labeled and unlabeled data.
$\mathcal{D}^t_{lab}$	Labeled data set at iteration t.
$\mathcal{D}^t_{pool}$	Unlabeled data pool at iteration t.
$\mathcal{D}^t_{new}$	Set of observations from $\mathcal{D}^t_{pool}$to be labeled and added to $\mathcal{D}^{t+1}_{lab}$.

Continued on next page

Table 5.1.: Description of all notations and symbols used throughout the manuscript.

Symbol	Meaning
T	Iteration budget.
n	Annotation budget per iteration.

5.2.1. Active Learning

This paper focuses on pool-based AL methods as defined in [304]. The goal of AL models is to maximize the performance of a classifier, f_c, while annotating as least observations, x_i, as possible. They use a data pool, $\mathcal{D}$, where $\mathcal{D} = \mathcal{D}_{lab} \cup \mathcal{D}_{pool}$ and $|\mathcal{D}_{pool}| \gg |\mathcal{D}_{lab}|$. $\mathcal{D}_{pool}$ and $\mathcal{D}_{lab}$ refer to the sets of unlabeled and labeled data, respectively. Having a budget of T iterations (where $t \in \{1, 2, \ldots, T\}$) and n annotations per iteration, at iteration t, f_c is trained using $\mathcal{D}^t_{lab}$ to produce, for each $x_i \in \mathcal{D}^t_{pool}$, an uncertainty score using an acquisition function $f_{acq}(x_i; f_c)$. These uncertainty scores are used to annotate the n observations with highest uncertainty from $\mathcal{D}^t_{pool}$ to form $\mathcal{D}^t_{new}$. The iteration ends with the update of $\mathcal{D}^{t+1}_{lab} = \mathcal{D}^t_{lab} \cup \mathcal{D}^t_{new}$ and $\mathcal{D}^{t+1}_{pool} = \mathcal{D}^t_{pool} \setminus \mathcal{D}^t_{new}$ [33, 34]. This process is shown in Figure 5.2. Before the start of the iterative process, assuming $\mathcal{D}^{t=0}_{lab} = \emptyset$, the data used to populate $\mathcal{D}^{t=1}_{lab}$ is typically collected randomly from $\mathcal{D} = \mathcal{D}^{t=0}_{pool}$ and is labeled by a supervisor [305, 31, 32].

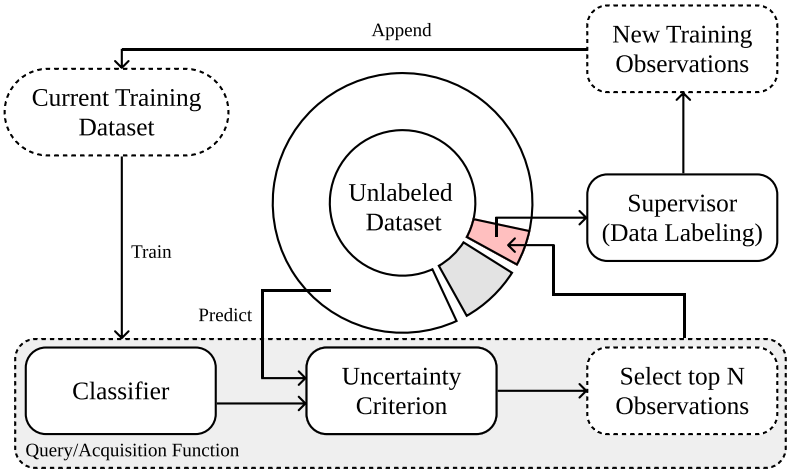

Figure 5.2.: Diagram depicting a typical AL iteration. In the first iteration, the training set collected during the initialization process becomes the "Current Training Dataset".

Research focused on AL has typically been focused on the specification of f_{acq} [306] and domain-specific applications, such as malware detection [307] or Land Use/Land Cover classification [308]. Acquisition functions can be divided into two different categories [309, 40]:

1. Informative-based. These strategies use the classifier's output to assess the importance of each observation towards the performance of the classifier [41].
2. Representative-based. These strategies estimate the optimal set of observations that will optimize the classifier's performance [40].

Although there are significant contributions toward the development of more robust query functions and classifiers in AL, modifications to AL's basic structure are rarely explored. In [31] the authors introduce a loss prediction module in the AL framework to replace the uncertainty criterion. This model implements

a second classifier to predict the expected loss of the unlabeled observations (using the actual losses collected during the training of the original classifier) and return the unlabeled observations with the highest expected loss. However, this contribution is specific to deep neural networks and was only tested for image classification.

AL techniques may also be used to complement other well-known learning challenges. For example, security bug report prediction tasks are typically developed in imbalanced learning environment, where it is necessary to manually label large amounts of data, which may result in mislabeled data [310]. Another related example is machinery fault diagnostics, where the quality and quantity of the data collected is often recognized as a bottleneck [311]. In this case, ML-based techniques frequently leverage unlabeled data to improve the classification performance [312] and rely on manual data acquisition [313]. In these examples, the application of an AL technique could reduce the amount of labeled data required, reduce the strain in the supervisor's labeling process and reduce the amount of label noise.

An under explored challenge in the AL literature is the effective handling of different data structures. One method to address this problem are autoencoder architectures [314] or, in the case of text data, semantic representation networks [315]. However, understanding how to integrate these two types of methods is a subject of future research. Within other research streams, such as deep reinforcement learning, some research also focus on optimizing observation efficiency during the learning process [316].

5.2.2. Data Augmentation

The standard AL model can be complemented with a data augmentation function, $f_{aug}(x_i; \tau)$, where τ defines the augmentation policy. In this context, τ refers to the transformation applied and its hyperparameters and f_{aug} produces a modified observation, $\tilde{x} \in \mathcal{D}_{aug}$ where $\mathcal{D}_{aug}$ is the set of modified observations. This involves the usage of a new set of data, $\mathcal{D}^t_{train} = \mathcal{D}^t_{lab} \cup \mathcal{D}^t_{aug}$, to train the classifier.

Data Augmentation methods expand the training dataset by introducing new and informative observations [15]. The production of artificial data may be done via the introduction of perturbations on the input [30], feature [17], or output space [15]. Data Augmentation methods may be divided into two categories [18]:

1. Heuristic approaches attempt to generate new and relevant observations by applying a predefined procedure, usually incorporating some degree of randomness [21]. Since these methods typically occur in the input space, they require fewer data and computational power when compared to Neural Network methods.

2. Neural Network approaches, on the other hand, map the original input space into a lower-dimensional representation, known as the feature space [17]. The generation of artificial data occurs in the feature space and is reconstructed into the input space. Although these methods allow the generation of less noisy data in high-dimensional contexts and more plausible artificial data, they are significantly more computationally intensive.

While some techniques may depend on the domain, others are domain-agnostic. For example, Random Erasing [16], Translation, Cropping and Flipping are examples of image data-specific augmentation methods. Other methods, such as autoencoders, may be considered domain agnostic.

5.2.3. Data Augmentation in Active Learning

The only AL model found that uses data augmentation outside of the computer vision or NLP domains implements a pipelined approach, described in [305]. In this study, the AL model proposed is applied for tabular data using an oversampling data augmentation policy (*i.e.*, the artificial data was only generated to balance the target class frequencies). However, this AL model was applied in a Land Use/Land Cover classification context with specific characteristics that are not necessarily found in other supervised learning problems. Specifically, these types of datasets are high dimensional and have limited data variability within each class (*i.e.,* cohesive spectral signatures within classes) due to their geographical proximity. Furthermore, this method does not allow augmentation policy optimization (i.e., every hyperparameter has to be hard-coded *a priori*).

The Bayesian Generative Active Deep Learning (BGDAL) [146] is another example of a pipelined combination of f_{acq} and f_{aug}, applied to image classification. BGDAL uses a Variational AutoEncoder (VAE) architecture to generate artificial observations. However, the proposed model is computationally expensive, requires a large data pool to train the VAE, and is not only dependent on the quality of the augmentations performed, but also on the performance of the discriminator and classifiers used.

The method proposed in [303], Look-Ahead Data Acquisition for Deep Active Learning, implements data augmentation to train a deep-learning classifier. However, adapting existing AL applications to use this approach is often impractical and implies the usage of image data since the augmentations used are image data specific and occur on the unlabeled observations, before the unlabeled data selection.

The Variational Adversarial Active Learning (VAAL) model [317] is a deep AL approach to image classification that uses as inputs the embeddings produced by a VAE into a secondary classifier, working as f_{acq}, to predict if $x_i \in \mathcal{D}$ belongs to $\mathcal{D}_{pool}$. The n true positives with the highest uncertainty are labeled by the supervisor and $\mathcal{D}_{pool}$ and $\mathcal{D}_{lab}$ are updated as described in Section 5.2.1. The Task-aware VAAL model [318] extends the VAAL model by introducing a ranker, which consists of the Learning Loss module introduced in [31]. These models use data augmentation techniques to train the different neural network-based components of the proposed models. However, the AL components used are specific image classification, computationally expensive and the analysis of the effect of data augmentation in these AL models is not discussed.

In [319], the proposed AL method was explicitly designed for image data classification, where a deep learning model was implemented as a classifier, but its architecture is not described, the augmentation policies used are unknown and the results reported correspond to single runs of the discussed model. The remaining AL models found implement data augmentation for NLP applications, in [320, 321]. However, these methods were designed for specific applications within that domain and are not necessarily transferable to other domains or tasks.

5.3. Proposed Method

Based on the literature found on AL, most of the contributions and novel implementations of AL algorithms have focused on the improvement of the choice/architecture of the classifier or the improvement of the uncertainty criterion. In addition, the resulting classification performance of AL-trained classifiers is frequently inconsistent and marginally improve the classification performance when compared to classifiers trained over the entire training set. In addition, there is also significant variability in the data selection efficiency during different runs of the AL iterative process [305].

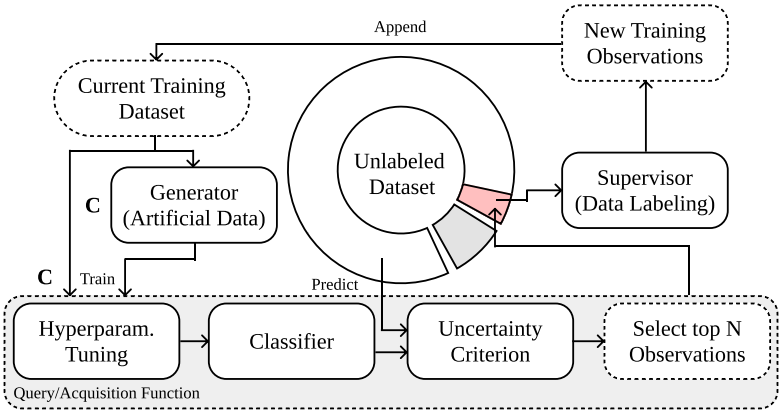

Figure 5.3.: Diagram depicting the proposed AL iteration. The proposed modifications are comprised within the red polygon and marked with a boldface "C."

This paper provides a context-agnostic AL framework for the integration of Data Augmentation within AL, with the following contributions:

1. Improvement of the AL framework by introducing a parameter tuning stage only using the labeled dataset available at the current iteration (*i.e.,* no labeled hold-out set is needed).
2. Generalization of the generator module proposed in [305] from oversampling techniques to any other data augmentation mechanism and/or policy.
3. Implementation of data augmentation outside the Deep AL realm, which was not previously found in the literature.
4. Analysis of the impact of Data Augmentation and Oversampling in AL over 15 different datasets of different domains, while comparing them with the standard AL framework.

The proposed AL framework is depicted in Figure 5.3. The generator element becomes an additional source of data and is expected to introduce additional data variability into the training dataset. This aspect should allow the classifier to generalize better and perform more consistently over unseen observations. However, in this scenario, the amount of data to generate per class at each iteration is unknown. Consequently, the hyperparameter tuning step was introduced to estimate the optimal data augmentation policy at each iteration. In our implementation, this step uses the current training dataset to perform an exhaustive search over specified generator parameters, tested over a 5-fold cross-validation method. The best augmentation policy found is used to train the iteration's classifier in the following step. This procedure is described in Algorithm 1.

We implemented a simple modification in the selection mechanism of the G-SMOTE algorithm to show the effectiveness of data augmentation in an AL implementation. We use the uncertainties produced by f_{acq} to compute the probabilities of observations to be selected for augmentation as an additional parameter. This modification is described in Algorithm 2

This modification facilitates the usage of G-SMOTE beyond its original oversampling purposes. However, in this paper, the data augmentation strategies are also used to ensure that class frequencies are balanced. Furthermore, the amount of artificial data produced for each class is defined by the *augmentation factor*, α_{af}, which represents a percentage of the majority class C_{maj} (*e.g.,* an augmentation factor of 1.2 will ensure there are $count(C_{maj}) \times 1.2$ observations in every class). In this paper's experiment, the data generation mechanism is similar to the one in [305]. This factor allows the direct comparison of the two frameworks and establishes a causality of the performance variations to the data generation mechanism

Algorithm 1: Proposed AL Framework (Single iteration)

Given: $t \geq 1$, performance metric f_{pm}
Input: $\mathcal{D}_{pool}$, $\mathcal{D}_{lab}$, f_c, f_{aug}, f_{acq}, τ_{grid}, k, n
Output: $\mathcal{D}_{pool}$, $\mathcal{D}_{lab}$

Function *ParameterTuning*(f_c, f_{aug}, τ_{grid}, $\mathcal{D}_{lab}$, k)**:**
    $p \leftarrow 0$
    $\tau \leftarrow \emptyset$
    $\{\mathcal{D}^1_{lab}, \dots \mathcal{D}^k_{lab}\} \leftarrow \mathcal{D}_{lab}$ // $\mathcal{D}^n_{lab} \cap \mathcal{D}^m_{lab} = \emptyset, \forall (n, m) \in 1, \dots, k$
    forall $\tau' \in \tau_{grid}$ **do**
        $p' \leftarrow \emptyset$
        forall $\mathcal{D}^i_{lab} \in \{\mathcal{D}^1_{lab}, \dots \mathcal{D}^k_{lab}\}$ **do**
            $\mathcal{D}'_{test} \leftarrow \mathcal{D}^i_{lab}$
            $\mathcal{D}'_{train} \leftarrow \mathcal{D}_{lab} \setminus \mathcal{D}^i_{lab}$
            $\mathcal{D}'_{train} \leftarrow f_{aug}(\mathcal{D}'_{train}; \tau')$
            train f_c using $\mathcal{D}'_{train}$
            $p' \leftarrow p' \cup \{f_{pm}(f_c(\mathcal{D}_{test}))\}$
        $p' \leftarrow \frac{\sum_{x_i \in p'} x_i}{k}$
        if $p' > p$ **then**
            $p \leftarrow p'$
            $\tau \leftarrow \tau'$
    return τ
begin
    $\tau \leftarrow ParameterTuning(f_c, f_{aug}, \tau_{grid}, \mathcal{D}_{lab}, k)$
    $\mathcal{D}_{train} \leftarrow f_{aug}(\mathcal{D}_{lab}; \tau)$
    train f_c using $\mathcal{D}_{train}$
    $\mathcal{D}_{new} = \arg\max_{\mathcal{D}'_{pool} \subset \mathcal{D}_{pool}, |\mathcal{D}'_{pool}| = n} \sum_{x \in \mathcal{D}'_{pool}} f_{acq}(x; f_c)$
    annotate $\mathcal{D}_{new}$
    $\mathcal{D}_{pool} \leftarrow \mathcal{D}_{pool} \setminus \mathcal{D}_{new}$
    $\mathcal{D}_{lab} \leftarrow \mathcal{D}_{lab} \cup \mathcal{D}_{new}$

(*i.e.,* augmentation vs normal oversampling) and hyperparameter tuning steps. However, in this case, the hyperparameter tuning is solely going to be used for augmentation policy optimization.

In the proposed framework, we (1) generalize the generator module to accept any data augmentation method or policy and (2) introduce a hyperparameter tuning module to estimate the optimal data augmentation policy. This framework was designed to be task-agnostic. Specifically, any data augmentation method (domain-specific or not) may be applied, as well as any other parameter search method. It is also expected to be compatible with other AL modifications, including those that do not affect solely the classifier or uncertainty criterion, such as the one proposed in [31].

5.4. Methodology

This section describes the different elements included in the experimental procedure. The datasets used were acquired in open data repositories. Their sources and preprocessing steps are defined in Subsection 5.4.1. The classifiers used in the experiment are defined in Subsection 5.4.2. The metrics

Algorithm 2: G-SMOTE Modified for Data Augmentation in AL

Given: $t \geq 1$, $\mathcal{D}^t_{lab} \neq \emptyset$, $\mathcal{D}_{lab} = \mathcal{D}^{min}_{lab} \cup \mathcal{D}^{maj}_{lab}$, $GSMOTE$
Input: $\mathcal{D}^t_{pool}$, $\mathcal{D}^t_{lab}$, f_c^{t-1}, f_{acq}, τ
Output: $\mathcal{D}^t_{train}$

Function *DataSelection*($\mathcal{D}^t_{lab}$, f_{acq}, f_c^{t-1})**:**
  $U \leftarrow \emptyset$
  $P \leftarrow \emptyset$
  $p_s \sim \mathcal{U}(0, 1)$
  forall $x_i \in \mathcal{D}^t_{lab}$ **do**
    $u_{x_i} \leftarrow f_{acq}(x_i; f_c^{t-1})$
    $U \leftarrow U \cup \{u_{x_i}\}$
  forall $u_{x_i} \in U$ **do**
    $p_{x_i} \leftarrow \frac{u_{x_i}}{\sum U} + \sum P$
    $P \leftarrow P \cup \{p_{x_i}\}$
  $i \leftarrow argmax(P < p_s)$
  return i-th element in $\mathcal{D}^t_{lab}$
begin
  $\mathcal{D}^{min}_{aug} \leftarrow \emptyset$
  $\mathcal{D}^{maj}_{aug} \leftarrow \emptyset$
  $\alpha_{af}, \alpha_{trunc}, \alpha_{def} \leftarrow \tau$
  $N \leftarrow count(C_{maj}) \times \alpha_{af}$
  forall $\mathcal{D}'_{aug} \in \{\mathcal{D}^{min}_{aug}, \mathcal{D}^{maj}_{aug}\}$, $\mathcal{D}'_{lab} \in \{\mathcal{D}^{min}_{lab}, \mathcal{D}^{maj}_{lab}\}$ **do**
    while $|\mathcal{D}'_{aug}| < N$ **do**
      $x_{center} \leftarrow DataSelection(\mathcal{D}'_{lab}, f_{acq}, f_c^{t-1})$
      $x_{gen} \leftarrow GSMOTE(x_{center}, \mathcal{D}^t_{lab}, \alpha_{trunc}, \alpha_{def})$
      $\mathcal{D}'_{aug} \leftarrow \mathcal{D}'_{aug} \cup \{x_{gen}\}$
  $\mathcal{D}_{aug} \leftarrow \mathcal{D}^{min}_{aug} \cup \mathcal{D}^{maj}_{aug}$
  $\mathcal{D}^t_{train} \leftarrow \mathcal{D}^t_{lab} \cup \mathcal{D}_{aug}$

chosen to measure AL performance and overall classification performance are defined in Subsection 5.4.3. The experimental procedure is described in Subsection 5.4.4.

The methodology developed serves a two-fold purpose: (1) Compare classification performance once all the AL procedures are completed (*i.e.,* optimal performance of a classifier trained via iterative data selection) and (2) Compare the amount of data required to reach specific performance thresholds (*i.e.,* the number of AL iterations required to reach similar classification performances).

5.4.1. Datasets

The datasets used to test the proposed method are publicly available in open data repositories. Specifically, they were retrieved from the OpenML and the UCI Machine Learning Repository websites. They were chosen considering diverse application domains, imbalance ratios, dimensionality and number of target classes, all of them focused on classification tasks. The goal is to demonstrate the performance of the different AL frameworks in various scenarios and domains. The data preprocessing approach was similar

Table 5.2.: Description of the datasets collected after data preprocessing. The sampling strategy is similar across datasets. Legend: (IR) Imbalance Ratio

Dataset	Features	Instances	Minority instances	Majority instances	IR	Classes
Image Segmentation	14	1155	165	165	1.0	7
Mfeat Zernike	47	1994	198	200	1.01	10
Texture	40	1824	165	166	1.01	11
Waveform	40	1666	551	564	1.02	3
Pendigits	16	1832	176	191	1.09	10
Vehicle	18	846	199	218	1.1	4
Mice Protein	69	1073	105	150	1.43	8
Gas Drift	128	1987	234	430	1.84	6
Japanese Vowels	12	1992	156	323	2.07	9
Usps	256	1859	142	310	2.18	10
Gesture Segmentation	32	1974	200	590	2.95	5
Volkert	147	1943	45	427	9.49	10
Steel Plates	24	1941	55	673	12.24	7
Baseball	15	1320	57	1196	20.98	3
Wine Quality	11	1599	10	681	68.1	6

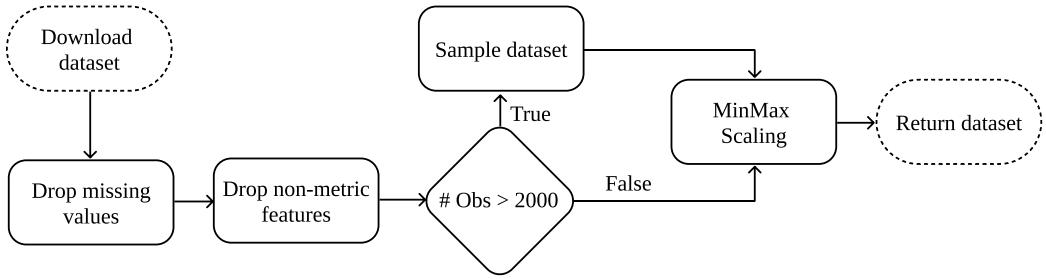

Figure 5.4.: Data preprocessing pipeline.

across all datasets. Table 5.2 describes the key properties of the 15 preprocessed datasets where the experimental procedure was applied.

The data preprocessing pipeline is depicted as a flowchart in Figure 5.4. The missing values are removed from each dataset by removing the corresponding observations. This step ensures that the input data in the experiment is kept as close to its original form as possible. The non-metric features (*i.e.,* binary, categorical, and ordinal variables) were removed since the application of G-SMOTE is limited to continuous and discrete features. The datasets containing over 2000 observations were downsampled in order to maintain the datasets to a manageable size. The data sampling procedure preserves the relative class frequency of the dataset, in order to maintain the Imbalance Ratio (IR) originally found in each dataset (where $IR = \frac{count(C_{maj})}{count(C_{\min})}$). The remaining features of each dataset are scaled to the range of $[-1, 1]$ to ensure a common range across features.

The preprocessed datasets were stored into an SQLite database file and is available along with the experiment's source code in the project's GitHub repository (see final remarks regarding data and software availability).

5.4.2. Machine Learning Algorithms

We used a total of four classification algorithms and a heuristic data augmentation mechanism. The choice of classifiers was based on the popularity and family of the classifiers (tree-based, nearest neighbors-based, ensemble-based and linear models). Our proposed method was tested using a Decision Tree (DT) [322], a K-nearest neighbors classifier (KNN) [251], a Random Forest Classifier (RF) [288] and a Logistic Regression (LR) [250]. Since the target variables are multi-class, the LR classifier was implemented using the one-versus-all approach. The predicted class is assigned to the label with the highest likelihood.

The oversampler G-SMOTE was used as a data augmentation method. The typical data generation policy of oversampling methods is to generate artificial observations on non-majority classes such that the number of majority class observations matches those of each non-majority class. We modified this data generation policy to generate observations for all classes, as a percentage of the number of observations in the majority class. In addition, the original G-SMOTE algorithm was modified to accept data selection probabilities based on classification uncertainty. These modifications are discussed in Section 5.3.

Every AL procedure was tested with different selection criteria: Random Selection, Entropy, and Breaking Ties. The baseline used is the standard AL procedure. As a benchmark, we add the AL procedure using G-SMOTE as a standard oversampling method, as proposed in [305]. Our proposed method was implemented using G-SMOTE as a data augmentation method to generate artificial observations for all classes, while still balancing the class distribution, as described in Section 5.3.

5.4.3. Evaluation Metrics

Considering the imbalanced nature of the datasets used in the experiment, commonly used performance metrics such as Overall Accuracy (OA), although being intuitive to interpret, are insufficient to quantify a model's classification performance [255]. The Cohen's Kappa performance metric, similar to OA, is also biased towards high-frequency classes since its definition is closely related to the OA metric, making its behavior consistent with OA [323]. However, these metrics remain popular choices for the evaluation of classification performance. Other performance metrics like $Precision = \frac{TP}{TP+FP}$, $Recall = \frac{TP}{TP+FN}$ (also known as Sensitivity) or $Specificity = \frac{TN}{TN+FP}$ are calculated as a function of True/False Positives (TP and FP) and True/False Negatives (TN and FN) and can be used on a per-class basis instead. In a multiple dataset scenario with varying amounts of target classes and meanings, comparing the performance of different models using these metrics becomes impractical.

Based on the recommendations found in [255, 289], we used two metrics found to be less sensitive to the class imbalance bias, along with OA as a reference for easier interpretability:

- The Geometric-mean scorer (G-mean) consists of the geometric mean of Specificity and Recall [289]. Both metrics are calculated in a multi-class context considering a one-versus-all approach. For multi-class problems, the G-mean scorer is calculated as its average per class values:

$$G\text{-}mean = \sqrt{\overline{Recall} \times \overline{Specificity}}$$

- The F-score metric consists of the harmonic mean of Precision and Recall. The two metrics are also calculated considering a one-versus-all approach. The F-score for the multi-class case can be calculated using its average per class values [255]:

$$F\text{-}score = 2 \times \frac{\overline{Precision} \times \overline{Recall}}{\overline{Precision} + \overline{Recall}}$$

- The OA consists of the number of TP divided by the total amount of observations. Considering c as the label for the different classes present in a target class, OA is given by the following formula:

$$OA = \frac{\sum_c \mathrm{TP}_c}{\sum_c (\mathrm{TP}_c + \mathrm{FP}_c)}$$

The comparison of the performance of AL frameworks is based on its data selection and augmentation efficacy. Specifically, an efficient data selection/generation policy allows the production of classifiers with high performance on unseen data while using as least non-artificial training data as possible. We follow the recommendations found in [36]. To measure the performance of the different AL setups, the performance of an AL setup will be compared using two AL-specific performance metrics:

- Area Under the Learning Curve (AULC). It is the sum of the classification performance over a validation/test set of the classifiers trained of all AL iterations. The resulting AULC scores are fixed within the range $[0, 1]$ by dividing the AULC scores by the total amount of iterations (*i.e.*, the maximum performance area) to facilitate the interpretability of this metric.
- Data Utilization Rate (DUR) [290]. Measures the percentage of training data required to reach a given performance threshold, as a ratio of the percentage of training data required by the baseline framework. This metric is also presented as a percentage of the total amount of training data, without making it relative to the baseline framework. The DUR metric is measured at 45 different performance thresholds, ranging between $[0.10, 1.00]$ at a 0.02 step.

5.4.4. Experimental Procedure

The evaluation of different active learners in a live setting is generally expensive, time-consuming, and prone to human error. Instead, a common practice is to compare them in an offline environment using labeled datasets [291]. Since the dataset is already labeled, the annotation process is done at zero cost in this scenario. Figure 5.5 depicts the experiment designed for one dataset over a single run.

A single run starts with the splitting of a preprocessed dataset into five different partitions, stratified according to the class frequencies of the target variable using the K-fold Cross Validation method. During this run, an active learner or classifier is trained five times using a different partition as the Test set each time. For each training process, a validation set containing 25% of the subset is created and is used to measure the data selection efficiency (*i.e.,* AULC and DUR using the classification performance metrics, specific to AL). Therefore, for a single training procedure, 20% of the original dataset is used as the validation set, 20% is used as the Test set and 60% is used as the training set. The AL simulations and the classifiers' training occur within the training set. However, the classifiers used to find the maximum performance classification scores are trained over the full training set. The AL simulations are run over a maximum of 50 iterations (including the initialization step), adding 1.6% of the training set each time (*i.e.,* all AL simulations use less than 80% of the training set). Once the training phase is completed, the Test set classification scores are calculated using the trained classifiers. For the case of AL, the classifier with the optimal validation set score is used to estimate the AL's optimal classification performance over unseen data.

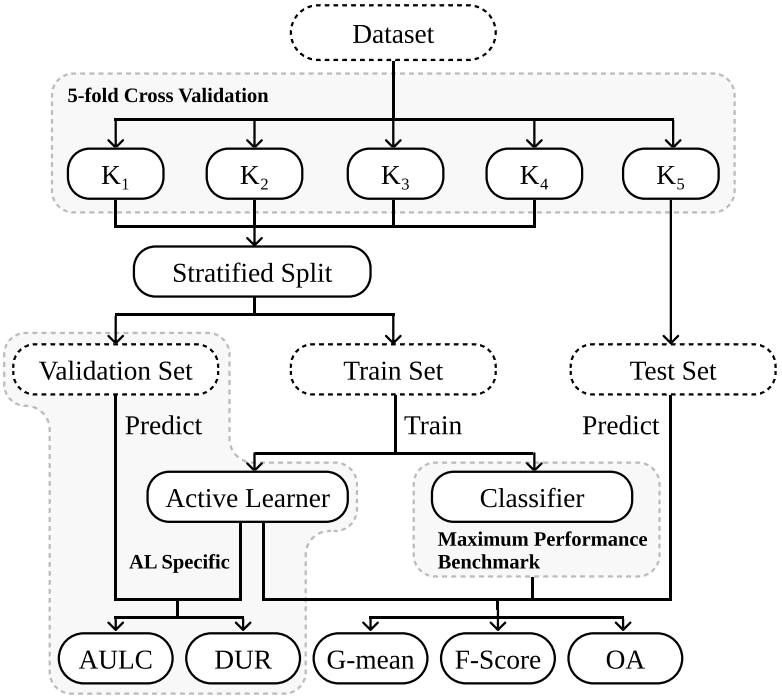

Figure 5.5.: Experimental procedure flowchart. The preprocessed datasets are split into five folds. One of the folds is used to test the best-found classifiers using AL and the classifiers trained using the entire training dataset (containing the remaining folds). The training set is used to run both the AL simulations as well as train the normal classifiers. The validation set is used to measure AL-specific performance metrics over each iteration. We use different subsets for overall classification performance and AL-specific performance to avoid data leakage.

The process shown in Figure 5.5 is repeated over three runs using different random seeds over the 15 different datasets collected. The final scores of each AL configuration and classifier correspond to the average of the three runs and 5-fold Cross-Validation estimations (*i.e.,* the mean score of 15 fits, across 15 datasets).

The hyperparameters defined for the AL frameworks, Classifiers, and Generators are shown in Table 5.3. In the Generators table, we distinguish the G-SMOTE algorithm working as a normal oversampling method from G-SMOTE-AUGM, which generates additional artificial data on top of the usual oversampling mechanism. Since the G-SMOTE-AUGM method is intended to be used with varying parameter values (via within-iteration parameter tuning), the parameters were defined as a list of various possible values. The remaining parameters were selected based on knowledge gathered in previous literature and typical default values for each of the algorithms. This choice was motivated by the impossibility of parameter tuning in a real-world setting when applying the benchmark AL methods. Although the proposed method addresses this limitation, we show that exclusively tuning the parameters on the augmentation policy is already sufficient to achieve superior, statistically significant performance.

5.4.5. Software Implementation

The experiment was implemented using the Python programming language, along with the Python libraries Scikit-Learn [257], Imbalanced-Learn [258], Geometric-SMOTE [23], Research-Learn and ML-Research libraries. All functions, algorithms, experiments, and results are provided in the project's GitHub

Table 5.3.: Hyperparameter definition for the active learners, classifiers, and generators used in the experiment.

Active Learners	Hyperparameters	Inputs
Standard	# initial obs.	1.6%
	# additional obs. per iteration	1.6%
	max. iterations + initialization	50
	evaluation metrics	G-mean, F-score, OA
	selection strategy	Random, Entropy, Breaking Ties
	within-iteration param. tuning	None
	generator	None
	classifier	DT, LR, KNN, RF
Oversampling	generator	G-SMOTE
Proposed	generator	G-SMOTE-AUGM
	within-iteration param. tuning	Grid Search K-fold CV
Classifier		
DT	min. samples split	2
	criterion	gini
LR	maximum iterations	100
	multi-class	One-vs-All
	solver	liblinear
	penalty	L2 (Ridge)
KNN	# neighbors	5
	weights	uniform
	metric	euclidean
RF	min. samples split	2
	# estimators	100
	criterion	gini
Generator		
G-SMOTE	# neighbors	4
	deformation factor	0.5
	truncation factor	0.5
G-SMOTE-AUGM	# neighbors	3, 4, 5
	deformation factor	0.5
	truncation factor	0.5
	augmentation factor	$[1.1, 2.0]$ at 0.1 step

repository. The original datasets used in this study are publicly available in open data repositories. They were retrieved from OpenML and the UCI Machine Learning Repository.

5.5. Results & Discussion

In a multiple dataset experiment, the analysis of results should not rely upon the average performance scores across datasets uniquely. The domain of application and fluctuations of performance scores between datasets make the analysis of these averaged results less accurate. Instead, it is generally recommended to use the mean ranking scores to extend the analysis [259]. Since mean performance scores are still intuitive to interpret; we will present and discuss both results. The rank values are assigned based on the mean scores of three different 5-fold Cross-Validation runs (15 performance estimations per dataset) for each combination of dataset, AL configuration, classifier, and performance metric.

5.5.1. Results

The average rankings of the AL methods' AULC estimations are shown in Table 5.4. The proposed method almost always improves AL performance and ensures higher data selection efficiency.

Table 5.4.: Mean rankings of the AULC metric over the different datasets (15), folds (5), and runs (3) used in the experiment. The proposed method constantly improves the results of the original framework and, on average, almost always improves the results of the oversampling framework.

Classifier	Evaluation Metric	Standard	Oversampling	Proposed
DT	Accuracy	2.13 ± 0.96	2.40 ± 0.49	**1.47 ± 0.62**
DT	F-score	2.47 ± 0.81	2.20 ± 0.40	**1.33 ± 0.70**
DT	G-mean	2.73 ± 0.57	1.93 ± 0.44	**1.33 ± 0.70**
KNN	Accuracy	2.07 ± 0.93	2.07 ± 0.68	**1.87 ± 0.81**
KNN	F-score	2.47 ± 0.81	1.87 ± 0.50	**1.67 ± 0.87**
KNN	G-mean	2.87 ± 0.34	**1.47 ± 0.50**	1.67 ± 0.70
LR	Accuracy	2.13 ± 0.88	2.20 ± 0.65	**1.67 ± 0.79**
LR	F-score	2.80 ± 0.40	1.87 ± 0.50	**1.33 ± 0.70**
LR	G-mean	2.80 ± 0.40	1.80 ± 0.54	**1.40 ± 0.71**
RF	Accuracy	2.27 ± 0.85	**1.87 ± 0.50**	**1.87 ± 0.96**
RF	F-score	2.73 ± 0.57	1.80 ± 0.54	**1.47 ± 0.72**
RF	G-mean	2.87 ± 0.34	**1.53 ± 0.50**	1.60 ± 0.71

Table 5.5 shows the average AULC scores, grouped by the classifier, Evaluation Metric and AL framework. The performance of the proposed method is almost always superior when considering the F-score and G-mean. On some occasions, the average AULC score is significantly improved when compared with the oversampling AL method.

The average DUR scores were calculated for various G-mean thresholds, varying between 0.1 and 1.0 at a 0.02 step (45 different thresholds in total). Table 5.6 shows the results obtained for these scores starting from a G-mean score of 0.6 and was filtered to show the thresholds ending with 0 or 6 only. In most cases, the proposed method reduces the amount of data annotation required to reach each G-mean score threshold.

Table 5.5.: Average AULC of each AL configuration tested. Each AULC score is calculated using the performance scores of each iteration in the validation set. By the end of the iterative process, each AL configuration used a maximum of 80% instances of the 60% instances that compose the training sets (*i.e.,* 48% of the entire preprocessed dataset).

Classifier	Evaluation Metric	Standard	Oversampling	Proposed
DT	Accuracy	0.663 ± 0.149	0.658 ± 0.153	**0.664 ± 0.155**
DT	F-score	0.610 ± 0.176	0.612 ± 0.179	**0.618 ± 0.181**
DT	G-mean	0.744 ± 0.129	0.751 ± 0.127	**0.755 ± 0.129**
KNN	Accuracy	**0.741 ± 0.160**	0.730 ± 0.178	0.734 ± 0.179
KNN	F-score	0.678 ± 0.208	0.684 ± 0.211	**0.687 ± 0.213**
KNN	G-mean	0.786 ± 0.152	**0.804 ± 0.139**	**0.804 ± 0.141**
LR	Accuracy	**0.736 ± 0.152**	0.723 ± 0.185	0.731 ± 0.184
LR	F-score	0.644 ± 0.228	0.673 ± 0.220	**0.682 ± 0.221**
LR	G-mean	0.767 ± 0.162	0.811 ± 0.134	**0.814 ± 0.136**
RF	Accuracy	**0.789 ± 0.148**	0.786 ± 0.153	0.785 ± 0.156
RF	F-score	0.724 ± 0.214	**0.735 ± 0.204**	**0.735 ± 0.205**
RF	G-mean	0.818 ± 0.150	**0.834 ± 0.135**	0.833 ± 0.135

The DUR scores relative to the Standard AL method are shown in Figure 5.6. A DUR below 1 means that the Proposed/Oversampling method requires less data than the Standard AL method to reach the same performance threshold. For example, running an AL simulation using the KNN classifier requires 80.7% of the amount of data required by the Standard AL method using the same classifier to reach an F-Score of 0.62 (*i.e.,* requires 19.3% less data).

The comparison of mean optimal classification scores of AL methods with Classifiers (using the entire training set, without AL) is shown in Table 5.7. Aside from the case of overall accuracy, the proposed AL method produces classifiers that almost consistently outperform classifiers using the whole training set (*i.e.,* the ones labeled as MP).

5.5.2. Statistical Analysis

When checking for statistical significance in a multiple dataset context it is critical to account for the multiple comparison problem. Consequently, our statistical analysis focuses on the recommendations found in [259]. Overall, we perform three statistical tests. The Friedman test [260] is used to understand whether there is a statistically significant difference in performance between the three AL frameworks. As *post hoc* analysis, the Wilcoxon signed-rank test [261] was utilized to check for statistical significance between the performance of the proposed AL method and the oversampling AL method across datasets. As a second *post hoc* analysis, the Holm-Bonferroni [324] method was employed to check for statistical significance between the methods using data generators and the Standard AL framework across classifiers and evaluation metrics.

Table 5.8 displays the *p-values* obtained with the Friedman test. The difference in performance across AL frameworks is statistically significant at a level of $\alpha = 0.05$ regardless of the classifier or evaluation metric being considered.

Table 5.9 contains the *p-values* obtained with the Wilcoxon signed-rank test. The proposed method was able to outperform both the standard AL framework, as well as the AL framework using a typical oversampling policy with statistical significance in 14 and 12 out of 15 datasets, respectively.

Table 5.6.: AL algorithms' mean data utilization as a percentage of the training set.

G-mean Score	Classifier	Standard	Oversampling	Proposed
0.60	DT	19.8%	**18.9%**	19.3%
0.60	KNN	18.4%	**11.8%**	12.8%
0.60	LR	23.0%	**9.7%**	**9.7%**
0.60	RF	14.1%	**7.7%**	7.8%
0.66	DT	23.1%	23.3%	**22.9%**
0.66	KNN	23.9%	**21.7%**	21.9%
0.66	LR	25.6%	**20.5%**	**20.5%**
0.66	RF	22.0%	17.6%	**17.5%**
0.70	DT	25.5%	25.0%	**24.8%**
0.70	KNN	26.8%	24.1%	**23.9%**
0.70	LR	29.9%	23.6%	**23.4%**
0.70	RF	23.8%	**22.1%**	22.3%
0.76	DT	33.4%	30.5%	**30.1%**
0.76	KNN	34.0%	27.7%	**27.3%**
0.76	LR	38.0%	27.6%	**26.2%**
0.76	RF	28.2%	**24.5%**	24.7%
0.80	DT	48.2%	43.8%	**41.2%**
0.80	KNN	38.8%	**34.4%**	34.6%
0.80	LR	43.7%	32.6%	**31.3%**
0.80	RF	32.4%	**27.2%**	27.7%
0.86	DT	69.6%	66.5%	**64.8%**
0.86	KNN	53.9%	**52.0%**	52.5%
0.86	LR	48.7%	45.3%	**45.0%**
0.86	RF	43.9%	**40.0%**	**40.0%**
0.90	DT	81.2%	79.4%	**76.6%**
0.90	KNN	60.9%	61.1%	**60.4%**
0.90	LR	62.1%	62.9%	**59.9%**
0.90	RF	57.1%	**55.7%**	56.2%
0.96	DT	100.0%	**99.7%**	100.0%
0.96	KNN	82.4%	79.7%	**77.1%**
0.96	LR	86.5%	84.0%	**81.8%**
0.96	RF	70.8%	71.1%	**70.3%**

The *p-values* shown in Table 5.10 refer to the results of the Holm-Bonferroni test. The proposed method's superior performance was statistically significant in 9 out of 12 cases.

5.5.3. Discussion

In this paper, we study the application of data augmentation methods through the modification of the standard AL framework. This is done to further reduce the amount of labeled data required to produce a reliable classifier, at the expense of artificial data generation. Overall, the proposed method achieves better and more consistent performance when compared to the remaining benchmark approaches. It was implemented to focus on the optimization of the data augmentation policy, as well as the introduction of a more informed AL-based data augmentation approach. The proposed method could be further extended and achieve an even higher performance by optimizing parameters of the ML classification using the

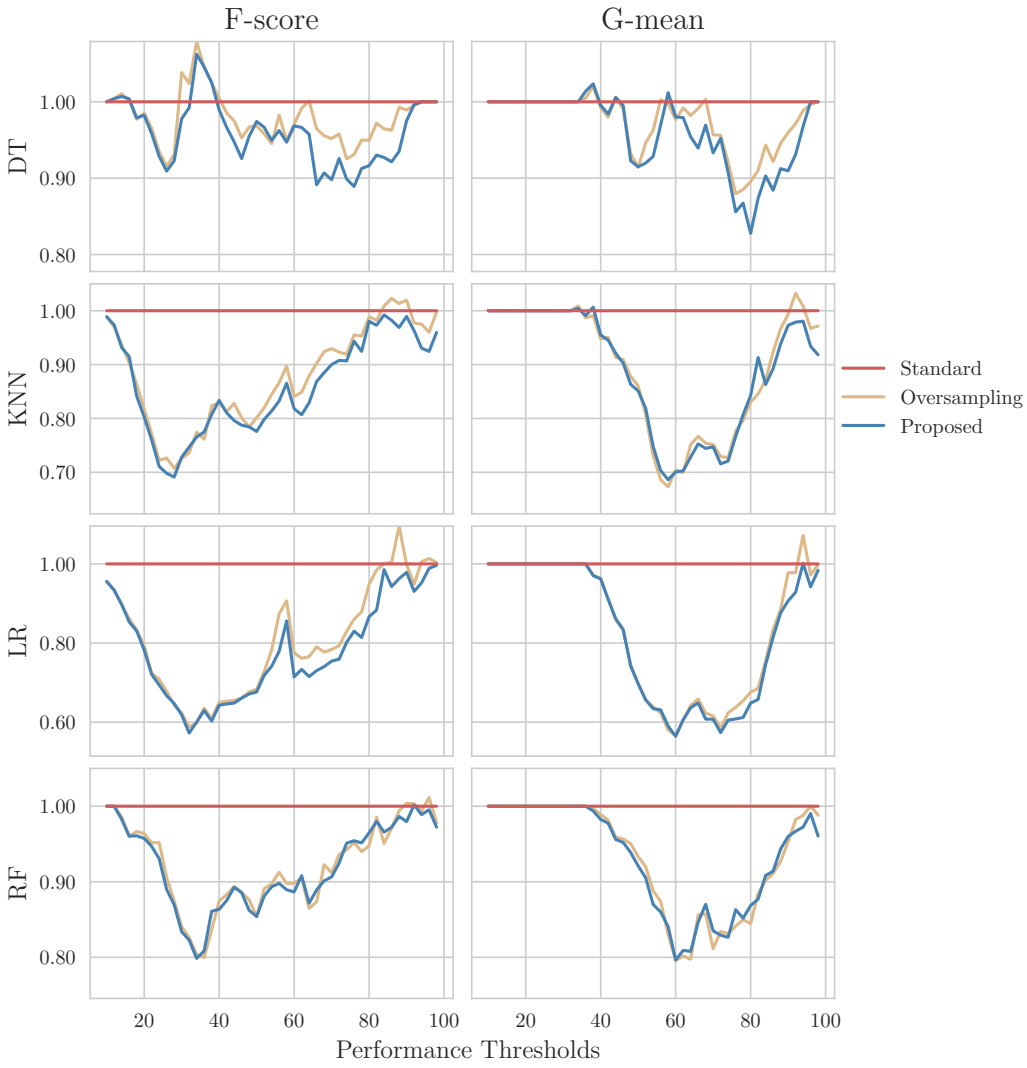

Figure 5.6.: Mean data utilization rates. The y-axis shows the percentage of data (relative to the baseline AL framework) required to reach the different performance thresholds.

hyperparameter optimizer. In addition, this framework could be further generalized by searching, within AL iterations, for the optimal ML classifier as well; at different stages of the data collection procedure some ML classifiers might be more useful than others. Although the proposed framework significantly improves the flexibility of AL implementations, we found that even a superficial parameter search is sufficient to ensure a superior performance when compared to related approaches.

In Table 5.4, we found that the proposed method was able to outperform the Standard AL framework in all scenarios. Except for the overall accuracy metric, the mean rankings are consistent with the mean AULC scores found in Table 5.5, while showing performance improvements between the proposed method and both the standard and oversampling methods. The Friedman test in Table 5.8 showed that the difference in the performance of these AL frameworks are statistically significant, regardless of the classifier or performance metric being used.

The proposed method evidenced more consistent data utilization requirements in most of the assessed G-mean score thresholds when compared to the remaining AL methods, as seen in Table 5.6. For example, to reach a G-mean score of 0.9 using the KNN and LR classifiers, the average amount of data required with the Oversampling AL approach increased when compared to the standard approach. However, the

Table 5.7.: Optimal classification scores. The Maximum Performance (MP) classification scores are calculated using classifiers trained using the entire training set.

Classifier	Evaluation Metric	MP	Standard	Oversampling	Proposed
DT	Accuracy	**0.732 ± 0.155**	0.726 ± 0.157	0.721 ± 0.167	0.727 ± 0.168
DT	F-score	0.682 ± 0.194	0.679 ± 0.193	0.679 ± 0.197	**0.684 ± 0.200**
DT	G-mean	0.792 ± 0.138	0.791 ± 0.136	0.797 ± 0.134	**0.800 ± 0.137**
KNN	Accuracy	**0.801 ± 0.164**	0.799 ± 0.168	0.784 ± 0.183	0.789 ± 0.183
KNN	F-score	0.742 ± 0.224	0.744 ± 0.223	0.741 ± 0.223	**0.746 ± 0.224**
KNN	G-mean	0.827 ± 0.160	0.829 ± 0.158	0.839 ± 0.146	**0.840 ± 0.147**
LR	Accuracy	0.778 ± 0.157	**0.791 ± 0.158**	0.764 ± 0.184	0.773 ± 0.185
LR	F-score	0.693 ± 0.243	0.717 ± 0.241	0.718 ± 0.222	**0.727 ± 0.226**
LR	G-mean	0.796 ± 0.171	0.814 ± 0.165	0.839 ± 0.130	**0.842 ± 0.137**
RF	Accuracy	0.827 ± 0.145	**0.832 ± 0.148**	0.827 ± 0.154	0.829 ± 0.153
RF	F-score	0.767 ± 0.215	0.775 ± 0.216	0.781 ± 0.204	**0.784 ± 0.204**
RF	G-mean	0.844 ± 0.148	0.849 ± 0.149	0.863 ± 0.131	**0.865 ± 0.131**

Table 5.8.: Friedman test results. Statistical significance is tested at a level of $\alpha = 0.05$. The null hypothesis is that there is no difference in the classification outcome across oversamplers.

Classifier	Evaluation Metric	p-value	Significance
DT	Accuracy	1.1e-15	True
DT	F-score	2.4e-31	True
DT	G-mean	2.3e-23	True
KNN	Accuracy	5.9e-20	True
KNN	F-score	8.8e-69	True
KNN	G-mean	8.8e-52	True
LR	Accuracy	1.1e-30	True
LR	F-score	4.0e-98	True
LR	G-mean	2.3e-83	True
RF	Accuracy	2.8e-26	True
RF	F-score	1.8e-88	True
RF	G-mean	1.8e-61	True

proposed method was able to decrease the amount of data required in both situations. The robustness of the proposed method is clearer in Figure 5.6. In most cases, this method was able to outperform the Oversampling method. At the same time, the proposed method also addresses inconsistencies in situations where the Oversampling method was unable to outperform the standard method.

The statistical analyses found in Tables 5.9 and 5.10 revealed that the proposed method's superiority was statistically significant in all datasets except three (Baseball, Usps, and Volkert) and established statistical significance when compared to the standard AL method for all combinations of classifier and performance metric, except for three cases regarding the use of the overall accuracy metric. These results show that the proposed method increased the reliability of the new AL framework and improved the quality of the final classifier while using fewer data.

Even though it was not the core purpose of this study, we found that the proposed AL method consistently outperformed the maximum performance threshold. Specifically, in Table 5.7, the performance of the classifiers originating from the proposed method was able to outperform classifiers trained using the full training dataset in 9 out of 12 scenarios. This outcome suggests that the selection of a meaningful training

Table 5.9.: Adjusted p-values using the Wilcoxon signed-rank method. Bold values are statistically significant at a level of $\alpha = 0.05$. The null hypothesis is that the performance of the proposed framework is similar to that of the oversampling or standard framework.

Dataset	Oversampling	Standard
Baseball	5.0e-01	3.4e-01
Gas Drift	**3.7e-26**	**4.6e-57**
Gesture Segmentation	**1.3e-02**	**8.7e-04**
Image Segmentation	**9.6e-18**	**2.1e-44**
Japanese Vowels	**2.4e-09**	**1.6e-32**
Mfeat Zernike	**1.2e-12**	**9.5e-40**
Mice Protein	**6.5e-32**	**1.5e-61**
Pendigits	**5.0e-18**	**2.3e-45**
Steel Plates	**3.4e-04**	**1.3e-08**
Texture	**1.5e-22**	**6.7e-57**
Usps	3.8e-01	**2.1e-29**
Vehicle	**7.4e-11**	**7.9e-13**
Volkert	2.5e-01	**1.3e-02**
Waveform	**8.9e-08**	**2.6e-02**
Wine Quality	**3.8e-05**	**6.1e-03**

Table 5.10.: Adjusted p-values using the Holm-Bonferroni method. Bold values are statistically significant at a level of $\alpha = 0.05$. The null hypothesis is that the Oversampling or Proposed method does not perform better than the control method (Standard AL framework).

Classifier	Evaluation Metric	Oversampling	Proposed
DT	Accuracy	7.7e-01	**1.1e-04**
DT	F-score	6.3e-02	**2.0e-06**
DT	G-mean	**1.0e-08**	**2.9e-12**
KNN	Accuracy	**1.0e-02**	8.5e-01
KNN	F-score	**7.1e-07**	**8.3e-13**
KNN	G-mean	**1.9e-11**	**1.0e-12**
LR	Accuracy	**3.2e-02**	8.3e-01
LR	F-score	**1.5e-09**	**5.8e-17**
LR	G-mean	**1.9e-13**	**5.6e-16**
RF	Accuracy	4.3e-01	4.3e-01
RF	F-score	**1.4e-11**	**1.1e-12**
RF	G-mean	**1.5e-10**	**1.2e-10**

subset training dataset paired with data augmentation not only matches the classification performance of ML algorithms, as it also improves them. Even in a setting with fully labeled training data, the proposed method may be used as a preprocessing technique to further optimize classification performance.

This study discussed the effect of data augmentation within the AL framework, along with the exploration of optimal augmentation methods within AL iterations. However, the conceptual nature of this study implies some limitations. Specifically, the large number of experiments required to test the method's efficacy, along with the limited computational power available, led to a limited exploration of the grid search's potential. Future work should focus on understanding how the usage of a more comprehensive parameter tuning approach improves the quality of the AL method. In addition, the proposed method was not able to outperform the standard AL method at 100% of scenarios. The exploration of other, more complex data augmentation techniques might further improve its performance by producing more meaningful training observations. Specifically, in this study, we assume that all datasets used follow a manifold, allowing the usage of G-SMOTE as a data augmentation approach. However, this method cannot be used in more complex, non-euclidean spaces. In this scenario, the usage of G-SMOTE is not valid and might lead to the production of noisy data. Deep Learning-based data augmentation techniques are able to address this limitation and improve the overall quality of the artificial data being generated. We also encountered significant standard errors throughout our experimental results (see Subsection 5.5.1), consistent with the findings in [305, 36]. This facet suggests that the usage of more robust generators did not decrease the standard error of AL performance. Instead, AL's performance variability is likely dependent on the quality of its initialization.

5.6. Conclusion and Future Directions

The ability to train ML classifiers is usually limited to the availability of labeled data. However, manually labeling data is often expensive, which makes the usage of AL particularly appealing for selecting the most informative observations and reducing the amount of required labeled data. On the other hand, the introduction of data variability in the training dataset can also be conducted via data augmentation. However, most, if not all, AL configurations that use some form of data augmentation are domain and/or task-specific. These methods typically apply deep learning approaches to both classification and data augmentation. Consequently, they may not apply to other classification tasks or when the available computational power is insufficient.

In this paper, we proposed a domain-agnostic AL framework that implements Data Augmentation and hyperparameter tuning. We found that a heuristic Data Augmentation algorithm is sufficient to improve the data selection efficiency in AL. Specifically, the data augmentation method used almost always increased AL performance, regardless of the target goal (*i.e.,* optimizing classification or data selection efficiency). The usage of data augmentation reduced the number of iterations required to train a classifier with a performance as good as (or better than) classifiers trained with the entire training dataset (*i.e.,* without using AL). In addition, the proposed method reduced the size of the training dataset, which is expanded with artificial data.

With this revised AL configuration, data selection in AL iterations aims towards observations that optimize the quality of the artificial data produced. The substitution of less informative labeled data with artificial data is especially useful in this context since it reduces some of the user interaction necessary to reach a sufficiently informative dataset. In order to further improve the proposed method, future work should (1) focus on the development of methods with varying data augmentation policies depending on the different input space regions, (2) develop augmentation-sensitive query functions capable of avoiding the unnecessary selection of similar observations from the unlabeled dataset, (3) understand the gap between randomized data augmentation techniques and neural network/feature space data augmentation

techniques in an AL context better, (4) explore more efficient ways to leverage the information collected in AL queries for better augmentation strategies and (5) expand the current framework to integrate alternative learning strategies using unlabeled data, such as self and semi supervised learning techniques.

Finally, the proposed method may be applied to any classification problem where labeled data is not readily available and an easily accessible unlabeled data pool. For more complex data structures, the application of this framework will require the learning of a manifold space as an additional preprocessing step. After that, this AL framework may be used as is.

6. Geometric SMOTE for Imbalanced Datasets with Nominal and Continuous Features

Submitted as Joao Fonseca, Fernando Bacao, to a Q1 Journal, 2023

Imbalanced learning can be addressed in 3 different ways: resampling, algorithmic modifications and cost-sensitive solutions. Resampling, and specifically oversampling, are more general approaches when opposed to algorithmic and cost-sensitive methods. Since the proposal of the Synthetic Minority Oversampling TEchnique (SMOTE), various SMOTE variants and neural network-based oversampling methods have been developed. However, the options to oversample datasets with nominal and continuous features are limited. We propose Geometric SMOTE for Nominal and Continuous features (G-SMOTENC), based on a combination of G-SMOTE and SMOTENC. Our method modifies SMOTENC's encoding and generation mechanism for nominal features while using G-SMOTE's data selection mechanism to determine the center observation and k-nearest neighbors and generation mechanism for continuous features. G-SMOTENC's performance is compared against SMOTENC's along with two other baseline methods, a State-of-the-art oversampling method and no oversampling. The experiment was performed over 20 datasets with varying imbalance ratios, number of metric and non-metric features and target classes. We found a significant improvement in classification performance when using G-SMOTENC as the oversampling method. An open-source implementation of G-SMOTENC is made available in the Python programming language.

Keywords: Imbalanced Learning; Oversampling; SMOTE; Data Generation; Nominal Data

6.1. Introduction

Various Machine Learning (ML) tasks deal with highly imbalanced datasets, such as fraud transactions detection, fault detection and medical diagnosis [325]. In these situations, predicting false positives is often a more acceptable error, since the class of interest is usually the minority class [326]. However, using standard ML classifiers on imbalanced datasets induces a bias in favor of the classes with the highest frequency, while limiting the predictive power on lower frequency classes [327, 328]. This effect is known in the ML community as the Imbalanced Learning problem.

Imbalanced learning involves a dataset with two or more target classes with varying class frequencies. The minority class is defined as the class with the least amount of observations and the majority class is the one with the highest amount of observations [329]. There are three main approaches to address imbalanced learning [9]:

1. Cost-sensitive solutions attribute a higher misclassification cost to the minority class observations to minimize higher cost errors;
2. Algorithmic level solutions modify ML classifiers to improve the learning of the minority class;
3. Resampling solutions generate synthetic minority class observations and/or remove majority class observations to balance the training dataset;

Since it is an external approach to imbalanced learning, the latter method becomes particularly useful. It dismisses the required domain knowledge to build a cost matrix and the technical complexity or knowledge to apply an imbalanced learning-specific classifier. Resampling can be done via undersampling, oversampling, or hybrid approaches [330]. In this paper, we will focus on oversampling approaches.

The presence of nominal features in imbalanced learning tasks limits the options available to deal with class imbalance. Even though it is possible to use encoding methods such as one-hot or ordinal encoding to convert nominal features into numerical, applying a distance metric on mixed-type datasets is questionable since the nominal feature values are unordered [331]. In this case, one possible approach is to use models that can handle different scales (*e.g.*, Decision Tree). However, this assumption may be limiting since there are few ML algorithms where this condition is verified. Another possible approach is transforming the variables to meet scale assumptions [331]. This method was explored in the algorithm Synthetic Minority Oversampling Technique for Nominal and Continuous features (SMOTENC) [22] (explained in Section 6.2).

In the presence of datasets with mixed data types, using most of the well-known resampling algorithms becomes unfeasible. This happens because these methods consider exclusively continuous data; they were not adapted to also use nominal features. Specifically, since the proposal of SMOTE, various other SMOTE-variants have been developed to address some of its limitations. Although, there was not a significant development in research to oversample datasets with both nominal and continuous features.

In this paper, we propose Geometric SMOTE for Nominal and Continuous features (G-SMOTENC). It generates the continuous feature values of a synthetic observation within a truncated hyper-spheroid with its nominal feature values using the most common value of its nearest neighbors. In addition, G-SMOTENC uses G-SMOTE's data selection strategy and SMOTENC's approach to find the center observation's nearest neighbors. G-SMOTENC is a generalization of both SMOTENC and G-SMOTE [23]. With the correct hyperparameters, our G-SMOTENC implementation can mimic the behavior of SMOTE, SMOTENC, or G-SMOTE. It is available in the open-source Python library "ML-Research" and is fully compatible with the Scikit-Learn ecosystem. These contributions can be summarized as follows:

1. We propose G-SMOTENC, an oversampling algorithm for datasets with nominal and continuous features;
2. We test the proposed oversampler using 20 datasets and compare its performance to SMOTENC, Random Oversampling, Random Undersampling and a State-of-the-art oversampler;
3. We provide an implementation of G-SMOTENC in the Python programming language;

The rest of this paper is structured as follows: Section 6.2 describes the related work and its limitations, Section 6.3 describes the proposed method (G-SMOTENC), Section 6.4 lays out the methodology used to test G-SMOTENC, Section 6.5 shows and discusses the results obtained in the experiment and Section 6.6 presents the conclusions drawn from this study.

6.2. Related Work

A classification problem contains n classes, having C_{maj} as the set of majority class observations (*i.e.*, observations belonging to the most common target class) and C_{min} as the set of minority class observations (*i.e.*, observations belonging to the least common target class). Typically, an oversampling algorithm will generate synthetic data in order to ensure $|C'_{min}| = |C_{maj}| = |C_i|, i \in \{1, \ldots, n\}$.

Since the proposal of SMOTE, other methods modified or extended SMOTE to improve the quality of the data generated. The process of generating synthetic data using SMOTE-based algorithms can be divided into two distinct phases [332]:

1. Data selection. A synthetic observation, x^{gen}, is generated based on two existing observations. A SMOTE-based algorithm employs a given heuristic to select a non-majority class observation as the center observation, x^c, and one of its nearest neighbors, x^{nn}, selected randomly. For the case of SMOTE, x^c is randomly selected from each non-majority class.
2. Data generation. Once x^c and x^{nn} have been selected, x^{gen} is generated based on a transformation between the two selected observations. In the case of SMOTE, this transformation is a linear interpolation between the two observations: $x^{gen} = \alpha x^c + (1 - \alpha)x^{nn}, \alpha \sim \mathcal{U}(0, 1)$.

Modifications to the SMOTE algorithm can be distinguished according to the phase where they were applied. This distinction is especially relevant for the case of oversampling on datasets with mixed data types since it raises the challenge of calculating meaningful distances and k-nearest neighbors among observations. For example, State-of-the-art oversampling methods, such as Borderline-SMOTE [24], ADASYN [246], K-means SMOTE [25] and LR-SMOTE [125] modify the data selection mechanism and show promising results in imbalanced learning [30]. However, these algorithms select x^c using procedures that include calculating each observation's k-nearest neighbors or clustering methods, which are not prepared to handle nominal data.

Modifications to SMOTE's generation mechanism are uncommon. A few oversampling methods, such as Safe-level SMOTE [124] and Geometric-SMOTE [23] proposed this type of modification and have shown promising results [2]. However, these methods are also unable to handle datasets with nominal data. Other methods attempt to replace the SMOTE data generation mechanism altogether using different Generative Adversarial Networks (GAN) architectures [333, 334, 335]. Network-based architectures, however, are computationally expensive to train and sensitive to the training initialization. It is also difficult to ensure a balanced training of the two networks involved and tuning their hyperparameters is often challenging or unfeasible [336].

As discussed in Section 6.1, research on resampling methods with mixed data types is scarce. The original paper proposing SMOTE also proposed SMOTE for Nominal and Continuous (SMOTENC), an adaptation of SMOTE to handle datasets with nominal and continuous features [22]. To determine the k-nearest neighbors of x^c, the Euclidean distance is modified to include the median of the standard deviations of the continuous features for every nominal feature with different values. Once x^c and x^{nn} are defined, the continuous feature values in x^{gen} are generated using the SMOTE generation mechanism. The nominal features are given the most common values occurring in the k-nearest neighbors.

Recently, a new SMOTE-based oversampling method for datasets with mixed data types, SMOTE-ENC [337], was proposed. This method modifies the encoding mechanism for nominal features used in the SMOTENC algorithm to account for nominal features' change of association with minority classes. The Multivariate Normal Distribution-based Oversampling for Numerical and Categorical features (MNDO-NC) [338] uses the original MNDO method [339] along with the SMOTENC encoding mechanism to find the values of the categorical features for the synthetic observation. However, the results reported in the

paper showed that MNDO-NC was consistently outperformed by SMOTENC, which led us to discard this approach from further consideration.

Alternatively to SMOTE-based methods, it is possible to use non-informed over and undersampling methods for datasets with nominal and continuous features, specifically Random Oversampling (ROS) and Random Undersampling (RUS). These methods consist of randomly duplicating minority class observations (in the case of ROS), which can lead to overfitting [340, 341], or randomly removing majority class observations (in the case of RUS), which may lead to underfitting [342].

6.3. Proposed Method

We propose G-SMOTENC to oversample imbalanced datasets with both nominal and continuous features. Our method builds on top of G-SMOTE's selection and generation mechanisms coupled with a modified version of SMOTENC. It attributes less importance to the nominal features (relative to the continuous features) when computing distances among observations compared to SMOTENC. However, this method can be extended with further modifications to the nominal data encoding and selection mechanisms in future work.

Similar to G-SMOTE being an extension of SMOTE, G-SMOTENC is also an extension of SMOTENC since any method or ML pipeline using the SMOTENC generation mechanism can replace it with G-SMOTENC without any further modifications. The proposed method is described in pseudo-code in Algorithm 3. The functions $SelectionMechanism$ and $GenerationMechanism$ are described in Algorithms 4 and 5, respectively.

Algorithm 3: G-SMOTENC.

Given: Dataset with binary target classes C_{min} and C_{maj}
Input: $C_{maj}, C_{min}, \alpha_{sel}, \alpha_{trunc}, \alpha_{def}$
Output: C^{gen}

begin
  $N \leftarrow |C_{maj}| - |C_{min}|$
  $C^{gen} \leftarrow \emptyset$
  while $|C^{gen}| < N$ **do**
    $x^c, x^{nn}, X^{nn} \leftarrow SelectionMechanism(C_{maj}, C_{min}, \alpha_{sel})$
    $x^{gen} \leftarrow GenerationMechanism(x^c, x^{nn}, X^{nn}, \alpha_{trunc}, \alpha_{def})$
    $C^{gen} \leftarrow C^{gen} \cup \{x^{gen}\}$

G-SMOTENC's implementation involves additional considerations regarding the management of the nominal features. During the selection mechanism (identified as the function $SelectionMechanism$), the nominal features are encoded using the one-hot encoding technique, while the non-zero constant assumes the value of the median of the standard deviations of the continuous features in C_{min}, divided by two. This encoding mechanism varies from the one in SMOTENC in order to attribute less weight to the nominal features relative to the continuous features.

The selection strategy, α_{sel}, as well as C_{min} and C_{maj} are used to determine a central observation, x^c, its nearest neighbors, X^{nn}, and one of its nearest neighbors, $x^{nn} \in X^{nn}$. X^{nn} is calculated using the euclidean distance and both the continuous and encoded nominal features. The outcome of this step is dependent on the choice of α_{sel}:

1. If $\alpha_{sel} = minority$, X^{nn} will consist of x^c's k-nearest neighbors within C_{min};

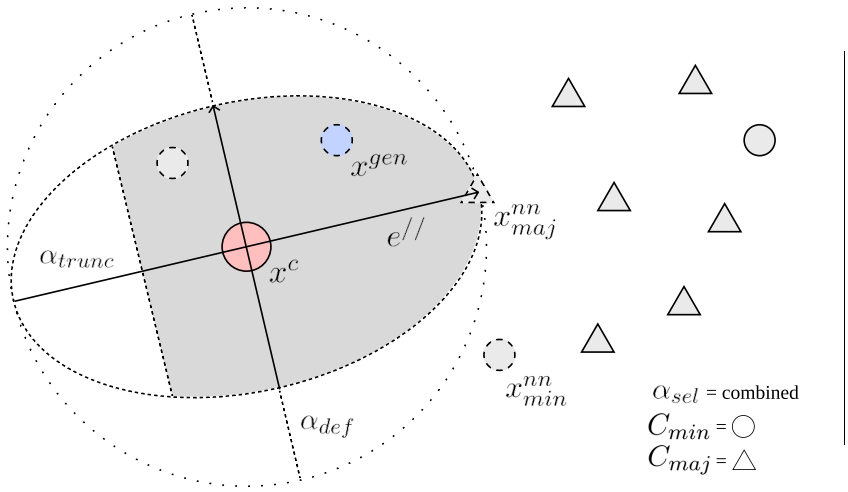

X^{nn}		f_1^{nom}	f_2^{nom}	f_3^{nom}
x^{nn}_{maj}	△	A	C	B
x^{nn}_{min}	○	B	B	B
n/a	○	B	C	A
x^{gen}_{nom}	○	B	C	B

Figure 6.1.: A visual depiction of G-SMOTENC. In this example, α_{trunc} is approximately 0.5 and α_{def} is approximately 0.4.

2. If $\alpha_{sel} = majority$, X^{nn} will consist of x^c's nearest neighbor within C_{maj};
3. If $\alpha_{sel} = combined$, X^{nn} will consist of the union between x^c's k-nearest neighbors within C_{min} and x^c's nearest neighbor within C_{maj}, *i.e.*, $C_{min,k} \cup C_{maj,1}$. In this case, x^{nn} is selected using the majority class observation within X^{nn} as well as another randomly selected nearest neighbor, such that $x^{nn} = argmin(||x^{nn}_{min} - x^c||, ||x^{nn}_{maj} - x^c||)$;

Unlike in the original G-SMOTE generation mechanism, X^{nn} is used in the to determine the nominal feature values of x^{gen} based on the mode of these features within X^{nn}. G-SMOTENC's generation mechanism (identified as $GenerationMechanism$) uses two hyperparameters to generate the continuous features in x^{gen}: the truncation factor, α_{trunc}, and the deformation factor, α_{def}. They are generated by forming a hyper-sphere with center x^c and is modified according to the parameters:

1. α_{trunc} truncates the hyper-sphere to induce the generation of the artificial instance within a subset of the hypersphere. It varies between 1 and -1, where 1 would split the generation area in half and use the area between x^c and x^{nn}, -1 achieves the same effect and uses the other semi-hyper-sphere, and 0 applies no truncation.
2. α_{def} deforms the hyper-sphere as shown in Figure 6.1. It varies between 0 and 1, where 0 applies no deformation and 1 fully deforms the hyper-sphere into a line segment, corresponding to $e^{//}$.

Figure 6.1 depicts the effect of those hyperparameters in the data selection and generation phases. For an in-depth explanation of these hyperparameters, the reader is referred to [23].

6.3.1. Selection Mechanism

The data selection mechanism is preceded by the numerical encoding of the nominal features. It combines the selection mechanisms of SMOTENC and G-SMOTE, as shown in Algorithm 4. The selection mechanism inherits the minority, majority, and combined mechanisms proposed in G-SMOTE. The nominal features in the minority and majority class observations, C_{maj} and C_{min} are first encoded using a one-hot encoding approach and replacing the constant 1 with the median of the standard deviations of the continuous features in C_{min} divided by 2. The nearest-neighbors (X^{nn}) of x^c are determined based on α_{sel}, which are passed on to the generation mechanism to determine the nominal features' values of x^{gen} in the

generation mechanism. Simultaneously, x^{nn} is randomly selected from X^{nn} and will be used to generate x^{gen}'s continuous features' values.

Algorithm 4: G-SMOTENC's selection mechanism.

Input: $C_{maj}, C_{min}, \alpha_{sel}$
Output: x^c, x^{nn}, X^{nn}

Function *CatEncoder(C_{maj}, C_{min})*:
  $S \leftarrow$ Standard deviations of the continuous features in C_{min}
  $\sigma_{med} \leftarrow median(S)$
  forall $i \in \{maj, min\}$ **do**
    forall $f \in C_i^T$ **do**
      if f *is nominal* **then**
        $f' \leftarrow OneHotEncode(f) \times \sigma_{med}/2$
        $C_i' \leftarrow (C_i^T \setminus f)^T$
        $C_i' \leftarrow (C_i'^T \cup f')^T$
  return C'_{maj}, C'_{min}
Function *Surface(α_{sel}, x^c, C_{maj}, C_{min})*:
  if $\alpha_{sel} = minority$ **then**
    $x^{nn} \in C_{min,k}$ `// One of the` k`-nearest neighbors of` x^c `from` C_{min}
    $X^{nn} \leftarrow C_{min,k}$
  if $\alpha_{sel} = majority$ **then**
    $x^{nn} \in C_{maj,1}$ `// Nearest neighbor of` x^c `from` C_{maj}
    $X^{nn} \leftarrow C_{maj,1}$
  if $\alpha_{sel} = combined$ **then**
    $x^{nn}_{min} \in C_{min,k}$
    $x^{nn}_{maj} \in C_{maj,1}$
    $x^{nn} \leftarrow argmin(||x^{nn}_{min} - x^c||, ||x^{nn}_{maj} - x^c||)$
    $X^{nn} \leftarrow C_{min,k} \cup C_{maj,1}$
  return x^{nn}, X^{nn} `//` X^{nn} `is the set of` k`-nearest neighbors`
begin
  $C'_{maj}, C'_{min} \leftarrow CatEncoder(C_{maj}, C_{min})$
  $x^c \in C'_{min}$ `// Randomly select` x^c `from` C'_{min}
  $x^{nn}, X^{nn} \leftarrow Surface(\alpha_{sel}, x^c, C'_{maj}, C'_{min})$
  Reverse encoding of nominal features in x^c, x^{nn} and X^{nn}

6.3.2. Generation Mechanism

G-SMOTENC's generation mechanism is shown in Algorithm 5. It divides the generation of x^{gen} into two parts: (1) generation of continuous feature values and (2) generation of nominal feature values. First, the nominal features from x^c and x^{nn} are discarded. Afterward, the continuous features are generated using G-SMOTE's generation mechanism; within a hyper-spheroid defined with α_{trunc} and α_{def}, which allows the non-linear generation of synthetic observations between x^c and x^{nn}. Finally, the nominal feature values are generated by the mode of each feature within the observations in X^{nn}.

Algorithm 5: G-SMOTENC's generation mechanism.

Input: $x^c, x^{nn}, X^{nn}, \alpha_{trunc}, \alpha_{def}$

Output: x^{gen}

Function *Hyperball()*:
- $v_i \sim \mathcal{N}(0,1)$
- $r \sim \mathcal{U}(0,1)$
- $x^{gen} \leftarrow r^{1/p} \frac{(v_1,\ldots,v_p)}{||(v_1,\ldots,v_p)||}$
- **return** x^{gen}

Function *Vectors(x^c, x^{nn}, x^{gen})*:
- $e^{//} \leftarrow \frac{x^{nn}-x^c}{||x^{nn}-x^c||}$
- $x^{//} \leftarrow (x^{gen} \cdot e^{//})e^{//}$
- $x^{\perp} \leftarrow x^{gen} - x^{//}$
- **return** $x^{//}, x^{\perp}$

Function *Truncate($x^c, x^{nn}, x^{gen}, x^{//}, \alpha_{trunc}$)*:
- **if** $|\alpha_{trunc} - x^{//}| > 1$ **then**
  - $x^{gen} \leftarrow x^{gen} - 2x^{//}$
- **return** x^{gen}

Function *Deform($x^{gen}, x^{\perp}, \alpha_{def}$)*:
- **return** $x^{gen} - \alpha_{def} x^{\perp}$

Function *Translate(x^c, x^{gen}, R)*:
- **return** $x^c + Rx^{gen}$

Function *GenNominal(X^{nn})*:
- $x^{gen}_{nom} = \emptyset$
- **forall** $f \in (X^{nn})^T$ **do**
  - **if** *f is nominal* **then**
    - $x^{gen}_{nom} \cup \{mode(f)\}$ `// Ties are decided with random selection`
- **return** x^{gen}_{nom}

begin
- Discard nominal features from x^c and x^{nn}
- $x^{gen} \leftarrow Hyperball()$
- $x^{//}, x^{\perp} \leftarrow Vectors(x^c, x^{nn}, x^{gen})$
- $x^{gen} \leftarrow Truncate(x^c, x^{nn}, x^{gen}, x^{//}, \alpha_{trunc})$
- $x^{gen} \leftarrow Deform(x^{gen}, x^{\perp}, \alpha_{def})$
- $x^{gen} \leftarrow Translate(x^c, x^{gen}, ||x^{nn}_{cont} - x^c||)$
- $x^{gen}_{nom} \leftarrow GenNominal(X^{nn})$
- $x^{gen} \leftarrow x^{gen} \cup x^{gen}_{nom}$

6.4. Methodology

This section describes how the evaluation of G-SMOTENC was performed. We describe the datasets used in the experiment, their source and preprocessing steps executed in Section 6.4.1. The resampling and classification methods used to analyze G-SMOTE's performance are listed in Section 6.4.2. The performance metrics used are defined in Section 6.4.3. Finally, the experimental procedure is described in Section 6.4.4.

6.4.1. Experimental Data

The datasets used in this experiment were extracted from the UC Irvine Machine Learning Repository. All of the datasets are publicly available and cover a range of different domains. The criteria to select the datasets ensured that all datasets are imbalanced and contained non-metric features (*i.e.*, ordinal, nominal or binary). These datasets are used to show how the performance of different classifiers varies across over/undersamplers.

All datasets were initially preprocessed manually with minimal manipulations. We removed features and/or observations with missing values and identified the non-metric features. The second stage of preprocessing was done systematically. It starts with the generation of artificially imbalanced datasets with different Imbalance Ratios ($IR = \frac{|C_{maj}|}{|C_{min}|}$). For each original dataset, we create its more imbalanced versions at intervals of 10, while ensuring that $|C_{min}| \geq 15$. The sampling strategy was determined for class $n \in \{1, \ldots, n, \ldots, m\}$ as a linear interpolation using $|C_{maj}|$ and $|C'_{min}| = \frac{|C_{maj}|}{IR_{new}}$, as shown in equation 6.1.

$$|C_i|^{imb} = \min(\frac{|C'_{min}| - |C_{maj}|}{n-1}.|C_i| + |C_{max}|, |C_i|) \tag{6.1}$$

The new, artificially imbalanced dataset, is formed by sampling observations without replacement from each C_i such that $C'_i \subseteq C_i, |C'_i| = |C_i|^{imb}$. The artificially imbalanced datasets are marked with its imbalance ratio as a suffix in Table 6.1.

The datasets (both original and artificially imbalanced versions) are then filtered to ensure all datasets have a minimum of 500 observations. The remaining datasets with a number of observations larger than 5000 are randomly sampled to match this number of observations. Afterward, we remove target classes with a frequency lower than 15 observations for each remaining dataset. Finally, the continuous and discrete features are scaled to the range $[0, 1]$ to ensure a common range between all features. The description of the resulting datasets is shown in Table 6.1.

Table 6.1.: Description of the datasets collected after data preprocessing. The sampling strategy is similar across datasets. Legend: (IR) Imbalance Ratio

Dataset	Metric	Non-Metric	Obs.	Min. Obs.	Maj. Obs.	IR	Classes
Abalone	1	7	4139	15	689	45.93	18
Adult	8	6	5000	1268	3732	2.94	2
Adult (10)	8	6	5000	451	4549	10.09	2
Annealing	4	6	790	34	608	17.88	4

Continued on next page

Table 6.1.: Description of the datasets collected after data preprocessing. The sampling strategy is similar across datasets. Legend: (IR) Imbalance Ratio

Dataset	Metric	Non-Metric	Obs.	Min. Obs.	Maj. Obs.	IR	Classes
Census	24	7	5000	337	4663	13.84	2
Contraceptive	4	5	1473	333	629	1.89	3
Contraceptive (10)	4	5	1036	62	629	10.15	3
Contraceptive (20)	4	5	990	31	629	20.29	3
Contraceptive (31)	4	5	973	20	629	31.45	3
Contraceptive (41)	4	5	966	15	629	41.93	3
Covertype	2	10	5000	20	2449	122.45	7
Credit Approval	9	6	653	296	357	1.21	2
German Credit	13	7	1000	300	700	2.33	2
German Credit (10)	13	7	770	70	700	10.00	2
German Credit (20)	13	7	735	35	700	20.00	2
German Credit (30)	13	7	723	23	700	30.43	2
German Credit (41)	13	7	717	17	700	41.18	2
Heart Disease	5	5	740	22	357	16.23	5
Heart Disease (21)	5	5	735	17	357	21.00	5

6.4.2. Machine Learning Algorithms

The choice of classifiers used in the experimental procedure was based on their type (tree-based, nearest neighbors-based, linear model and ensemble-based), popularity and consistency in performance. We used Decision Tree (DT), a K-Nearest Neighbors (KNN) classifier, a Logistic Regression (LR) and a Random Forest (RF).

Given the lack of existing oversamplers that address imbalanced learning problems with mixed data types, the amount of benchmark methods used is also limited. We used three appropriate, well-known methods and one state-of-the-art oversampling method: SMOTENC, RUS, ROS and SMOTE-ENC. Table 6.2 shows the hyperparameters used for the parameter search described in Section 6.4.4.

6.4.3. Performance Metrics

The choice of the performance metric plays a critical role in assessing the effect on classification tasks. The typical performance metrics, *e.g.*, Overall Accuracy (OA), are intuitive to interpret but are often inappropriate to measure a classifier's performance in an imbalanced learning context [343]. For example, to estimate an event that occurs in 1% of the dataset, a constant classifier would obtain an OA of 0.99 and still be unusable. However, this metric is still reported in some of our results to maintain interpretability.

Recent surveys consider Geometric-mean (G-mean), F1-score (F-score), $Sensitivity = \frac{TP}{FN+TP}$ and $Specificity = \frac{TN}{TN+FP}$ appropriate and common performance metrics in imbalanced learning contexts [344, 255, 345]. G-mean and F-score are defined equations 6.2 and 6.3, respectively.

$$G\text{-}mean = \sqrt{\overline{Sensitivity} \times \overline{Specificity}} \tag{6.2}$$

Table 6.2.: Hyperparameter definition for the classifiers and resamplers used in the experiment.

Classifier	Hyperparameter	Values
DT	min. samples split	2
	criterion	gini
	max depth	3, 6
LR	maximum iterations	10000
	multi-class	One-vs-All
	solver	saga
	penalty	None, L1, L2
KNN	# neighbors	3, 5
	weights	uniform
	metric	euclidean
RF	min. samples split	2
	# estimators	50, 100
	Max depth	3, 6
	criterion	gini
Resampler		
SMOTENC	# neighbors	3, 5
SMOTE-ENC	# neighbors	3, 5
G-SMOTENC	# neighbors	3, 5
	deformation factor	0.0, 0.25, 0.5, 0.75, 1.0
	truncation factor	-1.0, -0.5, 0.0, 0.5, 1.0
	selection strategy	"combined", "minority", "majority"
RUS	replacement	False
ROS	(no applicable parameters)	

$$F\text{-}score = 2 \times \frac{\overline{Precision} \times \overline{Recall}}{\overline{Precision} + \overline{Recall}} \tag{6.3}$$

They are calculated as a function of the number of False/True Positives (FP and TP) and False/True Negatives (FN and TN), with $Precision = \frac{TP}{TP+FP}$ and $Recall = \frac{TP}{TP+FN}$. This led us to use, along with OA, both F-score and G-mean as the main performance metrics for this study.

6.4.4. Experimental Procedure

The experimental procedure was applied similarly to all combinations of resamplers, classifiers and hyperparameter combinations across all datasets. The evaluation of the models' performance was tested using a 5-fold Cross-Validation (CV) approach. The mean performance in the test set is calculated over the five folds and three different runs of the experimental procedure for each combination of resampling/classifier hyperparameters. For each dataset, we select the results of the hyperparameters that optimize the performance of a resampler/classifier. Figure 6.2 shows a diagram of the experimental procedure described.

A CV run consists of a stratified partitioning (*i.e.*, each partition contains the same relative frequencies of target labels) of the dataset into five parts. A given resampler/classifier combination with a specific set of hyperparameters is fit and tested five times, using one of the partitions as a test set and the remaining

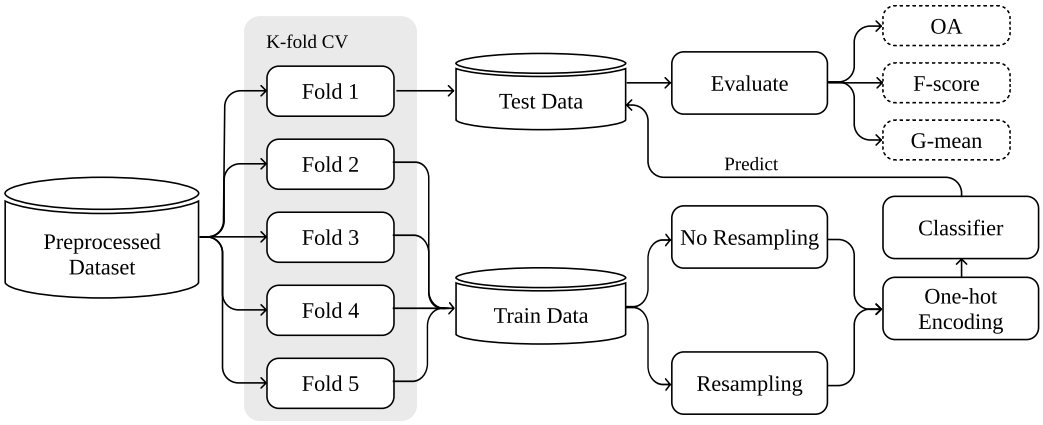

Figure 6.2.: Experimental procedure used in this study.

ones as the training set. In the ML pipeline defined for each run, the nominal features are one-hot encoded after oversampling and before passing the data to the classifier. The estimated performance consists of the average classification performance across the five tests and three runs (*i.e.*, a total of 15 tests).

6.4.5. Software Implementation

The algorithmic implementation of G-SMOTENC was written using the Python programming language and is available in the open-source package ML-Research [305], along with other utilities used to produce the experiment and outputs used in Section 6.5. In addition, the packages Scikit-Learn [257], Imbalanced-Learn [258] and Research-Learn were also used in the experimental procedure to get the implementations of the classifiers, benchmark over/undersamplers and run the experimental procedure. The original SMOTE-ENC implementation was retrieved from the authors' GitHub repository. The Latex code, Python scripts (including data pulling and preprocessing, experiment setup and analysis of results), as well as the datasets used, are available in this GitHub repository.

6.5. Results and Discussion

In this section, we present the experimental results. We focus on the comparison of classification performance using oversamplers whose generation mechanism is compatible with datasets containing both nominal and continuous features. The experimental results were analyzed in two stages: (1) in Section 6.5.1 we analyze mean rankings and absolute performances and in Section 6.5.2 we show the results of our statistical analysis. Section 6.5.3 discusses the main insights extracted by analyzing the experimental results.

6.5.1. Results

Table 6.3 presents the mean rankings of CV scores between the different combinations of oversamplers, metrics and classifiers. These results were calculated by assigning a ranking score for each oversampler from 1 (best) to 4 (worst) for each dataset, metric and classifier.

Table 6.3.: Mean rankings over the different datasets, folds and runs used in the experiment.

Classifier	Metric	G-SMOTENC	NONE	SMOTENC	ROS	RUS	SMOTE-ENC
DT	OA	1.66 ± 0.13	**1.61 ± 0.27**	3.58 ± 0.20	4.68 ± 0.15	5.42 ± 0.27	4.05 ± 0.23
DT	F-Score	**1.32 ± 0.11**	3.84 ± 0.40	3.13 ± 0.20	4.32 ± 0.19	5.47 ± 0.23	2.92 ± 0.34
DT	G-Mean	**1.68 ± 0.24**	5.84 ± 0.09	2.82 ± 0.21	2.95 ± 0.32	4.26 ± 0.32	3.45 ± 0.30
KNN	OA	2.50 ± 0.17	**1.37 ± 0.28**	4.21 ± 0.25	3.34 ± 0.35	5.68 ± 0.22	3.89 ± 0.15
KNN	F-Score	**1.37 ± 0.16**	3.95 ± 0.35	3.11 ± 0.29	3.47 ± 0.36	5.53 ± 0.23	3.58 ± 0.23
KNN	G-Mean	**1.74 ± 0.17**	5.84 ± 0.12	2.89 ± 0.23	3.76 ± 0.33	3.00 ± 0.45	3.76 ± 0.23
LR	OA	2.74 ± 0.19	**1.37 ± 0.28**	3.08 ± 0.21	4.34 ± 0.30	5.74 ± 0.17	3.74 ± 0.28
LR	F-Score	**2.11 ± 0.24**	4.53 ± 0.35	2.37 ± 0.28	3.47 ± 0.32	5.21 ± 0.27	3.32 ± 0.38
LR	G-Mean	2.13 ± 0.26	6.00 ± 0.00	3.61 ± 0.21	**2.11 ± 0.23**	3.32 ± 0.40	3.84 ± 0.28
RF	OA	1.82 ± 0.11	**1.24 ± 0.09**	3.97 ± 0.16	4.32 ± 0.21	5.92 ± 0.06	3.74 ± 0.22
RF	F-Score	**1.32 ± 0.13**	5.05 ± 0.31	3.16 ± 0.22	3.05 ± 0.31	5.37 ± 0.14	3.05 ± 0.27
RF	G-Mean	**1.68 ± 0.22**	5.79 ± 0.21	3.26 ± 0.28	2.47 ± 0.30	3.89 ± 0.35	3.89 ± 0.19

Table 6.4 presents the mean CV scores. Except for the OA metric, G-SMOTENC either outperformed or matched the remaining oversamplers.

Table 6.4.: Mean scores over the different datasets, folds and runs used in the experiment

Classifier	Metric	G-SMOTENC	NONE	SMOTENC	ROS	RUS	SMOTE-ENC
DT	OA	0.74 ± 0.05	**0.75 ± 0.04**	0.68 ± 0.04	0.66 ± 0.04	0.58 ± 0.04	0.65 ± 0.04
DT	F-Score	**0.56 ± 0.04**	0.52 ± 0.04	0.54 ± 0.04	0.52 ± 0.04	0.48 ± 0.04	0.51 ± 0.04
DT	G-Mean	**0.69 ± 0.03**	0.60 ± 0.02	0.68 ± 0.03	0.67 ± 0.03	0.65 ± 0.03	0.66 ± 0.03
KNN	OA	0.69 ± 0.04	**0.73 ± 0.05**	0.67 ± 0.04	0.69 ± 0.05	0.57 ± 0.04	0.68 ± 0.05
KNN	F-Score	**0.53 ± 0.04**	0.50 ± 0.04	0.52 ± 0.04	0.52 ± 0.04	0.46 ± 0.04	0.51 ± 0.04
KNN	G-Mean	**0.66 ± 0.03**	0.58 ± 0.03	0.64 ± 0.03	0.62 ± 0.03	0.65 ± 0.03	0.63 ± 0.03
LR	OA	0.68 ± 0.05	**0.75 ± 0.04**	0.68 ± 0.05	0.66 ± 0.05	0.58 ± 0.04	0.67 ± 0.04
LR	F-Score	**0.54 ± 0.04**	0.52 ± 0.04	**0.54 ± 0.04**	0.53 ± 0.04	0.48 ± 0.04	0.52 ± 0.04
LR	G-Mean	**0.69 ± 0.02**	0.60 ± 0.03	0.68 ± 0.02	**0.69 ± 0.03**	0.67 ± 0.03	0.67 ± 0.03
RF	OA	0.74 ± 0.04	**0.76 ± 0.04**	0.69 ± 0.04	0.69 ± 0.04	0.59 ± 0.04	0.68 ± 0.05
RF	F-Score	**0.57 ± 0.04**	0.48 ± 0.04	0.55 ± 0.04	0.55 ± 0.04	0.49 ± 0.04	0.53 ± 0.04
RF	G-Mean	**0.70 ± 0.02**	0.57 ± 0.02	0.68 ± 0.03	0.69 ± 0.03	0.68 ± 0.03	0.68 ± 0.02

6.5.2. Statistical Analysis

It is necessary to use methods that account for the multiple comparison problem to conduct an appropriate statistical analysis in an experiment with multiple datasets. Based on the recommendations found in [259], we applied a Friedman test followed by a Holm-Bonferroni test for post-hoc analysis.

In Section 6.4.3 we explained that OA, although easily interpretable, is not an appropriate performance metric for imbalanced learning problems. Therefore, the statistical analysis was developed using the two imbalance-appropriate metrics used in the study: F-Score and G-Mean. Based on the Friedman test [260], there is a statistically significant difference in performance across resampling methods. The results of this test are shown in Table 6.5. The null hypothesis is rejected in all cases.

Table 6.5.: Results for the Friedman test. Statistical significance is tested at a level of $\alpha = 0.05$. The null hypothesis is that there is no difference in the classification outcome across resamplers.

Classifier	Metric	p-value	Significance
DT	F-Score	2.2e-10	True
DT	G-Mean	1.2e-10	True
KNN	F-Score	2.3e-09	True
KNN	G-Mean	9.4e-10	True
LR	F-Score	2.1e-07	True
LR	G-Mean	9.7e-11	True
RF	F-Score	8.5e-12	True
RF	G-Mean	2.0e-10	True

We performed a Holm-Bonferroni test to understand whether the difference in the performance of G-SMOTENC is statistically significant to the remaining resampling methods. The results of this test are shown in Table 6.6. The null hypothesis is rejected in 33 out of 40 trials.

Table 6.6.: Adjusted p-values using the Holm-Bonferroni test. Statistical significance is tested at a level of $\alpha = 0.05$. The null hypothesis is that the benchmark methods perform similarly to the control method (G-SMOTENC).

Classifier	Metric	NONE	SMOTENC	ROS	RUS	SMOTE-ENC
DT	F-Score	**1.5e-04**	**1.5e-04**	**7.3e-06**	**1.2e-06**	1.0e-01
DT	G-Mean	**5.6e-07**	**2.7e-03**	**2.8e-02**	**3.9e-04**	**2.3e-02**
KNN	F-Score	**6.4e-04**	**2.2e-04**	**7.2e-04**	**6.4e-04**	**5.9e-06**
KNN	G-Mean	**1.6e-05**	**9.6e-03**	**6.5e-03**	2.0e-01	**3.5e-03**
LR	F-Score	**4.0e-03**	6.1e-01	**9.2e-03**	**3.6e-04**	5.6e-02
LR	G-Mean	**1.6e-07**	**4.0e-04**	8.6e-01	2.4e-01	**4.7e-03**
RF	F-Score	**1.7e-06**	**2.4e-04**	**8.0e-03**	**1.7e-06**	**8.0e-03**
RF	G-Mean	**3.8e-06**	**8.8e-03**	2.5e-01	**2.3e-02**	**1.7e-03**

6.5.3. Discussion

The results reported in Section 6.5.1 show that G-SMOTENC consistently outperforms the remaining oversampling approaches. Based on the two metrics appropriate for imbalanced learning problems, G-Mean and F-Score, in the average rankings shown in Table 6.3 G-SMOTENC was only outperformed once by a small margin. Unlike the results reported in [337], SMOTE-ENC's performance was rarely superior to SMOTENC's.

The relative difference in the classifiers' performance is better visible in Table 6.4. Using an RF classifier, for example, the impact of using G-SMOTENC compared to no oversampling improves, on average, 13 percentual points on G-mean and nine percentual points using F-Score.

The difference in performance between oversamplers was found to be statistically significant across classifiers and performance metrics in the Friedman test. The p-values of this test are reported in Table 6.5. The superiority of G-SMOTENC was confirmed with the results from the Holm-Bonferroni test shown in Table 6.6. This test showed that G-SMOTENC outperformed with statistical significance the remaining resamplers in 82.5% of the comparisons done.

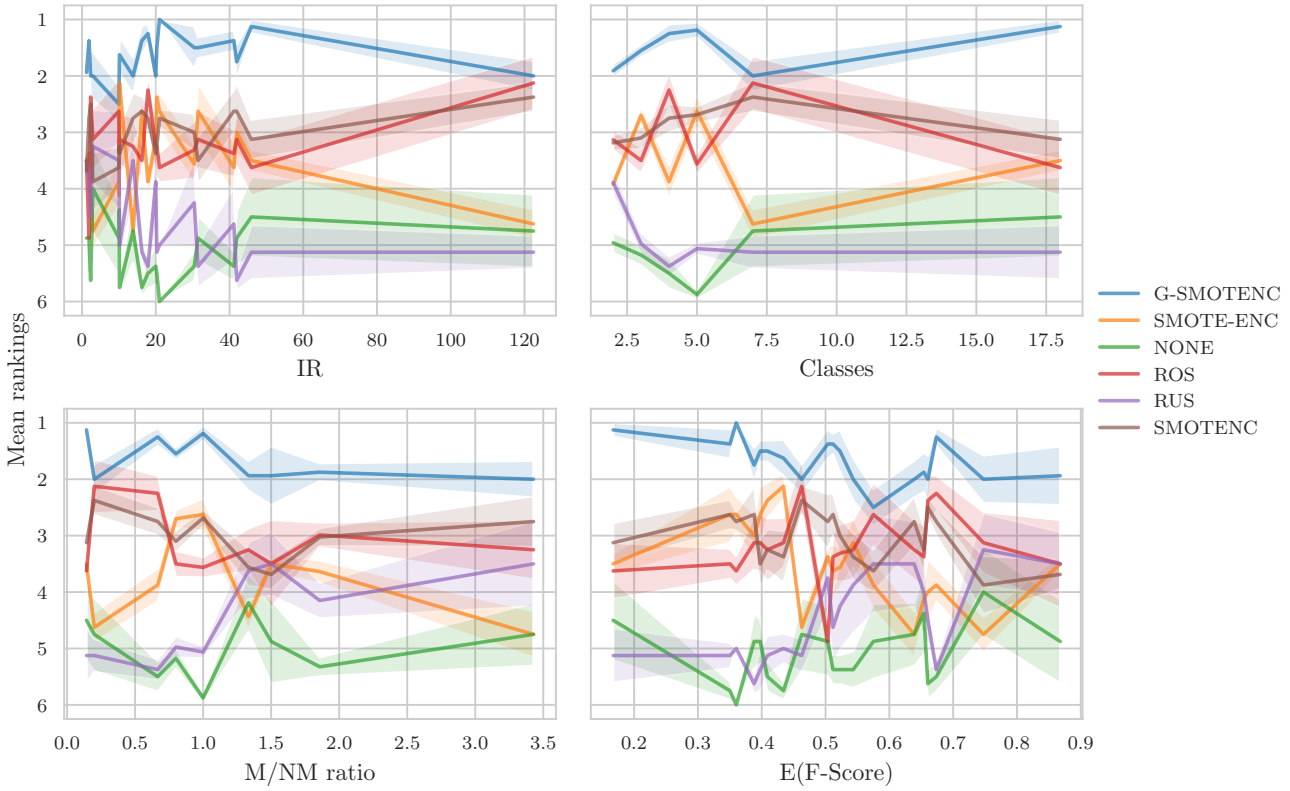

Figure 6.3.: Average ranking of oversamplers over different characteristics of the datasets used in the experiment. Legend: IR — Imbalance Ratio, Classes — Number of classes in the dataset, M/NM ratio — ratio between the number of metric and non-metric features, E(F-Score) — Mean F-Score of dataset across all combinations of classifiers and oversamplers.

The results from this experiment expose some well-known limitations of SMOTE, which become particularly evident with SMOTENC. Specifically, the lack of diversity in the generated data and, on some occasions, the near-duplication of observations discussed in [23] may be a possible explanation for the performance of SMOTENC being comparable to ROS' performance, visible in Figure 6.3. In this figure, three groups of resampling methods with comparable performance are visible: (1) G-SMOTENC, the top-performing method, (2) SMOTENC, ROS and SMOTE-ENC, where SMOTE-ENC has the most inconsistent behavior and (3) RUS and no oversampling, the worst-performing approaches. In addition, G-SMOTENC's superiority seems invariable to the dataset's characteristics, with little overlap with the remaining benchmark methods.

6.6. Conclusion

This paper presented G-SMOTENC, a new oversampling algorithm that combines G-SMOTE and SMOTENC. This oversampling algorithm leverages G-SMOTE's data selection and generation mechanisms into datasets with mixed data types. This was achieved by encoding and generating nominal feature values using SMOTENC's approach. The quality of the data generated with G-SMOTENC was tested over 20 datasets with different imbalance ratios, metric/non-metric feature ratios and number of classes. These results were compared to no oversampling, SMOTENC, Random Oversampling, Random Undersampling

and SMOTE-ENC using a Decision Tree, K-Nearest Neighbors, Logistic Regression and Random Forest as classifiers.

G-SMOTENC can be seen as a drop-in replacement of SMOTENC, since when $\alpha_{trunc} = 1$, $\alpha_{def} = 1$ and $\alpha_{sel} = minority$, SMOTENC is reproduced. G-SMOTENC has three additional hyperparameters that allow for greater customization of the selection and generation mechanisms. However, determining the optimal parameters a priori (*i.e.*, with reduced parameter tuning) is a topic for future work.

The results show that G-SMOTENC performs significantly better when compared to its more popular counterparts (SMOTENC, Random Oversampling and Random Undersampling), as well as a recently proposed oversampling algorithm for mixed data types (SMOTE-ENC). This performance improvement is related to G-SMOTENC's selection mechanism, which finds a safer region for data generation, along with its generation mechanism which increases the diversity of the generated observations compared to SMOTENC. The G-SMOTENC implementation used in this study is available in the open-source Python library "ML-Research" and is fully compatible with the Scikit-Learn ecosystem.

7. Moving Forward

In Chapter **??** we studied the state-of-the-art in data augmentation algorithms, which was necessary to proceed to subsequent steps of the work plan. Based on these findings, in Chapter 3 we used an oversampling method to address a know limitation of imbalanced learning in LULC. An additional limitation we found in oversampling methods was the lack of models capable of addressing datasets with both metric and non-metric features. We plan to address this limitation by modifying a state-of-the-art oversampling method, based on RQ4, as described in Subsection 1.4. This work will be added as a new Chapter between Chapters **??** and 3. At the time of writing, the algorithmic implementation, dataset collection and preprocessing, and experimental results have been completed. The writing of the Chapter is in progress.

The Geometric-SMOTENC oversampler will use the generation mechanism described in [23], while encoding the continuous features, calculating the selected observations' nearest neighbors and generating the categorical feature values for the synthetic data using the method described in [22]. This approach allows the usage of a state-of-the-art oversampling method with categorical features. The experimental results have shown that G-SMOTENC outperforms the oversamplers compatible with this type of data (*i.e.*, Random Oversampling and SMOTENC).

In Chapters 4 and 5 we modify the AL framework as a means to address RQ3. However, the work presented can be further enriched with the application of other methods that leverage information from unlabeled data, specifically semi-supervised and self-supervised learning techniques to form a single framework, the Self-Supervised Semi-Supervised Active Deep Learning (S^4AD-Learning) framework. This work is also under development and is intended to follow Chapter 5. At the time of writing, the algorithmic implementation is in progress.

The last chapter will close the thesis with the conclusions, discussion of the proposed research questions and recommendations for future work based on the results presented in previous chapters.

Bibliography

[1] Reza Khatami, Giorgos Mountrakis, and Stephen V. Stehman. "A meta-analysis of remote sensing research on supervised pixel-based land-cover image classification processes: General guidelines for practitioners and future research". In: *Remote Sensing of Environment* 177 (May 2016), pp. 89–100. ISSN: 0034-4257. DOI: 10.1016/J.RSE.2016.02.028. URL: https://www.sciencedirect.com/science/article/abs/pii/S0034425716300578.

[2] Georgios Douzas, Fernando Bacao, Joao Fonseca, and Manvel Khudinyan. "Imbalanced learning in land cover classification: Improving minority classes' prediction accuracy using the geometric SMOTE algorithm". In: *Remote Sensing* 11.24 (Dec. 2019), p. 3040. ISSN: 20724292. DOI: 10.3390/rs11243040. URL: https://www.mdpi.com/2072-4292/11/24/3040.

[3] Andrew P Tewkesbury, Alexis J Comber, Nicholas J Tate, Alistair Lamb, and Peter F Fisher. "A critical synthesis of remotely sensed optical image change detection techniques". In: *Remote Sensing of Environment* 160 (2015), pp. 1–14.

[4] Charlotte Pelletier, Silvia Valero, Jordi Inglada, Nicolas Champion, Claire Marais Sicre, and Gérard Dedieu. "Effect of Training Class Label Noise on Classification Performances for Land Cover Mapping with Satellite Image Time Series". In: *Remote Sensing* 9.2 (Feb. 2017), p. 173. ISSN: 2072-4292. DOI: 10.3390/rs9020173. URL: http://www.mdpi.com/2072-4292/9/2/173.

[5] Oliver Stromann, Andrea Nascetti, Osama Yousif, and Yifang Ban. "Dimensionality Reduction and Feature Selection for Object-Based Land Cover Classification based on Sentinel-1 and Sentinel-2 Time Series Using Google Earth Engine". In: *Remote Sensing* 12.1 (2020), p. 76. ISSN: 20724292. DOI: 10.3390/RS12010076.

[6] Francisco Alonso-Sarria, Carmen Valdivieso-Ros, and Francisco Gomariz-Castillo. "Isolation Forests to Evaluate Class Separability and the Representativeness of Training and Validation Areas in Land Cover Classification". In: *Remote Sensing* 11.24 (Dec. 2019), p. 3000. ISSN: 2072-4292. DOI: 10.3390/rs11243000. URL: https://www.mdpi.com/2072-4292/11/24/3000.

[7] Wei Feng, Wenjiang Huang, Huichun Ye, and Longlong Zhao. "Synthetic minority over-sampling technique based rotation forest for the classification of unbalanced hyperspectral data". In: *International Geoscience and Remote Sensing Symposium (IGARSS)*. Vol. 2018-July. Institute of Electrical and Electronics Engineers Inc., Oct. 2018, pp. 2651–2654. ISBN: 9781538671504. DOI: 10.1109/IGARSS.2018.8518242.

[8] Oriane Siméoni, Mateusz Budnik, Yannis Avrithis, and Guillaume Gravier. "Rethinking deep active learning: Using unlabeled data at model training". In: *Proceedings - International Conference on Pattern Recognition* (2020), pp. 1220–1227. ISSN: 10514651.

[9] Alberto Fernández, Victoria López, Mikel Galar, María José del Jesus, and Francisco Herrera. "Analysing the classification of imbalanced data-sets with multiple classes: Binarization techniques and ad-hoc approaches". In: *Knowledge-Based Systems* 42 (Apr. 2013), pp. 97–110. ISSN: 0950-7051. DOI: 10.1016/J.KNOSYS.2013.01.018. URL: https://www.sciencedirect.com/science/article/abs/pii/S0950705113000300.

[10] Yassine Ouali, Céline Hudelot, and Myriam Tami. "An overview of deep semi-supervised learning". In: *arXiv preprint arXiv:2006.05278* (2020).

[11] Olivier Chapelle, Bernhard Scholkopf, and Alexander Zien. "Semi-supervised learning (chapelle, o. et al., eds.; 2006)[book reviews]". In: *IEEE Transactions on Neural Networks* 20.3 (2009), pp. 542–542.

[12] Jean-Bastien Grill, Florian Strub, Florent Altché, Corentin Tallec, Pierre Richemond, Elena Buchatskaya, Carl Doersch, Bernardo Avila Pires, Zhaohan Guo, Mohammad Gheshlaghi Azar, et al. "Bootstrap your own latent: A new approach to self-supervised learning". In: *Advances in Neural Information Processing Systems* 33 (2020), pp. 21271–21284.

[13] Xiao Liu, Fanjin Zhang, Zhenyu Hou, Li Mian, Zhaoyu Wang, Jing Zhang, and Jie Tang. "Self-supervised learning: Generative or contrastive". In: *IEEE Transactions on Knowledge and Data Engineering* (2021).

[14] Samuel Budd, Emma C Robinson, and Bernhard Kainz. "A survey on active learning and human-in-the-loop deep learning for medical image analysis". In: *Medical Image Analysis* 71 (2021), p. 102062.

[15] Sima Behpour, Kris M Kitani, and Brian D Ziebart. "Ada: Adversarial data augmentation for object detection". In: *2019 IEEE Winter Conference on Applications of Computer Vision (WACV)*. IEEE. 2019, pp. 1243–1252.

[16] Zhun Zhong, Liang Zheng, Guoliang Kang, Shaozi Li, and Yi Yang. "Random erasing data augmentation". In: *Proceedings of the AAAI Conference on Artificial Intelligence*. Vol. 34. 07. 2020, pp. 13001–13008.

[17] Terrance DeVries and Graham W. Taylor. "Dataset augmentation in feature space". In: *5th International Conference on Learning Representations, ICLR 2017 - Workshop Track Proceedings*. International Conference on Learning Representations, ICLR, Feb. 2017.

[18] Connor Shorten and Taghi M Khoshgoftaar. "A survey on image data augmentation for deep learning". In: *Journal of Big Data* 6.1 (2019), pp. 1–48.

[19] Brian Kenji Iwana and Seiichi Uchida. "An empirical survey of data augmentation for time series classification with neural networks". In: *Plos one* 16.7 (2021), e0254841.

[20] Sebastien C Wong, Adam Gatt, Victor Stamatescu, and Mark D McDonnell. "Understanding data augmentation for classification: when to warp?" In: *2016 international conference on digital image computing: techniques and applications (DICTA)*. IEEE. 2016, pp. 1–6.

[21] Omid Kashefi and Rebecca Hwa. "Quantifying the Evaluation of Heuristic Methods for Textual Data Augmentation". In: *Proceedings of the Sixth Workshop on Noisy User-generated Text (W-NUT 2020)*. Online: Association for Computational Linguistics, Nov. 2020, pp. 200–208.

[22] Nitesh V. Chawla, Kevin W. Bowyer, Lawrence O. Hall, and W. Philip Kegelmeyer. "SMOTE: Synthetic minority over-sampling technique". In: *Journal of Artificial Intelligence Research* 16 (June 2002), pp. 321–357. ISSN: 10769757.

[23] Georgios Douzas and Fernando Bacao. "Geometric SMOTE a geometrically enhanced drop-in replacement for SMOTE". In: *Information sciences* 501 (2019), pp. 118–135.

[24] Hui Han, Wen-Yuan Wang, and Bing-Huan Mao. "Borderline-SMOTE: a new over-sampling method in imbalanced data sets learning". In: *International conference on intelligent computing*. Springer. 2005, pp. 878–887.

[25] Georgios Douzas, Fernando Bacao, and Felix Last. "Improving imbalanced learning through a heuristic oversampling method based on k-means and SMOTE". In: *Information Sciences* 465 (Oct. 2018), pp. 1–20. ISSN: 00200255. DOI: 10.1016/j.ins.2018.06.056.

[26] Xiangyong Cao, Jing Yao, Zongben Xu, and Deyu Meng. "Hyperspectral Image Classification with Convolutional Neural Network and Active Learning". In: *IEEE Transactions on Geoscience and Remote Sensing* 58.7 (July 2020), pp. 4604–4616. ISSN: 15580644. DOI: 10.1109/TGRS.2020.2964627.

[27] Pengzhen Ren, Yun Xiao, Xiaojun Chang, Po-Yao Huang, Zhihui Li, Brij B Gupta, Xiaojiang Chen, and Xin Wang. "A survey of deep active learning". In: *ACM Computing Surveys (CSUR)* 54.9 (2021), pp. 1–40.

[28] Vimal K. Shrivastava and Monoj K. Pradhan. "Hyperspectral Remote Sensing Image Classification Using Active Learning". In: *Studies in Computational Intelligence* 907 (2021), pp. 133–152. ISSN: 18609503.

[29] Pengzhen Ren, Yun Xiao, Xiaojun Chang, Po-Yao Huang, Zhihui Li, Xiaojiang Chen, and Xin Wang. "A survey of deep active learning". In: *arXiv preprint arXiv:2009.00236* (2020).

[30] Joao Fonseca, Georgios Douzas, and Fernando Bacao. "Improving imbalanced land cover classification with K-Means SMOTE: Detecting and oversampling distinctive minority spectral signatures". In: *Information* 12.7 (2021), p. 266.

[31] Donggeun Yoo and In So Kweon. "Learning Loss for Active Learning". In: *Proceedings of the IEEE/CVF Conference on Computer Vision and Pattern Recognition (CVPR)*. June 2019, pp. 93–102.

[32] Hamed H Aghdam, Abel Gonzalez-Garcia, Antonio Lopez, and Joost Weijer. "Active learning for deep detection neural networks". In: *Proceedings of the IEEE International Conference on Computer Vision*. Vol. 2019-Octob. 2019, pp. 3671–3679. ISBN: 9781728148038. DOI: 10.1109/ICCV.2019.00377. arXiv: 1911.09168. URL: www.gitlab.com/haghdam/deep%7B%5C_%7Dactive%7B%5C_%7Dlearning.

[33] Tengfei Su, Shengwei Zhang, and Tingxi Liu. "Multi-spectral image classification based on an object-based active learning approach". In: *Remote Sensing* 12.3 (Feb. 2020), p. 504. ISSN: 20724292. URL: https://www.mdpi.com/2072-4292/12/3/504.

[34] Yuriy Sverchkov and Mark Craven. "A review of active learning approaches to experimental design for uncovering biological networks". In: *PLoS Computational Biology* 13 (6 June 2017). Ed. by Haiyan Huang, e1005466. ISSN: 15537358. URL: https://dx.plos.org/10.1371/journal.pcbi.1005466.

[35] Zachary del Rosario, Matthias Rupp, Yoolhee Kim, Erin Antono, and Julia Ling. "Assessing the frontier: Active learning, model accuracy, and multi-objective candidate discovery and optimization". In: *The Journal of Chemical Physics* 153 (2 July 2020), p. 024112. ISSN: 0021-9606.

[36] Daniel Kottke, Adrian Calma, Denis Huseljic, Georg Krempl, and Bernhard Sick. "Challenges of reliable, realistic and comparable active learning evaluation". In: *CEUR Workshop Proceedings*. Vol. 1924. Sept. 2017, pp. 2–14. URL: http://dspace.library.uu.nl/handle/1874/359528.

[37] Jiayi Li, Xin Huang, and Xiaoyu Chang. "A label-noise robust active learning sample collection method for multi-temporal urban land-cover classification and change analysis". In: *ISPRS Journal of Photogrammetry and Remote Sensing* 163.January (2020), pp. 1–17. ISSN: 09242716. DOI: 10.1016/j.isprsjprs.2020.02.022. URL: https://doi.org/10.1016/j.isprsjprs.2020.02.022.

[38] Hieu T Nguyen and Arnold Smeulders. "Active learning using pre-clustering". In: *Proceedings of the twenty-first international conference on Machine learning*. 2004, p. 79.

[39] Bin Gu, Zhou Zhai, Cheng Deng, and Heng Huang. "Efficient Active Learning by Querying Discriminative and Representative Samples and Fully Exploiting Unlabeled Data". In: *IEEE Transactions on Neural Networks and Learning Systems* 32 (9 Sept. 2021), pp. 4111–4122. ISSN: 21622388.

[40] Punit Kumar and Atul Gupta. "Active Learning Query Strategies for Classification, Regression, and Clustering: A Survey". In: *Journal of Computer Science and Technology 2020 35:4* 35 (4 July 2020), pp. 913–945. ISSN: 1860-4749.

[41] Yifan Fu, Xingquan Zhu, and Bin Li. "A survey on instance selection for active learning". In: *Knowledge and information systems* 35.2 (2013), pp. 249–283.

[42] Alim Samat, Paolo Gamba, Sicong Liu, Peijun Du, and Jilili Abuduwaili. "Jointly Informative and Manifold Structure Representative Sampling Based Active Learning for Remote Sensing Image Classification". In: *IEEE Transactions on Geoscience and Remote Sensing* 54 (11 Nov. 2016), pp. 6803–6817. ISSN: 01962892.

[43] Sheng Jun Huang, Rong Jin, and Zhi Hua Zhou. "Active Learning by Querying Informative and Representative Examples". In: *IEEE Transactions on Pattern Analysis and Machine Intelligence* 36 (10 Oct. 2014), pp. 1936–1949. ISSN: 01628828.

[44] Xiao Li, Da Kuang, and Charles X. Ling. "Active Learning for Hierarchical Text Classification". In: *Lecture Notes in Computer Science (including subseries Lecture Notes in Artificial Intelligence and Lecture Notes in Bioinformatics)* 7301 LNAI (PART 1 2012), pp. 14–25. ISSN: 03029743.

[45] Dino Ienco, Albert Bifet, Indre Žliobaite, and Bernhard Pfahringer. "Clustering Based Active Learning for Evolving Data Streams". In: *Lecture Notes in Computer Science (including subseries Lecture Notes in Artificial Intelligence and Lecture Notes in Bioinformatics)* 8140 LNAI (2013), pp. 79–93. ISSN: 16113349.

[46] Klaus Brinker. "Incorporating diversity in active learning with support vector machines". In: *Proceedings of the 20th international conference on machine learning (ICML-03)*. 2003, pp. 59–66.

[47] Junteng Jia, Michael T Schaub, Santiago Segarra, and Austin R Benson. "Graph-based semi-supervised & active learning for edge flows". In: *Proceedings of the 25th ACM SIGKDD International Conference on Knowledge Discovery & Data Mining*. 2019, pp. 761–771.

[48] Burr Settles. "From theories to queries: Active learning in practice". In: *Active Learning and Experimental Design workshop In conjunction with AISTATS 2010*. JMLR Workshop and Conference Proceedings. 2011, pp. 1–18.

[49] David D Lewis and William A Gale. "A sequential algorithm for training text classifiers". In: *SIGIR'94*. Springer. 1994, pp. 3–12.

[50] Tong Luo, Kurt Kramer, Dmitry B Goldgof, Lawrence O Hall, Scott Samson, Andrew Remsen, Thomas Hopkins, and David Cohn. "Active learning to recognize multiple types of plankton." In: *Journal of Machine Learning Research* 6.4 (2005).

[51] Wensong Liu, Jie Yang, Pingxiang Li, Yue Han, Jinqi Zhao, and Hongtao Shi. "A novel object-based supervised classification method with active learning and random forest for PolSAR imagery". In: *Remote Sensing* 10.7 (2018), p. 1092. ISSN: 20724292. DOI: 10.3390/rs10071092.

[52] Jun Li, José M Bioucas-Dias, and Antonio Plaza. "Spectral–spatial classification of hyperspectral data using loopy belief propagation and active learning". In: *IEEE Transactions on Geoscience and remote sensing* 51.2 (2012), pp. 844–856.

[53] Naoki Abe. "Query learning strategies using boosting and bagging". In: *Proc. of* 15^{th} *Int. Cmf. on Machine Learning (ICML98)* (1998), pp. 1–9.

[54] Prem Melville and Raymond J Mooney. "Diverse ensembles for active learning". In: *Proceedings of the twenty-first international conference on Machine learning*. 2004, p. 74.

[55] Michael Bloodgood. "Support Vector Machine Active Learning Algorithms with Query-by-Committee Versus Closest-to-Hyperplane Selection". In: *Proceedings - 12th IEEE International Conference on Semantic Computing, ICSC 2018* 2018-January (Apr. 2018), pp. 148–155.

[56] Xiong Zhou, Saurabh Prasad, and Melba Crawford. "Wavelet domain multi-view active learning for hyperspectral image analysis". In: *Workshop on Hyperspectral Image and Signal Processing, Evolution in Remote Sensing*. Vol. 2014-June. IEEE Computer Society, June 2014. ISBN: 9781467390125. DOI: 10.1109/WHISPERS.2014.8077528.

[57] Jinsung Yoon, Yao Zhang, James Jordon, and Mihaela van der Schaar. "Vime: Extending the success of self-and semi-supervised learning to tabular domain". In: *Advances in Neural Information Processing Systems* 33 (2020), pp. 11033–11043.

[58] Diederik P Kingma, Max Welling, et al. "An introduction to variational autoencoders". In: *Foundations and Trends® in Machine Learning* 12.4 (2019), pp. 307–392.

[59] Terrance DeVries and Graham W Taylor. "Dataset augmentation in feature space". In: *arXiv preprint arXiv:1702.05538* (2017).

[60] Samuel A Assefa, Danial Dervovic, Mahmoud Mahfouz, Robert E Tillman, Prashant Reddy, and Manuela Veloso. "Generating synthetic data in finance: opportunities, challenges and pitfalls". In: *Proceedings of the First ACM International Conference on AI in Finance*. 2020, pp. 1–8.

[61] Yulin Wang, Gao Huang, Shiji Song, Xuran Pan, Yitong Xia, and Cheng Wu. "Regularizing deep networks with semantic data augmentation". In: *IEEE Transactions on Pattern Analysis and Machine Intelligence* (2021).

[62] Neha Patki, Roy Wedge, and Kalyan Veeramachaneni. "The synthetic data vault". In: *2016 IEEE International Conference on Data Science and Advanced Analytics (DSAA)*. IEEE. 2016, pp. 399–410.

[63] Samuli Laine and Timo Aila. "Temporal ensembling for semi-supervised learning". In: *International Conference on Learning Representations (ICLR)*. Vol. 4. 5. 2017, p. 6.

[64] Joao Fonseca, Georgios Douzas, and Fernando Bacao. "Improving imbalanced land cover classification with K-Means SMOTE: Detecting and oversampling distinctive minority spectral signatures". In: *Information* 12.7 (2021), p. 266.

[65] Yoon-Yeong Kim, Kyungwoo Song, JoonHo Jang, and Il-Chul Moon. "LADA: Look-Ahead Data Acquisition via Augmentation for Deep Active Learning". In: *Advances in Neural Information Processing Systems* 34 (2021), pp. 22919–22930.

[66] Jiang-Jing Lv, Xiao-Hu Shao, Jia-Shui Huang, Xiang-Dong Zhou, and Xi Zhou. "Data augmentation for face recognition". In: *Neurocomputing* 230 (2017), pp. 184–196.

[67] Georgios Douzas, Fernando Bacao, Joao Fonseca, and Manvel Khudinyan. "Imbalanced learning in land cover classification: Improving minority classes' prediction accuracy using the geometric SMOTE algorithm". In: *Remote Sensing* 11.24 (2019), p. 3040.

[68] Xin Yi, Ekta Walia, and Paul Babyn. "Generative adversarial network in medical imaging: A review". In: *Medical image analysis* 58 (2019), p. 101552.

[69] Steven Y Feng, Varun Gangal, Jason Wei, Sarath Chandar, Soroush Vosoughi, Teruko Mitamura, and Eduard Hovy. "A Survey of Data Augmentation Approaches for NLP". In: *Findings of the Association for Computational Linguistics: ACL-IJCNLP 2021*. Online: Association for Computational Linguistics, Aug. 2021, pp. 968–988.

[70] Talha Mahboob Alam, Kamran Shaukat, Ibrahim A Hameed, Suhuai Luo, Muhammad Umer Sarwar, Shakir Shabbir, Jiaming Li, and Matloob Khushi. "An investigation of credit card default prediction in the imbalanced datasets". In: *IEEE Access* 8 (2020), pp. 201173–201198.

[71] Rasool Fakoor, Jonas W Mueller, Nick Erickson, Pratik Chaudhari, and Alexander J Smola. "Fast, accurate, and simple models for tabular data via augmented distillation". In: *Advances in Neural Information Processing Systems* 33 (2020), pp. 8671–8681.

[72] L Theis, A van den Oord, and M Bethge. "A note on the evaluation of generative models". In: *International Conference on Learning Representations (ICLR 2016)*. 2016, pp. 1–10.

[73] Vikram S Chundawat, Ayush K Tarun, Murari Mandal, Mukund Lahoti, and Pratik Narang. "TabSynDex: A Universal Metric for Robust Evaluation of Synthetic Tabular Data". In: *arXiv preprint arXiv:2207.05295* (2022).

[74] Ahmed Alaa, Boris Van Breugel, Evgeny S Saveliev, and Mihaela van der Schaar. "How faithful is your synthetic data? sample-level metrics for evaluating and auditing generative models". In: *International Conference on Machine Learning*. PMLR. 2022, pp. 290–306.

[75] Miro Mannino and Azza Abouzied. "Is this real? Generating synthetic data that looks real". In: *Proceedings of the 32nd Annual ACM Symposium on User Interface Software and Technology*. 2019, pp. 549–561.

[76] Mikel Hernandez, Gorka Epelde, Ane Alberdi, Rodrigo Cilla, and Debbie Rankin. "Synthetic Data Generation for Tabular Health Records: A Systematic Review". In: *Neurocomputing* (2022).

[77] Trivellore E Raghunathan. "Synthetic data". In: *Annual Review of Statistics and Its Application* 8 (2021), pp. 129–140.

[78] Jakub Nalepa, Michal Marcinkiewicz, and Michal Kawulok. "Data augmentation for brain-tumor segmentation: a review". In: *Frontiers in computational neuroscience* 13 (2019), p. 83.

[79] Markus Bayer, Marc-André Kaufhold, and Christian Reuter. "A survey on data augmentation for text classification". In: *ACM Computing Surveys* (2021).

[80] Connor Shorten, Taghi M Khoshgoftaar, and Borko Furht. "Text data augmentation for deep learning". In: *Journal of big Data* 8.1 (2021), pp. 1–34.

[81] Jiaao Chen, Derek Tam, Colin Raffel, Mohit Bansal, and Diyi Yang. "An empirical survey of data augmentation for limited data learning in NLP". In: *arXiv preprint arXiv:2106.07499* (2021).

[82] Pei Liu, Xuemin Wang, Chao Xiang, and Weiye Meng. "A survey of text data augmentation". In: *2020 International Conference on Computer Communication and Network Security (CCNS)*. IEEE. 2020, pp. 191–195.

[83] Xiang Wang, Kai Wang, and Shiguo Lian. "A survey on face data augmentation for the training of deep neural networks". In: *Neural computing and applications* 32.19 (2020), pp. 15503–15531.

[84] Connor Shorten and Taghi M Khoshgoftaar. "A survey on image data augmentation for deep learning". In: *Journal of big data* 6.1 (2019), pp. 1–48.

[85] Cherry Khosla and Baljit Singh Saini. "Enhancing performance of deep learning models with different data augmentation techniques: A survey". In: *2020 International Conference on Intelligent Engineering and Management (ICIEM)*. IEEE. 2020, pp. 79–85.

[86] Nour Eldeen Khalifa, Mohamed Loey, and Seyedali Mirjalili. "A comprehensive survey of recent trends in deep learning for digital images augmentation". In: *Artificial Intelligence Review* (2021), pp. 1–27.

[87] Brian Kenji Iwana and Seiichi Uchida. "An empirical survey of data augmentation for time series classification with neural networks". In: *Plos one* 16.7 (2021), e0254841.

[88] Qingsong Wen, Liang Sun, Fan Yang, Xiaomin Song, Jingkun Gao, Xue Wang, and Huan Xu. "Time series data augmentation for deep learning: a survey". In: *Proceedings of the Thirtieth International Joint Conference on Artificial Intelligence, IJCAI-21*. Ed. by Zhi-Hua Zhou. International Joint Conferences on Artificial Intelligence Organization, Aug. 2021, pp. 4653–4660.

[89] Tong Zhao, Gang Liu, Stephan Günnemann, and Meng Jiang. "Graph Data Augmentation for Graph Machine Learning: A Survey". In: *arXiv preprint arXiv:2202.08871* (2022).

[90] Fida K Dankar and Mahmoud Ibrahim. "Fake it till you make it: Guidelines for effective synthetic data generation". In: *Applied Sciences* 11.5 (2021), p. 2158.

[91] Chiyuan Zhang, Samy Bengio, Moritz Hardt, Benjamin Recht, and Oriol Vinyals. "Understanding deep learning (still) requires rethinking generalization". In: *Communications of the ACM* 64.3 (2021), pp. 107–115.

[92] Yi Zeng, Han Qiu, Gerard Memmi, and Meikang Qiu. "A data augmentation-based defense method against adversarial attacks in neural networks". In: *International Conference on Algorithms and Architectures for Parallel Processing*. Springer. 2020, pp. 274–289.

[93] John X Morris, Eli Lifland, Jin Yong Yoo, Jake Grigsby, Di Jin, and Yanjun Qi. "Textattack: A framework for adversarial attacks, data augmentation, and adversarial training in nlp". In: *arXiv preprint arXiv:2005.05909* (2020).

[94] José A Sáez, Bartosz Krawczyk, and Michał Woźniak. "Analyzing the oversampling of different classes and types of examples in multi-class imbalanced datasets". In: *Pattern Recognition* 57 (2016), pp. 164–178.

[95] Joao Fonseca, Georgios Douzas, and Fernando Bacao. "Increasing the Effectiveness of Active Learning: Introducing Artificial Data Generation in Active Learning for Land Use/Land Cover Classification". In: *Remote Sensing* 13.13 (2021), p. 2619.

[96] Jesper E Van Engelen and Holger H Hoos. "A survey on semi-supervised learning". In: *Machine Learning* 109.2 (2020), pp. 373–440.

[97] Ryan McKenna, Gerome Miklau, and Daniel Sheldon. "Winning the NIST Contest: A scalable and general approach to differentially private synthetic data". In: *Journal of Privacy and Confidentiality* 11.3 (2021).

[98] Moritz Hardt, Katrina Ligett, and Frank McSherry. "A simple and practical algorithm for differentially private data release". In: *Proceedings of the 25th International Conference on Neural Information Processing Systems-Volume 2*. 2012, pp. 2339–2347.

[99] Ryan McKenna, Daniel Sheldon, and Gerome Miklau. "Graphical-model based estimation and inference for differential privacy". In: *International Conference on Machine Learning*. PMLR. 2019, pp. 4435–4444.

[100] Jun Zhang, Graham Cormode, Cecilia M Procopiuc, Divesh Srivastava, and Xiaokui Xiao. "Privbayes: Private data release via bayesian networks". In: *ACM Transactions on Database Systems (TODS)* 42.4 (2017), pp. 1–41.

[101] Liyang Xie, Kaixiang Lin, Shu Wang, Fei Wang, and Jiayu Zhou. "Differentially private generative adversarial network". In: *arXiv preprint arXiv:1802.06739* (2018).

[102] Lucas Rosenblatt, Xiaoyan Liu, Samira Pouyanfar, Eduardo de Leon, Anuj Desai, and Joshua Allen. "Differentially private synthetic data: Applied evaluations and enhancements". In: *arXiv preprint arXiv:2011.05537* (2020).

[103] James Jordon, Jinsung Yoon, and Mihaela Van Der Schaar. "PATE-GAN: Generating synthetic data with differential privacy guarantees". In: *International conference on learning representations*. 2018.

[104] Giuseppe Vietri, Grace Tian, Mark Bun, Thomas Steinke, and Steven Wu. "New oracle-efficient algorithms for private synthetic data release". In: *International Conference on Machine Learning*. PMLR. 2020, pp. 9765–9774.

[105] Sergul Aydore, William Brown, Michael Kearns, Krishnaram Kenthapadi, Luca Melis, Aaron Roth, and Ankit A Siva. "Differentially private query release through adaptive projection". In: *International Conference on Machine Learning*. PMLR. 2021, pp. 457–467.

[106] Christopher De Sa, Ihab Ilyas, Benny Kimelfeld, Christopher Re, and Theodoros Rekatsinas. "A Formal Framework for Probabilistic Unclean Databases". In: *22nd International Conference on Database Theory (ICDT 2019)*. 2019.

[107] Dan Suciu, Dan Olteanu, Christopher Ré, and Christoph Koch. "Probabilistic databases". In: *Synthesis lectures on data management* 3.2 (2011), pp. 1–180.

[108] Chang Ge, Shubhankar Mohapatra, Xi He, and Ihab F Ilyas. "Kamino: constraint-aware differentially private data synthesis". In: *Proceedings of the VLDB Endowment* 14.10 (2021), pp. 1886–1899.

[109] Thee Chanyaswad, Changchang Liu, and Prateek Mittal. "Ron-gauss: Enhancing utility in non-interactive private data release". In: *Proceedings on Privacy Enhancing Technologies* 2019.1 (2019), pp. 26–46.

[110] Ryan McKenna, Gerome Miklau, Michael Hay, and Ashwin Machanavajjhala. "Optimizing error of high-dimensional statistical queries under differential privacy". In: *Proceedings of the VLDB Endowment* 11.10 (2018).

[111] Marco Gaboardi, Emilio Jesús Gallego Arias, Justin Hsu, Aaron Roth, and Zhiwei Steven Wu. "Dual query: Practical private query release for high dimensional data". In: *International Conference on Machine Learning*. PMLR. 2014, pp. 1170–1178.

[112] Giovanna Menardi and Nicola Torelli. “Training and assessing classification rules with imbalanced data”. In: *Data mining and knowledge discovery* 28.1 (2014), pp. 92–122.

[113] Nitesh V Chawla, Kevin W Bowyer, Lawrence O Hall, and W Philip Kegelmeyer. “SMOTE: synthetic minority over-sampling technique”. In: *Journal of artificial intelligence research* 16 (2002), pp. 321–357.

[114] Hui Han, Wen-Yuan Wang, and Bing-Huan Mao. “Borderline-SMOTE: a new over-sampling method in imbalanced data sets learning”. In: *International conference on intelligent computing*. Springer. 2005, pp. 878–887.

[115] Georgios Douzas and Fernando Bacao. “Geometric SMOTE a geometrically enhanced drop-in replacement for SMOTE”. In: *Information Sciences* 501 (2019), pp. 118–135.

[116] Haibo He, Yang Bai, Edwardo A Garcia, and Shutao Li. “ADASYN: Adaptive synthetic sampling approach for imbalanced learning”. In: *2008 IEEE international joint conference on neural networks (IEEE world congress on computational intelligence)*. IEEE. 2008, pp. 1322–1328.

[117] Bo Tang and Haibo He. “KernelADASYN: Kernel based adaptive synthetic data generation for imbalanced learning”. In: *2015 IEEE congress on evolutionary computation (CEC)*. IEEE. 2015, pp. 664–671.

[118] Chin-Teng Lin, Tsung-Yu Hsieh, Yu-Ting Liu, Yang-Yin Lin, Chieh-Ning Fang, Yu-Kai Wang, Gary Yen, Nikhil R Pal, and Chun-Hsiang Chuang. “Minority oversampling in kernel adaptive subspaces for class imbalanced datasets”. In: *IEEE Transactions on Knowledge and Data Engineering* 30.5 (2017), pp. 950–962.

[119] Georgios Douzas and Fernando Bacao. “Self-Organizing Map Oversampling (SOMO) for imbalanced data set learning”. In: *Expert systems with Applications* 82 (2017), pp. 40–52.

[120] Georgios Douzas, Rene Rauch, and Fernando Bacao. “G-SOMO: An oversampling approach based on self-organized maps and geometric SMOTE”. In: *Expert Systems with Applications* 183 (2021), p. 115230.

[121] Meng Xing, Yanbo Zhang, Hongmei Yu, Zhenhuan Yang, Xueling Li, Qiong Li, Yanlin Zhao, Zhiqiang Zhao, and Yanhong Luo. “Predict DLBCL patients’ recurrence within two years with Gaussian mixture model cluster oversampling and multi-kernel learning”. In: *Computer Methods and Programs in Biomedicine* 226 (2022), p. 107103.

[122] Zhaozhao Xu, Derong Shen, Yue Kou, and Tiezheng Nie. “A Synthetic Minority Oversampling Technique Based on Gaussian Mixture Model Filtering for Imbalanced Data Classification”. In: *IEEE Transactions on Neural Networks and Learning Systems* (2022).

[123] Wangzhi Dai, Kenney Ng, Kristen Severson, Wei Huang, Fred Anderson, and Collin Stultz. “Generative oversampling with a contrastive variational autoencoder”. In: *2019 IEEE International Conference on Data Mining (ICDM)*. IEEE. 2019, pp. 101–109.

[124] Chumphol Bunkhumpornpat, Krung Sinapiromsaran, and Chidchanok Lursinsap. “Safe-level-smote: Safe-level-synthetic minority over-sampling technique for handling the class imbalanced problem”. In: *Pacific-Asia conference on knowledge discovery and data mining*. Springer. 2009, pp. 475–482.

[125] XW Liang, AP Jiang, T Li, YY Xue, and GT Wang. “LR-SMOTE — An improved unbalanced data set oversampling based on K-means and SVM”. In: *Knowledge-Based Systems* 196 (2020), p. 105845.

[126] Georgios Douzas, Fernando Bacao, and Felix Last. “Improving imbalanced learning through a heuristic oversampling method based on k-means and SMOTE”. In: *Information Sciences* 465 (2018), pp. 1–20.

[127] Chumphol Bunkhumpornpat, Krung Sinapiromsaran, and Chidchanok Lursinsap. “DBSMOTE: density-based synthetic minority over-sampling technique”. In: *Applied Intelligence* 36.3 (2012), pp. 664–684.

[128] Georgios Douzas and Fernando Bacao. “Effective data generation for imbalanced learning using conditional generative adversarial networks”. In: *Expert Systems with applications* 91 (2018), pp. 464–471.

[129] Chunsheng An, Jingtong Sun, Yifeng Wang, and Qingjie Wei. “A K-means Improved CTGAN Oversampling Method for Data Imbalance Problem”. In: *2021 IEEE 21st International Conference on Software Quality, Reliability and Security (QRS)*. IEEE. 2021, pp. 883–887.

[130] Luís Torgo, Rita P Ribeiro, Bernhard Pfahringer, and Paula Branco. “Smote for regression”. In: *Portuguese conference on artificial intelligence*. Springer. 2013, pp. 378–389.

[131] Luís Camacho, Georgios Douzas, and Fernando Bacao. “Geometric SMOTE for regression”. In: *Expert Systems with Applications* (2022), p. 116387.

[132] Barnan Das, Narayanan C Krishnan, and Diane J Cook. “RACOG and wRACOG: Two probabilistic oversampling techniques”. In: *IEEE transactions on knowledge and data engineering* 27.1 (2014), pp. 222–234.

[133] Huaxiang Zhang and Mingfang Li. “RWO-Sampling: A random walk over-sampling approach to imbalanced data classification”. In: *Information Fusion* 20 (2014), pp. 99–116.

[134] Ming Gao, Xia Hong, Sheng Chen, Chris J Harris, and Emad Khalaf. “PDFOS: PDF estimation based over-sampling for imbalanced two-class problems”. In: *Neurocomputing* 138 (2014), pp. 248–259.

[135] Hongyi Zhang, Moustapha Cisse, Yann N Dauphin, and David Lopez-Paz. “mixup: Beyond Empirical Risk Minimization”. In: *International Conference on Learning Representations*. 2018.

[136] Vikas Verma, Alex Lamb, Christopher Beckham, Amir Najafi, Ioannis Mitliagkas, David Lopez-Paz, and Yoshua Bengio. “Manifold mixup: Better representations by interpolating hidden states”. In: *International Conference on Machine Learning*. PMLR. 2019, pp. 6438–6447.

[137] Hongyu Guo. “Nonlinear mixup: Out-of-manifold data augmentation for text classification”. In: *Proceedings of the AAAI Conference on Artificial Intelligence*. Vol. 34. 04. 2020, pp. 4044–4051.

[138] Xiexing Feng, QM Jonathan Wu, Yimin Yang, and Libo Cao. “An autuencoder-based data augmentation strategy for generalization improvement of DCNNs”. In: *Neurocomputing* 402 (2020), pp. 283–297.

[139] Tsz-Him Cheung and Dit-Yan Yeung. “Modals: Modality-agnostic automated data augmentation in the latent space”. In: *International Conference on Learning Representations*. 2020.

[140] Xiaofeng Liu, Yang Zou, Lingsheng Kong, Zhihui Diao, Junliang Yan, Jun Wang, Site Li, Ping Jia, and Jane You. “Data augmentation via latent space interpolation for image classification”. In: *2018 24th International Conference on Pattern Recognition (ICPR)*. IEEE. 2018, pp. 728–733.

[141] Karim Armanious, Chenming Jiang, Marc Fischer, Thomas Küstner, Tobias Hepp, Konstantin Nikolaou, Sergios Gatidis, and Bin Yang. “MedGAN: Medical image translation using GANs”. In: *Computerized medical imaging and graphics* 79 (2020), p. 101684.

[142] Yishuo Zhang, Nayyar A Zaidi, Jiahui Zhou, and Gang Li. “GANBLR: a tabular data generation model”. In: *2021 IEEE International Conference on Data Mining (ICDM)*. IEEE. 2021, pp. 181–190.

[143] Noseong Park, Mahmoud Mohammadi, Kshitij Gorde, Sushil Jajodia, Hongkyu Park, and Youngmin Kim. “Data Synthesis based on Generative Adversarial Networks”. In: *Proceedings of the VLDB Endowment* 11.10 (2018).

[144] Lei Xu, Maria Skoularidou, Alfredo Cuesta-Infante, and Kalyan Veeramachaneni. “Modeling tabular data using conditional gan”. In: *Advances in Neural Information Processing Systems* 32 (2019).

[145] Juan Manuel Davila Delgado and Lukumon Oyedele. “Deep learning with small datasets: using autoencoders to address limited datasets in construction management”. In: *Applied Soft Computing* 112 (2021), p. 107836.

[146] Toan Tran, Thanh-Toan Do, Ian Reid, and Gustavo Carneiro. "Bayesian generative active deep learning". In: *International Conference on Machine Learning*. PMLR. 2019, pp. 6295–6304.

[147] Antti Rasmus, Mathias Berglund, Mikko Honkala, Harri Valpola, and Tapani Raiko. "Semi-supervised learning with ladder networks". In: *Advances in neural information processing systems* 28 (2015).

[148] Laine Samuli and Aila Timo. "Temporal ensembling for semi-supervised learning". In: *International Conference on Learning Representations (ICLR)*. Vol. 4. 5. 2017, p. 6.

[149] Antti Tarvainen and Harri Valpola. "Mean teachers are better role models: Weight-averaged consistency targets improve semi-supervised deep learning results". In: *Advances in neural information processing systems* 30 (2017).

[150] Vikas Verma, Kenji Kawaguchi, Alex Lamb, Juho Kannala, Arno Solin, Yoshua Bengio, and David Lopez-Paz. "Interpolation consistency training for semi-supervised learning". In: *Neural Networks* 145 (2022), pp. 90–106.

[151] David Berthelot, Nicholas Carlini, Ian Goodfellow, Nicolas Papernot, Avital Oliver, and Colin A Raffel. "Mixmatch: A holistic approach to semi-supervised learning". In: *Advances in neural information processing systems* 32 (2019).

[152] Junpeng Fang, Caizhi Tang, Qing Cui, Feng Zhu, Longfei Li, Jun Zhou, and Wei Zhu. "Semi-Supervised Learning with Data Augmentation for Tabular Data". In: *Proceedings of the 31st ACM International Conference on Information & Knowledge Management*. 2022, pp. 3928–3932.

[153] Xiaodi Li, Latifur Khan, Mahmoud Zamani, Shamila Wickramasuriya, Kevin W Hamlen, and Bhavani Thuraisingham. "MCoM: A Semi-Supervised Method for Imbalanced Tabular Security Data". In: *IFIP Annual Conference on Data and Applications Security and Privacy*. Springer. 2022, pp. 48–67.

[154] Sajad Darabi, Shayan Fazeli, Ali Pazoki, Sriram Sankararaman, and Majid Sarrafzadeh. "Contrastive Mixup: Self-and Semi-Supervised learning for Tabular Domain". In: *arXiv preprint arXiv:2108.12296* (2021).

[155] Talip Ucar, Ehsan Hajiramezanali, and Lindsay Edwards. "Subtab: Subsetting features of tabular data for self-supervised representation learning". In: *Advances in Neural Information Processing Systems* 34 (2021), pp. 18853–18865.

[156] Dara Bahri, Heinrich Jiang, Yi Tay, and Donald Metzler. "Scarf: Self-Supervised Contrastive Learning using Random Feature Corruption". In: *International Conference on Learning Representations*. 2022.

[157] Zhifeng Qiu, Wanxin Zeng, Dahua Liao, and Ning Gui. "A-SFS: Semi-supervised feature selection based on multi-task self-supervision". In: *Knowledge-Based Systems* 252 (2022), p. 109449.

[158] Jennifer Taub, Mark Elliot, Maria Pampaka, and Duncan Smith. "Differential correct attribution probability for synthetic data: an exploration". In: *International Conference on Privacy in Statistical Databases*. Springer. 2018, pp. 122–137.

[159] Jerome P Reiter. "New approaches to data dissemination: A glimpse into the future (?)" In: *Chance* 17.3 (2004), pp. 11–15.

[160] Bin Yu, Wenjie Mao, Yihan Lv, Chen Zhang, and Yu Xie. "A survey on federated learning in data mining". In: *Wiley Interdisciplinary Reviews: Data Mining and Knowledge Discovery* 12.1 (2022), e1443.

[161] Kalpana Singh and Lynn Batten. "Aggregating privatized medical data for secure querying applications". In: *Future Generation Computer Systems* 72 (2017), pp. 250–263.

[162] Ping Li, Tong Li, Heng Ye, Jin Li, Xiaofeng Chen, and Yang Xiang. "Privacy-preserving machine learning with multiple data providers". In: *Future Generation Computer Systems* 87 (2018), pp. 341–350.

[163] Cynthia Dwork, Aaron Roth, et al. "The algorithmic foundations of differential privacy". In: *Foundations and Trends® in Theoretical Computer Science* 9.3–4 (2014), pp. 211–407.

[164] Kevin Zhang, Neha Patki, and Kalyan Veeramachaneni. "Sequential Models in the Synthetic Data Vault". In: *arXiv preprint arXiv:2207.14406* (2022).

[165] Yuchao Tao, Ryan McKenna, Michael Hay, Ashwin Machanavajjhala, and Gerome Miklau. "Benchmarking differentially private synthetic data generation algorithms". In: *arXiv e-prints* (2021), arXiv–2112.

[166] Adam Kalai and Santosh Vempala. "Efficient algorithms for online decision problems". In: *Journal of Computer and System Sciences* 71.3 (2005), pp. 291–307.

[167] Aleksandar Nikolov, Kunal Talwar, and Li Zhang. "The geometry of differential privacy: the sparse and approximate cases". In: *Proceedings of the forty-fifth annual ACM symposium on Theory of computing*. 2013, pp. 351–360.

[168] Elizabeth Meckes. "Projections of probability distributions: A measure-theoretic Dvoretzky theorem". In: *Geometric aspects of functional analysis*. Springer, 2012, pp. 317–326.

[169] Jim Young, Patrick Graham, and Richard Penny. "Using Bayesian networks to create synthetic data". In: *Journal of Official Statistics* 25.4 (2009), p. 549.

[170] Nicolas Papernot, Martín Abadi, Ùlfar Erlingsson, Ian Goodfellow, and Kunal Talwar. "Semi-supervised Knowledge Transfer for Deep Learning from Private Training Data". In: *Proceedings of the International Conference on Learning Representations*. 2017. URL: https://arxiv.org/abs/1610.05755.

[171] Martin Benning and Martin Burger. "Modern regularization methods for inverse problems". In: *Acta Numerica* 27 (2018), pp. 1–111.

[172] Peter L Bartlett, Andrea Montanari, and Alexander Rakhlin. "Deep learning: a statistical viewpoint". In: *Acta numerica* 30 (2021), pp. 87–201.

[173] Alon Halevy, Peter Norvig, and Fernando Pereira. "The unreasonable effectiveness of data". In: *IEEE Intelligent Systems* 24.2 (2009), pp. 8–12.

[174] Pedro Domingos. "A few useful things to know about machine learning". In: *Communications of the ACM* 55.10 (2012), pp. 78–87.

[175] Shaeke Salman and Xiuwen Liu. "Overfitting mechanism and avoidance in deep neural networks". In: *arXiv preprint arXiv:1901.06566* (2019).

[176] Zeke Xie, Fengxiang He, Shaopeng Fu, Issei Sato, Dacheng Tao, and Masashi Sugiyama. "Artificial neural variability for deep learning: On overfitting, noise memorization, and catastrophic forgetting". In: *Neural computation* 33.8 (2021), pp. 2163–2192.

[177] Claudio Filipi Gonçalves dos Santos and João Paulo Papa. "Avoiding Overfitting: A Survey on Regularization Methods for Convolutional Neural Networks". In: *ACM Computing Surveys (CSUR)* (2022).

[178] David A Van Dyk and Xiao-Li Meng. "The art of data augmentation". In: *Journal of Computational and Graphical Statistics* 10.1 (2001), pp. 1–50.

[179] David A Van Dyk and Xiao-Li Meng. "The art of data augmentation". In: *Journal of Computational and Graphical Statistics* 10.1 (2001), pp. 1–50.

[180] Wei Feng, Wenjiang Huang, and Wenxing Bao. "Imbalanced hyperspectral image classification with an adaptive ensemble method based on SMOTE and rotation forest with differentiated sampling rates". In: *IEEE Geoscience and Remote Sensing Letters* 16.12 (2019), pp. 1879–1883.

[181] Roweida Mohammed, Jumanah Rawashdeh, and Malak Abdullah. "Machine learning with oversampling and undersampling techniques: overview study and experimental results". In: *2020 11th international conference on information and communication systems (ICICS)*. IEEE. 2020, pp. 243–248.

[182] Julio Hernandez, Jesús Ariel Carrasco-Ochoa, and José Francisco Martínez-Trinidad. "An empirical study of oversampling and undersampling for instance selection methods on imbalance datasets". In: *Iberoamerican Congress on Pattern Recognition*. Springer. 2013, pp. 262–269.

[183] Bartosz Krawczyk. "Learning from imbalanced data: open challenges and future directions". In: *Progress in Artificial Intelligence* 5.4 (2016), pp. 221–232.

[184] Teuvo Kohonen. "Emergence of invariant-feature detectors in the adaptive-subspace self-organizing map". In: *Biological cybernetics* 75.4 (1996), pp. 281–291.

[185] Abubakar Abid and James Zou. "Contrastive variational autoencoder enhances salient features". In: *arXiv preprint arXiv:1902.04601* (2019).

[186] Scott Cost and Steven Salzberg. "A weighted nearest neighbor algorithm for learning with symbolic features". In: *Machine learning* 10.1 (1993), pp. 57–78.

[187] Augustus Odena, Christopher Olah, and Jonathon Shlens. "Conditional image synthesis with auxiliary classifier gans". In: *International conference on machine learning*. PMLR. 2017, pp. 2642–2651.

[188] Max Jaderberg, Karen Simonyan, Andrew Zisserman, and Koray Kavukcuoglu. "Spatial transformer networks". In: *Proceedings of the 28th International Conference on Neural Information Processing Systems-Volume 2*. 2015, pp. 2017–2025.

[189] Timur Sattarov, Dayananda Herurkar, and Jörn Hees. "Explaining Anomalies using Denoising Autoencoders for Financial Tabular Data". In: *arXiv preprint arXiv:2209.10658* (2022).

[190] Ehsan Hajiramezanali, Max W Shen, Gabriele Scalia, and Nathaniel Lee Diamant. "STab: Self-supervised Learning for Tabular Data". In: *NeurIPS 2022 First Table Representation Workshop*. 2022.

[191] Sercan Ö Arik and Tomas Pfister. "Tabnet: Attentive interpretable tabular learning". In: *Proceedings of the AAAI Conference on Artificial Intelligence*. Vol. 35. 8. 2021, pp. 6679–6687.

[192] Yue Yu, Jie Chen, Tian Gao, and Mo Yu. "DAG-GNN: DAG structure learning with graph neural networks". In: *International Conference on Machine Learning*. PMLR. 2019, pp. 7154–7163.

[193] Ian Goodfellow, Jean Pouget-Abadie, Mehdi Mirza, Bing Xu, David Warde-Farley, Sherjil Ozair, Aaron Courville, and Yoshua Bengio. "Generative adversarial networks". In: *Communications of the ACM* 63.11 (2020), pp. 139–144.

[194] David H Ackley, Geoffrey E Hinton, and Terrence J Sejnowski. "A learning algorithm for Boltzmann machines". In: *Cognitive science* 9.1 (1985), pp. 147–169.

[195] Fida K Dankar, Mahmoud K Ibrahim, and Leila Ismail. "A Multi-Dimensional Evaluation of Synthetic Data Generators". In: *IEEE Access* 10 (2022), pp. 11147–11158.

[196] Markus Hittmeir, Andreas Ekelhart, and Rudolf Mayer. "On the utility of synthetic data: An empirical evaluation on machine learning tasks". In: *Proceedings of the 14th International Conference on Availability, Reliability and Security*. 2019, pp. 1–6.

[197] Zilong Zhao, Aditya Kunar, Robert Birke, and Lydia Y Chen. "Ctab-gan: Effective table data synthesizing". In: *Asian Conference on Machine Learning*. PMLR. 2021, pp. 97–112.

[198] Ishaan Gulrajani, Faruk Ahmed, Martin Arjovsky, Vincent Dumoulin, and Aaron C Courville. "Improved training of wasserstein gans". In: *Advances in neural information processing systems* 30 (2017).

[199] Andre Goncalves, Priyadip Ray, Braden Soper, Jennifer Stevens, Linda Coyle, and Ana Paula Sales. "Generation and evaluation of synthetic patient data". In: *BMC medical research methodology* 20.1 (2020), pp. 1–40.

[200] Mi-Ja Woo, Jerome P Reiter, Anna Oganian, and Alan F Karr. "Global measures of data utility for microdata masked for disclosure limitation". In: *Journal of Privacy and Confidentiality* 1.1 (2009).

[201] Joshua Snoke, Gillian M Raab, Beata Nowok, Chris Dibben, and Aleksandra Slavkovic. "General and specific utility measures for synthetic data". In: *Journal of the Royal Statistical Society: Series A (Statistics in Society)* 181.3 (2018), pp. 663–688.

[202] Mehdi SM Sajjadi, Olivier Bachem, Mario Lucic, Olivier Bousquet, and Sylvain Gelly. "Assessing generative models via precision and recall". In: *Advances in neural information processing systems* 31 (2018).

[203] Khaled El Emam. "Seven ways to evaluate the utility of synthetic data". In: *IEEE Security & Privacy* 18.4 (2020), pp. 56–59.

[204] Anat Reiner Benaim, Ronit Almog, Yuri Gorelik, Irit Hochberg, Laila Nassar, Tanya Mashiach, Mogher Khamaisi, Yael Lurie, Zaher S Azzam, Johad Khoury, et al. "Analyzing medical research results based on synthetic data and their relation to real data results: systematic comparison from five observational studies". In: *JMIR medical informatics* 8.2 (2020), e16492.

[205] Lucas Rosenblatt, Anastasia Holovenko, Taras Rumezhak, Andrii Stadnik, Bernease Herman, Julia Stoyanovich, and Bill Howe. "Epistemic Parity: Reproducibility as an Evaluation Metric for Differential Privacy". In: *arXiv preprint arXiv:2208.12700* (2022).

[206] Md Sakib Nizam Khan, Niklas Reje, and Sonja Buchegger. "Utility Assessment of Synthetic Data Generation Methods". In: *Privacy in Statistical Database*. 2022.

[207] Alan F Karr, Christine N Kohnen, Anna Oganian, Jerome P Reiter, and Ashish P Sanil. "A framework for evaluating the utility of data altered to protect confidentiality". In: *The American Statistician* 60.3 (2006), pp. 224–232.

[208] Tri Dao, Albert Gu, Alexander Ratner, Virginia Smith, Chris De Sa, and Christopher Ré. "A kernel theory of modern data augmentation". In: *International Conference on Machine Learning*. PMLR. 2019, pp. 1528–1537.

[209] Ekin D Cubuk, Barret Zoph, Dandelion Mane, Vijay Vasudevan, and Quoc V Le. "Autoaugment: Learning augmentation strategies from data". In: *Proceedings of the IEEE/CVF Conference on Computer Vision and Pattern Recognition*. 2019, pp. 113–123.

[210] Amy Zhao, Guha Balakrishnan, Fredo Durand, John V Guttag, and Adrian V Dalca. "Data augmentation using learned transformations for one-shot medical image segmentation". In: *Proceedings of the IEEE/CVF conference on computer vision and pattern recognition*. 2019, pp. 8543–8553.

[211] Jing Zhou, Yanan Zheng, Jie Tang, Jian Li, and Zhilin Yang. "Flipda: Effective and robust data augmentation for few-shot learning". In: *arXiv preprint arXiv:2108.06332* (2021).

[212] Stefan Hegselmann, Alejandro Buendia, Hunter Lang, Monica Agrawal, Xiaoyi Jiang, and David Sontag. "TabLLM: Few-shot Classification of Tabular Data with Large Language Models". In: *arXiv preprint arXiv:2210.10723* (2022).

[213] Katherina K Hauner, Richard E Zinbarg, and William Revelle. "A latent variable model approach to estimating systematic bias in the oversampling method". In: *Behavior Research Methods* 46.3 (2014), pp. 786–797.

[214] M. Drusch, U. Del Bello, S. Carlier, O. Colin, V. Fernandez, F. Gascon, B. Hoersch, C. Isola, P. Laberinti, P. Martimort, A. Meygret, F. Spoto, O. Sy, F. Marchese, and P. Bargellini. "Sentinel-2: ESA's Optical High-Resolution Mission for GMES Operational Services". In: *Remote Sensing of Environment* 120 (May 2012), pp. 25–36. ISSN: 00344257. DOI: 10.1016/j.rse.2011.11.026.

[215] Steffen Fritz, Linda See, Christoph Perger, Ian McCallum, Christian Schill, Dmitry Schepaschenko, Martina Duerauer, Mathias Karner, Christopher Dresel, Juan Carlos Laso-Bayas, Myroslava Lesiv, Inian Moorthy, Carl F. Salk, Olha Danylo, Tobias Sturn, Franziska Albrecht, Liangzhi You, Florian Kraxner, and Michael Obersteiner. "A global dataset of crowdsourced land cover and land use reference data". In: *Scientific Data* 4.1 (June 2017), pp. 1–8. ISSN: 20524463. DOI: 10.1038/sdata.2017.75. URL: www.nature.com/sdata/.

[216] Michael A. Wulder, Nicholas C. Coops, David P. Roy, Joanne C. White, and Txomin Hermosilla. "Land cover 2.0". In: *International Journal of Remote Sensing* 39.12 (2018), pp. 4254–4284. ISSN: 13665901. DOI: 10.1080/01431161.2018.1452075.

[217] Anil B. Gavade and Vijay S. Rajpurohit. "Systematic analysis of satellite image-based land cover classification techniques: literature review and challenges". In: *International Journal of Computers and Applications* (Feb. 2019), pp. 1–10. ISSN: 1206-212X. DOI: 10.1080/1206212x.2019.1573946.

[218] Harsurinder Kaur, Husanbir Singh Pannu, and Avleen Kaur Malhi. "A systematic review on imbalanced data challenges in machine learning: Applications and solutions". In: *ACM Computing Surveys (CSUR)* 52.4 (2019), pp. 1–36.

[219] Rongfang Wang, Jie Zhang, Jia-Wei Chen, Licheng Jiao, and Mi Wang. "Imbalanced Learning-based Automatic SAR Images Change Detection by Morphologically Supervised PCA-Net". In: *IEEE Geoscience and Remote Sensing Letters* (June 2019). arXiv: 1906.07923. URL: http://arxiv.org/abs/1906.07923.

[220] Wei Feng, Wenjiang Huang, and Wenxing Bao. "Imbalanced Hyperspectral Image Classification With an Adaptive Ensemble Method Based on SMOTE and Rotation Forest With Differentiated Sampling Rates". In: *IEEE Geoscience and Remote Sensing Letters* (2019), pp. 1–5. ISSN: 1545-598X. DOI: 10.1109/LGRS.2019.2913387. URL: https://ieeexplore.ieee.org/document/8713384/.

[221] Nitesh V Chawla, Nathalie Japkowicz, and Aleksander Kotcz. "Special issue on learning from imbalanced data sets". In: *ACM SIGKDD explorations newsletter* 6.1 (2004), pp. 1–6.

[222] Lida Abdi and Sattar Hashemi. "To Combat Multi-Class Imbalanced Problems by Means of Over-Sampling Techniques". In: *IEEE Transactions on Knowledge and Data Engineering* 28.1 (Jan. 2016), pp. 238–251. ISSN: 1041-4347. DOI: 10.1109/TKDE.2015.2458858. URL: http://ieeexplore.ieee.org/document/7163639/.

[223] Aaron E. Maxwell, Timothy A. Warner, and Fang Fang. "Implementation of machine-learning classification in remote sensing: An applied review". In: *International Journal of Remote Sensing* 39.9 (2018), pp. 2784–2817. ISSN: 13665901. DOI: 10.1080/01431161.2018.1433343. URL: https://doi.org/10.1080/01431161.2018.1433343.

[224] Julián Luengo, Diego García-Gil, Sergio Ramírez-Gallego, Salvador García, and Francisco Herrera. "Imbalanced Data Preprocessing for Big Data". In: *Big Data Preprocessing*. Cham: Springer International Publishing, 2020, pp. 147–160. DOI: 10.1007/978-3-030-39105-8_8. URL: http://link.springer.com/10.1007/978-3-030-39105-8%7B%5C_%7D8.

[225] Salvador García, Sergio Ramírez-Gallego, Julián Luengo, José Manuel Benítez, and Francisco Herrera. "Big data preprocessing: methods and prospects". In: *Big Data Analytics* 1.1 (Dec. 2016), p. 9. ISSN: 2058-6345. DOI: 10.1186/s41044-016-0014-0. URL: http://bdataanalytics.biomedcentral.com/articles/10.1186/s41044-016-0014-0.

[226] Guo Haixiang, Li Yijing, Jennifer Shang, Gu Mingyun, Huang Yuanyue, and Gong Bing. "Learning from Class-Imbalanced Data". In: *Expert Syst. Appl.* 73.C (May 2017), pp. 220–239. ISSN: 0957-4174. DOI: 10.1016/j.eswa.2016.12.035. URL: https://doi.org/10.1016/j.eswa.2016.12.035.

[227] Nathalie Japkowicz. "Concept-learning in the presence of between-class and within-class imbalances". In: *Lecture Notes in Computer Science (including subseries Lecture Notes in Artificial Intelligence and Lecture Notes in Bioinformatics)*. Vol. 2056. Springer Verlag, 2001, pp. 67–77. ISBN: 3540421440. DOI: 10.1007/3-540-45153-6_7. URL: https://link.springer.com/chapter/10.1007/3-540-45153-6_7.

[228] Taeho Jo and Nathalie Japkowicz. "Class imbalances versus small disjuncts". In: *ACM SIGKDD Explorations Newsletter* 6.1 (June 2004), pp. 40–49. ISSN: 1931-0145. DOI: 10.1145/1007730.1007737. URL: https://dl.acm.org/doi/10.1145/1007730.1007737.

[229] Rok Blagus and Lara Lusa. "Class prediction for high-dimensional class-imbalanced data." In: *BMC bioinformatics* 11.1 (Oct. 2010), p. 523. ISSN: 14712105. DOI: 10.1186/1471-2105-11-523.

[230] Andrew Mellor, Samia Boukir, Andrew Haywood, and Simon Jones. "Exploring issues of training data imbalance and mislabelling on random forest performance for large area land cover classification using the ensemble margin". In: *ISPRS Journal of Photogrammetry and Remote Sensing* 105 (July 2015), pp. 155–168. ISSN: 0924-2716. DOI: 10.1016/J.ISPRSJPRS.2015.03.014. URL: https://www.sciencedirect.com/science/article/pii/S0924271615000945.

[231] Yuan Hai Shao, Wei Jie Chen, Jing Jing Zhang, Zhen Wang, and Nai Yang Deng. "An efficient weighted Lagrangian twin support vector machine for imbalanced data classification". In: *Pattern Recognition* 47.9 (Sept. 2014), pp. 3158–3167. ISSN: 00313203. DOI: 10.1016/j.patcog.2014.03.008.

[232] Taehyung Lee, Ki Bum Lee, and Chang Ouk Kim. "Performance of Machine Learning Algorithms for Class-Imbalanced Process Fault Detection Problems". In: *IEEE Transactions on Semiconductor Manufacturing* 29.4 (Nov. 2016), pp. 436–445. ISSN: 08946507. DOI: 10.1109/TSM.2016.2602226. URL: http://ieeexplore.ieee.org/document/7549079/.

[233] Chen Huang, Yining Li, Chen Change Loy, and Xiaoou Tang. "Learning deep representation for imbalanced classification". In: *Proceedings of the IEEE Computer Society Conference on Computer Vision and Pattern Recognition*. Vol. 2016-Decem. 2016, pp. 5375–5384. ISBN: 9781467388504. DOI: 10.1109/CVPR.2016.580.

[234] Yin Cui, Menglin Jia, Tsung Yi Lin, Yang Song, and Serge Belongie. "Class-balanced loss based on effective number of samples". In: *Proceedings of the IEEE Computer Society Conference on Computer Vision and Pattern Recognition*. Vol. 2019-June. 2019, pp. 9260–9269. ISBN: 9781728132938. DOI: 10.1109/CVPR.2019.00949. arXiv: 1901.05555.

[235] Qi Dong, Shaogang Gong, and Xiatian Zhu. "Class Rectification Hard Mining for Imbalanced Deep Learning". In: *Proceedings of the IEEE International Conference on Computer Vision*. Vol. 2017-Octob. 2017, pp. 1869–1878. ISBN: 9781538610329. DOI: 10.1109/ICCV.2017.205. arXiv: 1712.03162.

[236] Amin Sharififar, Fereydoon Sarmadian, and Budiman Minasny. "Mapping imbalanced soil classes using Markov chain random fields models treated with data resampling technique". In: *Computers and Electronics in Agriculture* 159 (Apr. 2019), pp. 110–118. ISSN: 01681699. DOI: 10.1016/j.compag.2019.03.006.

[237] Kpade O.L. Hounkpatin, Karsten Schmidt, Felix Stumpf, Gerald Forkuor, Thorsten Behrens, Thomas Scholten, Wulf Amelung, and Gerhard Welp. "Predicting reference soil groups using legacy data: A data pruning and Random Forest approach for tropical environment (Dano catchment, Burkina Faso)". In: *Scientific Reports* 8.1 (Dec. 2018), pp. 1–16. ISSN: 20452322. DOI: 10.1038/s41598-018-28244-w.

[238] Bartosz Krawczyk. "Learning from imbalanced data: open challenges and future directions". In: *Progress in Artificial Intelligence* 5.4 (Nov. 2016), pp. 221–232. ISSN: 21926360. DOI: 10.1007/s13748-016-0094-0.

[239] Matheus Pinheiro Ferreira, Fabien Hubert Wagner, Luiz E.O.C. Aragão, Yosio Edemir Shimabukuro, and Carlos Roberto de Souza Filho. "Tree species classification in tropical forests using visible to shortwave infrared WorldView-3 images and texture analysis". In: *ISPRS Journal of Photogrammetry and Remote Sensing* 149 (Mar. 2019), pp. 119–131. ISSN: 09242716. DOI: 10.1016/j.isprsjprs.2019.01.019.

[240] Shahab Eddin Jozdani, Brian Alan Johnson, and Dongmei Chen. "Comparing Deep Neural Networks, Ensemble Classifiers, and Support Vector Machine Algorithms for Object-Based Urban Land Use/Land Cover Classification". In: *Remote Sensing* 11.14 (July 2019), p. 1713. ISSN: 2072-4292. DOI: 10.3390/rs11141713. URL: https://www.mdpi.com/2072-4292/11/14/1713.

[241] Christina Bogner, Bumsuk Seo, Dorian Rohner, and Björn Reineking. "Classification of rare land cover types: Distinguishing annual and perennial crops in an agricultural catchment in South Korea". In: *PLoS ONE* 13.1 (Jan. 2018). ISSN: 19326203. DOI: 10.1371/journal.pone.0190476.

[242] Ming Zhu, Bo Wu, Y. N. He, and Y. Q. He. "Land Cover Classification Using High Resolution Satellite Image Based On Deep Learning". In: *ISPRS - International Archives of the Photogrammetry, Remote Sensing and Spatial Information Sciences* XLII-3/W10 (2020), pp. 685–690. ISSN: 2194-9034. DOI: 10.5194/isprs-archives-xlii-3-w10-685-2020. URL: https://doi.org/10.5194/isprs-archives-XLII-3-W10-685-2020.

[243] Tjeng Wawan Cenggoro, Sani M. Isa, Gede Putra Kusuma, and Bens Pardamean. "Classification of imbalanced land-use/land-cover data using variational semi-supervised learning". In: *Proceedings - 2017 International Conference on Innovative and Creative Information Technology: Computational Intelligence and IoT, ICITech 2017*. Vol. 2018-Janua. IEEE, Nov. 2018, pp. 1–6. ISBN: 9781538640456. DOI: 10.1109/INNOCIT.2017.8319149. URL: http://ieeexplore.ieee.org/document/8319149/.

[244] Li Ma and Suohai Fan. "CURE-SMOTE algorithm and hybrid algorithm for feature selection and parameter optimization based on random forests". In: *BMC Bioinformatics* 18.1 (Mar. 2017), p. 169. ISSN: 14712105. DOI: 10.1186/s12859-017-1578-z. URL: http://bmcbioinformatics.biomedcentral.com/articles/10.1186/s12859-017-1578-z.

[245] Georgios Douzas and Fernando Bacao. "Self-Organizing Map Oversampling (SOMO) for imbalanced data set learning". In: *Expert Systems with Applications* 82 (Oct. 2017), pp. 40–52. ISSN: 09574174. DOI: 10.1016/j.eswa.2017.03.073.

[246] Haibo He, Yang Bai, Edwardo A. Garcia, and Shutao Li. "ADASYN: Adaptive synthetic sampling approach for imbalanced learning". In: *2008 IEEE International Joint Conference on Neural Networks (IEEE World Congress on Computational Intelligence)*. IEEE, June 2008, pp. 1322–1328. ISBN: 978-1-4244-1820-6. DOI: 10.1109/IJCNN.2008.4633969. URL: http://ieeexplore.ieee.org/document/4633969/.

[247] Robert C Holte, Liane Acker, Bruce W Porter, et al. "Concept Learning and the Problem of Small Disjuncts." In: *IJCAI*. Vol. 89. Citeseer. 1989, pp. 813–818.

[248] Miriam Seoane Santos, Pedro Henriques Abreu, Pedro J. García-Laencina, Adélia Simão, and Armando Carvalho. "A new cluster-based oversampling method for improving survival prediction of hepatocellular carcinoma patients". In: *Journal of Biomedical Informatics* 58 (Dec. 2015), pp. 49–59. ISSN: 15320464. DOI: 10.1016/j.jbi.2015.09.012.

[249] Marion F. Baumgardner, Larry L. Biehl, and David A. Landgrebe. "220 Band AVIRIS Hyperspectral Image Data Set: June 12, 1992 Indian Pine Test Site 3". In: *Purdue University Research Repository* (Sept. 2015). DOI: 10.4231/R7RX991C. URL: https://doi.org/10.4231/R7RX991C.

[250] John Ashworth Nelder and Robert WM Wedderburn. "Generalized linear models". In: *Journal of the Royal Statistical Society: Series A (General)* 135.3 (1972), pp. 370–384.

[251] T Cover and P Hart. "Nearest neighbor pattern classification". In: *IEEE Transactions on Information Theory* 13.1 (1967), pp. 21–27. ISSN: 0018-9448. DOI: 10.1109/TIT.1967.1053964. URL: http://ieeexplore.ieee.org/lpdocs/epic03/wrapper.htm?arnumber=1053964.

[252] Andy Liaw, Matthew Wiener, et al. "Classification and regression by randomForest". In: *R news* 2.3 (2002), pp. 18–22.

[253] Pontus Olofsson, Giles M. Foody, Stephen V. Stehman, and Curtis E. Woodcock. "Making better use of accuracy data in land change studies: Estimating accuracy and area and quantifying uncertainty using stratified estimation". In: *Remote Sensing of Environment* 129 (Feb. 2013), pp. 122–131. ISSN: 00344257. DOI: 10.1016/j.rse.2012.10.031.

[254] Robert Gilmore Pontius and Marco Millones. *Death to Kappa: Birth of quantity disagreement and allocation disagreement for accuracy assessment*. 2011. DOI: 10.1080/01431161.2011.552923.

[255] László A. Jeni, Jeffrey F. Cohn, and Fernando De La Torre. "Facing imbalanced data - Recommendations for the use of performance metrics". In: *Proceedings - 2013 Humaine Association Conference on Affective Computing and Intelligent Interaction, ACII 2013*. 2013, pp. 245–251. ISBN: 9780769550480. DOI: 10.1109/ACII.2013.47.

[256] Haibo He and Edwardo A Garcia. "Learning from Imbalanced Data". In: *IEEE Transactions on Knowledge and Data Engineering* 21.9 (2009), pp. 1263–1284. ISSN: 10414347. DOI: 10.1109/TKDE.2008.239. arXiv: arXiv:1011.1669v3.

[257] Fabian Pedregosa, Gaël Varoquaux, Alexandre Gramfort, Vincent Michel, Bertrand Thirion, Olivier Grisel, Mathieu Blondel, Peter Prettenhofer, Ron Weiss, Vincent Dubourg, Jake Vanderplas, Alexandre Passos, David Cournapeau, Matthieu Brucher, Matthieu Perrot, and Édouard Duchesnay. "Scikit-learn: Machine Learning in Python". In: *Journal of Machine Learning Research* 12.Oct (2011), pp. 2825–2830. ISSN: ISSN 1533-7928. URL: http://jmlr.csail.mit.edu/papers/v12/pedregosa11a.html.

[258] Guillaume Lemaître, Fernando Nogueira, and Christos K. Aridas. "Imbalanced-learn: A Python Toolbox to Tackle the Curse of Imbalanced Datasets in Machine Learning". In: *Journal of Machine Learning Research* 18.17 (2017), pp. 1–5. URL: http://jmlr.org/papers/v18/16-365.html.

[259] Janez Demšar. "Statistical Comparisons of Classifiers over Multiple Data Sets". In: *Journal of Machine Learning Research* 7 (2006), pp. 1–30. DOI: 10.5555/1248547.

[260] Milton Friedman. "The use of ranks to avoid the assumption of normality implicit in the analysis of variance". In: *Journal of the american statistical association* 32.200 (1937), pp. 675–701.

[261] Frank Wilcoxon. "Individual Comparisons by Ranking Methods". In: *Biometrics Bulletin* 1.6 (Dec. 1945), p. 80. ISSN: 00994987.

[262] Shin Nagai, Kenlo Nishida Nasahara, Tomoko Kawaguchi Akitsu, Taku M. Saitoh, and Hiroyuki Muraoka. "Importance of the Collection of Abundant Ground-Truth Data for Accurate Detection of Spatial and Temporal Variability of Vegetation by Satellite Remote Sensing". In: *Biogeochemical Cycles: Ecological Drivers and Environmental Impact*. American Geophysical Union (AGU), Feb. 2020, pp. 223–244. DOI: 10.1002/9781119413332.ch11. URL: https://onlinelibrary.wiley.com/doi/abs/10.1002/9781119413332.ch11.

[263] Yanbo Huang, Zhong xin CHEN, Tao YU, Xiang zhi HUANG, and Xing fa GU. "Agricultural remote sensing big data: Management and applications". In: *Journal of Integrative Agriculture* 17.9 (Sept. 2018), pp. 1915–1931. ISSN: 20953119. DOI: 10.1016/S2095-3119(17)61859-8.

[264] Xianwei Wang and Hongjie Xie. "A review on applications of remote sensing and geographic information systems (GIS) in water resources and flood risk management". In: *Water (Switzerland)* 10.5 (May 2018), p. 608. ISSN: 20734441. DOI: 10.3390/w10050608. URL: http://www.mdpi.com/2073-4441/10/5/608.

[265] H Costa, P Benevides, F Marcelino, and M Caetano. "Introducing automatic satellite image processing into land cover mapping by photo-interpretation of airborne data". In: *The International Archives of Photogrammetry, Remote Sensing and Spatial Information Sciences* 42 (2020), pp. 29–34.

[266] Eric F Vermote, Sergii Skakun, Inbal Becker-Reshef, and Keiko Saito. "Remote Sensing of Coconut Trees in Tonga Using Very High Spatial Resolution WorldView-3 Data". In: *Remote Sensing* 12.19 (2020), p. 3113.

[267] Domenica Costantino, Massimiliano Pepe, Gino Dardanelli, and Valerio Baiocchi. "Using Optical Satellite and Aerial Imagery for Automatic Coastline Mapping". In: *Geographia Technica* (Sept. 2020), pp. 171–190. ISSN: 18425135. DOI: 10.21163/gt_2020.152.17.

[268] Vít Růžička, Stefano D'Aronco, Jan Dirk Wegner, and Konrad Schindler. "Deep Active Learning in Remote Sensing for data efficient Change Detection". In: *arXiv preprint arXiv:2008.11201* (2020).

[269] Sheng-Jie Liu, Haowen Luo, and Qian Shi. "Active Ensemble Deep Learning for Polarimetric Synthetic Aperture Radar Image Classification". In: *IEEE Geoscience and Remote Sensing Letters* (2020), pp. 1–5. ISSN: 1545-598X. DOI: 10.1109/lgrs.2020.3005076. arXiv: 2006.15771.

[270] Edoardo Pasolli, Hsiuhan Lexie Yang, and Melba M. Crawford. "Active-metric learning for classification of remotely sensed hyperspectral images". In: *IEEE Transactions on Geoscience and Remote Sensing* 54.4 (Apr. 2016), pp. 1925–1939. ISSN: 01962892. DOI: 10.1109/TGRS.2015.2490482.

[271] G.C. Cawley. "Baseline Methods for Active Learning". In: *Proceedings of Active Learning and Experimental Design workshop In conjunction with AISTATS* 16 (Apr. 2011), pp. 47–57. ISSN: 1938-7228. URL: http://proceedings.mlr.press/v16/cawley11a.html.

[272] Xin Li and Yuhong Guo. "Active learning with multi-label SVM classification". In: *In IJCAI*. Aug. 2013, pp. 1479–1485.

[273] Devis Tuia, E Pasolli, and William J Emery. "Using active learning to adapt remote sensing image classifiers". In: *Remote Sensing of Environment* 115.9 (2011), pp. 2232–2242.

[274] Xin Wu, Wei Li, Danfeng Hong, Jiaojiao Tian, Ran Tao, and Qian Du. "Vehicle detection of multi-source remote sensing data using active fine-tuning network". In: *ISPRS Journal of Photogrammetry and Remote Sensing* 167 (Sept. 2020), pp. 39–53. ISSN: 09242716. DOI: 10.1016/j.isprsjprs.2020.06.016. arXiv: 2007.08494.

[275] Haixia Bi, Feng Xu, Zhiqiang Wei, Yong Xue, and Zongben Xu. "An Active Deep Learning Approach for Minimally Supervised PolSAR Image Classification". In: *IEEE Transactions on Geoscience and Remote Sensing* 57.11 (Nov. 2019), pp. 9378–9395. ISSN: 15580644. DOI: 10.1109/TGRS.2019.2926434.

[276] Lucas Hu, Caleb Robinson, and Bistra Dilkina. "Model Generalization in Deep Learning Applications for Land Cover Mapping". In: *arXiv preprint arXiv:2008.10351* (2020).

[277] Swalpa Kumar Roy, Gopal Krishna, Shiv Ram Dubey, and Bidyut B. Chaudhuri. "HybridSN: Exploring 3-D-2-D CNN Feature Hierarchy for Hyperspectral Image Classification". In: *IEEE Geoscience and Remote Sensing Letters* (June 2019), pp. 1–5. ISSN: 1545-598X. DOI: 10.1109/lgrs.2019.2918719. arXiv: 1902.06701.

[278] Ion Muslea, Steven Minton, and Craig A. Knoblock. "Active learning with multiple views". In: *Journal of Artificial Intelligence Research* 27 (Oct. 2006), pp. 203–233. ISSN: 10769757. DOI: 10.1613/jair.2005. arXiv: 1110.1073. URL: https://www.jair.org/index.php/jair/article/view/10470.

[279] Wei Di and Melba M. Crawford. "View generation for multiview maximum disagreement based active learning for hyperspectral image classification". In: *IEEE Transactions on Geoscience and Remote Sensing* 50.5 PART 2 (May 2012), pp. 1942–1954. ISSN: 01962892. DOI: 10.1109/TGRS.2011.2168566.

[280] Zhou Zhang, Edoardo Pasolli, Hsiuhan Lexie Yang, and Melba M. Crawford. "Multimetric Active Learning for Classification of Remote Sensing Data". In: *IEEE Geoscience and Remote Sensing Letters* 13.7 (July 2016), pp. 1007–1011. ISSN: 1545598X. DOI: 10.1109/LGRS.2016.2560623.

[281] Devis Tuia, Frdric Ratle, Fabio Pacifici, Mikhail F. Kanevski, and William J. Emery. "Active learning methods for remote sensing image classification". In: *IEEE Transactions on Geoscience and Remote Sensing* 47 (7 July 2009), pp. 2218–2232. ISSN: 01962892.

[282] Loris Copa, Devis Tuia, Michele Volpi, and Mikhail Kanevski. "Unbiased query-by-bagging active learning for VHR image classification". In: *Image and Signal Processing for Remote Sensing XVI*. Ed. by Lorenzo Bruzzone. Vol. 7830. SPIE, Oct. 2010, 78300K. ISBN: 9780819483478. DOI: 10.1117/12.864861. URL: http://proceedings.spiedigitallibrary.org/proceeding.aspx?doi=10.1117/12.864861.

[283] Begm Demir, Claudio Persello, and Lorenzo Bruzzone. "Batch-mode active-learning methods for the interactive classification of remote sensing images". In: *IEEE Transactions on Geoscience and Remote Sensing* 49.3 (Mar. 2011), pp. 1014–1031. ISSN: 01962892. DOI: 10.1109/TGRS.2010.2072929.

[284] Jun Li, José M. Bioucas-Dias, and Antonio Plaza. "Hyperspectral image segmentation using a new bayesian approach with active learning". In: *IEEE Transactions on Geoscience and Remote Sensing* 49.10 PART 2 (Oct. 2011), pp. 3947–3960. ISSN: 01962892. DOI: 10.1109/TGRS.2011.2128330.

[285] Tong Luo, Kurt Kramer, Dmitry Goldgof, Lawrence O. Hall, Scott Samson, Andrew Remsen, and Thomas Hopkins. "Learning to recognize plankton". In: *Proceedings of the IEEE International Conference on Systems, Man and Cybernetics*. Vol. 1. 2003, pp. 888–893. DOI: 10.1109/icsmc.2003.1243927.

[286] Jun Li, José M. Bioucas-Dias, and Antonio Plaza. "Spectral-spatial classification of hyperspectral data using loopy belief propagation and active learning". In: *IEEE Transactions on Geoscience and Remote Sensing* 51.2 (2013), pp. 844–856. ISSN: 01962892. DOI: 10.1109/TGRS.2012.2205263.

[287] Seyda Ertekin, Jian Huang, and C. Lee Giles. "Active learning for class imbalance problem". In: *Proceedings of the 30th Annual International ACM SIGIR Conference on Research and Development in Information Retrieval, SIGIR'07*. New York, New York, USA: ACM Press, 2007, pp. 823–824. ISBN: 1595935975. DOI: 10.1145/1277741.1277927. URL: http://portal.acm.org/citation.cfm?doid=1277741.1277927.

[288] Tin Kam Ho. "Random Decision Forests". In: *Proceedings of the Third International Conference on Document Analysis and Recognition (Volume 1) - Volume 1*. ICDAR '95. USA: IEEE Computer Society, 1995, p. 278. ISBN: 0818671289.

[289] Miroslav Kubat, Stan Matwin, et al. "Addressing the curse of imbalanced training sets: one-sided selection". In: *Icml*. Vol. 97. Citeseer. 1997, pp. 179–186.

[290] Tobias Reitmaier and Bernhard Sick. "Let us know your decision: Pool-based active training of a generative classifier with the selection strategy 4DS". In: *Information Sciences* 230 (May 2013), pp. 106–131. ISSN: 0020-0255.

[291] Jean-François Kagy, Tolga Kayadelen, Ji Ma, Afshin Rostamizadeh, and Jana Strnadova. "The Practical Challenges of Active Learning: Lessons Learned from Live Experimentation". In: *arXiv preprint arXiv:1907.00038* (June 2019).

[292] Vishwesh Nath, Dong Yang, Bennett A. Landman, Daguang Xu, and Holger R. Roth. "Diminishing Uncertainty Within the Training Pool: Active Learning for Medical Image Segmentation". In: *IEEE Transactions on Medical Imaging* 40.10 (2021), pp. 2534–2547.

[293] Yayong Li, Jie Yin, and Ling Chen. "SEAL: Semisupervised Adversarial Active Learning on Attributed Graphs". In: *IEEE Transactions on Neural Networks and Learning Systems* 32.7 (2021), pp. 3136–3147.

[294] Jesper E Van Engelen and Holger H Hoos. "A survey on semi-supervised learning". In: *Machine Learning* 109.2 (2020), pp. 373–440.

[295] Ozan Sener and Silvio Savarese. "Active Learning for Convolutional Neural Networks: A Core-Set Approach". In: *International Conference on Learning Representations*. 2018.

[296] Yan Leng, Xinyan Xu, and Guanghui Qi. "Combining active learning and semi-supervised learning to construct SVM classifier". In: *Knowledge-Based Systems* 44 (2013), pp. 121–131.

[297] Hualong Yu, Xibei Yang, Shang Zheng, and Changyin Sun. "Active Learning from Imbalanced Data: A Solution of Online Weighted Extreme Learning Machine". In: *IEEE Transactions on Neural Networks and Learning Systems* 30 (4 Apr. 2019), pp. 1088–1103. ISSN: 21622388.

[298] Hang Zhang, Weike Liu, and Qingbao Liu. "Reinforcement online active learning ensemble for drifting imbalanced data streams". In: *IEEE Transactions on Knowledge and Data Engineering* (2020).

[299] Weiwei Zong, Guang-Bin Huang, and Yiqiang Chen. "Weighted extreme learning machine for imbalance learning". In: *Neurocomputing* 101 (2013), pp. 229–242.

[300] Jiongming Qin, Cong Wang, Qinhong Zou, Yubin Sun, and Bin Chen. "Active learning with extreme learning machine for online imbalanced multiclass classification". In: *Knowledge-Based Systems* 231 (2021), p. 107385.

[301] Hanxiao Liu, Zihang Dai, David R So, and Quoc V Le. "Pay Attention to MLPs". In: *arXiv preprint arXiv:2105.08050* (2021).

[302] Alaa Tharwat and Wolfram Schenck. "Balancing Exploration and Exploitation: A novel active learner for imbalanced data". In: *Knowledge-Based Systems* 210 (2020), p. 106500.

[303] Yoon-Yeong Kim, Kyungwoo Song, JoonHo Jang, and Il-chul Moon. "LADA: Look-Ahead Data Acquisition via Augmentation for Deep Active Learning". In: *Advances in Neural Information Processing Systems* 34 (2021).

[304] Julian Katz-Samuels, Jifan Zhang, Lalit Jain, and Kevin Jamieson. "Improved algorithms for agnostic pool-based active classification". In: *International Conference on Machine Learning*. PMLR. 2021, pp. 5334–5344.

[305] Joao Fonseca, Georgios Douzas, and Fernando Bacao. "Increasing the Effectiveness of Active Learning: Introducing Artificial Data Generation in Active Learning for Land Use/Land Cover Classification". In: *Remote Sensing 2021, Vol. 13, Page 2619* 13.13 (July 2021), p. 2619.

[306] Timothy M Hospedales, Shaogang Gong, and Tao Xiang. "Finding rare classes: Active learning with generative and discriminative models". In: *IEEE transactions on knowledge and data engineering* 25.2 (2011), pp. 374–386.

[307] Yuanzhang Li, Xinxin Wang, Zhiwei Shi, Ruyun Zhang, Jingfeng Xue, and Zhi Wang. "Boosting training for PDF malware classifier via active learning". In: *International Journal of Intelligent Systems* 37.4 (2022), pp. 2803–2821.

[308] Jiayi Li, Xin Huang, and Xiaoyu Chang. "A label-noise robust active learning sample collection method for multi-temporal urban land-cover classification and change analysis". In: *ISPRS Journal of Photogrammetry and Remote Sensing* 163 (2020), pp. 1–17.

[309] Cong Su, Zhongmin Yan, and Guoxian Yu. "Cost-effective multi-instance multilabel active learning". In: *International Journal of Intelligent Systems* 36.12 (2021), pp. 7177–7203.

[310] Xiaoxue Wu, Wei Zheng, Xin Xia, and David Lo. "Data quality matters: A case study on data label correctness for security bug report prediction". In: *IEEE Transactions on Software Engineering* (2021).

[311] Wei Zhang, Ziwei Wang, and Xiang Li. "Blockchain-based decentralized federated transfer learning methodology for collaborative machinery fault diagnosis". In: *Reliability Engineering & System Safety* 229 (2023), p. 108885.

[312] Wei Zhang, Xiang Li, Hui Ma, Zhong Luo, and Xu Li. "Open-set domain adaptation in machinery fault diagnostics using instance-level weighted adversarial learning". In: *IEEE Transactions on Industrial Informatics* 17.11 (2021), pp. 7445–7455.

[313] Miao He and David He. "Deep learning based approach for bearing fault diagnosis". In: *IEEE Transactions on Industry Applications* 53.3 (2017), pp. 3057–3065.

[314] Jun Li, Kai Xu, Siddhartha Chaudhuri, Ersin Yumer, Hao Zhang, and Leonidas Guibas. "Grass: Generative recursive autoencoders for shape structures". In: *ACM Transactions on Graphics (TOG)* 36.4 (2017), pp. 1–14.

[315] Wenfeng Zheng, Xiangjun Liu, and Lirong Yin. "Sentence representation method based on multi-layer semantic network". In: *Applied Sciences* 11.3 (2021), p. 1316.

[316] Kai Zhang, Zhongzheng Wang, Guodong Chen, Liming Zhang, Yongfei Yang, Chuanjin Yao, Jian Wang, and Jun Yao. "Training effective deep reinforcement learning agents for real-time life-cycle production optimization". In: *Journal of Petroleum Science and Engineering* 208 (2022), p. 109766.

[317] Samarth Sinha, Sayna Ebrahimi, and Trevor Darrell. "Variational adversarial active learning". In: *Proceedings of the IEEE/CVF International Conference on Computer Vision*. 2019, pp. 5972–5981.

[318] Kwanyoung Kim, Dongwon Park, Kwang In Kim, and Se Young Chun. "Task-aware variational adversarial active learning". In: *Proceedings of the IEEE/CVF Conference on Computer Vision and Pattern Recognition*. 2021, pp. 8166–8175.

[319] Yu Ma, Shaoxing Lu, Erya Xu, Tian Yu, and Lijian Zhou. "Combining Active Learning and Data Augmentation for Image Classification". In: *Proceedings of the 2020 3rd International Conference on Big Data Technologies*. 2020, pp. 58–62.

[320] Husam Quteineh, Spyridon Samothrakis, and Richard Sutcliffe. "Textual Data Augmentation for Efficient Active Learning on Tiny Datasets". In: *Proceedings of the 2020 Conference on Empirical Methods in Natural Language Processing (EMNLP)*. 2020, pp. 7400–7410.

[321] Qingqing Li, Zhen Huang, Yong Dou, and Ziwen Zhang. "A Framework of Data Augmentation While Active Learning for Chinese Named Entity Recognition". In: *International Conference on Knowledge Science, Engineering and Management*. Springer. 2021, pp. 88–100.

[322] Chialin Wu. *The decision tree approach to classification*. Purdue University, 1975.

[323] Mehrdad Fatourechi, Rabab K Ward, Steven G Mason, Jane Huggins, Alois Schloegl, and Gary E Birch. "Comparison of evaluation metrics in classification applications with imbalanced datasets". In: *2008 seventh international conference on machine learning and applications*. IEEE. 2008, pp. 777–782.

[324] Sture Holm. "A simple sequentially rejective multiple test procedure". In: *Scandinavian journal of statistics* (1979), pp. 65–70.

[325] Shivani Tyagi and Sangeeta Mittal. "Sampling approaches for imbalanced data classification problem in machine learning". In: *Proceedings of ICRIC 2019*. Springer, 2020, pp. 209–221.

[326] Pattaramon Vuttipittayamongkol, Eyad Elyan, and Andrei Petrovski. "On the class overlap problem in imbalanced data classification". In: *Knowledge-based systems* 212 (2021), p. 106631.

[327] Victoria López, Alberto Fernández, Salvador Garcia, Vasile Palade, and Francisco Herrera. "An insight into classification with imbalanced data: Empirical results and current trends on using data intrinsic characteristics". In: *Information sciences* 250 (2013), pp. 113–141.

[328] Swagatam Das, Shounak Datta, and Bidyut B Chaudhuri. "Handling data irregularities in classification: Foundations, trends, and future challenges". In: *Pattern Recognition* 81 (2018), pp. 674–693.

[329] Harsurinder Kaur, Husanbir Singh Pannu, and Avleen Kaur Malhi. "A systematic review on imbalanced data challenges in machine learning: Applications and solutions". In: *ACM Computing Surveys (CSUR)* 52.4 (2019), pp. 1–36.

[330] Adane Nega Tarekegn, Mario Giacobini, and Krzysztof Michalak. "A review of methods for imbalanced multi-label classification". In: *Pattern Recognition* 118 (2021), p. 107965.

[331] Janne Lumijärvi, Jorma Laurikkala, and Martti Juhola. "A comparison of different heterogeneous proximity functions and Euclidean distance". In: *MEDINFO 2004*. IOS Press. 2004, pp. 1362–1366.

[332] Alberto Fernández, Salvador Garcia, Francisco Herrera, and Nitesh V Chawla. "SMOTE for learning from imbalanced data: progress and challenges, marking the 15-year anniversary". In: *Journal of artificial intelligence research* 61 (2018), pp. 863–905.

[333] Addisson Salazar, Luis Vergara, and Gonzalo Safont. "Generative Adversarial Networks and Markov Random Fields for oversampling very small training sets". In: *Expert Systems with Applications* 163 (2021), p. 113819.

[334] Aki Koivu, Mikko Sairanen, Antti Airola, and Tapio Pahikkala. "Synthetic minority oversampling of vital statistics data with generative adversarial networks". In: *Journal of the American Medical Informatics Association* 27.11 (2020), pp. 1667–1674.

[335] Wonkeun Jo and Dongil Kim. "OBGAN: Minority oversampling near borderline with generative adversarial networks". In: *Expert Systems with Applications* 197 (2022), p. 116694.

[336] Liang Gonog and Yimin Zhou. "A review: generative adversarial networks". In: *2019 14th IEEE conference on industrial electronics and applications (ICIEA)*. IEEE. 2019, pp. 505–510.

[337] Mimi Mukherjee and Matloob Khushi. "SMOTE-ENC: A novel SMOTE-based method to generate synthetic data for nominal and continuous features". In: *Applied System Innovation* 4.1 (2021), p. 18.

[338] Kotaro Ambai and Hamido Fujita. "Multivariate normal distribution based over-sampling for numerical and categorical features". In: *Advancing Technology Industrialization Through Intelligent Software Methodologies, Tools and Techniques: Proceedings of the 18th International Conference on New Trends in Intelligent Software Methodologies, Tools and Techniques (SoMeT)*. Vol. 318. 2019, p. 107.

[339] Kotaro Ambai and Hamido Fujita. "MNDO: Multivariate Normal Distribution Based Over-Sampling for Binary Classification." In: *Advancing Technology Industrialization Through Intelligent Software Methodologies, Tools and Techniques: Proceedings of the 17th International Conference on New Trends in Intelligent Software Methodologies, Tools and Techniques (SoMeT)*. 2018, pp. 425–438.

[340] Seunghyun Park and Hyunhee Park. "Combined oversampling and undersampling method based on slow-start algorithm for imbalanced network traffic". In: *Computing* 103.3 (2021), pp. 401–424.

[341] Gustavo EAPA Batista, Ronaldo C Prati, and Maria Carolina Monard. "A study of the behavior of several methods for balancing machine learning training data". In: *ACM SIGKDD explorations newsletter* 6.1 (2004), pp. 20–29.

[342] Ankita Bansal and Abha Jain. "Analysis of Focussed Under-Sampling Techniques with Machine Learning Classifiers". In: *2021 IEEE/ACIS 19th International Conference on Software Engineering Research, Management and Applications (SERA)*. IEEE. 2021, pp. 91–96.

[343] Yanmin Sun, Andrew KC Wong, and Mohamed S Kamel. "Classification of imbalanced data: A review". In: *International journal of pattern recognition and artificial intelligence* 23.04 (2009), pp. 687–719.

[344] Neelam Rout, Debahuti Mishra, and Manas Kumar Mallick. "Handling imbalanced data: a survey". In: *International proceedings on advances in soft computing, intelligent systems and applications*. Springer, 2018, pp. 431–443.

[345] Nathalie Japkowicz. "Assessment metrics for imbalanced learning". In: *Imbalanced learning: Foundations, algorithms, and applications* (2013), pp. 187–206.

A. Improving Imbalanced Land Cover Classification with K-means SMOTE: Detecting and Oversampling Distinctive Minority Spectral Signatures

Dataset	Classifier	Metric	NONE	ROS	SMOTE	B-SMOTE	K-SMOTE
Botswana	LR	Accuracy	0.920	0.917	0.920	0.921	**0.927**
Botswana	LR	F-score	0.913	0.909	0.913	0.914	**0.921**
Botswana	LR	G-mean	0.952	0.950	0.952	0.952	**0.956**
Botswana	KNN	Accuracy	0.875	0.862	0.881	0.869	**0.889**
Botswana	KNN	F-score	0.859	0.850	0.873	0.859	**0.879**
Botswana	KNN	G-mean	0.924	0.918	0.930	0.923	**0.933**
Botswana	RF	Accuracy	0.873	0.884	0.877	0.877	**0.890**
Botswana	RF	F-score	0.865	0.877	0.872	0.870	**0.883**
Botswana	RF	G-mean	0.925	0.933	0.929	0.928	**0.936**
PC	LR	Accuracy	0.954	0.955	0.955	0.950	**0.956**
PC	LR	F-score	0.944	0.947	0.947	0.941	**0.948**
PC	LR	G-mean	0.968	0.972	0.972	0.966	**0.973**
PC	KNN	Accuracy	**0.926**	0.920	0.923	0.924	**0.926**
PC	KNN	F-score	**0.915**	0.909	0.913	0.913	**0.915**
PC	KNN	G-mean	0.953	0.955	**0.957**	0.954	**0.957**
PC	RF	Accuracy	0.938	0.941	0.940	0.938	**0.942**
PC	RF	F-score	0.928	0.932	0.931	0.928	**0.933**
PC	RF	G-mean	0.959	0.964	**0.965**	0.961	**0.965**
KSC	LR	Accuracy	0.904	0.905	0.905	0.899	**0.909**
KSC	LR	F-score	0.868	0.873	0.874	0.862	**0.877**
KSC	LR	G-mean	0.928	0.932	0.932	0.924	**0.934**
KSC	KNN	Accuracy	0.855	0.859	0.862	0.857	**0.865**
KSC	KNN	F-score	0.808	0.819	**0.827**	0.810	0.826
KSC	KNN	G-mean	0.893	0.901	**0.906**	0.895	0.905
KSC	RF	Accuracy	0.860	0.859	0.863	0.859	**0.868**
KSC	RF	F-score	0.817	0.815	0.826	0.816	**0.832**
KSC	RF	G-mean	0.898	0.899	0.905	0.898	**0.907**
SA	LR	Accuracy	0.979	0.981	0.983	0.979	**0.984**
SA	LR	F-score	0.976	0.979	**0.982**	0.977	**0.982**
SA	LR	G-mean	0.985	0.988	**0.990**	0.987	0.989
SA	KNN	Accuracy	0.987	0.979	0.982	0.983	**0.988**
SA	KNN	F-score	0.986	0.979	0.981	0.982	**0.987**
SA	KNN	G-mean	0.992	0.989	0.990	0.991	**0.993**
SA	RF	Accuracy	0.980	0.983	0.984	0.979	**0.985**
SA	RF	F-score	0.979	0.982	0.983	0.978	**0.984**
SA	RF	G-mean	0.987	0.988	0.989	0.986	**0.990**

Dataset	Classifier	Metric	NONE	ROS	SMOTE	B-SMOTE	K-SMOTE
PU	LR	Accuracy	**0.905**	0.897	0.897	0.891	0.904
PU	LR	F-score	0.890	0.894	0.894	0.888	**0.898**
PU	LR	G-mean	0.932	0.947	0.947	0.942	**0.949**
PU	KNN	Accuracy	**0.895**	0.867	0.865	0.873	**0.895**
PU	KNN	F-score	**0.891**	0.868	0.868	0.874	**0.891**
PU	KNN	G-mean	0.940	0.935	0.936	0.936	**0.941**
PU	RF	Accuracy	**0.912**	0.908	0.907	0.908	0.911
PU	RF	F-score	**0.909**	0.906	0.906	0.908	**0.909**
PU	RF	G-mean	0.946	0.946	0.948	0.948	**0.949**
Salinas	LR	Accuracy	**0.990**	**0.990**	0.989	**0.990**	**0.990**
Salinas	LR	F-score	0.985	**0.986**	0.985	0.985	**0.986**
Salinas	LR	G-mean	0.992	**0.993**	0.992	0.992	**0.993**
Salinas	KNN	Accuracy	**0.970**	0.967	0.969	0.967	**0.970**
Salinas	KNN	F-score	0.959	0.957	**0.960**	0.957	**0.960**
Salinas	KNN	G-mean	0.977	0.978	**0.981**	0.976	**0.981**
Salinas	RF	Accuracy	0.984	0.983	0.983	0.983	**0.985**
Salinas	RF	F-score	0.979	0.979	0.977	0.978	**0.980**
Salinas	RF	G-mean	0.989	0.989	0.989	0.989	**0.990**
IP	LR	Accuracy	0.687	0.681	0.680	0.678	**0.692**
IP	LR	F-score	0.662	0.663	0.659	0.659	**0.674**
IP	LR	G-mean	0.798	0.801	0.798	0.797	**0.807**
IP	KNN	Accuracy	**0.644**	0.602	0.589	0.557	0.632
IP	KNN	F-score	0.593	0.591	0.603	0.560	**0.604**
IP	KNN	G-mean	0.757	0.764	**0.782**	0.751	0.781
IP	RF	Accuracy	0.742	0.747	0.747	0.740	**0.752**
IP	RF	F-score	0.673	0.704	0.713	0.701	**0.714**
IP	RF	G-mean	0.806	0.826	0.835	0.831	**0.838**

Table A.1.: Mean cross-validation scores for each dataset. Legend: IP - Indian Pines, KSC - Kennedy Space Center, PC - Pavia Center, PU - Pavia University, SA - Salinas A.

NOVA Information Management School
Instituto Superior de Estatística e Gestão de Informação

Universidade Nova de Lisboa